

Supplemental Information

Redox-neutral Photocatalytic C–H Carboxylation of Arenes and Styrenes with CO₂

Matthias Schmalzbauer,^{1,5} Thomas D. Svejstrup,^{2,5} Florian Fricke,¹ Peter Brandt,² Magnus J. Johansson,^{2,3} Giulia Bergonzini,^{2,*} and Burkhard König^{1,4,**}

¹Faculty of Chemistry and Pharmacy, University of Regensburg, Germany

²Medicinal Chemistry, Research and Early Development Cardiovascular, Renal and Metabolism, BioPharmaceuticals R&D, AstraZeneca, Gothenburg, Sweden

³Department of Organic Chemistry, Stockholm University, Stockholm 10691, Sweden

⁴Lead Contact

⁵These authors contributed equally

*Correspondence: giulia.bergonzini@astrazeneca.com

**Correspondence: burkhard.koenig@ur.de

Table of contents

1 - General Experimental Details	2
2 - Catalyst Synthesis and Physicochemical Properties	5
2.1 - Synthesis of the Photocatalyst.....	5
2.2 - Spectroscopic and Photochemical Characteristics	6
3 - Substrate Synthesis	13
4 - Carboxylation Reactions	17
4.1 - Reaction Optimization	17
4.2 - Substrate Scope	20
5 - Spectra.....	43
6 - Mechanistic Studies	96
6.1 - General Procedure for High-throughput Screening of Arenes.....	96
6.2 - Deuterium Labeling Experiments	96
6.3 - Time-resolved Luminescence Quenching studies.....	101
6.4 - Computational Analysis.....	104
7 - Miscellaneous.....	109
7.1 - Synthetic route towards FDCA and DMFDC	109
7.2 - Carboxylation of biphenyl	109
7.3 - Unsuccessful Substrates.....	110
8 - References.....	111

1 - General Experimental Details

All required fine chemicals were purchased from commercial suppliers (abcr, Acros, Alfa Aesar, Fluka, Fluorochem, Merck, Sigma Aldrich, TCI) and were used directly without purification unless stated otherwise. All air and moisture sensitive reactions were carried out under nitrogen atmosphere using standard Schlenk manifold technique. Anhydrous DMSO was used directly from the bottle or dried using activated 4Å molecular sieves. ¹H and ¹³C Nuclear Magnetic Resonance (NMR) spectra were acquired at room temperature with field strengths as indicated and were referenced to CDCl₃ (7.26 and 77.16 ppm for ¹H and ¹³C respectively), DMSO-d₆ (2.50 and 39.52 for ¹H and ¹³C respectively) or CD₃OD (3.31 and 49.0 ppm for ¹H and ¹³C respectively). ¹H-NMR coupling constants are reported in Hertz and refer to apparent multiplicities and not true coupling constants. Data are reported as follows: chemical shift, multiplicity (s = singlet, bs = broad singlet, d = doublet, t = triplet, q = quartet, qi = quintet, sx = sextet, sp = septet, m = multiplet, dd = doublet of doublets, etc.), coupling constants, integration, proton assignment (determined by 2D NMR experiments: COSY, HSQC and HMBC) where possible. ¹³C-NMR assignment was aided using DEPT 135 techniques (DEPT = distortion less enhancement by polarization transfer) to distinguish CH₂ groups from CH and CH₃ groups and to assign quaternary carbon atoms (C_q). ¹⁹F-NMR spectra were recorded for compounds containing fluorine atoms.

Analytical TLC was performed on silica gel coated aluminium sheets (Merck, TLC Silica gel 60 F₂₅₄) Compounds were visualized by exposure to UV-light (254 or 366 nm) or by dipping the plates in staining solutions (permanganate stain, bromocresol green stain, ceric ammonium molybdate stain) followed by heating. Flash column chromatography was performed using Merck Silica Gel 60 (40–63 μm) & Medium pressure liquid chromatography (MPLC) was performed on a Grace Reveleris® X2 from Büchi with built-in UV-detector and fraction collector using Biotage® sfär silica HC D 20 μm column cartridges or on a Biotage® Isolera One flash purification system using flash silica gel. All mixed solvent eluents are reported as v/v solutions. High resolution mass spectrometry (HRMS) were performed at the Central Analytical Laboratory of the University of Regensburg. Mass spectra were recorded on a Finnigan MAT 95, ThermoQuest Finnigan TSQ 7000, Finnigan MAT SSQ 710 A or Agilent Q-TOF 6540 UHD instrument and a Waters Acquity UPLC system equipped with Waters PDA, sample manager, sample organiser, column oven and Waters Xevo QTOF mass spectrometer. Photoreactions in regular scale were irradiated with blue LEDs (OSRAM Oslon SSL 80 royal-blue, λ = 455 nm (± 15), average radiant flux 232 ± 23 mW, 2.9 V, 350 mA) or green LEDs (λ = 535 nm, average radiant flux, 29 ± 5 mW) and were exposed to light from the flat bottom side of the vial. The temperature of the reaction mixtures was controlled by a water-cooling circuit consisting of an aluminium cooling block connected to a thermostat (Figure S1). An exemplary reaction in larger scale was carried out in a

custom-built glass reactor which upon vigorous stirring generates a thin film of the reaction mixture between the reaction vessel and an attached cold finger. A hose which was dipped in the solution provided CO₂ gas from the cylinder. The reaction vessel was surrounded by blue LED arrays (OSRAM Oslon SSL 80 LT-2010, $\lambda = 451$ nm, 700 mA) generating a total radiant flux of 12 W (Figure S2). For the high-throughput screening experiments, Kessil PR160L 456 nm LEDs were used. Cyclic voltammetry measurements were performed with a three-electrode system consisting of a glassy carbon working electrode, a platinum wire counter electrode and a silver wire as a reference electrode. Data was processed on a potentiostat PGSTAT302N from Metrohm Autolab. Prior to the measurement the solvent DMSO (dry) was degassed with argon and TBATFB (0.1M) was added as supporting electrolyte. All experiments were performed under argon atmosphere. Ferrocene was used as an internal reference. Measurements were performed at a scan rate of 0.05 Vs⁻¹. Potentials are reported against saturated calomel electrode (SCE) as reference. UV-Vis measurements were performed on an Agilent Cary 4000 UV-Vis Spectrophotometer. Prior to measurements a solvent blank was recorded and subtracted. Precision cells (1×1 cm) made of quartz SUPRASIL® from Hellma® Analytics were used. Luminescence measurements were performed on a Horiba® Scientific FluoroMax-4 instrument using the above-mentioned quartz cells. Luminescence lifetime measurements were performed on a Horiba® Scientific DeltaPro™ fluorescence lifetime system using a 452 nm laser diode from Horiba® Scientific DeltaDiode™ as excitation source and above-mentioned quartz cells. The instrument response function (IRF) was determined prior to measurements by using colloidal silica (LUDOX®) in water.

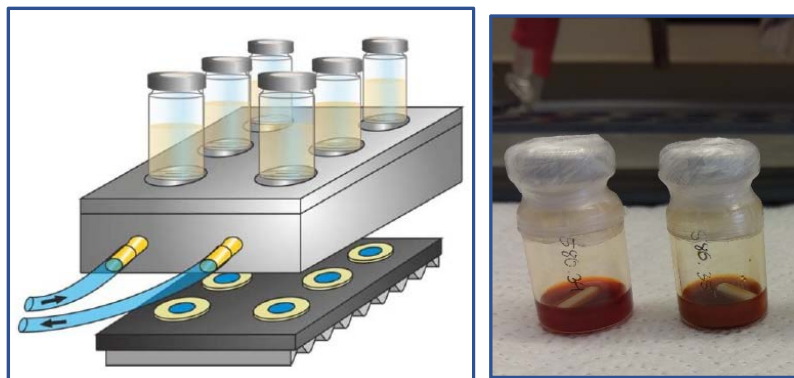


Figure S1. Schematic picture of the setup for photoreactions (left); crimp vials charged with stirring bar and reaction mixture and sealed with aluminium crimp seal with septum and Parafilm®

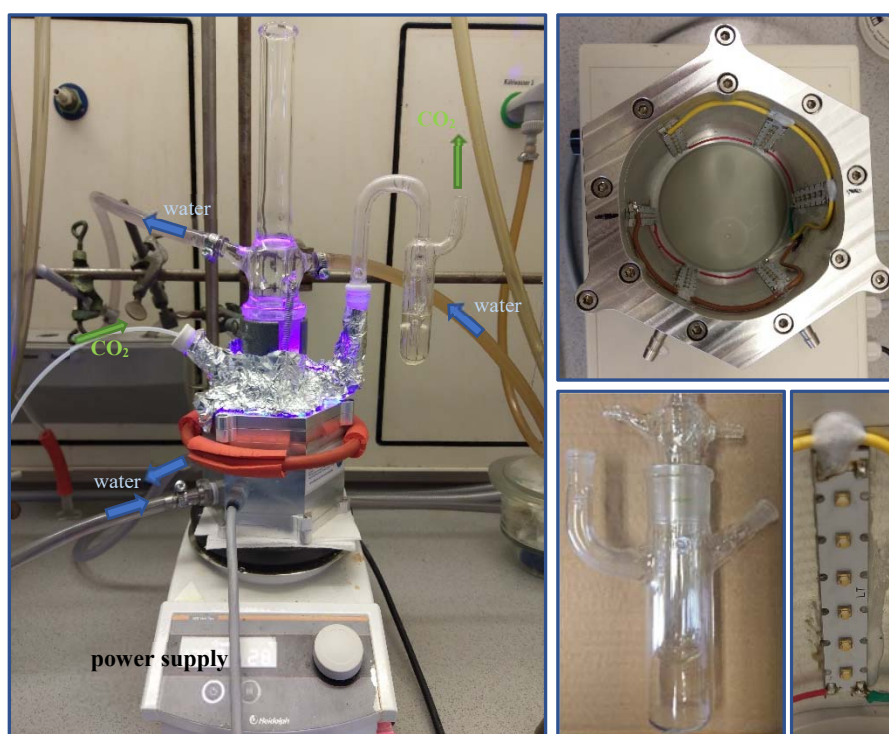
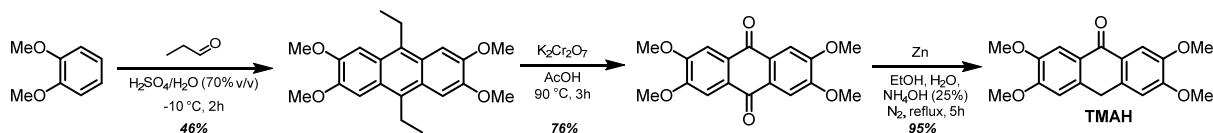


Figure S2. Custom-built glass reactor for upscaling of the photocatalytic carboxylation reaction.

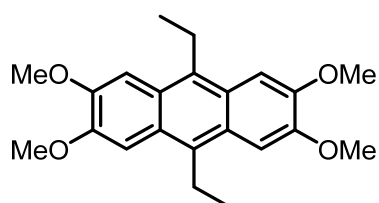
2 - Catalyst Synthesis and Physicochemical Properties

2.1 - Synthesis of the Photocatalyst

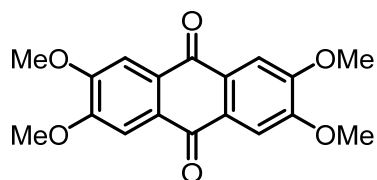
2,3,6,7-tetramethoxyanthracen-9(10*H*)-one **TMAH** was synthesized in three steps with an overall yield of 33%. The catalyst in its neutral form is a bench stable compound and can be stored easily.



Scheme S1. Overview of the synthetic steps in the synthesis of the used photocatalyst **TMAH**; overall yield 33% (3 steps).

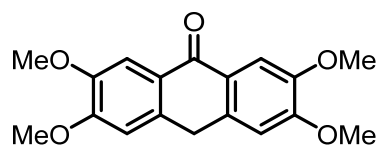


Synthesis of 9,10-diethyl-2,3,6,7-tetramethoxyanthracene: Referring to literature known procedures^{1,2}, a 250 mL round bottom flask equipped with stirring bar was charged with H₂SO₄ (70 mL, 70% v/v in H₂O) and veratrole (12.8 mL, 0.1 mol, 1 equiv.) and the resulting mixture was cooled to -10 °C. Under vigorous stirring, propanal (14.3 mL, 0.2 mol, 2 equiv.) was added dropwise *via* a syringe pump within 2 hrs. Care was taken, that the reaction temperature during addition of aldehyde was kept below 0 °C. The reaction mixture was poured into ice water (ca. 500 mL) and the resulting precipitate was filtered off and washed with water. The filter cake was dried over night by lyophilization and was washed in boiling EtOH. The precipitate was filtered off, washed with EtOH and dried under vacuo to give the title compound (8.06 g, 23 mmol, 46%) as pale-yellow powder. ¹H-NMR (400 MHz, Chloroform-*d*) δ 7.41 (s, 4H), 4.07 (s, 12H), 3.47 (q, *J* = 7.6 Hz, 4H), 1.44 (t, *J* = 7.6 Hz, 6H). ¹³C-NMR (101 MHz, CDCl₃) δ 149.0 (C_q), 130.7 (C_q), 125.1 (C_q), 102.4, 55.8, 22.0 (CH₂), 14.6.



Synthesis of 2,3,6,7-tetramethoxy-9,10-anthraquinone: According to a literature known procedure³ a 500 mL round bottom flask was charged with 9,10-diethyl-2,3,6,7-tetramethoxyanthracene (8.0 g, 22.6 mmol, 1 equiv.) and K₂Cr₂O₇ (33.2 g, 113 mmol, 5 equiv.) and the solids were suspended in glacial acetic acid (270 mL). The resulting mixture was heated to 90 °C for 3 hrs. After the mixture was cooled

to ambient temperature the yellow precipitate was filtered off and washed several times with water to remove excess of $K_2Cr_2O_7$. The filter cake was freeze-dried and finally washed with Et_2O and dried in vacuo to afford the title compound as yellow powder (5.67 g, 17.3 mmol, 76%), which was used without further purification for the next step. 1H -NMR (300 MHz, Chloroform-*d*) δ 7.68 (s, 4H), 4.07 (s, 12H). ^{13}C -NMR (101 MHz, $CDCl_3$) δ 182.1(C_q), 153.6 (C_q), 128.6 (C_q), 108.5, 56.7.



Synthesis of 2,3,6,7-tetramethoxyanthracen-9(10H)-one (TMAH): Referring to a literature known procedure⁴ a 500 mL Schlenk flask equipped with stirring bar and condenser was charged with 2,3,6,7-tetramethoxy-9,10-anthraquinone (5.60 g, 17.1 mmol, 1 equiv) and zinc dust (3.40 g, 52.0 mmol, 3.1 equiv.). The flask was set under N_2 atmosphere and a mixture of aq. ammonia solution (135 mL, 25%), EtOH (135 mL) and water (135 mL) was added. The resulting mixture was refluxed for 5 hrs under N_2 atmosphere and vigorous stirring. The mixture was allowed to cool to ambient temperature and was poured in ice water (ca. 1 L). Conc. HCl (150 mL) was added to dissolve excess zinc and the mixture was stirred overnight. The turbid solution was filtered and the residue was washed several times with water and was freeze-dried to yield **TMAH** as pale-yellow powder (5.10 g, 16.2 mmol, 95%). 1H -NMR (400 MHz, Chloroform-*d*) δ 7.79 (s, 2H), 6.82 (s, 2H), 4.15 (s, 2H), 3.98 (d, $J = 7.3$ Hz, 12H). ^{13}C -NMR (101 MHz, $CDCl_3$) δ 182.4 (C_q), 153.1 (C_q), 148.6 (C_q), 135.1 (C_q), 125.4 (C_q), 109.7, 108.5, 56.2, 32.0 (CH_2). Data in accordance with the literature.³

2.2 - Spectroscopic and Photochemical Characteristics

The properties of the used photocatalyst (PC) were investigated in various spectroscopic experiments.

2.2.1 - UV-Vis absorption

The absorption of the photocatalyst was recorded in dry, degassed DMSO (50 μ M) by using a quartz cuvette (1 \times 1 cm) with septum screw cap. The cuvette was degassed *in vacuo* and backfilled with N_2 (5 \times) before the solvent and the catalyst solution were added *via* syringe. In presence of cesium carbonate, a distinct absorption band arises in the visible range of the spectrum (Figure S3). This process can also be followed by naked eye, as the solution turns from colorless into yellow.

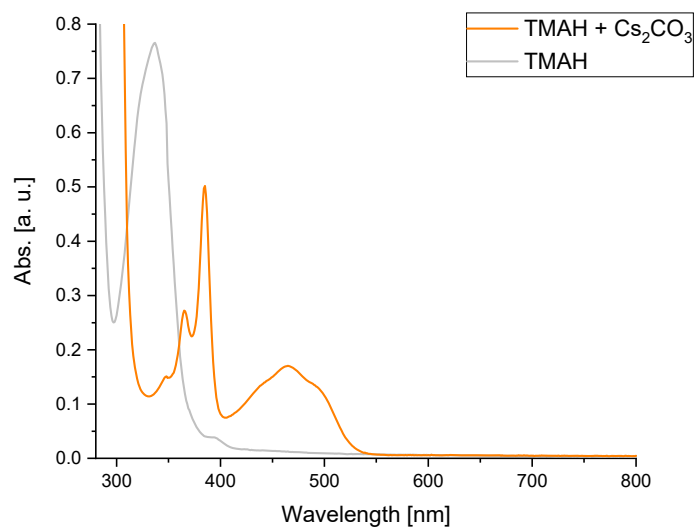


Figure S3. UV-vis spectra of (PC) in DMSO and in presence and absence of cesium carbonate.

2.2.2 - Emission spectra

The emission spectrum of the photocatalyst was recorded in dry, degassed DMSO in presence of cesium carbonate by using a quartz cuvette (1×1 cm) with septum screw cap. The cuvette was degassed *in vacuo* and backfilled with N₂ (5×) before the solvent and the catalyst solution were added *via* syringe. The excitation wavelength was set to 420 nm (entrance-/exit slit 1 nm) and the emission was measured starting from 450 nm to 800 nm (Increment 1 nm, entrance-/exit slit 2 nm). Relative intensities are plotted for absorption and emission (Figure S4a). To determine the intersection between normalized symmetrical absorption- and emission spectra, relative intensities for the lowest energy absorption band ($\lambda > 400$ nm) were calculated and plotted (Figure S4b).

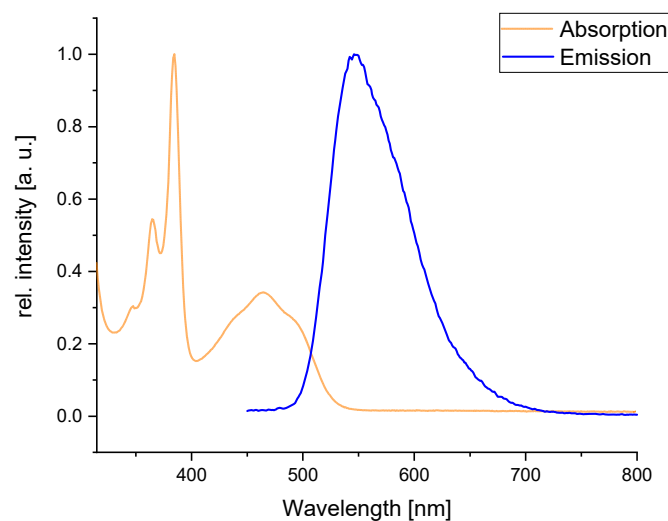


Figure S4a: Superimposed absorption and emission spectra of the photocatalyst in DMSO and in presence of cesium carbonate

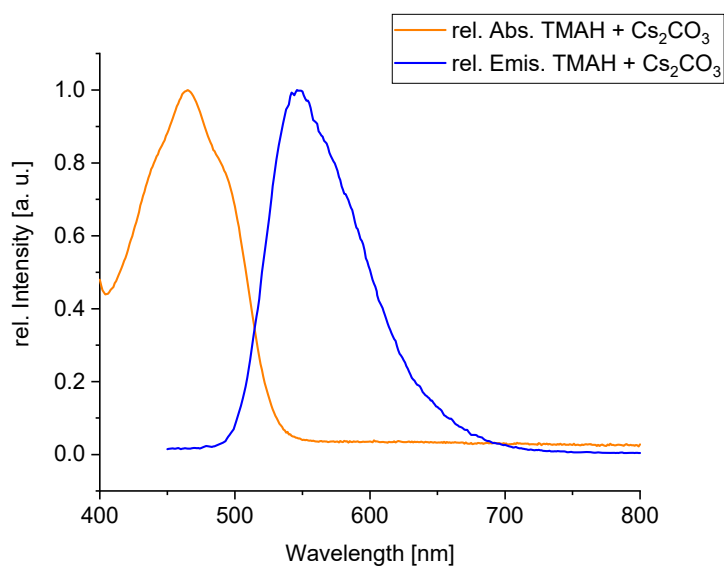


Figure S5b: Superimposed normalized absorption- and emission spectra of the photocatalyst in DMSO and in presence of cesium carbonate with an intersection at $\lambda_{\text{isec}} = 514$ nm.

2.2.3 - Excited state lifetime

The luminescence lifetime of the PC was recorded in dry, degassed DMSO in presence of cesium carbonate by using a quartz cuvette (1×1 cm) with septum screw cap. The cuvette was degassed *in vacuo* and backfilled with N₂ (5×) before the solvent and the catalyst solution were added *via* syringe. For excitation of the sample, a 452 nm laser diode was used and an optical longpass filter (cut-on wavelength

500 nm) was installed before the detection unit. The time range for the measurement was set to 400 ns. The experimental data were fitted with a mono-exponential function.

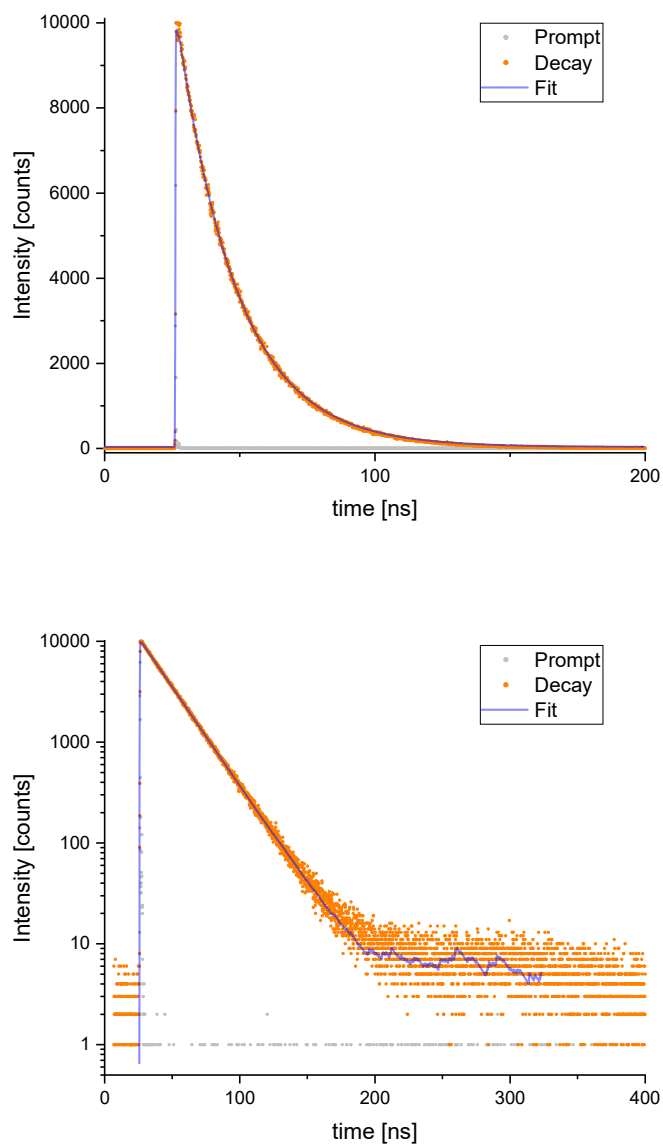


Figure S6. Luminescence decay of the excited photocatalyst with fit function in a linear plot (top) and logarithmic plot (bottom).

According to the parameters of the single-exponential fit function, a luminescence lifetime of 22.08 ns (CHISQ = 1.416859) was found.

2.2.4 - $^1\text{H-NMR}$ spectroscopy of TMAH

Proton NMR spectra of **TMAH** were recorded in absence and presence of Cs_2CO_3 (Figure S6a-b) in dried, degassed DMSO-d_6 . For the measurement in presence of base, a NMR tube with septum and screw-cap was used and the spectra was recorded under N_2 atmosphere. Integration over the NMR signals in presence of Cs_2CO_3 confirms the quantitative formation of the anionic species TMA^- .

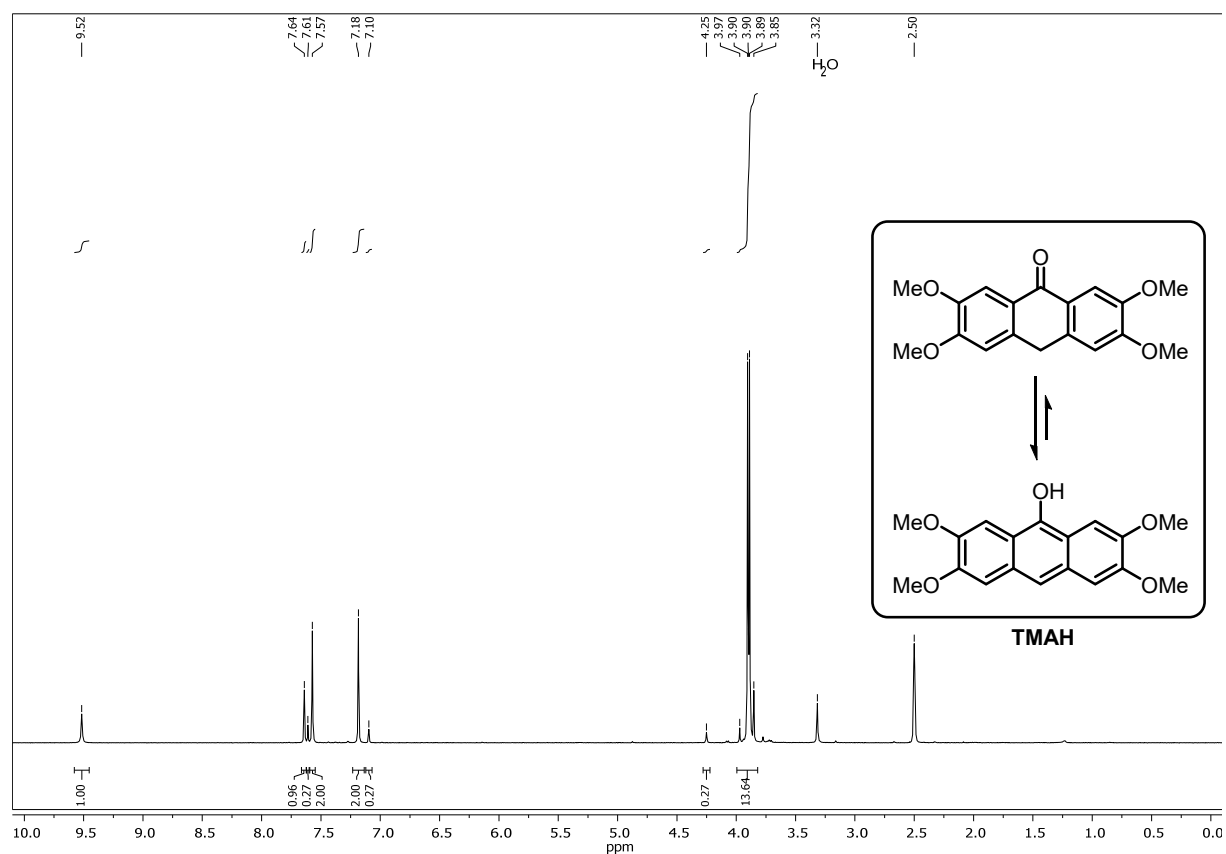


Figure S7a. $^1\text{H-NMR}$ of TMAH in DMSO-d_6 . The keto-enol tautomerism causes two sets of signals; The peak at 3.32 ppm is caused by residual water in the sample.

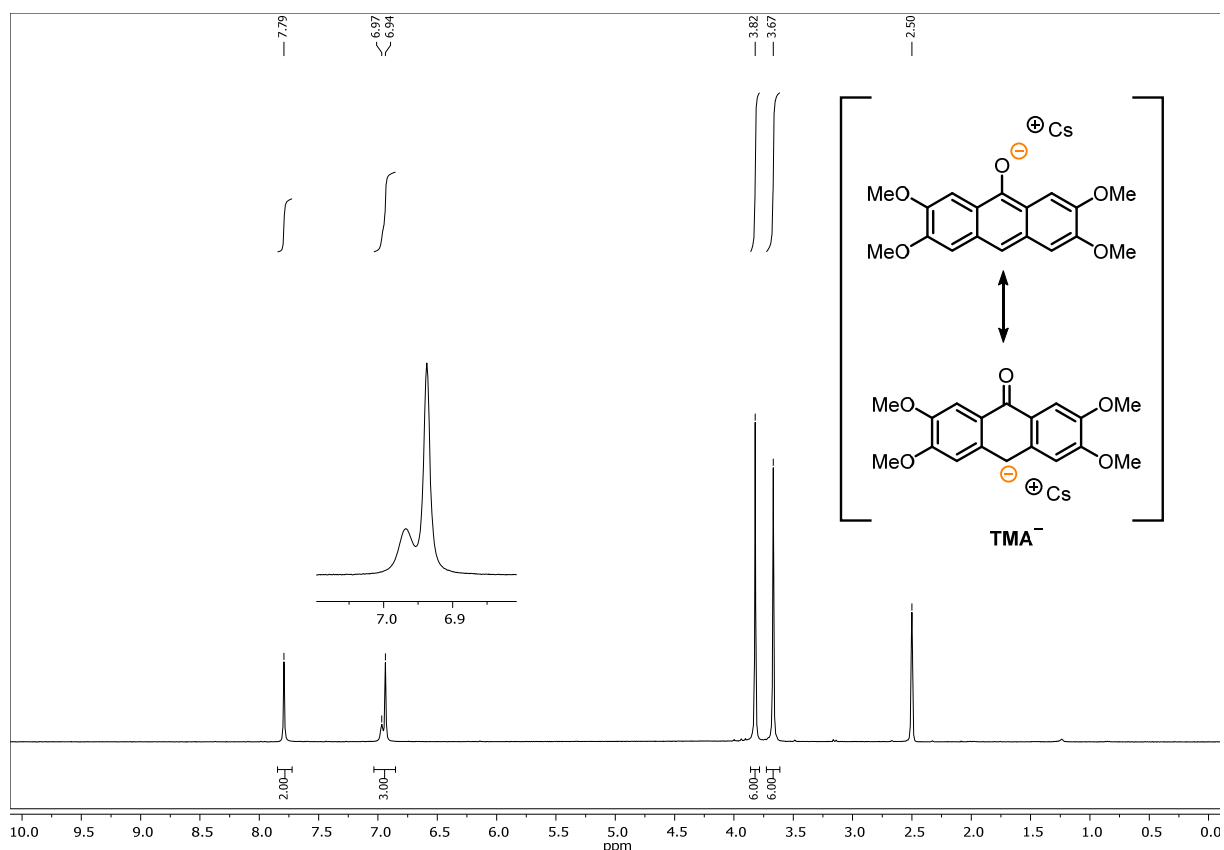


Figure S6b. $^1\text{H-NMR}$ of TMAH in presence of Cs_2CO_3 (6 eq.) in DMSO-d_6 .

2.2.5 - Ground state and excited state potential

The ground state potential of the photocatalyst was investigated by cyclic voltammetry. In presence of 1,1,3,3-tetramethylguanidine the anionic photocatalyst was oxidized (Figure S7) upon sweeping to positive potentials. Obtained potentials vs. Fc^+/Fc were converted to potentials against SCE.⁵ The estimated excited state oxidation potential ($E_{\text{ox}}^* = -2.92$ V vs. SCE) of the photocatalyst was determined according to the free enthalpy change of PET (neglecting the solvent-dependent electrostatic work term) as described in literature^{6,7} by taking the excited state energy ($E_{0,0} = 2.41$ eV, $\lambda_{\text{isec}} = 514$ nm) and the converted ground state potential ($E_{\text{p,ox}} = -0.51$ V vs. SCE) into account.

$$E_{\text{ox}}^* = E_{\text{p,ox}} - E_{0,0} + \omega$$

The obtained value for E_{ox}^* is based on following approximations: (a) As reported in literature,^{8,9} the single electron oxidation of an organic anion causes an irreversible peak in the cyclic voltammogram and an accurate value for the ground state oxidation potential is not accessible. Thus, for the anionic photocatalyst the peak potential $E_{\text{p,ox}}$ obtained for this irreversible process (Figure S7) was used to determine the excited state potential. (b) The excited state energy $E_{0,0}$ can be estimated in a number of ways. When using the wavelength at the luminescence maximum $\lambda_{\text{emis,max}}$ (546 nm) an underestimation of $E_{0,0}$ is likely.⁶ Furthermore, it is possible to use the midpoint between the absorption maximum of the

most red shifted absorption band and the emission maximum (506 nm). The most common way to determine $E_{0,0}$ is by taking the intersection between symmetric normalized absorption- and emission spectra (Figure S4b, $\lambda_{\text{isec}} = 514 \text{ nm}$) which was used for the calculation herein. (c) The solvent-dependent electrostatic work term ω contributes little to the free enthalpy change of PET when working in polar solvents like DMSO and hence was omitted in the calculation.

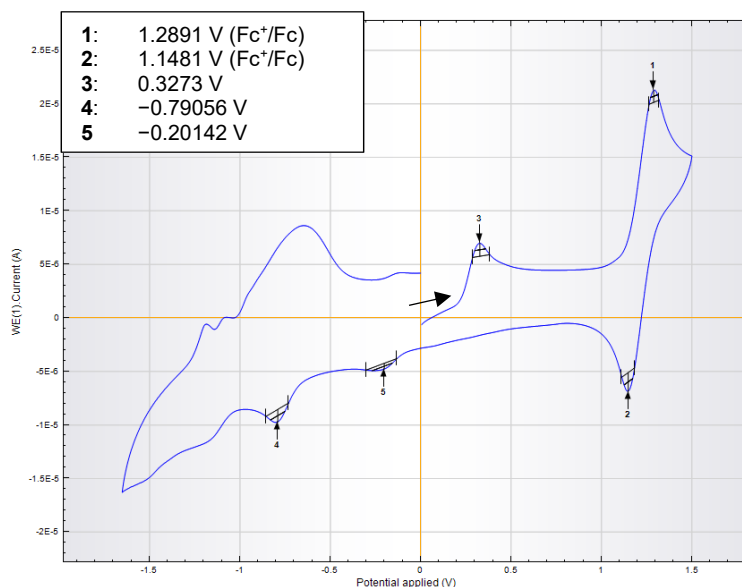
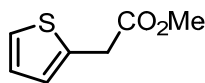


Figure S7. Cyclic voltammetry of the photocatalyst was recorded in anhydrous, degassed DMSO, in presence of 1,1,3,3-tetramethylguanidine as base and ferrocene (peaks 1, 2) as internal reference.

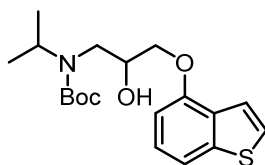
3 - Substrate Synthesis

Methyl 2-(thiophen-2-yl)acetate (3h)



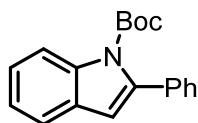
To a solution of 2-thiopheneacetic acid (123 mg, 0.2 mmol) in methanol (2 mL) was added conc. H₂SO₄ (2 drops) and the reaction was heated at reflux for 4 h. The solution was cooled, diluted with water (20 mL) and extracted with diethyl ether (3×20 mL). The combined organics were washed with brine (2×50 mL), dried via a phase separator and concentrated *in vacuo*. Purification by column chromatography on silica gel eluting with heptane:EtOAc (9:1) gave the title compound as a colorless oil (125 mg, 92%). ¹H-NMR (400 MHz, CDCl₃) δ 7.22 (dd, *J* = 4.9, 1.4 Hz, 1H), 6.98–6.95 (m, 2H), 3.85 (s, 2H), 3.73 (s, 3H); ¹³C-NMR (100 MHz, CDCl₃) δ 171.2, 135.3, 127.2, 127.1, 125.4, 52.6, 35.5. Data in accordance with the literature.¹⁰

tert-Butyl (3-(benzo[*b*]thiophen-4-yloxy)-2-hydroxypropyl)(isopropyl)carbamate (5e)



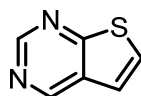
1-(Benzo[*b*]thiophen-4-yloxy)-3-(isopropylamino)propan-2-ol (239 mg, 0.9 mmol), triethylamine (0.377 mL, 2.70 mmol), and di-*tert*-butyl dicarbonate (0.236 g, 1.08 mmol) were added to a 50 mL round bottom flask. DCM (25 mL) was added and the mixture stirred at room temperature for 2 h. Water (25 mL) was subsequently added and the layers were separated. The organic layer was washed brine (2 x 25 mL) with then dried *via* a phase separator and concentrated *in vacuo*. Purification by column chromatography on silica gel eluting with heptane:EtOAc (9:1) gave the title compound as a yellow/orange oil (151 mg, 45%). *R*_f 0.56 [petrol–EtOAc (9:1)]; ¹H-NMR (400 MHz, DMSO) δ 7.66 (d, *J* = 5.4 Hz, 1H), 7.53 (dd, *J* = 10.5, 2.3 Hz, 2H), 7.30 (t, *J* = 8.0 Hz, 1H), 6.84 (d, *J* = 7.9 Hz, 1H), 5.76 (s, 1H), 5.17 (d, *J* = 5.2 Hz, 1H), 4.23 – 3.89 (m, 4H), 3.54 – 3.22 (m, 1H), 1.38 (s, 9H), 1.24 – 1.01 (m, 6H). ¹³C-NMR (125 MHz, DMSO) δ 156.4, 155.2, 141.5, 131.1, 130.0, 128.9, 123.2, 121.1, 109.1, 80.3, 71.5, 68.2, 49.0, 45.5, 28.3, 19.5.

tert-Butyl 2-phenyl-1*H*-indole-1-carboxylate (3v)



The compound was synthesized according to a literature known procedure.¹¹ In a flame dried 100 mL Schlenk flask under N₂ atmosphere equipped with stirring bar, (Boc)₂O (1.20 g, 5.50 mmol, 1.1 equiv.) was added to a solution of 2-phenylindole (0.966 g, 5.0 mmol, 1 equiv.) and 4-(*N,N*-dimethylamino)pyridine in dry MeCN (30 mL). The resulting mixture was stirred at room temperature for 24 h and was then concentrated *in vacuo*. After the addition of water, the mixture was extracted with EtOAc (3×). The combined organic layers were washed with brine, dried over Na₂SO₄, filtered and concentrated under reduced pressure. The crude material was purified by flash silica gel column chromatography using a mixture of hexanes/EtOAc to provide the title compound as white solid (1.40 g, 4.8 mmol, 96%). ¹H-NMR (400 MHz, Chloroform-*d*) δ 8.27 – 8.20 (m, 1H), 7.59 – 7.54 (m, 1H), 7.46 – 7.31 (m, 6H), 7.27 (td, *J* = 7.6, 0.9 Hz, 1H), 6.57 (s, 1H), 1.32 (s, 9H). ¹³C-NMR (101 MHz, CDCl₃) δ 150.3 (C_q), 140.6 (C_q), 137.6 (C_q), 135.1 (C_q), 129.3 (C_q), 128.9, 127.9, 127.7, 124.4, 123.0, 120.6, 115.3, 110.0, 83.5 (C_q), 27.7.

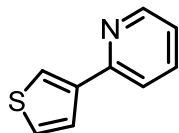
Thieno[2,3-*d*]pyrimidine (3y)



Based on a literature reported procedure for dehalogenation of aromatic compounds¹², a 5 mL crimp vial equipped with stirring bar was charged with 4-chlorothieno[2,3-*d*]pyrimidine (17.1 mg, 0.1 mmol, 1 equiv.) and 10-phenylphenothiazine (2.8 mg, 0.01 mmol, 10 mol%) and sealed with an aluminium crimp seal with septum. The vial was degassed and flushed with N₂ and tributylamine (119 μL, 0.5 mmol, 5 equiv.), formic acid (18.9 μL, 0.5 mmol, 5 equiv.) and dry MeCN (1 mL) were added. The reaction mixture was degassed by freeze-pump-thaw cycles (3×) and backfilled with N₂. The crimp vial was irradiated from the bottom side with 365 nm LED light for 22 hrs and a constant reaction temperature (25°C) was maintained by employing a water-cooling circuit connected to a thermostat. For isolation of the compound, 10 reactions were combined. The reactions were quenched by adding water and brine and the resulting mixture was extracted with EtOAc (3×). The combined organic layers were dried over Na₂SO₄, filtered and concentrated *in vacuo*. Purification was accomplished by flash silica gel chromatography using a mixture of hexanes/EtOAc as eluents and subsequent recrystallization from hexanes to afford the title compound as pale-yellow needles (31.8 mg, 0.23 mmol, 23%). ¹H-NMR (400

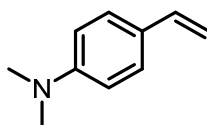
MHz, Chloroform-*d*) δ 9.16 (s, 1H), 9.10 (s, 1H), 7.57 (d, $J = 6.0$ Hz, 1H), 7.36 (d, $J = 6.0$ Hz, 1H). Data in accordance with the literature.¹³

2-(Thiophen-3-yl)pyridine (3z)



Following a literature known procedure¹⁴ a 10 mL crimp vial was charged with 3-thienylboronic acid (130 mg, 1.01 mmol, 1.2 equiv.), K_2CO_3 (326 mg, 2.36 mmol, 2.8 equiv.), $[Pd(PPh_3)_2Cl_2]$ (29.6 mg, 0.042 mmol, 0.05 equiv.), DME (2.5 mL) and water (1.17 mL). The vial was sealed with an aluminium crimp seal with septum and argon was bubbled through the solution for 10 minutes. Bromopyridine (81 μ L, 0.842 mmol, 1 equiv.) was added *via* syringe and the reaction was stirred in a pre-heated heating block for 18 hrs at 80 °C. The reaction was allowed to cool to ambient temperature, was quenched by adding water and was extracted with EtOAc (3 \times). The combined organic layers were washed with brine, dried over Na_2SO_4 , filtered and concentrated *in vacuo*. The crude product was purified by flash silica gel column chromatography using a mixture of hexanes/EtOAc and was obtained as colorless oil (127 mg, 0.79 mmol, 94%). ¹H-NMR (400 MHz, Chloroform-*d*) δ 8.62 (ddd, $J = 4.9, 1.8, 0.9$ Hz, 1H), 7.90 (dd, $J = 3.0, 1.3$ Hz, 1H), 7.70 (td, $J = 7.7, 1.8$ Hz, 1H), 7.66 (dd, $J = 5.0, 1.3$ Hz, 1H), 7.62 (dt, $J = 8.0, 1.1$ Hz, 1H), 7.40 (dd, $J = 5.0, 3.0$ Hz, 1H), 7.17 (ddd, $J = 7.4, 4.9, 1.2$ Hz, 1H). ¹³C-NMR (101 MHz, $CDCl_3$) δ 153.7 (C_q), 149.8, 142.3 (C_q), 136.8, 126.4, 126.3, 123.6, 121.9, 120.4.

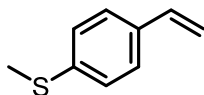
N,N-Dimethyl-4-vinylaniline (7g)



According to a literature known procedure¹⁵ a flame-dried 250 mL Schlenk flask was charged under N_2 atmosphere with methyltriphenylphosphonium bromide (14.4 g, 40.3 mmol, 1 equiv.) and dry THF (60 mL). The suspension was cooled to 0 °C and *n*-BuLi (1.6M in hexane, 25.2 mL, 40.3 mmol, 1 equiv.) was slowly added *via* syringe and the resulting mixture was stirred for 1 h. A solution of 4-(*N,N*-dimethylamino)benzaldehyde (6.02 g, 40.3 mmol, 1 equiv.) in dry THF (20 mL) was added dropwise and the reaction was further stirred at 0 °C for 1 h and at ambient temperature for 18 hrs. The reaction was quenched by adding sat. aq. NH_4Cl (30 mL) and the resulting mixture was extracted with DCM (3 \times 20 mL) and the combined organic layers were dried over Na_2SO_4 , filtered and concentrated *in vacuo*. Purification by vacuum distillation (0.8 mbar, 75 °C) afforded the title compound as yellowish oil

(4.70 g, 31.9 mmol, 79%). ¹H-NMR (300 MHz, Chloroform-*d*) δ 7.37 – 7.27 (m, 2H), 6.75 – 6.58 (m, 3H), 5.55 (dd, *J* = 17.6, 1.1 Hz, 1H), 5.03 (dd, *J* = 10.9, 1.1 Hz, 1H), 2.97 (s, 6H). ¹³C-NMR (75 MHz, CDCl₃) δ 150.4 (C_q), 136.7, 127.3, 126.3 (C_q), 112.5, 109.5 (CH₂), 40.7.

Methyl(4-vinylphenyl)sulfane (7h)

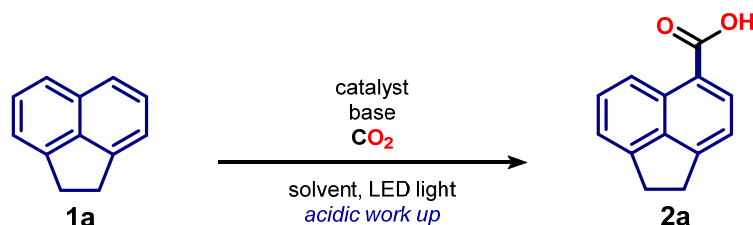


According to a literature known procedure¹⁵ a flame-dried 250 mL Schlenk flask was charged under N₂ atmosphere with methyltriphenylphosphonium bromide (14.1 g, 39.5 mmol, 1 equiv.) and dry THF (60 mL). The suspension was cooled to 0 °C and *n*-BuLi (1.6M in hexane, 30 mL, 48 mmol, 1.2 equiv.) was slowly added *via* syringe and the resulting mixture was stirred for 1 h. 4-(Methylthio)benzaldehyde (5.24 mL, 38.4 mmol, 1 equiv.) was added dropwise *via* syringe and the reaction mixture was stirred for further 2.5 h at 0 °C. After dilution with THF (20 mL) the reaction was stirred at ambient temperature overnight and was quenched by adding sat. aq. NH₄Cl (20 mL). The crude mixture was extracted with DCM (3×20 mL) and the combined organic layers were dried over Na₂SO₄, filtered and concentrated *in vacuo*. Purification by flash silica gel chromatography (hexanes/MTBE) afforded the title compound as colorless liquid (4.04 g, 26.9 mmol, 68%). ¹H-NMR (400 MHz, Chloroform-*d*) δ 7.37 – 7.32 (m, 2H), 7.25 – 7.20 (m, 2H), 6.69 (dd, *J* = 17.6, 10.9 Hz, 1H), 5.73 (dt, *J* = 17.6, 0.9 Hz, 1H), 5.23 (dt, *J* = 10.8, 0.9 Hz, 1H), 2.50 (s, 3H). ¹³C-NMR (101 MHz, CDCl₃) δ 138.1 (C_q), 136.3, 134.6 (C_q), 126.7, 126.7, 113.3 (CH₂), 15.9.

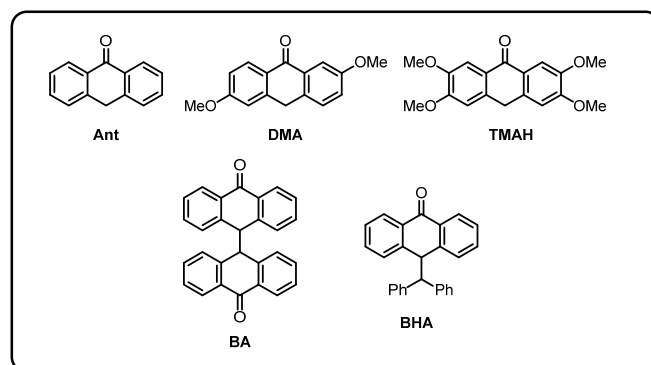
4 - Carboxylation Reactions

4.1 - Reaction Optimization

4.1.1 - General Procedure for the Reaction Optimization – GP1



To a dry flat-bottomed crimp vial (5 mL) equipped with stirring bar, was added acenaphthene (**1a**, 0.1-0.2 mmol, 1 equiv.) and photocatalyst (5-20 mol%, Scheme S2). Base (if solid) was quickly added and the vial was sealed with a Supelco aluminium crimp seal with septum (PTFE/butyl). The vial was then evacuated and refilled with CO₂ (5×) *via* syringe needle. The reaction mixture was dissolved in the solvent (dry and degassed by bubbling with N₂) and base (if liquid) was added *via* syringe. The vial was sealed with two layers of Parafilm® and then had gaseous CO₂ added *via* a Luer Lock Monoject™ (20 ccm) syringe, into the head space. The vial was then stirred and irradiated from the bottom side and a constant reaction temperature (0 °C or 25 °C) was maintained by employing a cooling circuit connected to a thermostat. After 18 hrs the reaction was transferred with aq. NaOH (0.1M) into a centrifuge tube and was washed with Et₂O (2×) to remove left over starting material or non-polar side products. The aqueous layer was acidified by adding aq. HCl (2M) and was extracted with EtOAc (3×). The combined organic layers were dried over Na₂SO₄, filtered and concentrated *in vacuo*. As internal standard a stock solution of 1,3,5-trimethoxybenzene in DMSO-d₆ (0.7 mL, 42.9 mM) was added and the mixture was analyzed by ¹H-NMR spectroscopy. The ¹H-NMR yield was determined by integration over product signals and internal standard signals.



Scheme S2. Tested 9-anthrone based derivatives for the optimization of the carboxylation reaction; 9-anthrone (**Ant**), 2,6-dimethoxyanthracen-9(10H)-one (**DMA**), 2,3,6,7-tetramethoxyanthracen-9(10H)-one (**TMAH**), bianthrone (**BA**), 10-benzhydryl-anthrone (**BHA**).

Table S1. Optimization of the photocatalyzed aromatic C-H carboxylation.

entry	PC (mol%)	base (eq.)	solvent	λ [nm]	V(CO ₂) added [ccm]	NMR yield [%]
1	Ant (20)	Cs ₂ CO ₃ (2)	DMSO	455	22	n.d. ^a
2	DMA (20)	Cs ₂ CO ₃ (2)	DMSO	455	22	n.d.
3	TMA (20)	Cs ₂ CO ₃ (2)	DMSO	455	22	37 ^b
4	BA (20)	Cs ₂ CO ₃ (2)	DMSO	455	22	trace
5	BHA (20)	Cs ₂ CO ₃ (2)	DMSO	455	22	n.d.
6	TMAH (20)	Cs ₂ CO ₃ (1)	DMSO	455	22	1
7	TMAH (20)	Cs ₂ CO ₃ (3)	DMSO	455	22	68 ^b
8	TMAH (20)	Cs ₂ CO ₃ (4)	DMSO	455	22	59
9	TMAH (5)	Cs ₂ CO ₃ (2)	DMSO	455	22	54
10	TMAH (10)	Cs ₂ CO ₃ (2)	DMSO	455	22	60
11	TMAH (10)	Cs ₂ CO ₃ (3)	DMSO	455	22	56
12 ^c	TMAH (20)	Cs ₂ CO ₃ (3)	DMSO	455	22	52
13	TMAH (20)	Na ₂ CO ₃ (2)	DMSO	455	22	1
14	TMAH (20)	K ₂ CO ₃ (2)	DMSO	455	22	17
15	TMAH (10)	K ₂ CO ₃ (3)	DMSO	455	22	25
16 ^c	TMAH (10)	K ₂ CO ₃ (3)	DMSO	455	22	47
17 ^c	TMAH (20)	K ₂ CO ₃ (3)	DMSO	455	22	38
18	TMAH (20)	(NH ₄) ₂ CO ₃ (3)	DMSO	455	22	2
19	TMAH (20)	Cs pivalate (3)	DMSO	455	22	6
20	TMAH (20)	K ₃ PO ₄ (3)	DMSO	455	22	trace
21	TMAH (20)	(NBu ₄)H ₂ PO ₄ (3)	DMSO	455	22	7
22	TMAH (20)	DBU (3)	DMSO	455	22	28
23	TMAH (20)	TMG (3)	DMSO	455	22	22
24	TMAH (20)	BTMG (3)	DMSO	455	22	25
25	TMAH (20)	Cs ₂ CO ₃ (3)	DMF	455	22	35
26	TMAH (20)	Cs ₂ CO ₃ (3)	DMA	455	22	12
27	TMAH (20)	Cs ₂ CO ₃ (3)	NMP	455	22	14
28	TMAH (20)	Cs ₂ CO ₃ (3)	ⁱ PrOH	455	22	n.d.
29	TMAH (20)	Cs ₂ CO ₃ (3)	DCM	455	22	n.d.
30	TMAH (20)	Cs ₂ CO ₃ (3)	acetone	455	22	trace
31	TMAH (20)	Cs ₂ CO ₃ (3)	DMSO	400	22	14
32	TMAH (20)	Cs ₂ CO ₃ (3)	DMSO	535	22	29
33	TMAH (20)	Cs ₂ CO ₃ (3)	DMSO	white ^d	22	27
34	TMAH (20)	Cs ₂ CO ₃ (3)	DMSO	455 ^e	22	23
35	TMAH (20)	Cs ₂ CO ₃ (3)	DMSO	455 ^f	22	56
36 ^g	TMAH (20)	Cs ₂ CO ₃ (3)	DMSO/DMF (1:1)	455	22	17
37	TMAH (20)	Cs ₂ CO ₃ (3)	DMSO	455	- ^h	37
38	TMAH (20)	Cs ₂ CO ₃ (3)	DMSO	455	11	48
39 ⁱ	TMAH (20)	Cs ₂ CO ₃ (3)	DMSO	455	22	39
40 ^j	TMAH (20)	Cs ₂ CO ₃ (3)	DMSO	455	22	51
41 ^k	TMAH (20)	Cs ₂ CO ₃ (3)	DMSO	455	22	13
42 ^l	TMAH (20)	Cs ₂ CO ₃ (3)	DMSO	455	22	34
43 ^m	TMAH (20)	Cs ₂ CO ₃ (3)	DMSO	455	22	49
44 ⁿ	TMAH (20)	Cs ₂ CO ₃ (3)	DMSO	455	22	57
45 ^o	TMAH (20)	Cs ₂ CO ₃ (3)	DMSO	455	22	52

All reactions, if not otherwise stated, were run following GP1: ^a product was not detected; ^b isolated yield following GP2a; ^c reaction was run with 18-crown-6 (1 equiv.); ^d cold white LED; ^e fan-cooled high-power LED setup (7 W) was used. Due to inefficient cooling, the reaction temperature was significantly elevated; ^f water-cooled high-power LED setup (1.4 W) was used. DMSO was saturated with CO₂ by bubbling gas through the solvent; ^g reaction was run at 0 °C; ^h reaction was run without pressure (1 atm) of CO₂; ⁱ reaction was run with 0.2 mmol of substrate; ^j concentration was changed to 0.05 M (0.1 mmol substrate in 2 mL DMSO); ^k reaction with chloro(pyridine)bis(dimethylglyoximate)cobalt(III) (5 mol%); ^l reaction with *p*-terphenyl (5 mol%); ^m reaction with *p*-quaterphenyl (5 mol%); ⁿ reaction with (^tPr)₃SiSH (10 mol%); ^o reaction with 1,4-cyclohexadiene (20 mol%).

4.1.2 - Kinetic profile of the aromatic carboxylation reaction

Under the optimized conditions the kinetic profile of the reaction was monitored within the first six hours of the reaction (Figure S8). Reactions were run following GP1.

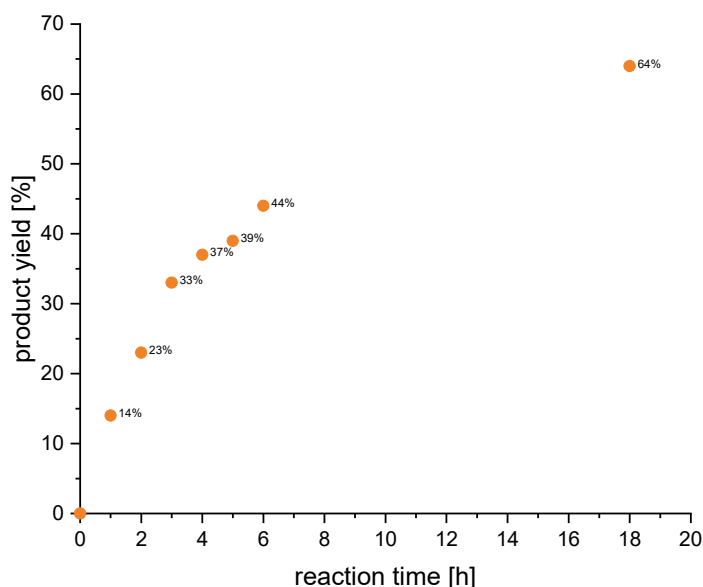


Figure S8. The progress of the carboxylation reaction was monitored within the first six hours.

4.1.3 - Control reactions

Conducted control experiments revealed that all compounds and light are crucial for product formation (Table S2). To exclude a base promoted carboxylation reaction, substrates **3c** & **3j** possessing acidic C-H bonds were tested in absence of catalyst and light and upon work-up, the respective products **4c** & **4j** could not be detected. Substrates **3b** and **3p** gave excellent yields of the respective carboxylation products following GP2a. No product was formed in absence of light and catalyst, demonstrating the photocatalytic nature of this reaction.

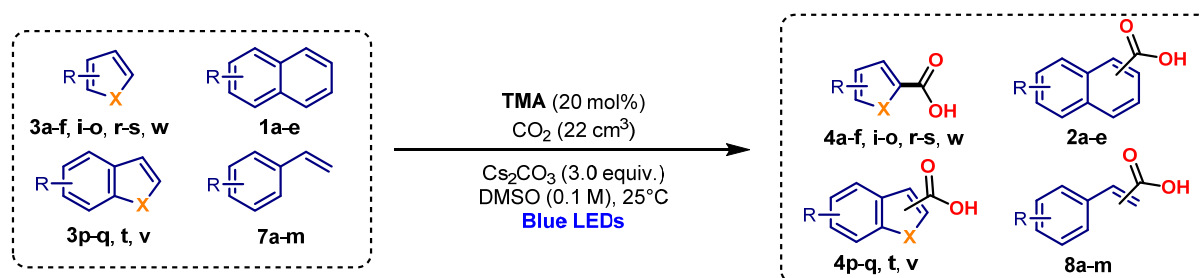
Table S2. Control reactions

entry	PC (mol%)	Substrate	base (eq.)	λ [nm]	V(CO ₂) added [ccm]	Product	NMR yield [%]
1	-	1a	Cs ₂ CO ₃ (3)	455	22	2a	n.d. ^a
2	TMAH (20)	1a	-	455	22	2a	n.d.
3	TMAH (20)	1a	Cs ₂ CO ₃ (3)	455	no CO ₂ ^b	2a	n.d.
4	TMAH (20)	1a	Cs ₂ CO ₃ (3)	dark ^c	22	2a	n.d.
5	-	3b ^d	Cs ₂ CO ₃ (3)	dark	22	4b	n.d.
6	-	3c ^e	Cs ₂ CO ₃ (3)	dark	22	4c	n.d.
7	-	3j ^f	Cs ₂ CO ₃ (3)	dark	22	4j	n.d.
8	-	3p ^g	Cs ₂ CO ₃ (3)	dark	22	4p	n.d.

All reactions, if not otherwise stated, were run following GP1: ^a product was not detected; ^b reaction was run under N₂ atmosphere; ^c reaction was stirred in the dark; ^d reaction was run following GP1 using **3b** (0.1 mmol) as substrate; ^e reaction was run following GP1 using **3c** (0.1 mmol) as substrate; ^f reaction was run following GP1 using **3j** (0.1 mmol) as substrate; ^g reaction was run following GP1 using **3p** (0.1 mmol) as substrate.

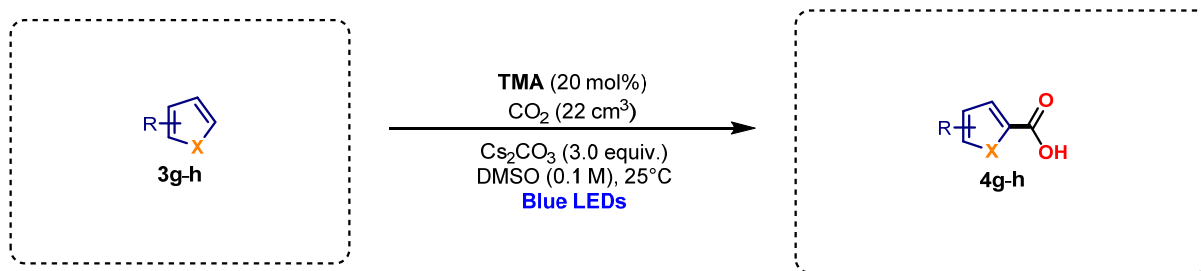
4.2 - Substrate Scope

General Procedure for Carboxylation of Hetero(arenes) and Styrenes– GP2a



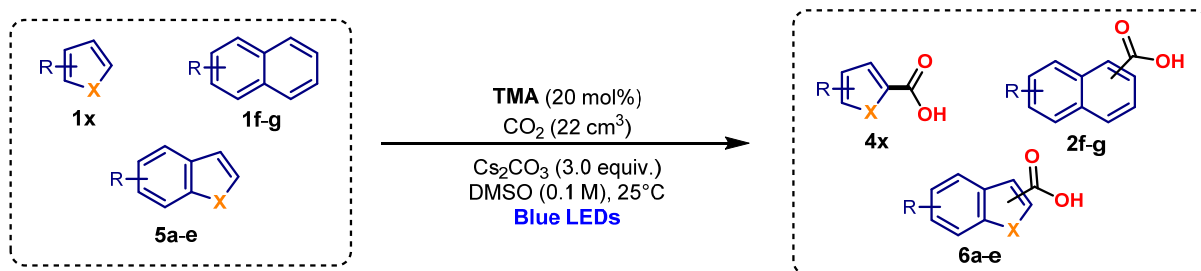
To a dry flat-bottomed crimp vial (5 mL) equipped with stirring bar, was added the arene (if solid) (0.1 mmol) and 2,3,6,7-tetramethoxyanthracen-9(10*H*)-one (6.3 mg, 0.02 mmol, 20 mol%). Cs₂CO₃ (98 mg, 3 equiv.) was quickly added and the vial was sealed with a Supelco aluminium crimp seal with septum (PTFE/butyl). The vial was then evacuated and refilled with CO₂ (5×) *via* syringe needle. The reaction mixture was dissolved in DMSO (1 mL, dry and degassed by bubbling with N₂) and the arene (0.1 mmol) (if liquid) was added *via* syringe. The vial was sealed with two layers of Parafilm® and then had gaseous CO₂ added *via* a Luer Lock Monoject™ (20 ccm) syringe, into the head space. The vial was then irradiated from the bottom side with blue LED light and a constant reaction temperature (25°C) was maintained by employing a water-cooling circuit connected to a thermostat. After 18 hrs of reaction time the pressure was released. For product isolation, the reaction mixtures of 4 reactions run in parallel were combined and transferred with water and Et₂O into a separating funnel. The ether layer was extracted with water (3×) and the combined aqueous layers were acidified with aq. HCl (2M) to adjust to an acidic pH. The aqueous layer was extracted with EtOAc (3×) and the combined EtOAc layers were dried over Na₂SO₄, filtered and concentrated *in vacuo*. The crude material was purified by silica flash column chromatography using mixtures of hexanes and ethyl acetate with 0.5% HOAc (v/v) as eluents.

General Procedure for Carboxylation of Arenes – GP2b (no glovebox)



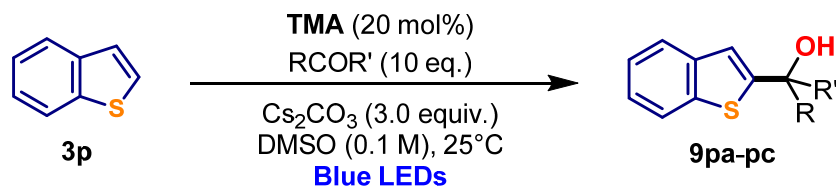
To a dry flat-bottomed crimp vial (5 mL) equipped with stirring bar, was added the arene (if solid) (0.1 mmol) and 2,3,6,7-tetramethoxyanthracen-9(10H)-one (6.3 mg, 0.02 mmol, 20 mol%). Cs₂CO₃ (98 mg, 3 equiv.) was quickly added and the vial was sealed with a Supelco aluminium crimp seal with septum (PTFE/butyl). The vial was then evacuated and refilled with N₂ (3×) *via* syringe needle. The reaction mixture was dissolved in DMSO (1 mL, dry and degassed by bubbling with N₂) and the arene (0.1 mmol) (if liquid) was added *via* syringe. The reaction mixture then had gaseous CO₂ (22 cm³) added *via* a gastight Hamilton® syringe, into the head space of the vial. The vial was then irradiated from the bottom side with blue light and a constant reaction temperature (25°C) was maintained by employing a water-cooling circuit connected to a thermostat. After the designated time the reactions were extracted *via* an acid base wash. The combined organic layers were dried over Na₂SO₄, filtered and concentrated *in vacuo*.

General Procedure for Carboxylation of Arenes – GP2c (glovebox)



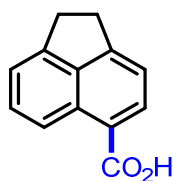
To a dry microwave vial (5 mL) equipped with stirring bar, was added the arene (if solid) (0.1 mmol) and 2,3,6,7-tetramethoxyanthracen-9(10H)-one (6.3 mg, 0.02 mmol, 20 mol%). The vials were sealed and transferred to a glovebox after the vial had evacuated and refilled with N₂ (×3) within the antechamber via syringe. Cs₂CO₃ (98 mg, 3 equiv.) and DMSO (1 mL) was added and the vial was sealed with a Supelco aluminium crimp seal with septum (PTFE/butyl). The vials were removed from the glovebox and the arene (0.1 mmol) (if liquid) was added via syringe. The reaction mixture then had gaseous CO₂ (22 cm³) added via a gastight Hamilton® syringe, into the head space of the vial. The vial was then irradiated from two sides by two kessil lamps (vials approximately 6 cm away from the light source) with fans placed in front of the vials for cooling (temperatures measured via IR ranged between 25-30 °C). After 18 hrs. the irradiation was stopped and the vials were decapped quenched with aq. HCl (1 mL, 0.3M) and monitored by LCMS and ¹H NMR. Reactions were filtered of any solids and purified directly *via* prep-HPLC.

General Procedure for the substitution reaction of benzo[*b*]thiophene with ketones– GP3



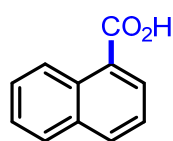
To a dry flat-bottomed crimp vial (5 mL) equipped with stirring bar, was added the benzo[*b*]thiophene (13.4 mg, 0.1 mmol, 1 equiv.) and 2,3,6,7-tetramethoxyanthracen-9(10*H*)-one (6.3 mg, 0.02 mmol, 20 mol%). Cs₂CO₃ (98 mg, 0.3 mmol, 3 equiv.) was quickly added and the vial was sealed with a Supelco aluminium crimp seal with septum (PTFE/butyl). The vial was then evacuated and refilled with N₂ (5×) *via* syringe needle. The reaction mixture was dissolved in DMSO (1mL, dry and degassed by bubbling with N₂) and the ketone (1.0 mmol, 10 equiv.) was added *via* syringe. The vial was then irradiated from the bottom side with blue LED light and a constant reaction temperature (25°C) was maintained by employing a water-cooling circuit connected to a thermostat. After 18 hrs the reaction was quenched by adding water. For product isolation, the reaction mixtures of 4 reactions run in parallel were combined and transferred with water and EtOAc into a separating funnel. The reaction mixture was extracted with EtOAc (3×) and the combined organic layers were dried over Na₂SO₄, filtered and concentrated *in vacuo*. The crude material was purified by silica flash column chromatography using mixtures of hexanes and ethyl acetate as eluents.

1,2-Dihydroacenaphthylene-5-carboxylic acid (2a)



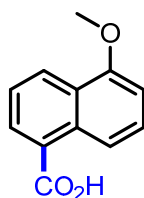
Following GP2a, acenaphthene (0.4 mmol) gave **2a** (68%) as a pale orange solid; **¹H-NMR** (400 MHz, Chloroform-*d*) δ 8.74 (d, $J = 8.5$ Hz, 1H), 8.45 (d, $J = 7.3$ Hz, 1H), 7.63 (dd, $J = 8.6, 6.9$ Hz, 1H), 7.37 (dd, $J = 12.2, 7.1$ Hz, 2H), 3.45 (s, 4H). **¹H-NMR** (400 MHz, DMSO-*d*₆) δ 12.85 (bs, 1H), 8.60 (d, $J = 8.5$ Hz, 1H), 8.22 (d, $J = 7.3$ Hz, 1H), 7.57 (dd, $J = 8.6, 6.9$ Hz, 1H), 7.36 (t, $J = 6.6$ Hz, 2H), 3.35 (s, 4H). **¹³C-NMR** (101 MHz, DMSO) δ 168.3 (*C*_q), 152.5 (*C*_q), 146.2 (*C*_q), 139.1 (*C*_q), 132.9, 129.8 (*C*_q), 129.6, 122.3 (*C*_q), 121.6, 119.9, 118.6, 29.9. **HRMS** (EI⁺): calculated m/z for C₁₃H₁₀O₂ [M⁺] 198.06753; found 198.06722. Data in accordance with the literature.¹⁶

1-Naphthoic acid (2b)



Following GP2a, naphthalene (0.3 mmol) gave **2b** (38%) as a white solid; **¹H-NMR** (400 MHz, DMSO-*d*₆) δ 13.13 (bs, 1H), 8.86 (d, $J = 8.5$ Hz, 1H), 8.20 – 8.10 (m, 2H), 8.02 (d, $J = 7.7$ Hz, 1H), 7.70 – 7.52 (m, 3H). **¹³C-NMR** (101 MHz, DMSO) δ 168.6 (*C*_q), 133.5 (*C*_q), 132.9, 130.7 (*C*_q), 129.8, 128.6, 127.7 (*C*_q), 127.5, 126.2, 125.5, 124.9. **HRMS** (EI⁺): calculated m/z for C₁₁H₈O₂ [M⁺] 172.05188; found 172.05143. Data in accordance with the literature.¹⁷

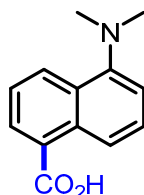
5-Methoxy-1-naphthoic acid (2c)



Following GP2a, 1-methoxynaphthalene (0.4 mmol) gave **2c** (22%) as a pale yellow solid; **¹H-NMR** (400 MHz, DMSO-*d*₆) δ 12.95 (bs, 1H), 8.45 – 8.35 (m, 2H), 8.13 (dd, $J = 7.2, 1.3$ Hz, 1H), 7.60 – 7.51 (m, 2H), 7.05 (d, $J = 7.8$ Hz, 1H), 3.99 (s, 3H). **¹³C-NMR** (101 MHz, DMSO) δ 168.8 (*C*_q), 154.9 (*C*_q),

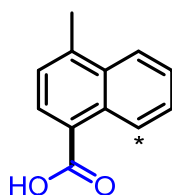
131.6 (C_q), 130.0, 127.8, 127.7 (C_q), 126.1, 125.3 (C_q), 124.2, 117.5, 104.7, 55.7. **HRMS** (EI⁺): calculated *m/z* for C₁₂H₁₀O₃ [M⁺] 202.06245; found 202.06283. Data in accordance with the literature.¹⁸

5-(Dimethylamino)-1-naphthoic acid (**2d**)



Following GP2a, 1-dimethylaminonaphthalen (0.4 mmol) gave **2d** (38%) as a yellow solid; **¹H-NMR** (400 MHz, DMSO-*d*₆) δ 13.04 (bs, 1H), 8.43 (dd, *J* = 15.9, 8.6 Hz, 2H), 8.08 (dd, *J* = 7.1, 1.0 Hz, 1H), 7.54 (ddd, *J* = 18.0, 8.6, 7.3 Hz, 2H), 7.19 (d, *J* = 7.3 Hz, 1H), 2.82 (s, 6H). **¹³C-NMR** (101 MHz, DMSO) δ 168.9 (C_q), 151.0 (C_q), 132.0 (C_q), 129.3, 128.6 (C_q), 128.5 (C_q), 128.4, 127.4, 124.0, 120.0, 114.4, 45.0. **HRMS** (ESI⁺): calculated *m/z* for C₁₃H₁₄NO₂ [(M+H)⁺] 216.1019; found 216.1022.

4-Methyl-1-naphthoic acid (**2e**) & 5-Methyl-1-naphthoic acid (**2e'**)



Following GP2a, 1-methylnaphthalene (0.1 mmol) gave **2e** (19%) and **2e'** (14%) as a beige solid. **2e:2e'** = 1.3:1. The ratio of products was determined by ¹H-NMR analysis. **HRMS** (EI⁺): calculated *m/z* for C₁₂H₁₀O₂ [M⁺] 186.06753; found 186.06731.

Data for **2e**: **¹H-NMR** (300 MHz, Chloroform-*d*) δ 9.22 – 9.13 (m, 1H), 8.34 (d, *J* = 7.5 Hz, 1H), 8.13 – 8.05 (m, 1H), 7.73 – 7.50 (m, 2H), 7.41 (d, *J* = 7.5 Hz, 1H), 2.78 (s, 3H). **¹H-NMR** (400 MHz, DMSO-*d*₆) δ 13.06 (bs, 1H), 9.00 – 8.88 (m, 1H), 8.11 (m, 1H), 8.06 (d, *J* = 7.4 Hz, 1H), 7.68 – 7.58 (m, 2H), 7.44 (d, *J* = 7.0 Hz, 1H), 2.70 (s, 3H). **¹³C-NMR** (101 MHz, DMSO) δ 168.7, 139.7, 132.4, 130.9, 129.8, 127.2, 126.1, 126.0, 125.9, 125.7, 124.7, 19.6. Data in accordance with literature.^{19,20}

Data for **2e'**: **¹H-NMR** (300 MHz, CD₃OD) δ 8.95 (d, *J* = 8.8 Hz, 1H), 8.40 (dd, *J* = 7.3, 1.3 Hz, 1H), 8.30 (dt, *J* = 8.5, 1.1 Hz, 1H), 7.71 – 7.51 (m, 2H), 7.41 (d, *J* = 7.5 Hz, 1H), 2.75 (s, 3H). **¹H-NMR** (400 MHz, DMSO-*d*₆) δ 13.06 (bs, 1H), 8.67 (d, *J* = 8.6 Hz, 1H), 8.25 (d, *J* = 8.5 Hz, 1H), 8.14 – 8.08 (m, 1H), 7.68 – 7.58 (m, 1H), 7.54 – 7.48 (m, 1H), 7.39 – 7.47 (m, 1H), 2.68 (s, 3H). **¹³C-NMR** (101 MHz,

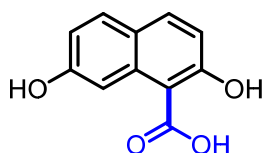
DMSO) δ 169.0, 134.5, 132.5, 130.8, 129.1, 128.7, 128.6, 127.1, 126.9, 124.8, 123.7, 19.5. Data in accordance with the literature.²¹

1-Hydroxy-4-naphthoic acid (2f) & 1-hydroxy-2-naphthoic acid (2f')



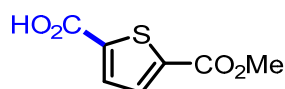
Following GP2c, 1-naphthol (0.1 mmol) gave **2f** & **2f'** (56%) as an inseparable mixture (1:1), as a waxy solid. ¹H-NMR (500 MHz, DMSO) δ 12.58 (s, 2H), 11.02 (s, 2H), 9.03 (d, J = 8.7 Hz, 1H), 8.23 (d, J = 7.7 Hz, 1H), 8.13 (d, J = 8.1 Hz, 1H), 7.87 (dd, J = 8.3, 1.0 Hz, 1H), 7.61 (ddd, J = 8.5, 6.8, 1.4 Hz, 1H), 7.50 (ddd, J = 8.2, 6.8, 1.2 Hz, 1H), 7.48 – 7.42 (m, 1H), 7.41 – 7.32 (m, 3H), 6.91 (d, J = 8.2 Hz, 1H), 6.87 (dd, J = 7.2, 1.3 Hz, 1H). ¹³C-NMR (126 MHz, DMSO) δ 171.88, 168.30, 157.80, 134.78, 133.04, 132.85, 128.74, 127.86, 126.98, 125.54, 125.08, 124.75, 124.56, 123.59, 122.43, 118.63, 116.69, 109.60, 106.95, 104.40. Data in accordance with the literature.^{18,22}

2,7-dihydroxy-1-naphthoic acid (2g)



Following GP2c, naphthalene-2,7-diol (0.1 mmol) gave **2g** (64%) as a yellow solid. ¹H-NMR (500 MHz, DMSO-d₆) δ 12.43 (bs, 1H), 9.82 (s, 2H), 7.95 (s, 1H), 7.84 (d, J = 8.8 Hz, 1H), 7.68 (d, J = 8.8 Hz, 1H), 6.95-6.77 (m, 2H); ¹³C-NMR (126 MHz, DMSO-d₆) δ 173.0, 161.8, 157.5, 135.1, 133.6, 130.5, 122.5, 115.1, 115.1 107.5, 105.8; HRMS (ESI⁺): calculated m/z for C₁₁H₉O₄ [(M+H)⁺] 205.0495; found 205.0497.

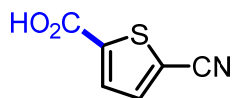
5-(methoxycarbonyl)thiophene-2-carboxylic acid (4a)



Following GP2a, methyl thiophene-2-carboxylate (0.4 mmol) gave **4a** (49%) as a white solid; ¹H-NMR (400 MHz, DMSO-d₆) δ 13.65 (bs, 1H), 7.78 (d, J = 3.9 Hz, 1H), 7.72 (d, J = 3.9 Hz, 1H), 3.85 (s, 3H).

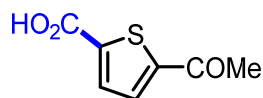
¹³C-NMR (101 MHz, DMSO) δ 162.3 (C_q), 161.4 (C_q), 140.4 (C_q), 137.5 (C_q), 133.7, 133.2, 52.7. **HRMS** (EI⁺): calculated m/z for C₇H₆O₄S [M⁺] 185.99813; found 185.99833. Data in accordance with the literature.²³

5-Cyanothiophene-2-carboxylic acid (**4b**)



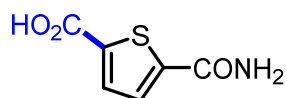
Following GP2a, thiophene-2-carbonitrile (0.4 mmol) gave **4b** (92%) as a pale yellow solid; **¹H-NMR** (400 MHz, DMSO-*d*₆) δ 13.98 (bs, 1H), 8.00 (d, $J = 4.0$ Hz, 1H), 7.79 (d, $J = 4.0$ Hz, 1H). **¹³C-NMR** (101 MHz, DMSO) δ 161.5 (C_q), 141.7 (C_q), 139.5 (C_q), 132.9 (C_q), 113.6, 113.3. **HRMS** (EI⁺): calculated m/z for C₆H₃NO₂S [M⁺] 152.98790; found 152.98804. Data in accordance with the literature.²⁴

5-Acetylthiophene-2-carboxylic acid (**4c**)



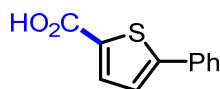
Following GP2a, 2-acetylthiophene (0.4 mmol) gave **4c** (39%) as a pale yellow solid; **¹H-NMR** (300 MHz, DMSO-*d*₆) δ 13.55 (bs, 1H), 7.92 (d, $J = 4.0$ Hz, 1H), 7.76 (d, $J = 3.9$ Hz, 1H), 2.58 (s, 3H). **¹³C-NMR** (75 MHz, DMSO) δ 191.5 (C_q), 162.5 (C_q), 148.2 (C_q), 141.0 (C_q), 133.7, 133.6, 26.8. **HRMS** (EI⁺): calculated m/z for C₇H₆O₃S [M⁺] 170.00322; found 170.00333. Data in accordance with literature.²⁴

5-Carbamoylthiophene-2-carboxylic acid (**4d**)



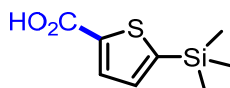
The title compound was prepared according to GP2a. Isolation of the compound was accomplished by employing C18 reversed-phase silica gel column chromatography using a mixture of water and acetonitrile as eluents. Thiophene-2-carboxamide (0.4 mmol) gave **4d** (91%) as a white solid; **¹H-NMR** (400 MHz, DMSO-*d*₆) δ 13.40 (bs, 1H), 8.17 (bs, 1H), 7.73 (d, $J = 3.9$ Hz, 1H), 7.69 (d, $J = 3.9$ Hz, 1H), 7.64 (bs, 1H). **¹³C-NMR** (101 MHz, DMSO) δ 162.7 (C_q), 162.2 (C_q), 145.7 (C_q), 137.9 (C_q), 133.3, 128.9. **HRMS** (ESI⁺): calculated m/z for C₆H₆O₃S [(M+H)⁺] 172.0063; found 172.0065.

5-Phenylthiophene-2-carboxylic acid (4e)



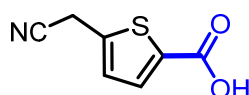
Following GP2a, 3-phenylthiophene (0.4 mmol) gave **4e** (99%) as a white solid; **¹H-NMR** (300 MHz, DMSO-*d*₆) δ 13.18 (bs, 1H), 7.77 – 7.68 (m, 3H), 7.55 (d, *J* = 4.0 Hz, 1H), 7.49 – 7.33 (m, 3H). **¹³C-NMR** (75 MHz, DMSO) δ 162.9 (*C_q*), 149.8 (*C_q*), 134.4, 133.4 (*C_q*), 132.9 (*C_q*), 129.3, 128.9, 125.9, 124.6. **HRMS** (ESI⁺): calculated *m/z* for C₁₁H₉O₂S [(M+H)⁺] 205.0318; found 205.0321. Data in accordance with the literature.²⁵

5-(Trimethylsilyl)thiophene-2-carboxylic acid (4f)



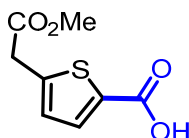
Following GP2a, trimethyl(thiophen-2-yl)silane (0.4 mmol) gave **4f** (28%) as a white solid; **¹H-NMR** (400 MHz, DMSO-*d*₆) δ 13.02 (bs, 1H), 7.75 (d, *J* = 3.5 Hz, 1H), 7.34 (d, *J* = 3.5 Hz, 1H), 0.31 (s, 9H). **¹³C-NMR** (101 MHz, DMSO) δ 162.6 (*C_q*), 148.1 (*C_q*), 139.5 (*C_q*), 135.0, 133.9, -0.4. **HRMS** (EI⁺): calculated *m/z* for C₈H₁₂O₂SiS [M⁺] 200.03218; found 200.03162.

5-(cyanomethyl)thiophene-2-carboxylic acid (4g)



Following GP2b, 2-(thiophen-2-yl)acetonitrile (0.1 mmol) gave **4g** (89%) as a white solid. **¹H-NMR** (500 MHz, CDCl₃) δ 7.78 (d, *J* = 3.8 Hz, 1H), 7.13 (d, *J* = 3.8 Hz, 1H), 3.96 (s, 2H); **¹³C-NMR** (126 MHz, CDCl₃) δ 165.6 (*C_q*), 139.8 (*C_q*), 135.3, 133.2 (*C_q*), 128.3, 115.9 (*C_q*), 19.3 (CH₂); **HRMS** (ESI): calculated *m/z* for C₇H₄NO₂S [(M-H)⁺] 165.9968; found 165.9967.

5-(2-methoxy-2-oxoethyl)thiophene-2-carboxylic acid (4h)



Following GP2b, methyl 2-(thiophen-2-yl)acetate (0.1 mmol) gave **4h** (99%) as a waxy solid. ¹H-NMR (500 MHz, CDCl₃) δ 7.76 (d, *J* = 3.8 Hz, 1H), 6.99 (d, *J* = 3.8 Hz, 1H), 3.8 (s, 2H), 3.76 (s, 3H); ¹³C-NMR (126 MHz, CDCl₃) δ 170.0, 167.4, 144.5, 135.2, 132.2, 128.2, 52.7, 35.9; HRMS (ESI): calculated *m/z* for C₈H₇O₄S [(M-H)⁺] 199.0065; found 199.0065.

3-Cyanothiophene-2-carboxylic acid (**4i**)



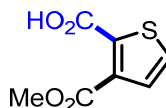
Following GP2a, thiophene-3-carbonitrile (0.4 mmol) gave **4i** (86%) as a pale yellow solid; ¹H-NMR (300 MHz, DMSO-*d*₆) δ 14.12 (bs, 1H), 8.06 (d, *J* = 5.2 Hz, 1H), 7.62 (d, *J* = 5.1 Hz, 1H). ¹³C-NMR (75 MHz, DMSO) δ 160.7 (*C_q*), 141.9 (*C_q*), 133.9, 131.6, 114.1 (*C_q*), 113.0 (*C_q*). HRMS (ESI⁺): calculated *m/z* for C₆H₄NO₂S [(M+H)⁺] 153.9957; found 153.9957. Data in accordance with the literature.²⁶

3-Acetylthiophene-2-carboxylic acid (**4j**)



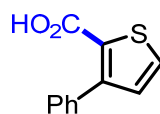
Following GP2a, 3-acetylthiophene (0.4 mmol) gave **4j** (41%) as a pale yellow solid; ¹H-NMR (300 MHz, Acetonitrile-*d*₃) δ 7.78 (d, *J* = 5.4 Hz, 1H), 7.71 (d, *J* = 5.4 Hz, 1H), 2.73 (s, 3H). ¹H-NMR (400 MHz, DMSO-*d*₆) δ 13.59 (bs, 1H), 7.85 (d, *J* = 5.0 Hz, 1H), 7.24 (d, *J* = 5.0 Hz, 1H), 2.50 (s, 3H). ¹³C-NMR (101 MHz, DMSO) δ 199.3 (*C_q*), 162.3 (*C_q*), 146.9 (*C_q*), 132.2 (*C_q*), 132.1, 128.1, 30.9. HRMS (EI⁺): calculated *m/z* for C₇H₆O₃S [M⁺] 170.00322; found 170.00304.

3-(Methoxycarbonyl)thiophene-2-carboxylic acid (**4k**)



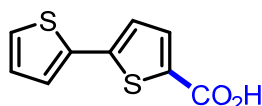
Following GP2a, methyl thiophene-2-carboxylate (0.4 mmol) gave **4k** (88%) as a white solid; ¹H-NMR (400 MHz, DMSO-*d*₆) δ 13.53 (bs, 1H), 7.86 (d, *J* = 5.1 Hz, 1H), 7.31 (d, *J* = 5.1 Hz, 1H), 3.80 (s, 3H). ¹³C-NMR (101 MHz, DMSO) δ 164.8 (*C_q*), 161.9 (*C_q*), 136.8 (*C_q*), 134.5 (*C_q*), 131.8, 128.3, 52.5. HRMS (ESI⁺): calculated *m/z* for C₇H₇O₄S [(M+H)⁺] 187.0060; found 187.0059.

3-Phenylthiophene-2-carboxylic acid (**4l**)



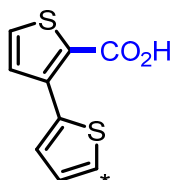
Following GP2a, 3-phenylthiophene (0.4 mmol) gave **4l** (71%) as a pale yellow solid; **¹H-NMR** (400 MHz, DMSO-*d*₆) δ 12.86 (bs, 1H), 7.85 (d, *J* = 5.0 Hz, 1H), 7.49 – 7.42 (m, 2H), 7.42 – 7.32 (m, 3H), 7.17 (d, *J* = 5.1 Hz, 1H). **¹³C-NMR** (101 MHz, DMSO) δ 162.8 (*C*_q), 147.1 (*C*_q), 135.5 (*C*_q), 131.7, 131.0, 129.3, 128.1 (*C*_q), 127.7, 127.6. **HRMS** (ESI+): calculated *m/z* for C₁₁H₉O₂S [(M+H)⁺] 205.0318; found 205.0319. Data in accordance with the literature.²⁷

[2,2'-Bithiophene]-5-carboxylic acid (**4m**)



Following GP2a, 2,2'-bithiophene (0.4 mmol) gave **4m** (53%) as a pale yellow solid; **¹H-NMR** (400 MHz, DMSO-*d*₆) δ 13.15 (bs, 1H), 7.66 (d, *J* = 3.9 Hz, 1H), 7.62 (dd, *J* = 5.1, 1.1 Hz, 1H), 7.48 (dd, *J* = 3.7, 1.1 Hz, 1H), 7.34 (d, *J* = 3.9 Hz, 1H), 7.13 (dd, *J* = 5.1, 3.6 Hz, 1H). **¹³C-NMR** (101 MHz, DMSO) δ 162.6 (*C*_q), 142.9 (*C*_q), 135.4 (*C*_q), 134.2, 132.5 (*C*_q), 128.6, 127.2, 125.9, 124.5. **HRMS** (ESI+): calculated *m/z* for C₉H₇O₂S₂ [(M+H)⁺] 210.9882; found 210.9884. Data in accordance with the literature.²⁸

[2,3'-Bithiophene]-2'-carboxylic acid (**4n**) & [2,3'-bithiophene]-5-carboxylic acid (**4n'**)



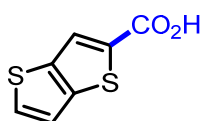
Following GP2a, 2,3'-bithiophene (0.4 mmol) gave **4n** (64%) as a white solid and **4n'** (23%) as a pale yellow solid. **4n:4n'** = 2.8:1.

Data for **4n**: **¹H-NMR** (400 MHz, Chloroform-*d*) δ 7.60 (dd, *J* = 3.7, 1.2 Hz, 1H), 7.56 (d, *J* = 5.2 Hz, 1H), 7.40 (dd, *J* = 5.1, 1.2 Hz, 1H), 7.27 (d, *J* = 5.2 Hz, 1H), 7.10 (dd, *J* = 5.1, 3.7 Hz, 1H). **¹H-NMR** (400 MHz, DMSO-*d*₆) δ 13.07 (bs, 1H), 7.84 (d, *J* = 5.2 Hz, 1H), 7.65 – 7.59 (m, 2H), 7.36 (d, *J* = 5.2

Hz, 1H), 7.11 (dd, $J = 5.1, 3.7$ Hz, 1H). $^{13}\text{C-NMR}$ (101 MHz, DMSO) δ 162.8 (C_q), 138.7 (C_q), 135.9 (C_q), 131.3, 131.2, 129.0, 127.3, 127.2, 126.7 (C_q). **HRMS** (ESI+): calculated m/z for $\text{C}_9\text{H}_7\text{O}_2\text{S}_2$ [(M+H) $^+$] 210.9882; found 210.9883. Data in accordance with the literature.²⁹

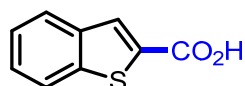
Data for **4n'**: $^1\text{H-NMR}$ (400 MHz, DMSO- d_6) δ 7.93 (dd, $J = 2.9, 1.4$ Hz, 1H), 7.69 – 7.64 (m, 2H), 7.49 (dd, $J = 5.0, 1.4$ Hz, 1H), 7.44 (d, $J = 3.8$ Hz, 1H). $^{13}\text{C-NMR}$ (101 MHz, DMSO) δ 162.9 (C_q), 144.7 (C_q), 134.3 (C_q), 134.0, 132.6 (C_q), 128.0, 126.0, 124.5, 122.4. Data in accordance with the literature.³⁰

Thieno[3,2-*b*]thiophene-2-carboxylic acid (**4o**)



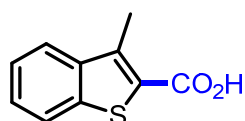
Following GP2a, thieno[3,2-*b*]thiophene (0.4 mmol) gave **4o** (48%) as a pale green solid; $^1\text{H-NMR}$ (400 MHz, DMSO- d_6) δ 13.20 (bs, 1H), 8.11 (s, 1H), 7.92 (d, $J = 5.3$ Hz, 1H), 7.51 (d, $J = 5.3$ Hz, 1H). $^{13}\text{C-NMR}$ (101 MHz, DMSO) δ 163.4 (C_q), 143.2 (C_q), 138.6 (C_q), 135.7 (C_q), 133.0, 126.1, 120.3. **HRMS** (ESI+): calculated m/z for $\text{C}_7\text{H}_5\text{O}_2\text{S}_2$ [(M+H) $^+$] 184.9725; found 184.9728. Data in accordance with the literature.³¹

Benzo[*b*]thiophene-2-carboxylic acid (**4p**)



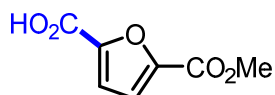
Following GP2a, benzo[*b*]thiophene (0.4 mmol) gave **4p** (97%) as a white solid; $^1\text{H-NMR}$ (400 MHz, DMSO- d_6) δ 13.45 (bs, 1H), 8.11 (s, 1H), 8.06 – 7.96 (m, 2H), 7.54 – 7.41 (m, 2H). $^{13}\text{C-NMR}$ (101 MHz, DMSO) δ 163.5 (C_q), 141.3 (C_q), 138.7 (C_q), 134.8 (C_q), 130.2, 127.0, 125.7, 125.1, 123.0. **HRMS** (ESI+): calculated m/z for $\text{C}_9\text{H}_7\text{O}_2\text{S}$ [(M+H) $^+$] 179.0161; found 179.0163. Data in accordance with the literature.³²

3-Methylbenzo[*b*]thiophene-2-carboxylic acid (**4q**)



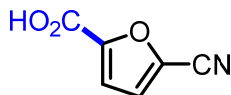
Following GP2a, 3-methylbenzo[*b*]thiophene (0.4 mmol) gave **4q** (95%) as a white solid; **¹H-NMR** (300 MHz, DMSO-*d*₆) δ 13.37 (bs, 1H), 8.01 – 7.88 (m, 2H), 7.55 – 7.41 (m, 2H), 2.70 (s, 3H). **¹³C-NMR** (75 MHz, DMSO) δ 164.4 (C_q), 140.0 (C_q), 139.8 (C_q), 139.4 (C_q), 127.9 (C_q), 127.3, 124.7, 123.9, 122.8, 12.8. **HRMS** (ESI+): calculated *m/z* for C₁₀H₉O₂S [(M+H)⁺] 193.0318; found 193.0319. Data in accordance with the literature.³³

5-(Methoxycarbonyl)furan-2-carboxylic acid (**4r**)



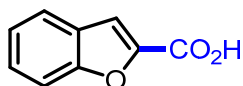
Following GP2a, methyl furan-2-carboxylate (0.4 mmol) gave **4r** (70%) as a pale yellow solid. **¹H-NMR** (400 MHz, DMSO-*d*₆) δ 13.72 (bs, 1H), 7.39 (d, *J* = 3.6 Hz, 1H), 7.32 (d, *J* = 3.6 Hz, 1H), 3.85 (s, 3H). **¹³C-NMR** (101 MHz, DMSO) δ 158.8 (C_q), 157.9 (C_q), 147.4 (C_q), 145.6 (C_q), 119.0, 118.4, 52.3. **HRMS** (ESI+): calculated *m/z* for C₇H₇O₅ [(M+H)⁺] 171.0288; found 171.0289. Data in accordance with the literature.³⁴

5-Cyanofuran-2-carboxylic acid (**4s**)



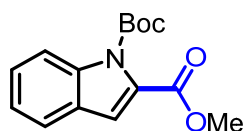
Following GP2a, furan-2-carbonitrile (0.4 mmol) gave **4s** (43%) as a pale yellow solid; **¹H-NMR** (400 MHz, DMSO-*d*₆) δ 13.98 (bs, 1H), 7.72 (d, *J* = 3.8 Hz, 1H), 7.40 (d, *J* = 3.8 Hz, 1H). **¹³C-NMR** (101 MHz, DMSO) δ 158.0 (C_q), 149.0 (C_q), 126.9 (C_q), 124.6, 117.8, 111.0 (C_q). **HRMS** (EI+): calculated *m/z* for C₆H₃NO₃ [M⁺] 137.01074; found 137.01037.

Benzofuran-2-carboxylic acid (**4t**)



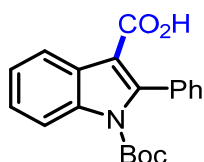
Following GP2a, benzofuran (0.4 mmol) gave **4t** (47%) as a pale yellow solid; **¹H-NMR** (400 MHz, DMSO-*d*₆) δ 13.55 (bs, 1H), 7.78 (d, *J* = 7.8 Hz, 1H), 7.69 (d, *J* = 8.4 Hz, 1H), 7.67 – 7.63 (m, 1H), 7.49 (ddd, *J* = 8.4, 7.1, 1.3 Hz, 1H), 7.38 – 7.32 (m, 1H). **¹³C-NMR** (101 MHz, DMSO) δ 160.1 (C_q), 155.0 (C_q), 146.3 (C_q), 127.5, 126.9 (C_q), 123.8, 123.1, 113.4, 112.1. **HRMS** (EI+): calculated *m/z* for C₉H₆O₃ [M⁺] 162.03115; found 162.03138. Data in accordance with the literature.¹⁷

1-(*tert*-butyl) 2-methyl 1*H*-indole-1,2-dicarboxylate (**4u**)



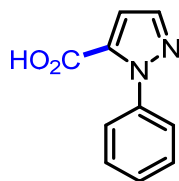
A dry microwave vial (5 mL) equipped with stirring bar, was charged with *tert*-butyl 1*H*-indole-1-carboxylate (0.1 mmol) and 2,3,6,7-tetramethoxyanthracen-9(10*H*)-one (20 mol%). The vial was sealed and transferred to a glovebox after the vial had evacuated and refilled with N₂ (3×) within the antechamber *via* syringe. Cs₂CO₃ (3.0 equiv.) and dry DMSO (1 mL) was added and the vial was sealed with a Supelco aluminium crimp seal with septum (PTFE/butyl). The vial was removed from the glovebox. The reaction mixture then had gaseous CO₂ (22 cm³) added *via* a gastight Hamilton® syringe, into the head space of the vial. The vial was then irradiated from two sides by two kessil lamps (vials approximately 6 cm away from the light source) with fans placed in front of the vials for cooling (temperatures measured *via* IR ranged between 25-30 °C). After 18 hrs the irradiation was stopped, the pressure was vented *via* syringe and MeI (31 μL, 0.5 mmol) was added. The reaction mixture was left to stir for 4 hrs. The vial was decapped and quenched with aq. HCl (1 mL, 0.3M). The reaction was diluted with brine (10 mL) extracted with EtOAc (3×5 mL). The organic layers were combined and washed with brine (3×10 mL) and then dried *via* phase separator and concentrated *in vacuo*. Purification by column chromatography on silica gel eluting with heptane:EtOAc (9:1) gave the title compound **4u** (40%) as a white waxy solid. R_f 0.51 [Heptane–EtOAc (9:1)]; 8.10 (dq, *J* = 8.5, 0.9 Hz, 1H), 7.60 (ddd, *J* = 7.8, 1.2, 0.8 Hz, 1H), 7.42 (ddd, *J* = 8.5, 7.2, 1.3 Hz, 1H), 7.27 (ddd, *J* = 8.1, 7.2, 1.0 Hz, 1H), 7.11 (d, *J* = 0.8 Hz, 1H), 3.93 (s, 3H), 1.63 (s, 9H). ¹³C-NMR (101 MHz, CDCl₃) δ 162.5, 149.4, 137.9, 130.5, 127.6, 126.9, 123.4, 122.3, 115.0, 115.0, 84.7, 52.5, 27.9. Data in accordance with the literature.³⁵

1-(*tert*-Butoxycarbonyl)-2-phenyl-1*H*-indole-3-carboxylic acid (**4v**)



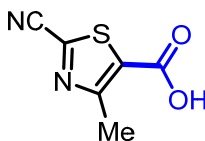
Following GP2a, *tert*-butyl 2-phenyl-1*H*-indole-1-carboxylate (0.4 mmol) gave **4v** (10%) as a white solid; ¹H-NMR (400 MHz, DMSO-*d*₆) δ 12.40 (bs, 1H), 8.17 – 8.12 (m, 1H), 8.12 – 8.07 (m, 1H), 7.48 – 7.32 (m, 7H), 1.16 (s, 9H). ¹³C-NMR (101 MHz, DMSO) δ 164.9 (C_q), 148.9 (C_q), 143.8 (C_q), 135.3 (C_q), 133.1 (C_q), 129.7, 128.1, 127.4, 126.9 (C_q), 124.9, 123.7, 121.6, 114.2, 111.4 (C_q), 84.3 (C_q), 26.8. HRMS (ESI⁺): calculated *m/z* for C₂₀H₂₀NO₄ [(M+H)⁺] 338.1387; found 338.1391.

1-Phenyl-1*H*-pyrazole-5-carboxylic acid (**4w**)



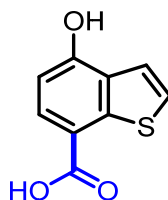
Following GP2a, 1-phenylpyrazole (0.4 mmol) gave **4w** (33%) as a white solid; **¹H-NMR** (300 MHz, Methanol-*d*₄) δ 7.72 (d, *J* = 2.0 Hz, 1H), 7.52 – 7.39 (m, 5H), 7.05 (d, *J* = 2.0 Hz, 1H). **¹H-NMR** (400 MHz, DMSO-*d*₆) δ 13.29 (bs, 1H), 7.77 (d, *J* = 1.9 Hz, 1H), 7.52 – 7.41 (m, 5H), 7.03 (d, *J* = 1.9 Hz, 1H). **¹³C-NMR** (101 MHz, DMSO) δ 160.0 (*C*_q), 140.2 (*C*_q), 139.7, 134.1 (*C*_q), 128.5, 128.2, 125.7, 112.5. **HRMS** (ESI+): calculated *m/z* for C₁₀H₉N₂O₂ [(M+H)⁺] 189.0659; found 189.0661. Data in accordance with the literature.³⁶

2-cyano-4-methylthiazole-5-carboxylic acid (**4x**)



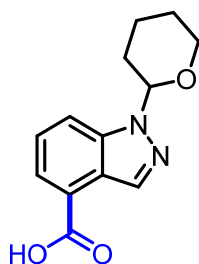
Following GP2c, 4-methylthiazole-2-carbonitrile (0.1 mmol) gave **4x** (53%) as a white solid. **¹H-NMR** (500 MHz, CDCl₃) δ 2.83 (3H, s); **¹³C-NMR** (126 MHz, CDCl₃) δ 165.4 (*C*_q), 163.3 (*C*_q), 139.3 (*C*_q), 126.6 (*C*_q), 112.1 (*C*_q), 17.7; **HRMS** (EI): calculated *m/z* for C₆H₄N₂O₂S [M⁺] 167.9992; found 168.0003.

4-hydroxybenzo[*b*]thiophene-7-carboxylic acid (**6a**)



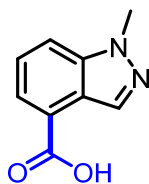
Following GP2c, 4-hydroxybenzo[*b*]thiophene (0.1 mmol) gave **6a** (99%) as a white solid. **¹H-NMR** (500 MHz, DMSO-*d*₆): δ 7.91 (d, *J* = 8.2 Hz, 1H), 7.66 (d, *J* = 5.6 Hz, 1H), 7.51 (d, *J* = 5.6 Hz, 1H), 6.85 (d, *J* = 8.2 Hz, 1H); **¹³C-NMR** (126 MHz, DMSO-*d*₆) δ 166.9 (*C*_q), 157.0 (*C*_q), 141.8 (*C*_q), 129.8 (*C*_q), 129.3, 127.7, 119.8, 115.6 (*C*_q), 108.9; **HRMS** (ESI): calculated *m/z* for C₉H₅O₃S [(M-H)⁺] 192.9965; found 192.9965.

1-(Tetrahydro-2H-pyran-2-yl)-1H-indazole-4-carboxylic acid (**6b**)



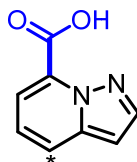
Following GP2c, 1-(tetrahydro-2H-pyran-2-yl)-1H-indazole (0.1 mmol) gave **6b** (60%) as a white solid. **¹H-NMR** (500 MHz, DMSO-d₆): δ 12.88 (bs, 1H), 8.42 (s, 1H), 8.03 (d, *J* = 8.4 Hz, 1H), 7.83 (d, *J* = 7.1 Hz, 1H), 7.63-7.43 (m, 1H), 5.92 (dd, *J* = 9.6, 2.1 Hz, 1H), 3.88 (d, *J* = 11.2 Hz, 1H), 3.80-3.71 (m, 1H), 2.42 (qd, *J* = 3.7, 13.0 Hz, 1H), 2.15-1.94 (m, 2H), 1.88-1.67 (m, 1H), 1.65-1.52 (m, 2H); **¹³C-NMR** (126 MHz, DMSO-d₆): δ 167.0, 139.8, 133.6, 125.9, 124.4, 123.3, 122.5, 115.3, 84.0, 66.5, 28.9, 24.7, 22.1; **HRMS** (ESI): calculated *m/z* for C₁₃H₁₅N₂O₃ [(M+H)⁺] 247.1077; found 247.1066.

1-Methyl-1H-indazole-4-carboxylic acid (**6c**)



Following GP2c, 1-methyl-1H-indazole (0.1 mmol) gave **6c** (58%) as a white solid. **¹H-NMR** (500 MHz, CDCl₃): δ 8.58 (s, 1H), 8.05 (d, *J* = 6.9 Hz, 1H), 7.69 (d, *J* = 8.8 Hz, 1H), 7.44-7.56 (m, 1H), 4.16 (s, 3H); **¹³C-NMR** (126 MHz, CDCl₃): 171.3, 140.5, 133.9, 125.7, 125.3, 122.8, 122.3, 114.9, 35.9; **HRMS** (ESI): calculated *m/z* for C₉H₉N₂O₂ [(M+H)⁺] 177.0664; found 177.0669.

Pyrazolo[1,5-*a*]pyridine-7-carboxylic acid (**6d**) & pyrazolo[1,5-*a*]pyridine-4-carboxylic acid (**6d'**)

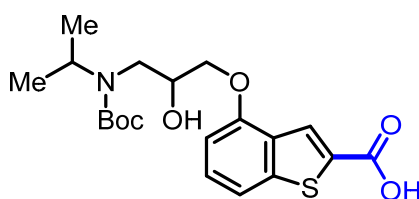


Following GP2c, pyrazolo[1,5-*a*]pyridine (0.1 mmol) gave **6d** (63%) as a white solid & **6d'** (22%) as a white solid. **6d:6d'** = 2.8:1.

Data for 6d: $^1\text{H-NMR}$ (500 MHz, DMSO-d_6) δ 8.20 (d, $J = 2.3$ Hz, 1H), 8.14–7.88 (m, 1H), 7.73–7.58 (m, 1H), 7.38 (dd, $J = 7.1, 8.8$ Hz, 1H), 6.87 (d, $J = 2.3$ Hz, 1H); $^{13}\text{C-NMR}$ (126 MHz, DMSO-d_6) δ 161.8, 140.8, 140.6, 129.3, 123.6, 122.3, 116.9, 98.5. Data in accordance with the literature.³⁷

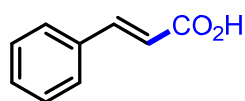
Data for 6d': $^1\text{H-NMR}$ (500 MHz, DMSO-d_6) δ 13.34 (bs, 1H), 8.94 (d, $J = 6.8$ Hz, 1H), 8.12 (d, $J = 2.1$ Hz, 1H), 7.95 (d, $J = 6.4$ Hz, 1H), 7.03–6.98 (m, 2H); $^{13}\text{C-NMR}$ (126 MHz, DMSO-d_6) δ 165.5, 142.9, 137.9, 133.0, 128.6, 120.7, 110.9, 98.6. Data in accordance with the literature.³⁷

4-(3-((*tert*-butoxycarbonyl)(isopropyl)amino)-2-hydroxypropoxy)benzo[*b*]thiophene-2-carboxylic acid (6e)



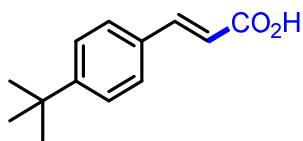
Following GP2c, *tert*-butyl (3-(benzo[*b*]thiophen-4-yloxy)-2-hydroxypropyl)(isopropyl)carbamate (0.1 mmol) gave **6e** (18%) as a yellow oil. $^1\text{H-NMR}$ (500 MHz, CDCl_3): δ 8.26 (s, 1H), 7.32–7.49 (m, 2H), 6.77 (d, $J = 7.5$ Hz, 1H), 4.28–4.11 (m, 3H), 4.10–3.99 (m, 1H), 3.47 (s, 2H), 2.05 (s, 1H), 1.50 (s, 9H), 1.18 (dd, $J = 6.5, 31.4$ Hz, 6H); $^{13}\text{C-NMR}$ (126 MHz, CDCl_3) δ 165.6, 154.3, 143.4, 131.0, 129.1, 127.7, 127.3, 114.4, 104.2, 80.0, 71.0, 69.1, 48.0, 46.1, 27.6, 19.7 **HRMS** (ESI): calculated m/z for $\text{C}_{20}\text{H}_{28}\text{NO}_6\text{S}$ [$(\text{M}+\text{H})^+$] 410.1637; found 410.1655.

Cinnamic acid (8a)



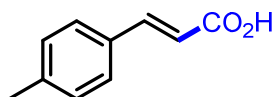
Following GP2a, styrene (0.4 mmol) gave **8a** (54%) as a white solid; $^1\text{H-NMR}$ (400 MHz, DMSO-d_6) δ 12.40 (bs, 1H), 7.72 – 7.64 (m, 2H), 7.59 (d, $J = 16.0$ Hz, 1H), 7.45 – 7.37 (m, 3H), 6.53 (d, $J = 16.0$ Hz, 1H). $^{13}\text{C-NMR}$ (101 MHz, DMSO) δ 167.6 (C_q), 143.9, 134.2 (C_q), 130.2, 128.9, 128.2, 119.3. **HRMS** (EI+): calculated m/z for $\text{C}_9\text{H}_8\text{O}_2$ [M^+] 148.05188; found 148.05161. Data in accordance with the literature.³⁸

(E)-3-(4-(*tert*-Butyl)phenyl)acrylic acid (8b)



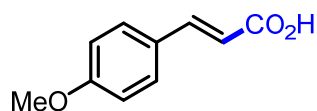
Following GP2a, 1-(*tert*-butyl)-4-vinylbenzene (0.4 mmol) gave **8b** (56%) as a white solid; ¹H-NMR (400 MHz, DMSO-*d*₆) δ 12.33 (bs, 1H), 7.62 – 7.53 (m, 3H), 7.46 – 7.38 (m, 2H), 6.47 (d, *J* = 16.0 Hz, 1H), 1.27 (s, 9H). ¹³C-NMR (101 MHz, DMSO) δ 167.7 (C_q), 153.1 (C_q), 143.8, 131.5 (C_q), 128.0, 125.7, 118.3, 34.6 (C_q), 30.9. HRMS (EI+): calculated *m/z* for C₁₃H₁₆O₂ [M⁺] 204.11448; found 204.11415.

(E)-3-(*p*-Tolyl)acrylic acid (8c)



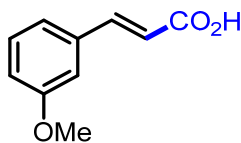
Following GP2a, 4-methylstyrene (0.4 mmol) gave **8c** (53%) as a white solid; ¹H-NMR (400 MHz, DMSO-*d*₆) δ 12.31 (bs, 1H), 7.60 – 7.51 (m, 3H), 7.22 (d, *J* = 7.9 Hz, 2H), 6.46 (d, *J* = 16.0 Hz, 1H), 2.32 (s, 3H). ¹³C-NMR (101 MHz, DMSO) δ 167.7 (C_q), 143.9, 140.1 (C_q), 131.5 (C_q), 129.5, 128.2, 118.1, 21.0. HRMS (EI+): calculated *m/z* for C₁₀H₁₀O₂ [M⁺] 162.06753; found 162.06783.

(E)-3-(4-Methoxyphenyl)acrylic acid (8d)



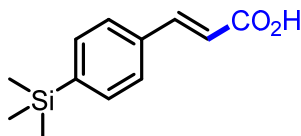
Following GP2a, 4-methoxystyrene (0.4 mmol) gave **8d** (40%) as a pale yellow solid; ¹H-NMR (400 MHz, DMSO-*d*₆) δ 12.21 (bs, 1H), 7.66 – 7.60 (m, 2H), 7.54 (d, *J* = 16.0 Hz, 1H), 7.00 – 6.93 (m, 2H), 6.37 (d, *J* = 15.9 Hz, 1H), 3.79 (s, 3H). ¹³C-NMR (101 MHz, DMSO) δ 167.8 (C_q), 160.9 (C_q), 143.7, 129.9, 126.8 (C_q), 116.5, 114.3, 55.3. HRMS (EI+): calculated *m/z* for C₁₀H₁₀O₃ [M⁺] 178.06245; found 178.06194.

(E)-3-(3-Methoxyphenyl)acrylic acid (8e):



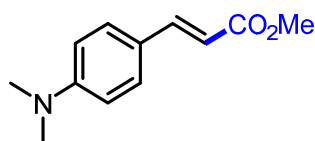
Following GP2a, 3-methoxystyrene (0.4 mmol) gave **8e** (46%) as a white solid; ¹H-NMR (400 MHz, DMSO-*d*₆) δ 12.40 (bs, 1H), 7.56 (d, *J* = 16.0 Hz, 1H), 7.36 – 7.20 (m, 3H), 7.03 – 6.92 (m, 1H), 6.55 (d, *J* = 16.0 Hz, 1H), 3.79 (s, 3H). ¹³C-NMR (101 MHz, DMSO) δ 167.6 (C_q), 159.6 (C_q), 143.9, 135.7 (C_q), 129.9, 120.8, 119.6, 116.2, 112.9, 55.2. HRMS (EI⁺): calculated *m/z* for C₁₀H₁₀O₃ [M⁺] 178.06245; found 178.06210.

(E)-3-(4-(Trimethylsilyl)phenyl)acrylic acid (8f)



Following GP2a, trimethyl(4-vinylphenyl)silane (0.4 mmol) gave **8f** (53%) as a pale yellow solid; ¹H-NMR (400 MHz, DMSO-*d*₆) δ 12.38 (bs, 1H), 7.67 – 7.62 (m, 2H), 7.61 – 7.52 (m, 3H), 6.54 (d, *J* = 16.0 Hz, 1H), 0.24 (s, 9H). ¹³C-NMR (101 MHz, DMSO) δ 167.5 (C_q), 143.9, 142.6 (C_q), 134.6 (C_q), 133.7, 127.3, 119.4, -1.3. HRMS (EI⁺): calculated *m/z* for C₁₂H₁₆O₂Si [M⁺] 220.09141; found 220.09148.

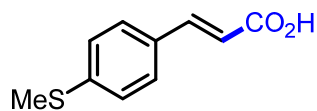
Methyl (E)-3-(4-(dimethylamino)phenyl)acrylate (8g)



The title compound was prepared according to GP2a with *N,N*-dimethyl-4-vinylaniline (0.4 mmol). After irradiating the mixture for 18 hrs the reaction vial was vented and MeI (18.7 μL, 0.3 mmol, 3 equiv.) was added *via* syringe. The resulting mixture was stirred for 2 hrs at 35 °C and was quenched by adding water. The crude mixture was extracted with DCM (3×) and the combined organic layers were dried over Na₂SO₄, filtered and concentrated *in vacuo*. Flash silica gel column chromatography with a mixture of hexanes+NEt₃ (1% v/v) and EtOAc provided the title compound **8g** (14%) as a pale brown solid; ¹H-NMR (400 MHz, Chloroform-*d*) δ 7.63 (d, *J* = 15.9 Hz, 1H), 7.45 – 7.38 (m, 2H), 6.70 – 6.62 (m, 2H), 6.22 (d, *J* = 15.8 Hz, 1H), 3.78 (s, 3H), 3.01 (s, 6H). ¹³C-NMR (101 MHz, CDCl₃) δ

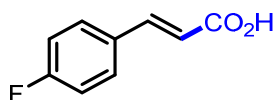
168.5 (C_q), 151.9 (C_q), 145.5, 129.9, 122.3 (C_q), 112.2, 112.0, 51.5, 40.3. **HRMS** (EI⁺): calculated *m/z* for C₁₂H₁₅NO₂ [M⁺] 205.10973; found 205.10937.

(E)-3-(4-(Methylthio)phenyl)acrylic acid (8h)



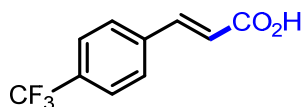
Following GP2a, methyl(4-vinylphenyl)sulfane (0.4 mmol) gave **8h** (38%) as a white solid; **¹H-NMR** (400 MHz, DMSO-*d*₆) δ 12.32 (bs, 1H), 7.65 – 7.60 (m, 2H), 7.55 (d, *J* = 16.0 Hz, 1H), 7.31 – 7.24 (m, 2H), 6.48 (d, *J* = 16.0 Hz, 1H), 2.51 (s, 3H). **¹³C-NMR** (101 MHz, DMSO) δ 167.7 (C_q), 143.4, 141.3 (C_q), 130.6 (C_q), 128.7, 125.6, 118.0, 14.2. **HRMS** (EI⁺): calculated *m/z* for C₁₀H₁₀O₂S [M⁺] 194.03960; found 194.03936.

(E)-3-(4-Fluorophenyl)acrylic acid (8i)



Following GP2a, 4-fluorostyrene (0.4 mmol) gave **8i** (46%) as a white solid; **¹H-NMR** (400 MHz, DMSO-*d*₆) δ 12.39 (bs, 1H), 7.80 – 7.71 (m, 2H), 7.59 (d, *J* = 16.0 Hz, 1H), 7.29 – 7.19 (m, 2H), 6.49 (d, *J* = 16.0 Hz, 1H). **¹³C-NMR** (101 MHz, DMSO-*d*₆) δ 167.5 (C_q), 163.1 (d, *J* = 248.3 Hz, C_q), 142.7, 130.9 (d, *J* = 3.2 Hz, C_q), 130.5 (d, *J* = 8.6 Hz), 119.1 (d, *J* = 2.2 Hz), 115.9 (d, *J* = 21.7 Hz). **¹⁹F-NMR** (376 MHz, DMSO) δ -110.0. **HRMS** (EI⁺): calculated *m/z* for C₉H₇FO₂ [M⁺] 166.04246; found 166.04203.

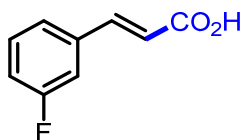
(E)-3-(4-(Trifluoromethyl)phenyl)acrylic acid (8j)



Following GP2a, 1-(trifluoromethyl)-4-vinylbenzene (0.4 mmol) gave **8j** (13%) as a white solid; **¹H-NMR** (400 MHz, DMSO-*d*₆) δ 12.58 (bs, 1H), 7.92 (d, *J* = 8.1 Hz, 2H), 7.76 (d, *J* = 8.1 Hz, 2H), 7.66 (d, *J* = 16.1 Hz, 1H), 6.68 (d, *J* = 16.1 Hz, 1H). **¹³C-NMR** (101 MHz, DMSO) δ 167.2 (C_q), 142.0, 138.3 (d, *J* = 1.3 Hz, C_q), 129.8 (q, *J* = 31.8 Hz, C_q), 128.8, 125.7 (q, *J* = 3.7 Hz), 124.0 (q, *J* = 272.1 Hz, C_q),

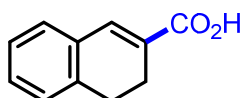
122.3. $^{19}\text{F-NMR}$ (376 MHz, DMSO) δ -60.8. **HRMS** (ESI+): calculated m/z for $\text{C}_{10}\text{H}_8\text{F}_3\text{O}_2$ $[(\text{M}+\text{H})^+]$ 217.0471; found 217.0472. Data in accordance with the literature.³⁸

(*E*)-3-(3-Fluorophenyl)acrylic acid (**8k**)



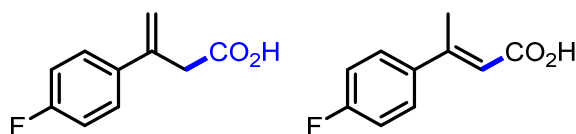
Following GP2a, 3-fluorostyrene (0.4 mmol) gave **8k** (38%) as a white solid; $^1\text{H-NMR}$ (400 MHz, DMSO- d_6) δ 12.49 (bs, 1H), 7.64 – 7.49 (m, 3H), 7.49 – 7.41 (m, 1H), 7.29 – 7.19 (m, 1H), 6.61 (d, J = 16.0 Hz, 1H). $^{13}\text{C-NMR}$ (101 MHz, DMSO- d_6) δ 167.4 (C_q), 162.42 (d, J = 243.7 Hz, C_q), 142.51 (d, J = 2.6 Hz), 136.82 (d, J = 8.1 Hz, C_q), 130.81 (d, J = 8.4 Hz), 124.63 (d, J = 2.6 Hz), 120.9, 116.86 (d, J = 21.3 Hz), 114.38 (d, J = 22.0 Hz). $^{19}\text{F-NMR}$ (377 MHz, DMSO) δ -112.4. **HRMS** (ESI+): calculated m/z for $\text{C}_9\text{H}_8\text{FO}_2$ $[(\text{M}+\text{H})^+]$ 167.0503; found 167.0502.

3,4-Dihydronaphthalene-2-carboxylic acid (**8l**)



Following GP2a, 1,2-dihydronaphthalene (0.4 mmol) gave **8l** (58%) as a white solid; $^1\text{H-NMR}$ (400 MHz, DMSO- d_6) δ 12.43 (bs, 1H), 7.47 (s, 1H), 7.34 – 7.18 (m, 4H), 2.81 (t, J = 8.3 Hz, 2H), 2.49 – 2.43 (m, 2H). $^{13}\text{C-NMR}$ (101 MHz, DMSO) δ 168.1 (C_q), 136.5 (C_q), 135.3, 132.3 (C_q), 130.0 (C_q), 129.3, 128.3, 127.5, 126.7, 26.9 (CH_2), 21.9 (CH_2). **HRMS** (EI+): calculated m/z for $\text{C}_{11}\text{H}_{10}\text{O}_2$ $[\text{M}^{++}]$ 174.06753; found 174.06707. Data in accordance with the literature.³⁹

3-(4-Fluorophenyl)but-3-enoic acid (**8m**) & (*E*)-3-(4-fluorophenyl)but-2-enoic acid (**8m'**)

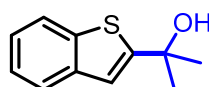


Following GP2a, 4-fluoro- α -methylstyrene (0.4 mmol) gave **8m** (43%) as a white solid and **8m'** (9%) as a pale yellow solid. **8m:8m'** = 4.8:1. **HRMS** (EI+): calculated m/z for $\text{C}_{10}\text{H}_9\text{FO}_2$ $[\text{M}^{++}]$ 180.05811; found 180.05831.

Data for 8m: $^1\text{H-NMR}$ (400 MHz, Chloroform-*d*) δ 9.83 (bs, 1H), 7.45 – 7.35 (m, 2H), 7.06 – 6.97 (m, 2H), 5.52 (s, 1H), 5.24 (s, 1H), 3.52 (s, 2H). $^{13}\text{C-NMR}$ (101 MHz, Chloroform-*d*) δ 177.5 (C_q), 162.7 (d, $J = 247.3$ Hz, C_q), 139.3 (C_q), 135.7 (d, $J = 3.3$ Hz, C_q), 127.61 (d, $J = 8.1$ Hz), 116.98 (d, $J = 1.3$ Hz, CH_2), 115.49 (d, $J = 21.5$ Hz), 41.1 (CH_2). $^{19}\text{F-NMR}$ (376 MHz, CDCl_3) δ -114.8.

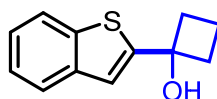
Data for 8m': $^1\text{H-NMR}$ (400 MHz, Chloroform-*d*) δ 7.51 – 7.45 (m, 2H), 7.11 – 7.04 (m, 2H), 6.13 (s, 1H), 2.58 (d, $J = 0.7$ Hz, 3H). $^{19}\text{F-NMR}$ (376 MHz, CDCl_3) δ -112.4. Data in accordance with the literature.⁴⁰

2-(Benzo[*b*]thiophen-2-yl)propan-2-ol (9pa)



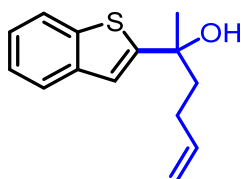
According to GP3 benzo[*b*]thiophene and acetone gave **9pa** (54%) as a white solid; $^1\text{H-NMR}$ (400 MHz, Chloroform-*d*) δ 7.80 (d, $J = 7.8$ Hz, 1H), 7.71 (d, $J = 7.7$ Hz, 1H), 7.31 (dt, $J = 15.1, 7.4$ Hz, 2H), 7.16 (s, 1H), 2.26 (s, 1H), 1.73 (s, 6H). $^{13}\text{C-NMR}$ (101 MHz, CDCl_3) δ 155.1 (C_q), 139.9 (C_q), 139.3 (C_q), 124.3, 124.1, 123.5, 122.4, 118.5, 71.8 (C_q), 32.1. **HRMS** (ESI+): calculated m/z for $\text{C}_{11}\text{H}_{13}\text{O}_2\text{S}$ [(M+H)⁺] 175.0576; found 175.0577.

1-(Benzo[*b*]thiophen-2-yl)cyclobutan-1-ol (9pb)



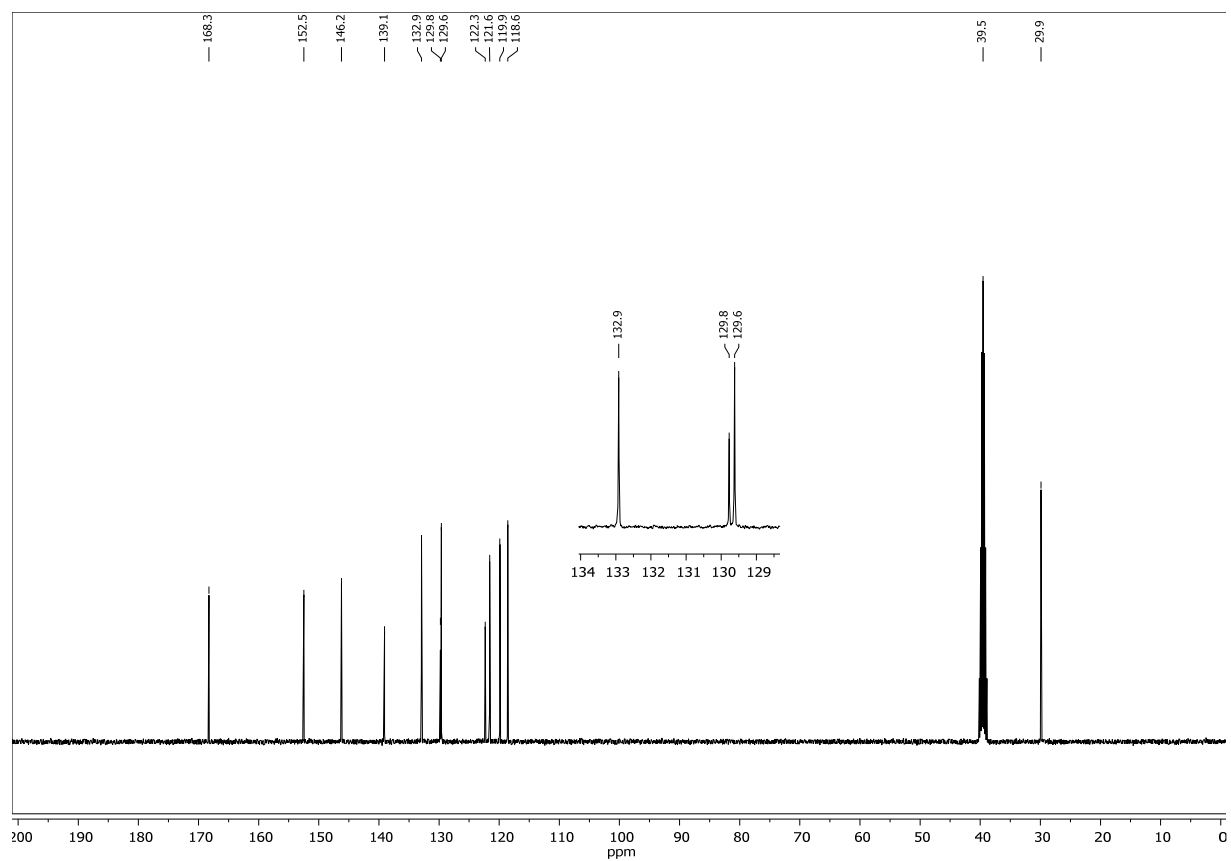
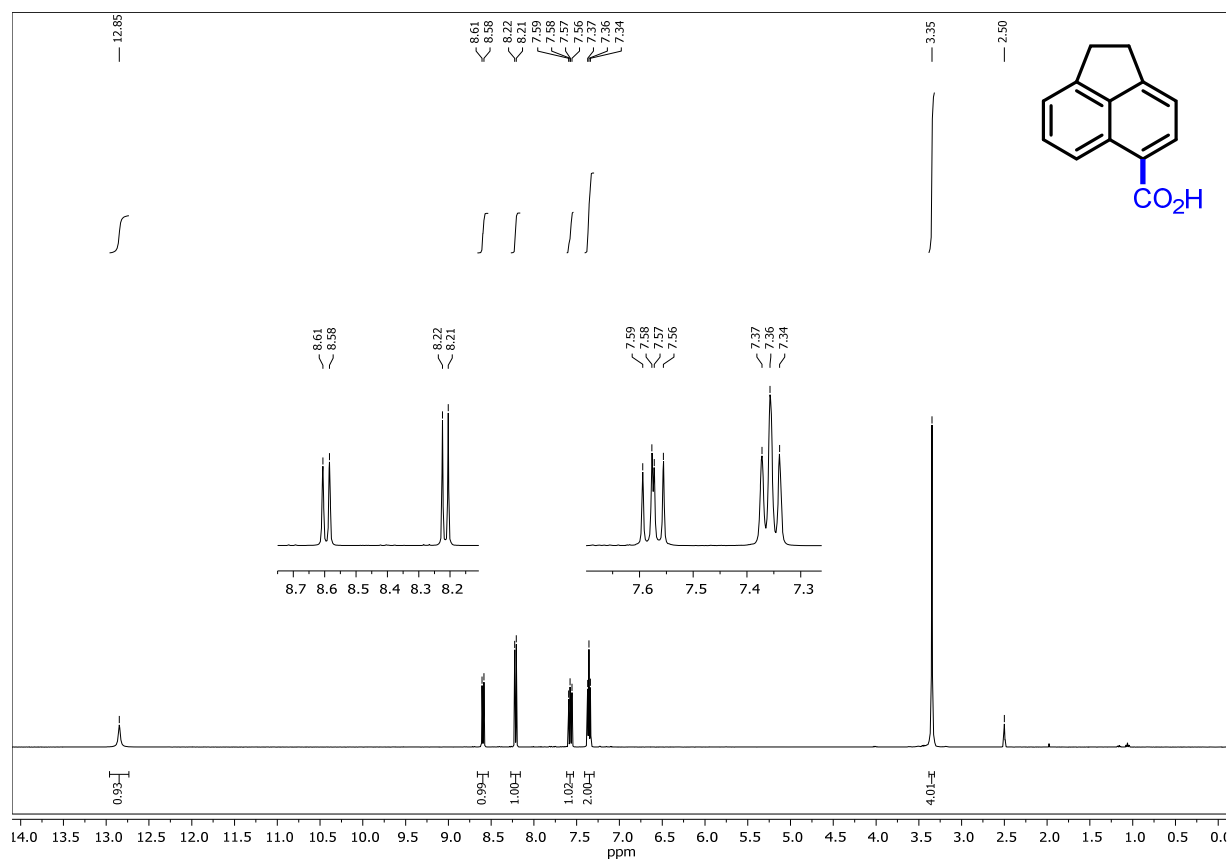
According to GP3 benzo[*b*]thiophene and cyclobutanone gave **9pb** (30%) as a pale yellow oil; $^1\text{H-NMR}$ (300 MHz, Methanol-*d*₄) δ 7.84 – 7.73 (m, 1H), 7.76 – 7.70 (m, 1H), 7.35 – 7.22 (m, 3H), 2.65 – 2.52 (m, 2H), 2.52 – 2.38 (m, 2H), 2.06 – 1.77 (m, 2H). $^{13}\text{C-NMR}$ (75 MHz, MeOD) δ 154.1 (C_q), 141.3 (C_q), 141.0 (C_q), 125.1, 125.0, 124.4, 123.2, 119.8, 75.7 (C_q), 39.0 (CH_2), 13.7 (CH_2). **HRMS** (ESI+): calculated m/z for $\text{C}_{12}\text{H}_{13}\text{OS}$ [(M+H)⁺] 187.0576; found 187.0577.

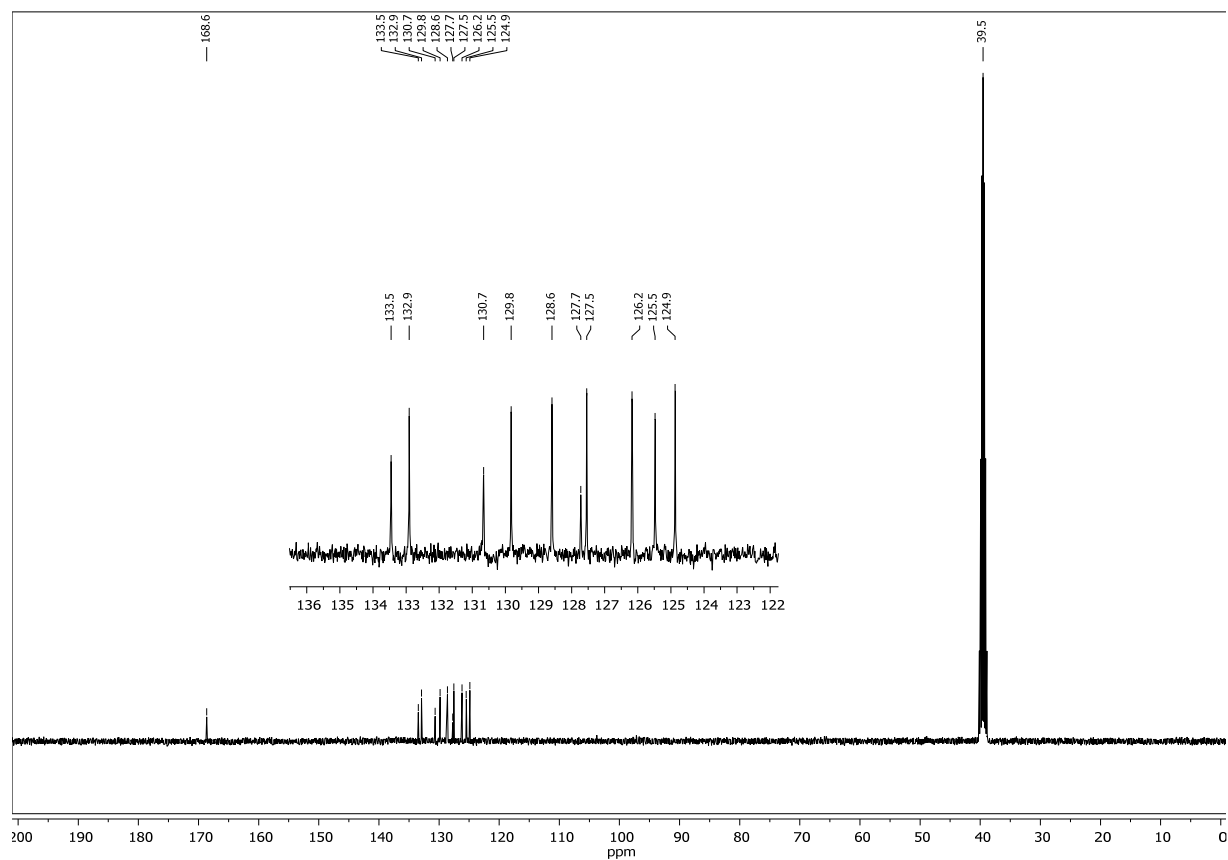
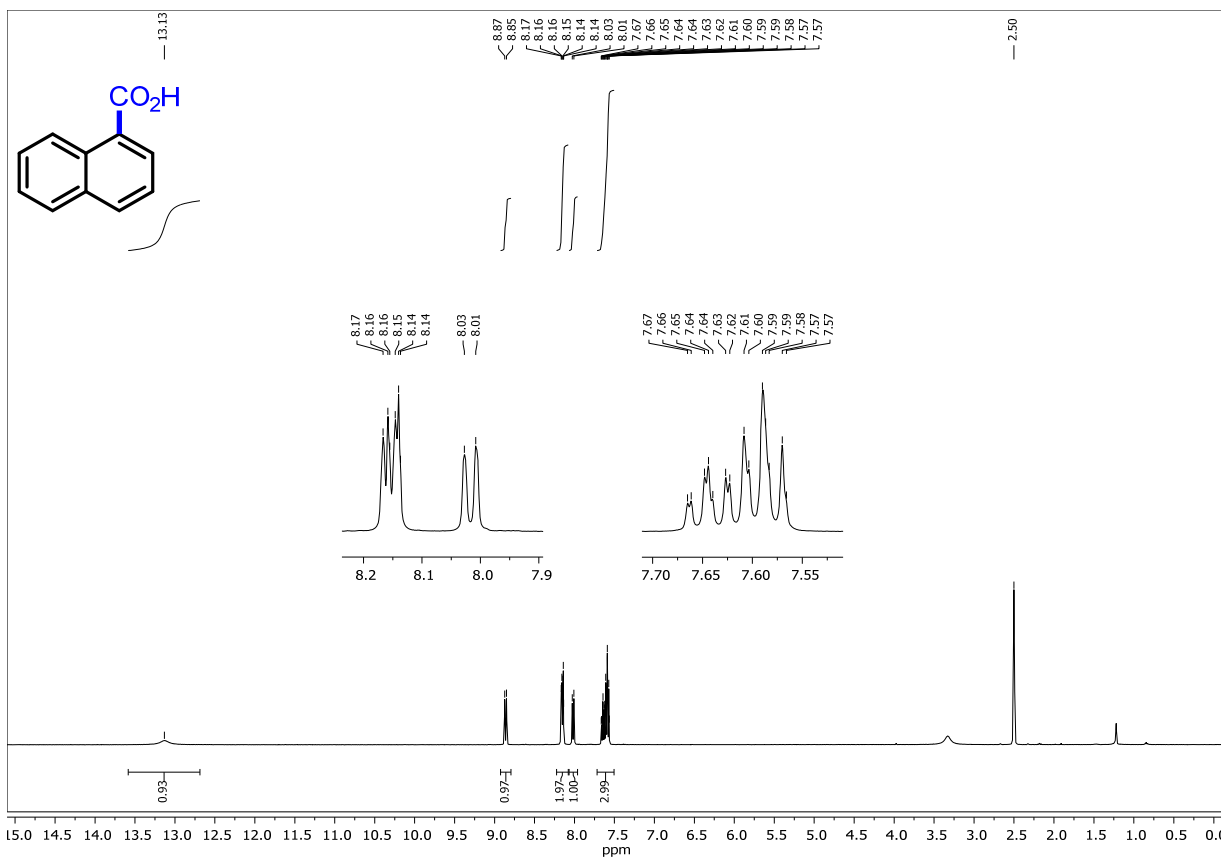
2-(Benzo[*b*]thiophen-2-yl)hex-5-en-2-ol (**9pc**)

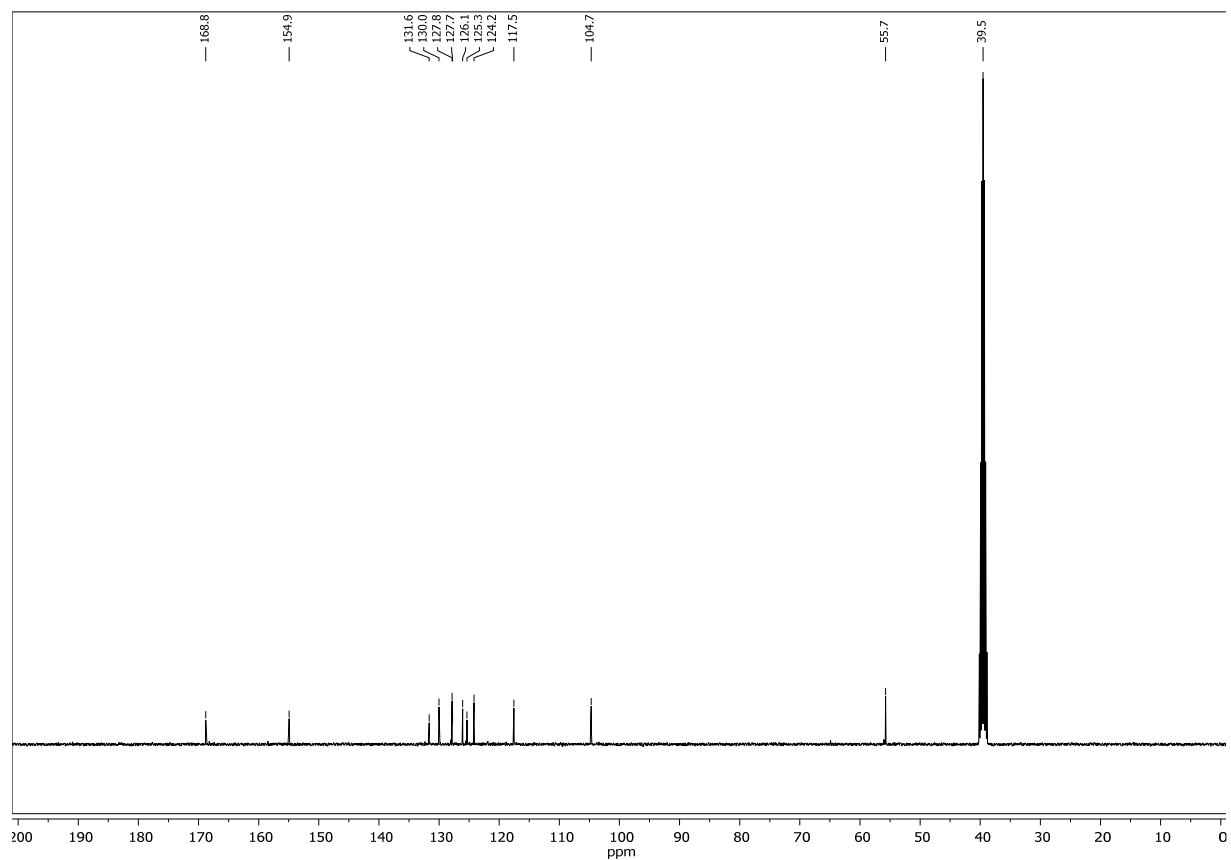
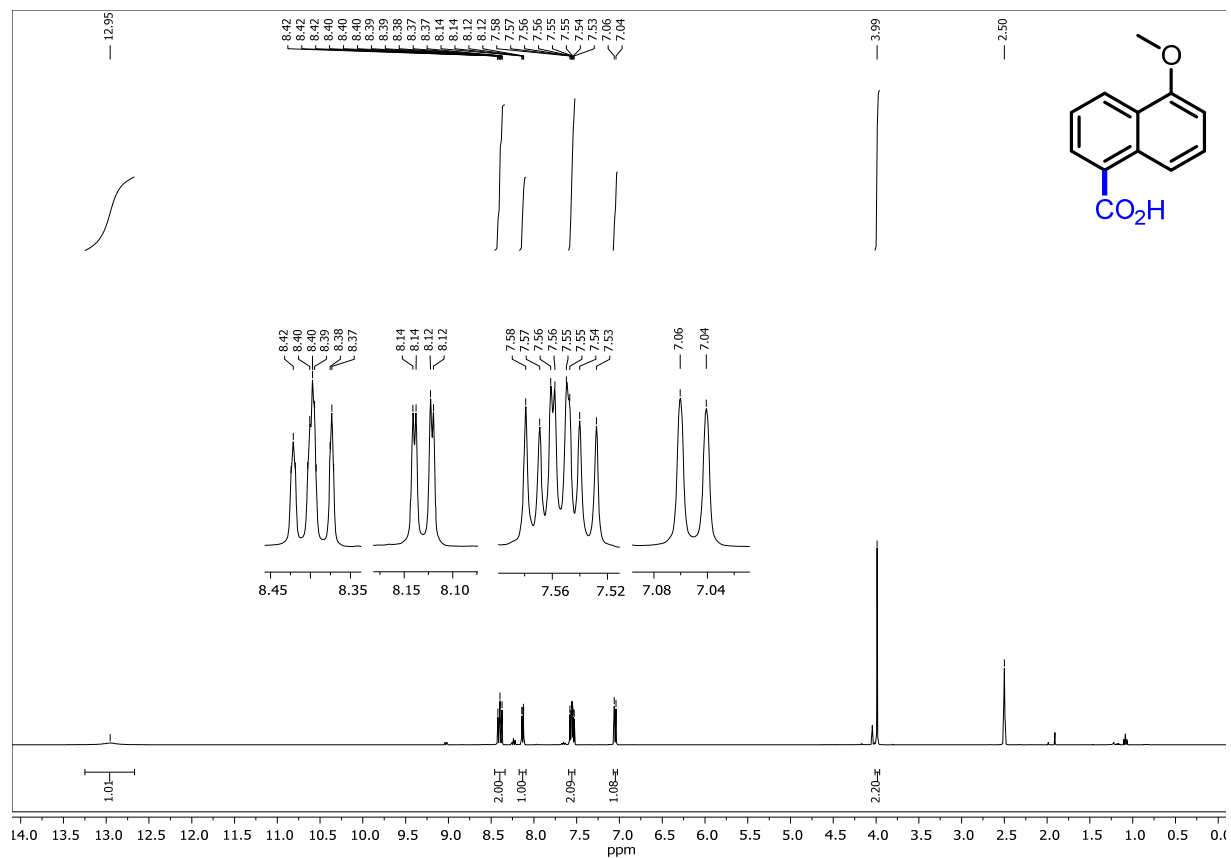


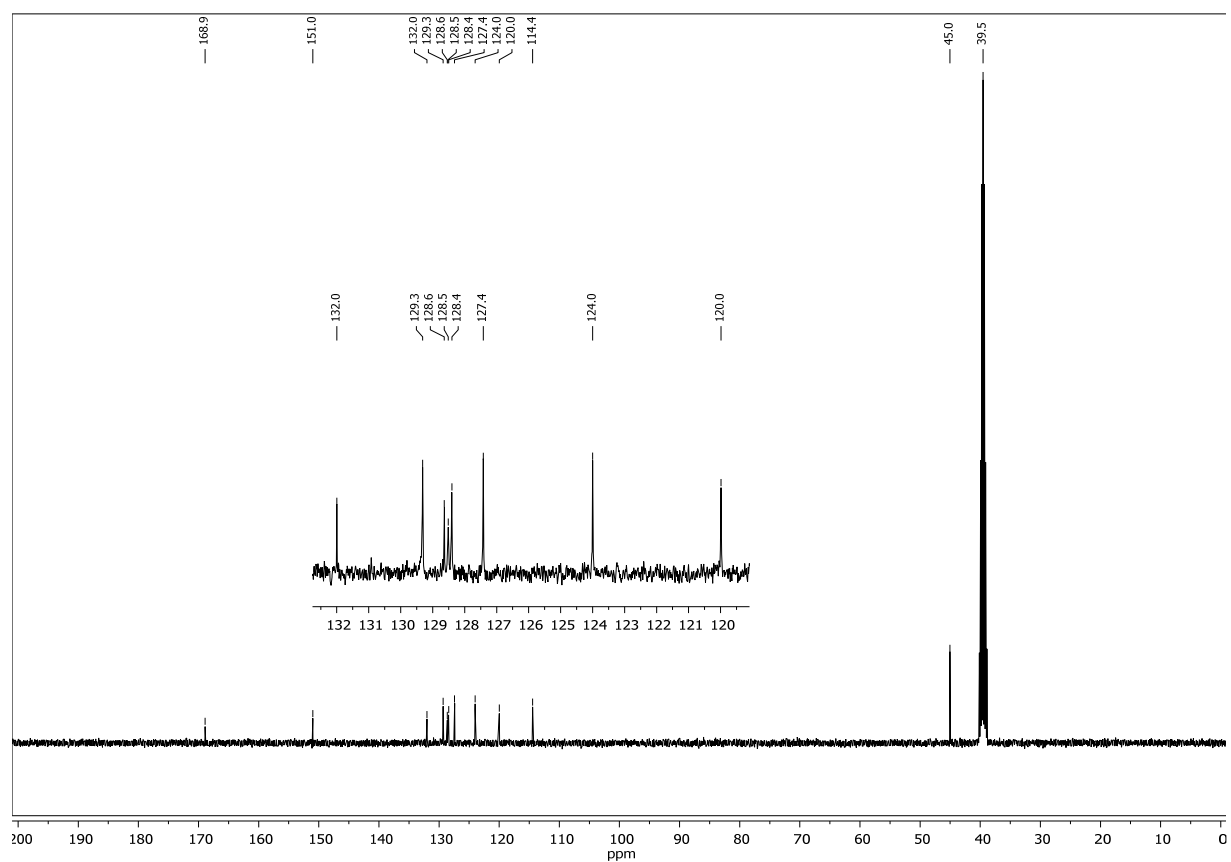
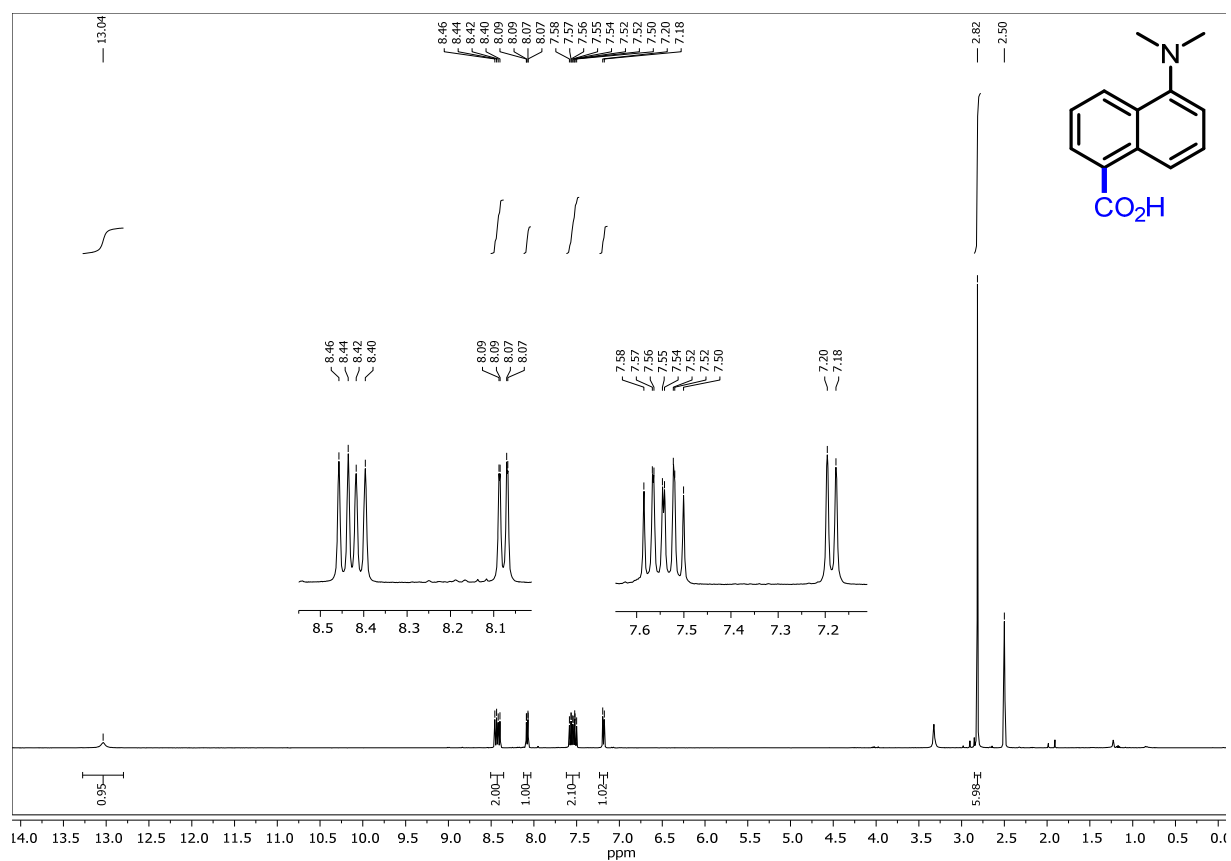
According to GP3 benzo[*b*]thiophene and hex-5-en-2-one gave **9pc** (19%) as a colorless oil; **¹H-NMR** (400 MHz, Chloroform-*d*) δ 7.83 – 7.77 (m, 1H), 7.74 – 7.68 (m, 1H), 7.37 – 7.26 (m, 2H), 7.14 (s, 1H), 5.84 (ddt, $J = 16.8, 10.2, 6.4$ Hz, 1H), 5.02 (dq, $J = 17.1, 1.7$ Hz, 1H), 4.96 (dq, $J = 9.9, 1.3$ Hz, 1H), 2.24 – 2.07 (m, 3H), 2.06 – 1.99 (m, 2H), 1.70 (s, 3H). **¹³C-NMR** (101 MHz, CDCl₃) δ 153.9 (C_q), 140.0 (C_q), 139.4 (C_q), 138.4, 124.4, 124.1, 123.4, 122.4, 119.1, 115.1 (CH₂), 74.4 (C_q), 43.5 (CH₂), 30.7, 28.8 (CH₂). **HRMS** (EI⁺): calculated m/z for C₁₄H₁₆OS [M^{+}] 232.09164; found 232.09159.

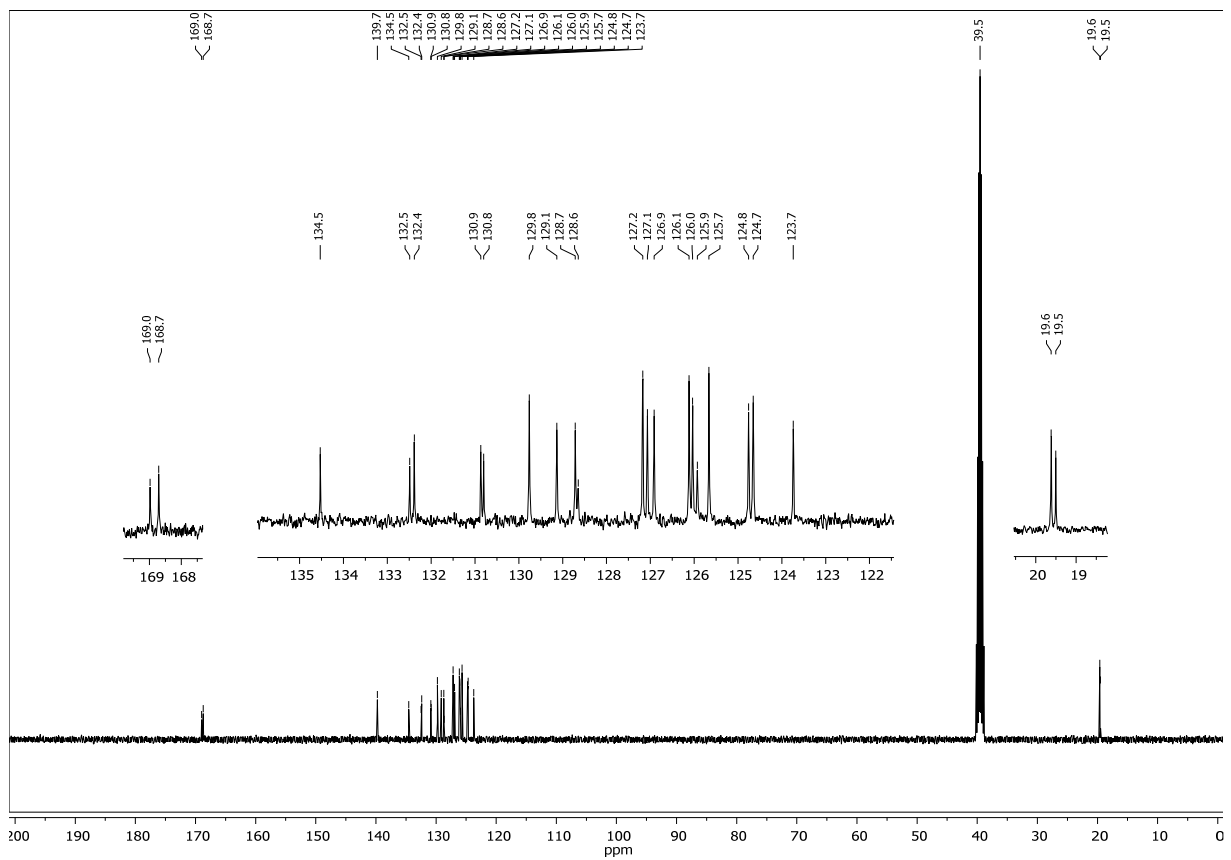
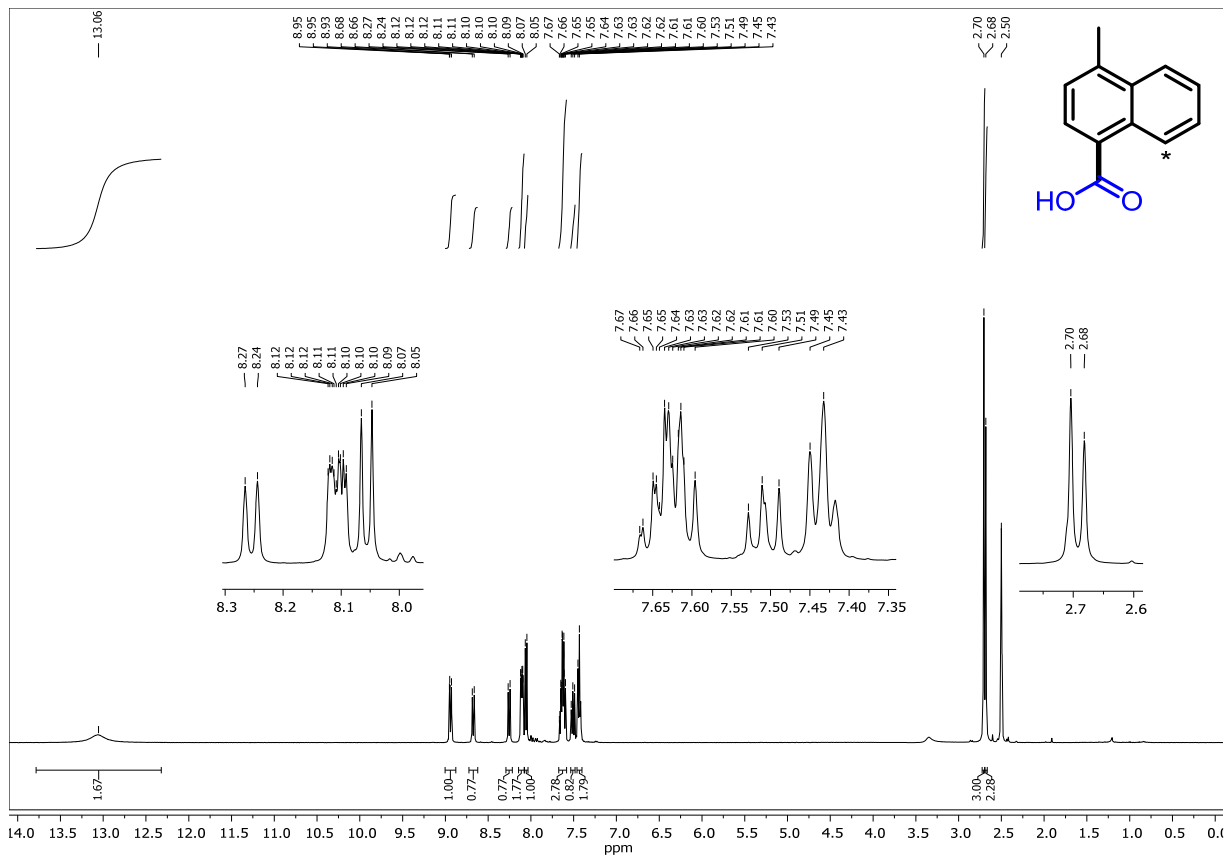
5 - Spectra

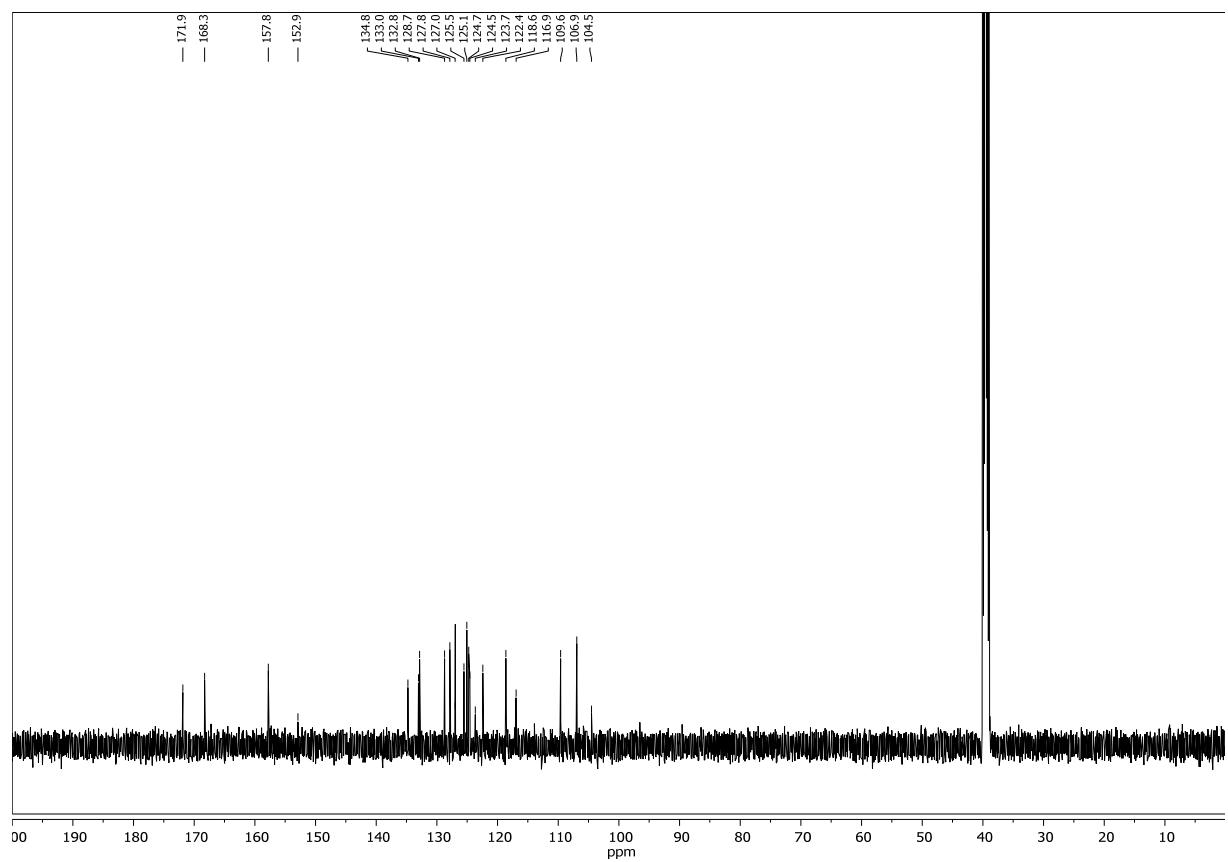
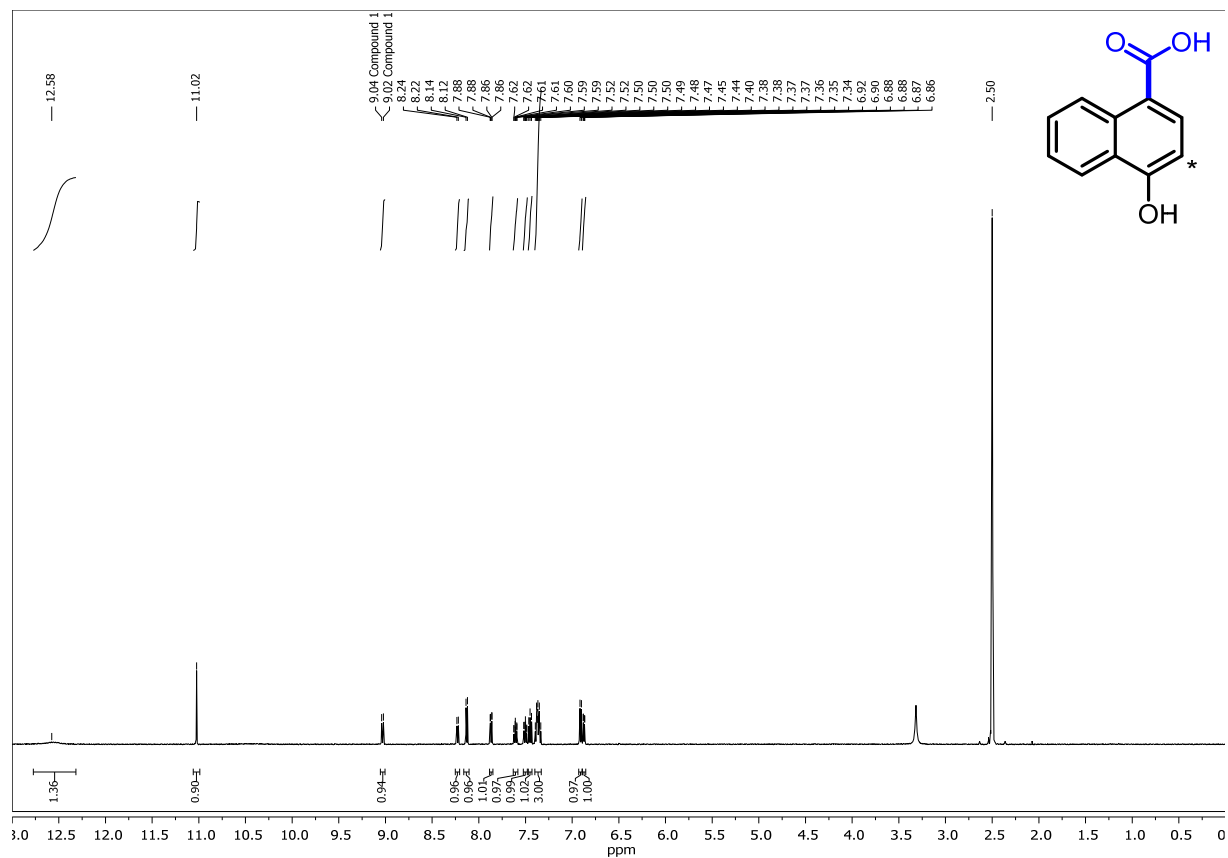


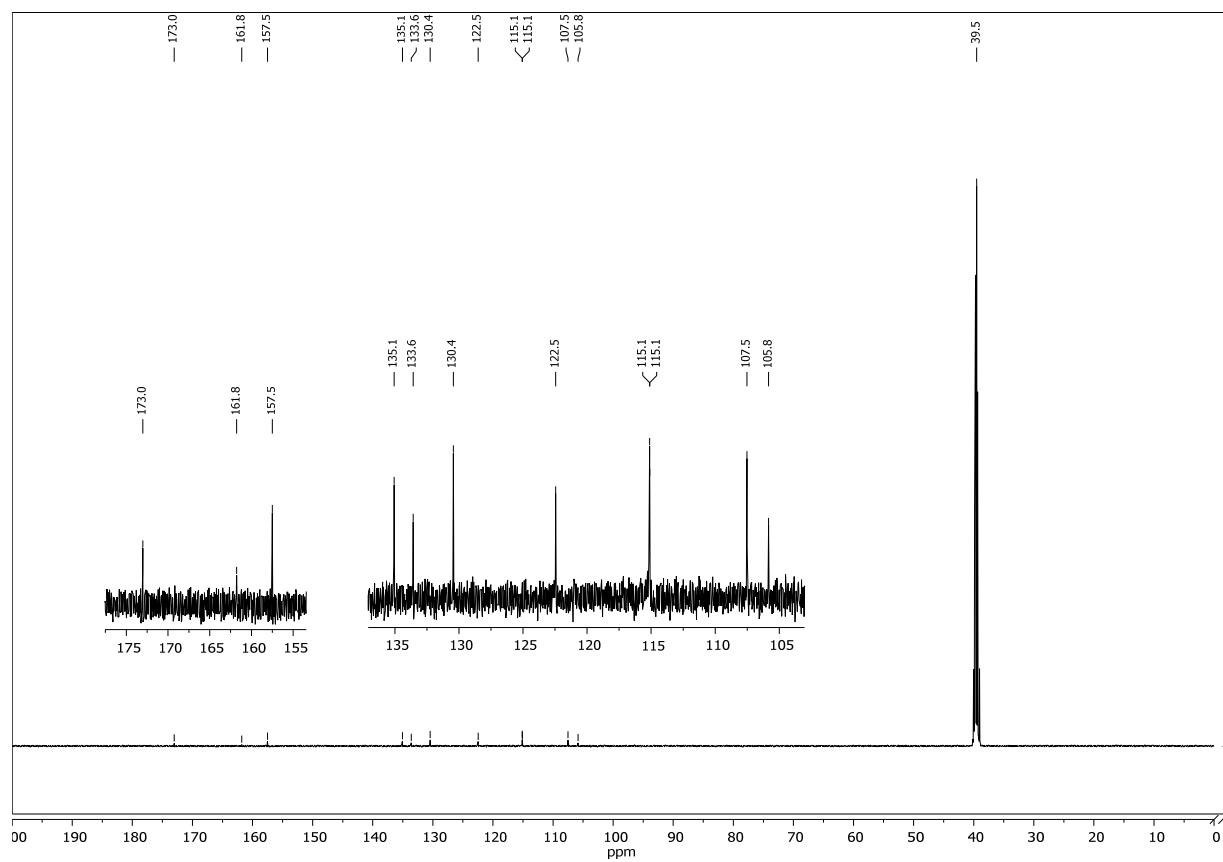
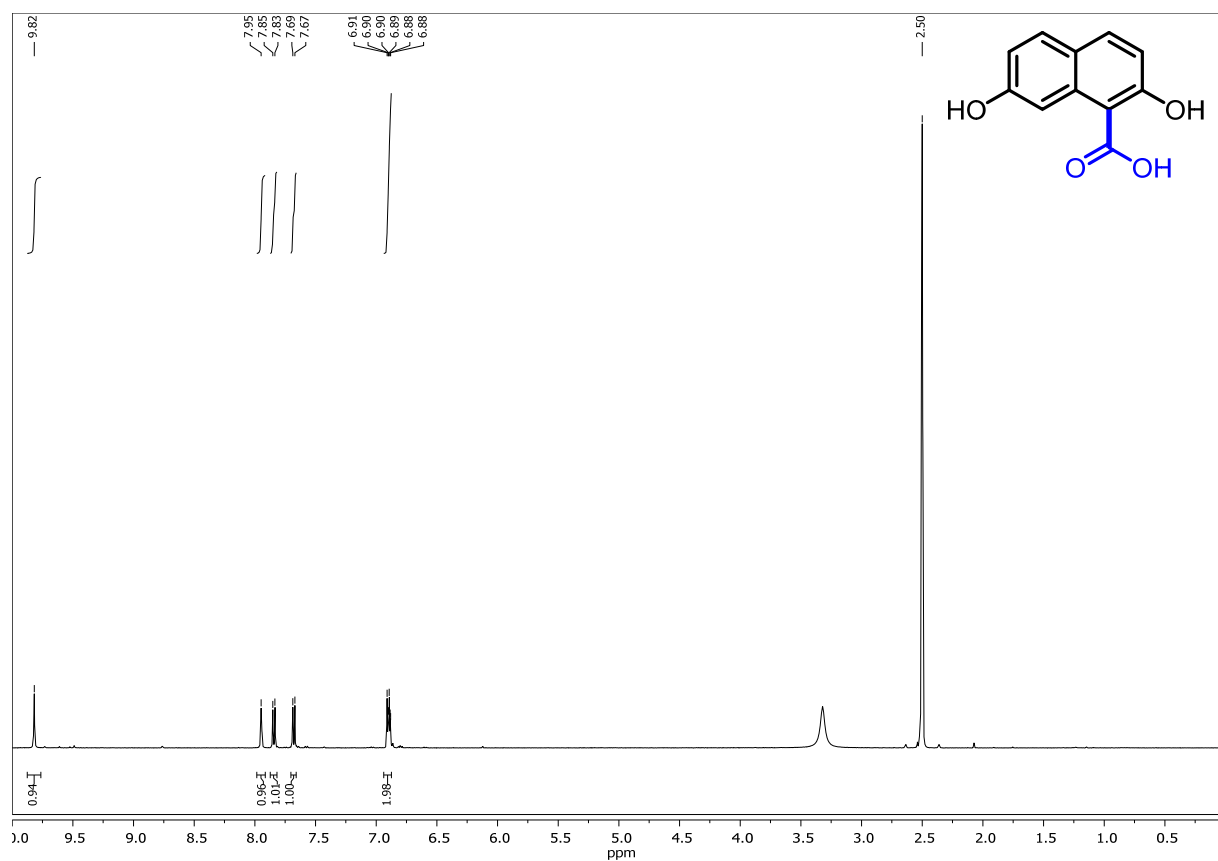


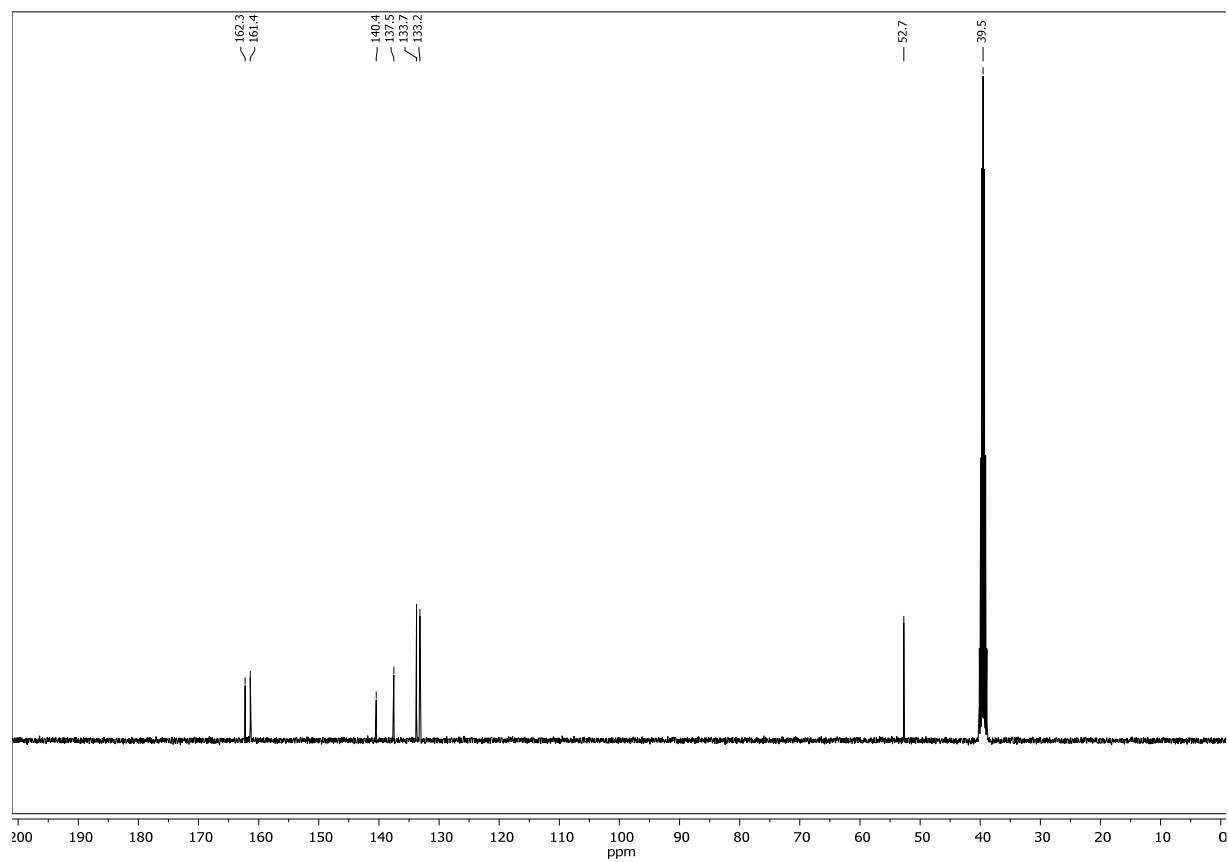
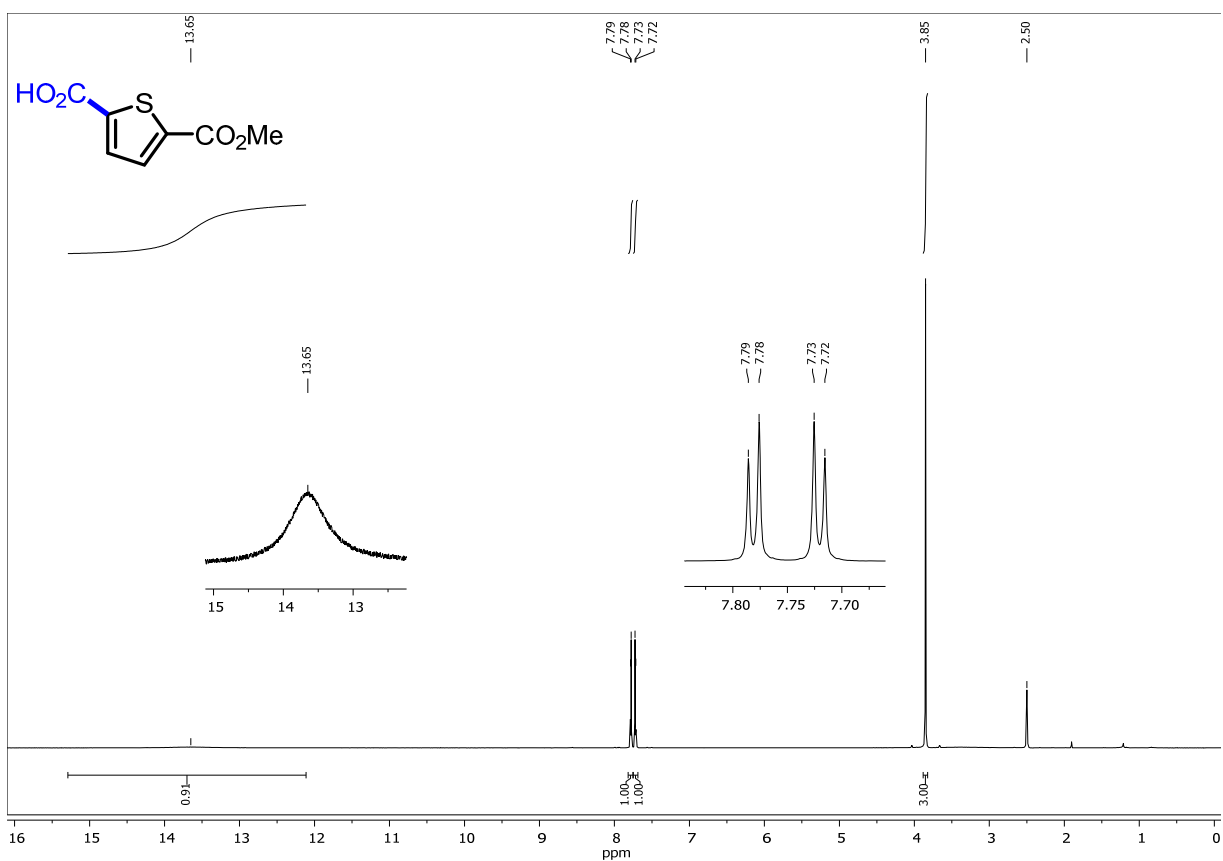


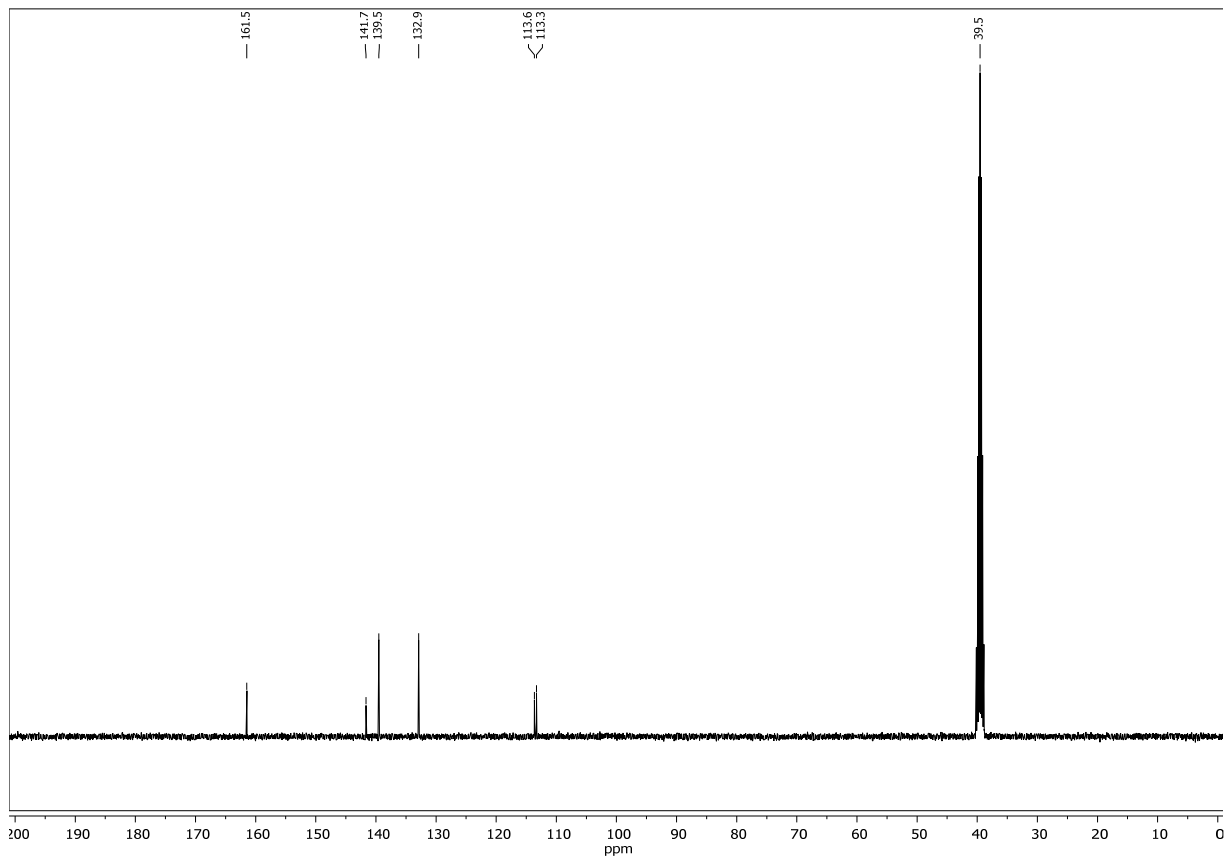
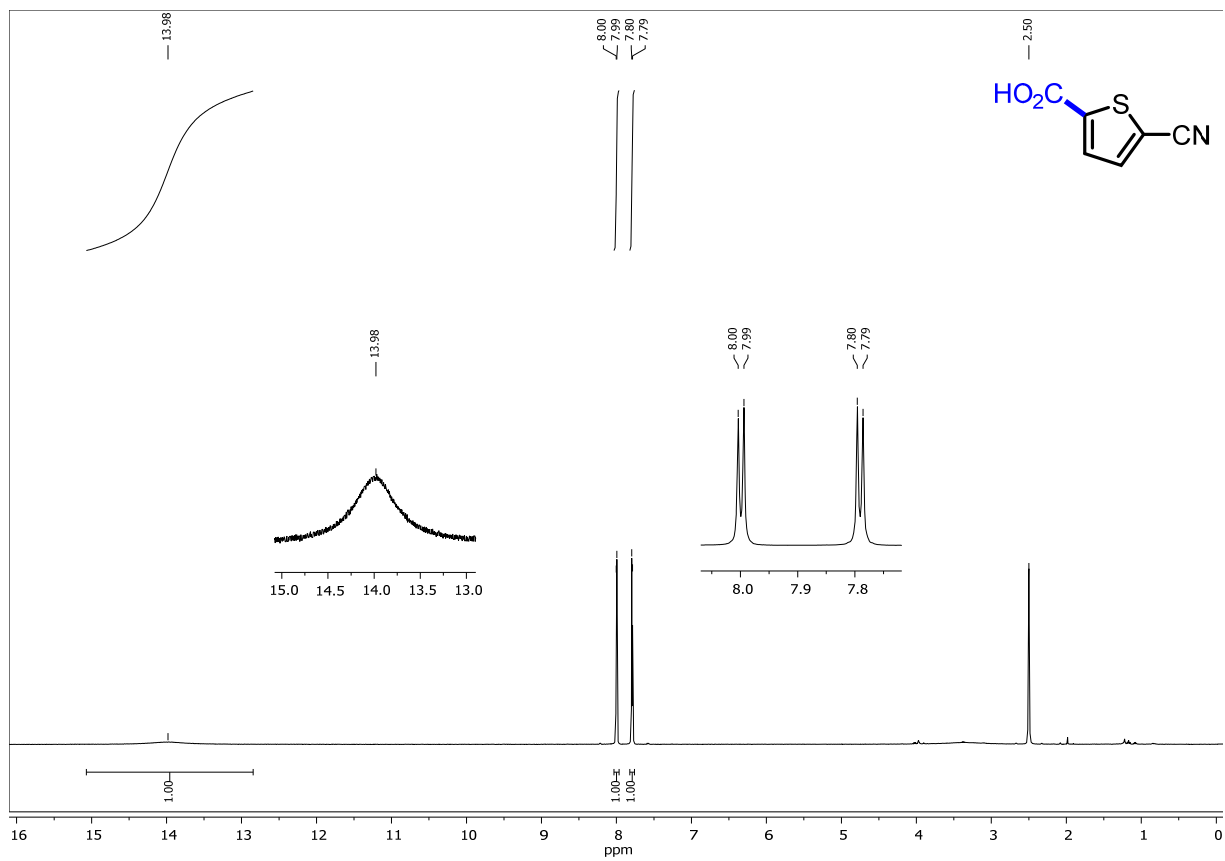


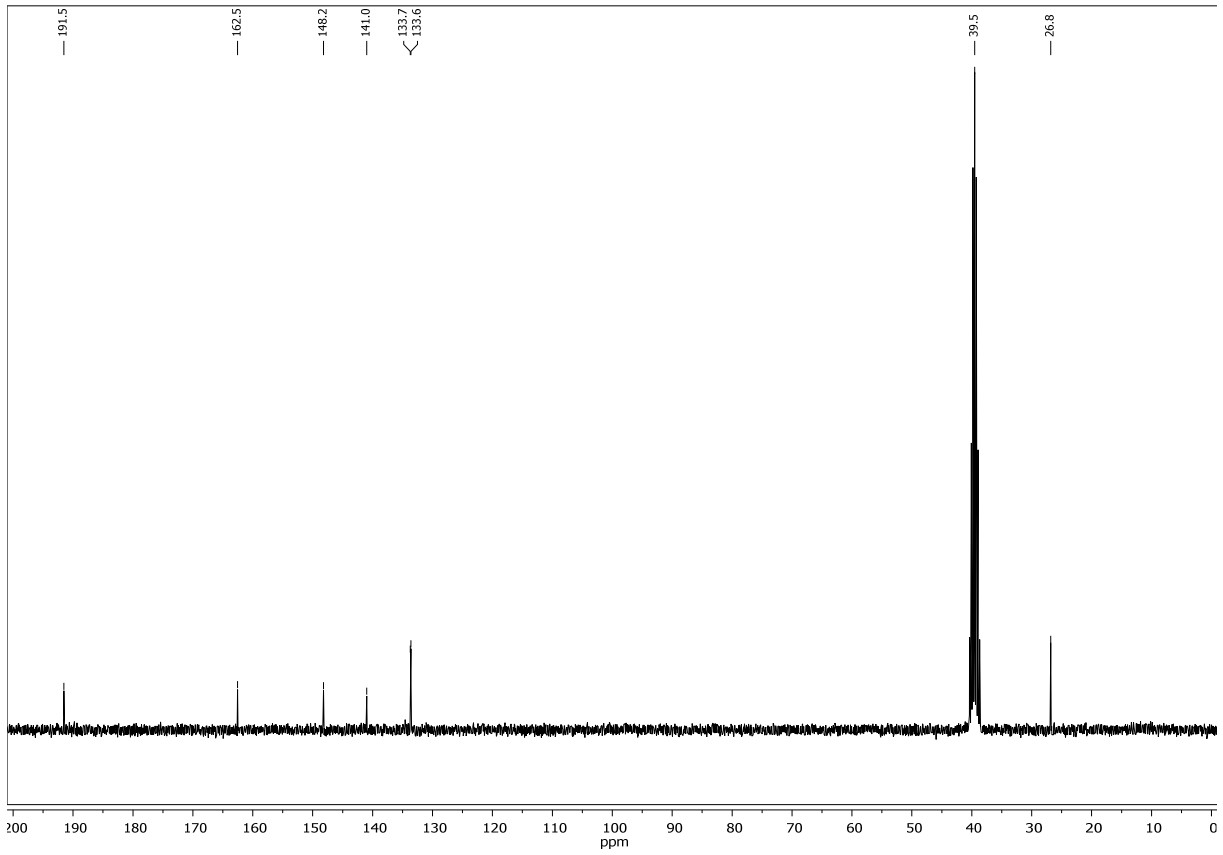
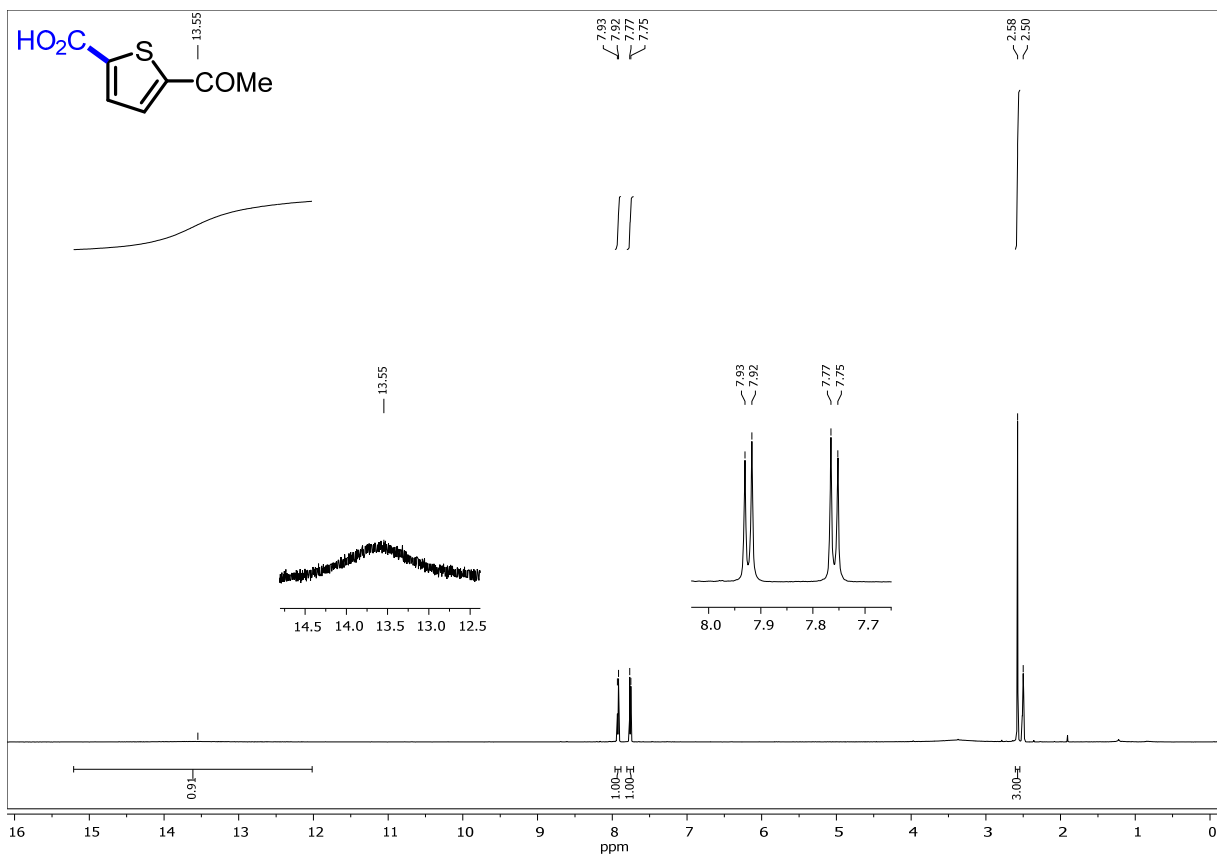


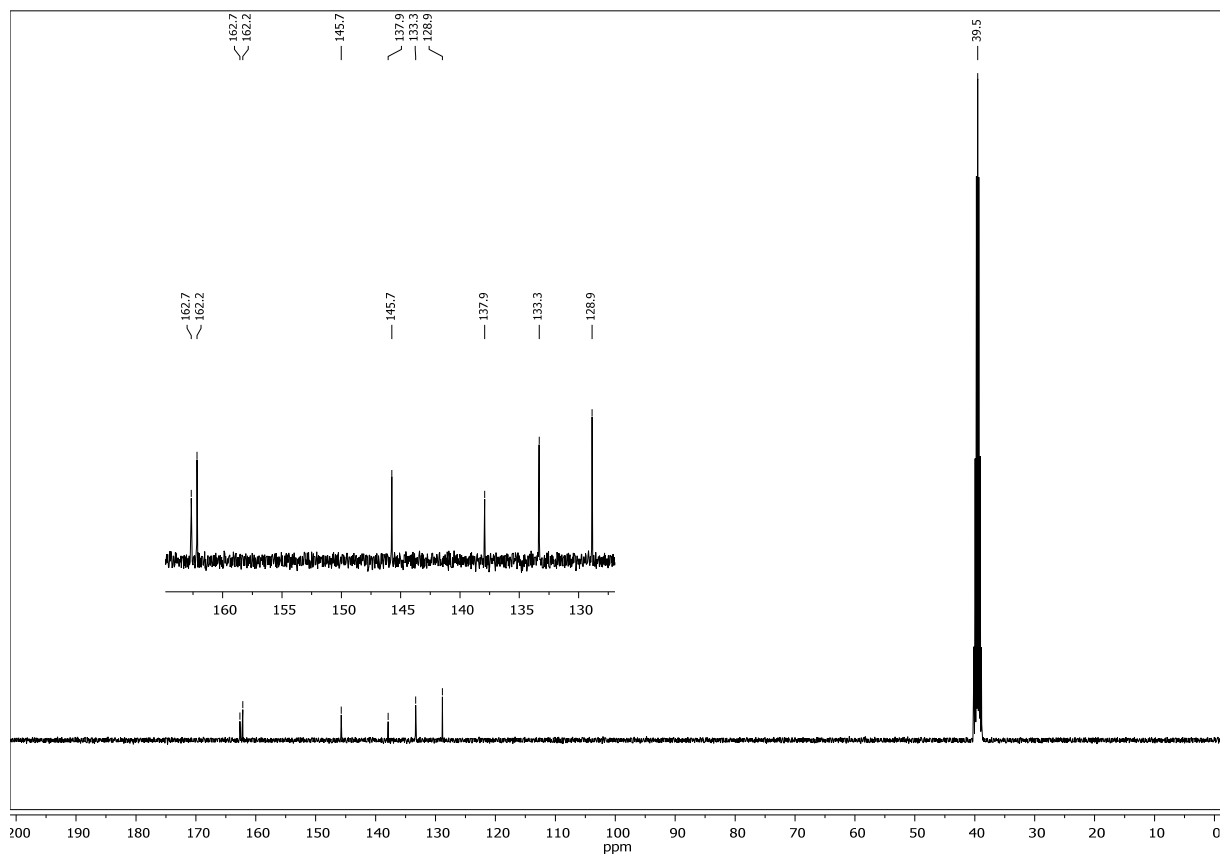
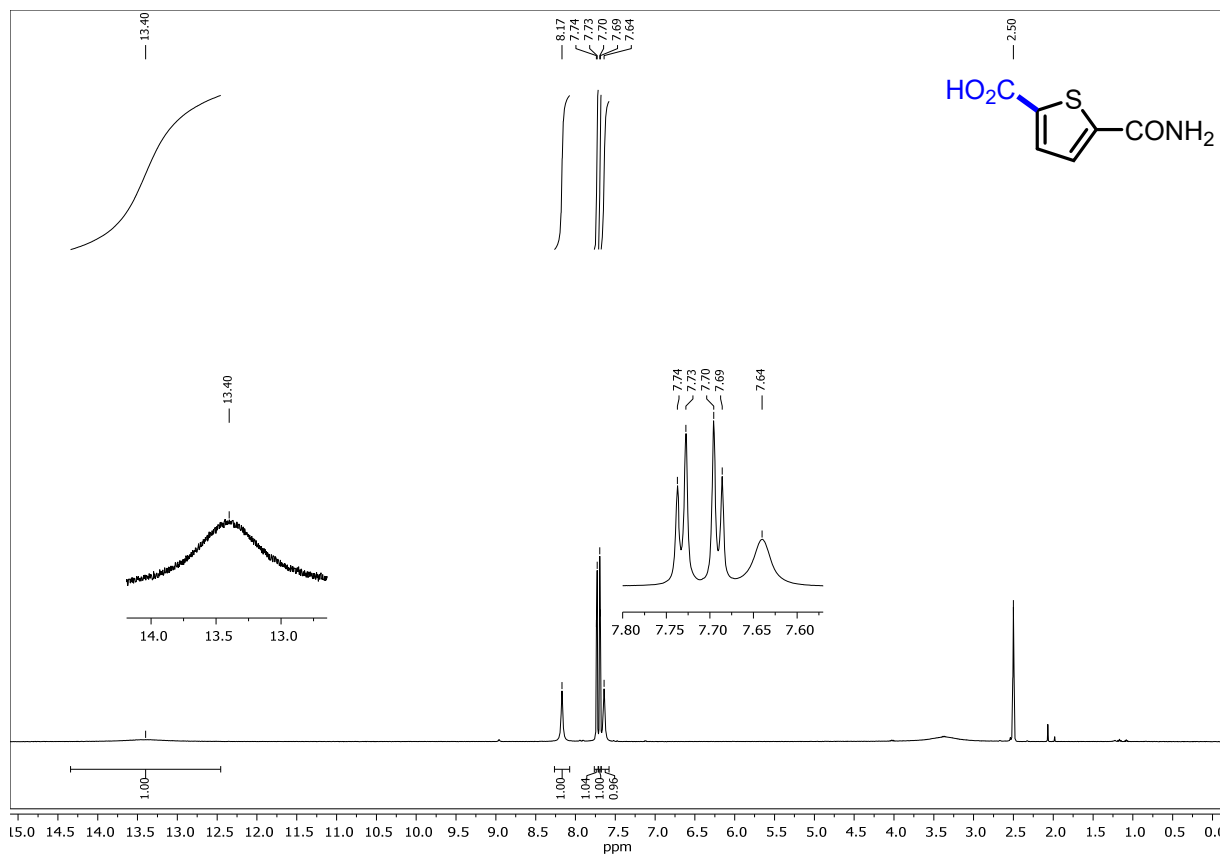


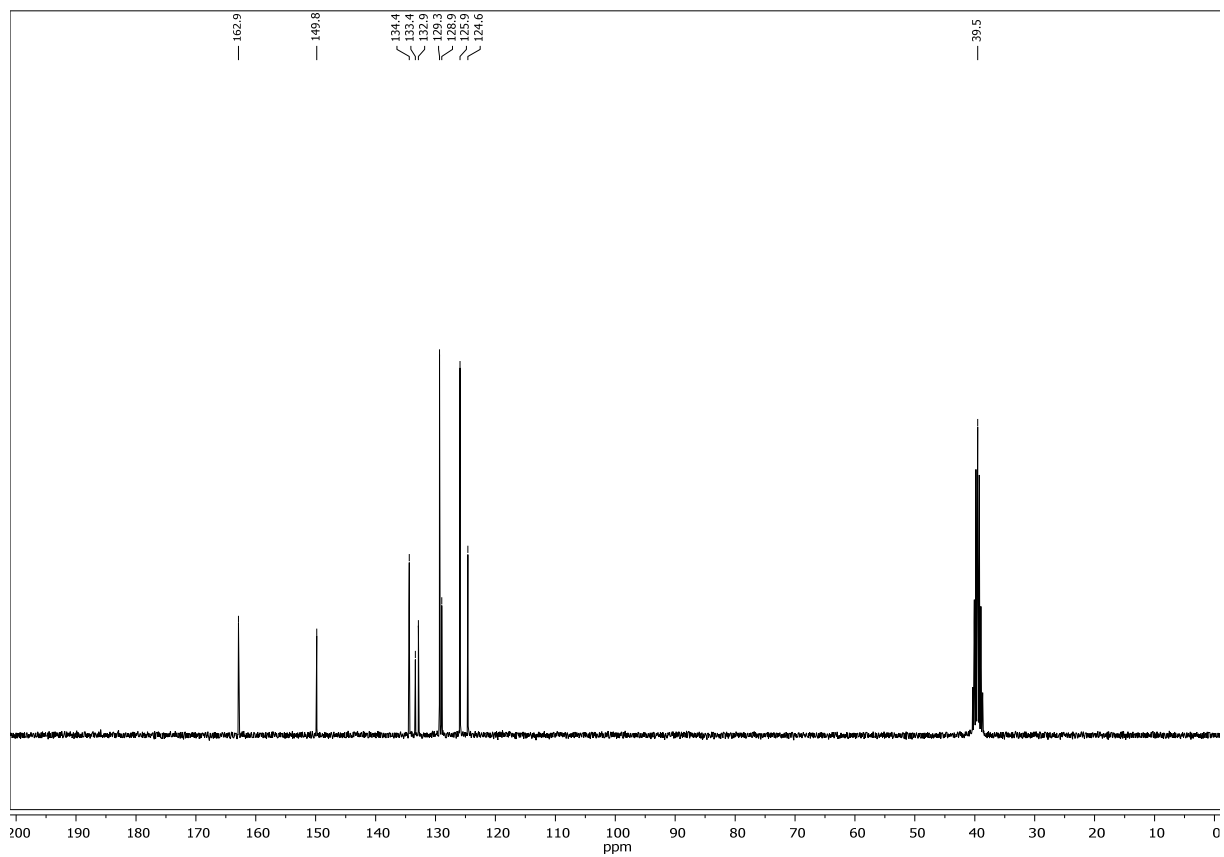
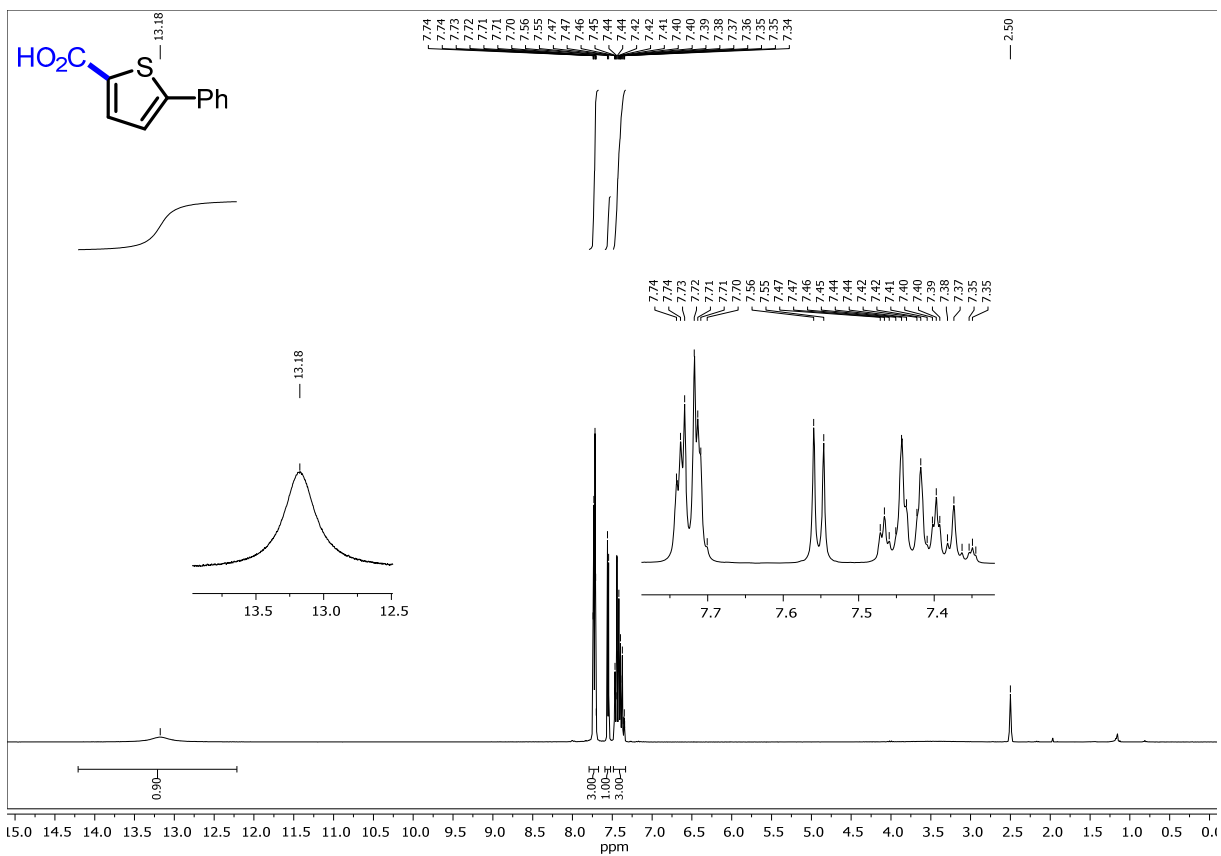


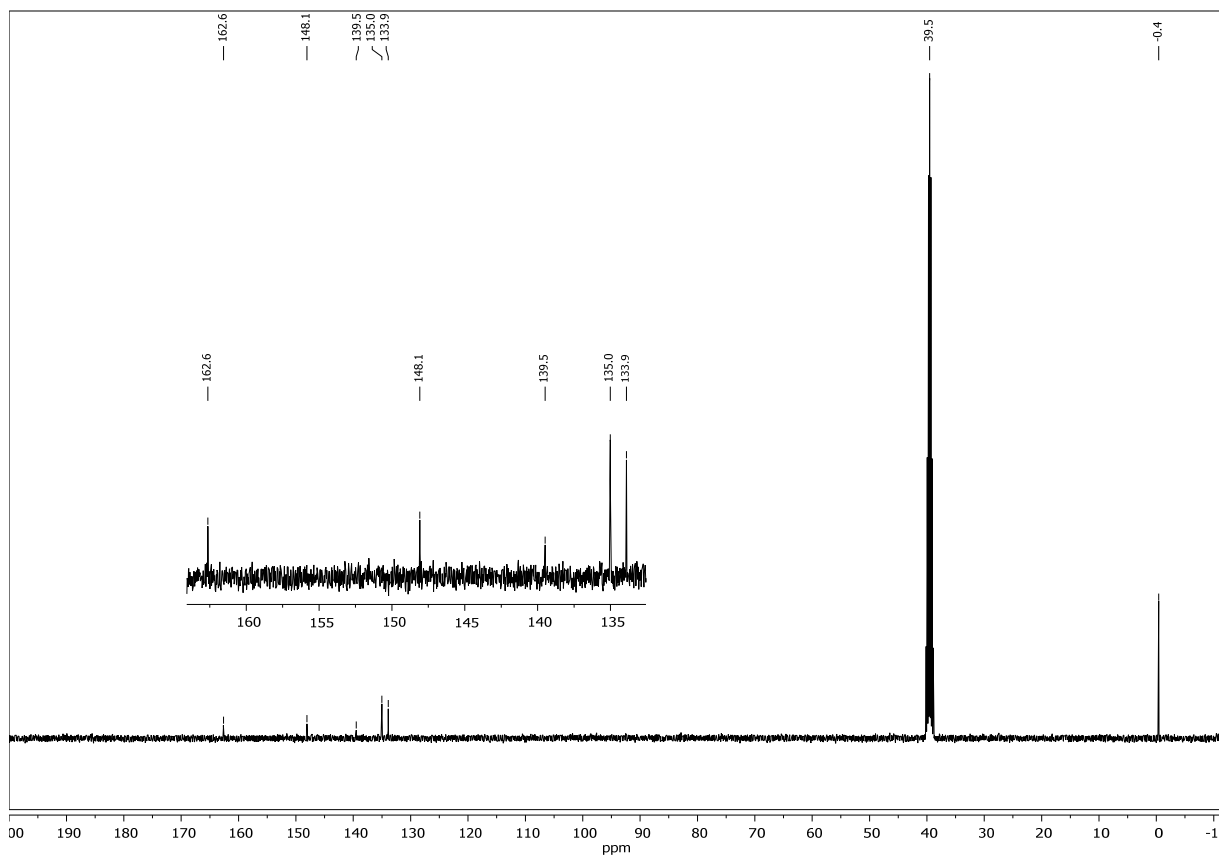
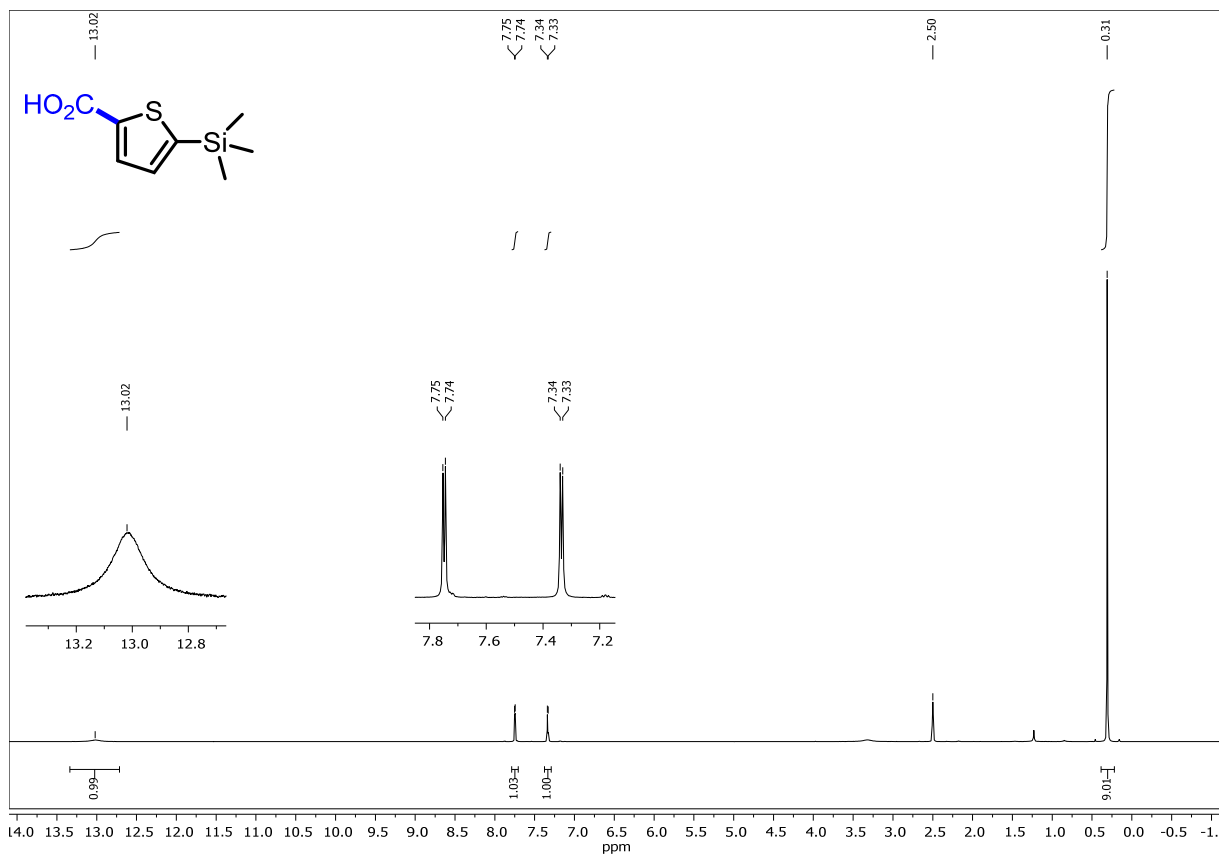


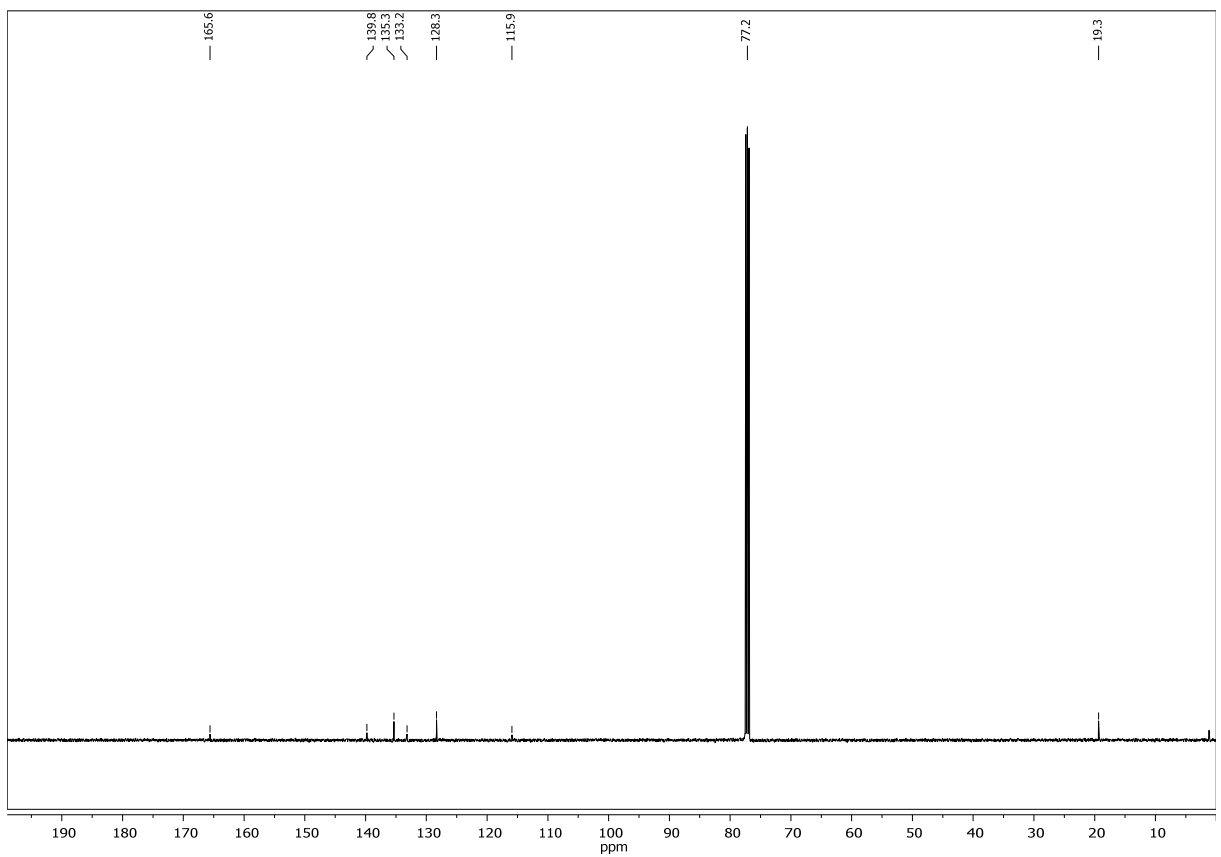
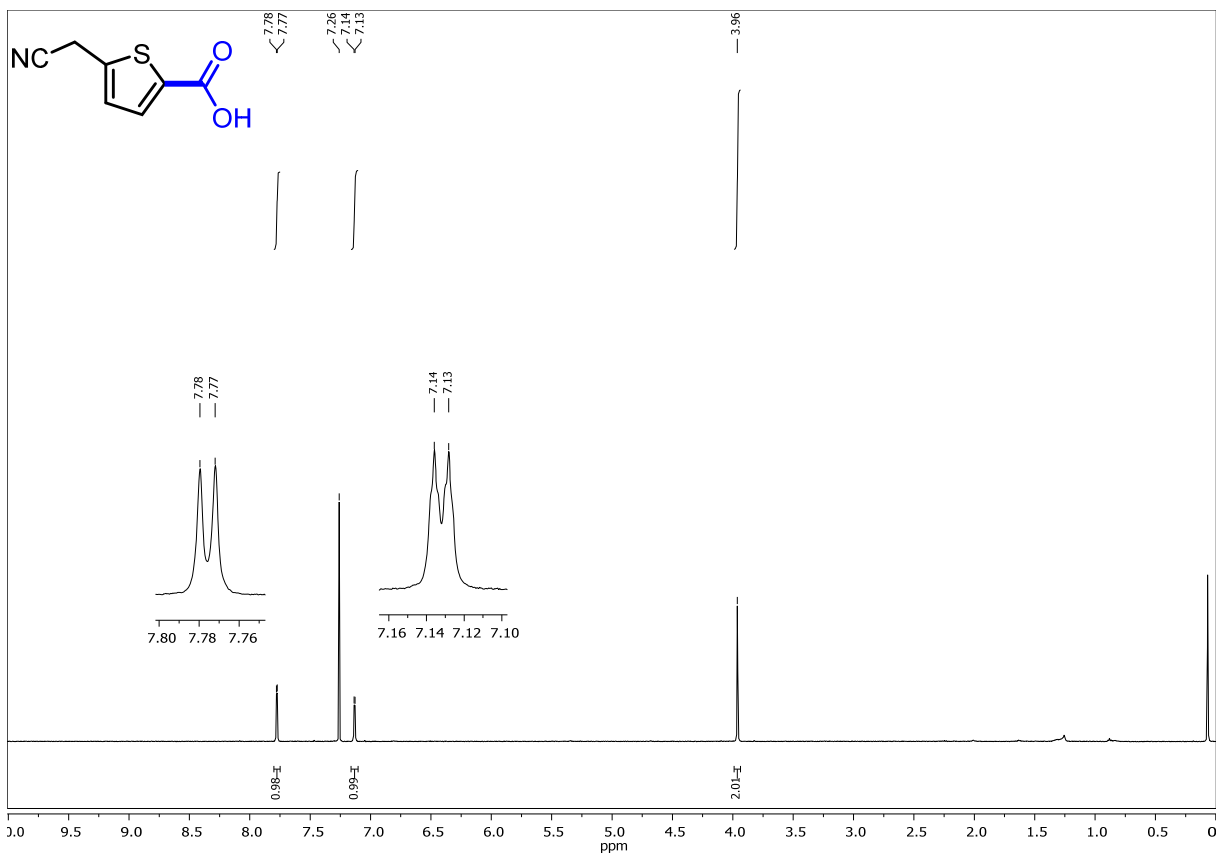


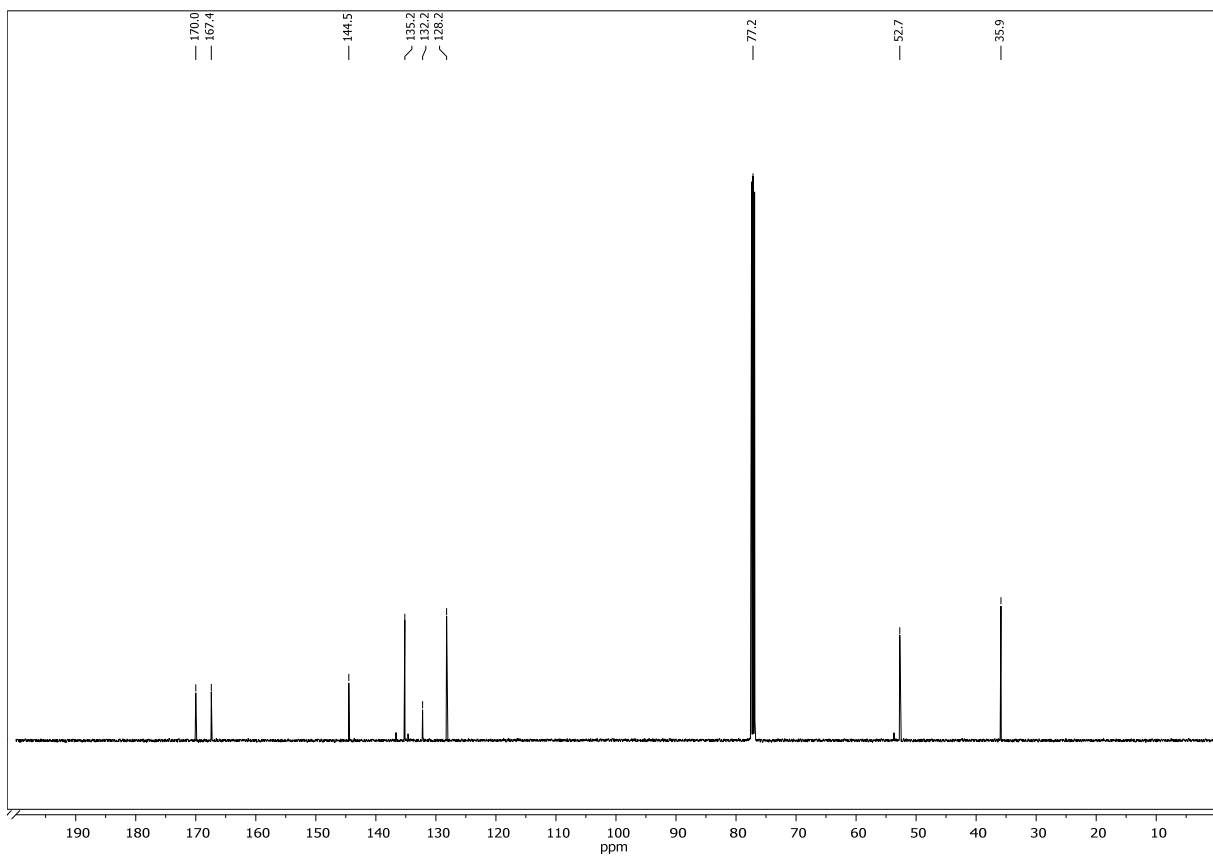
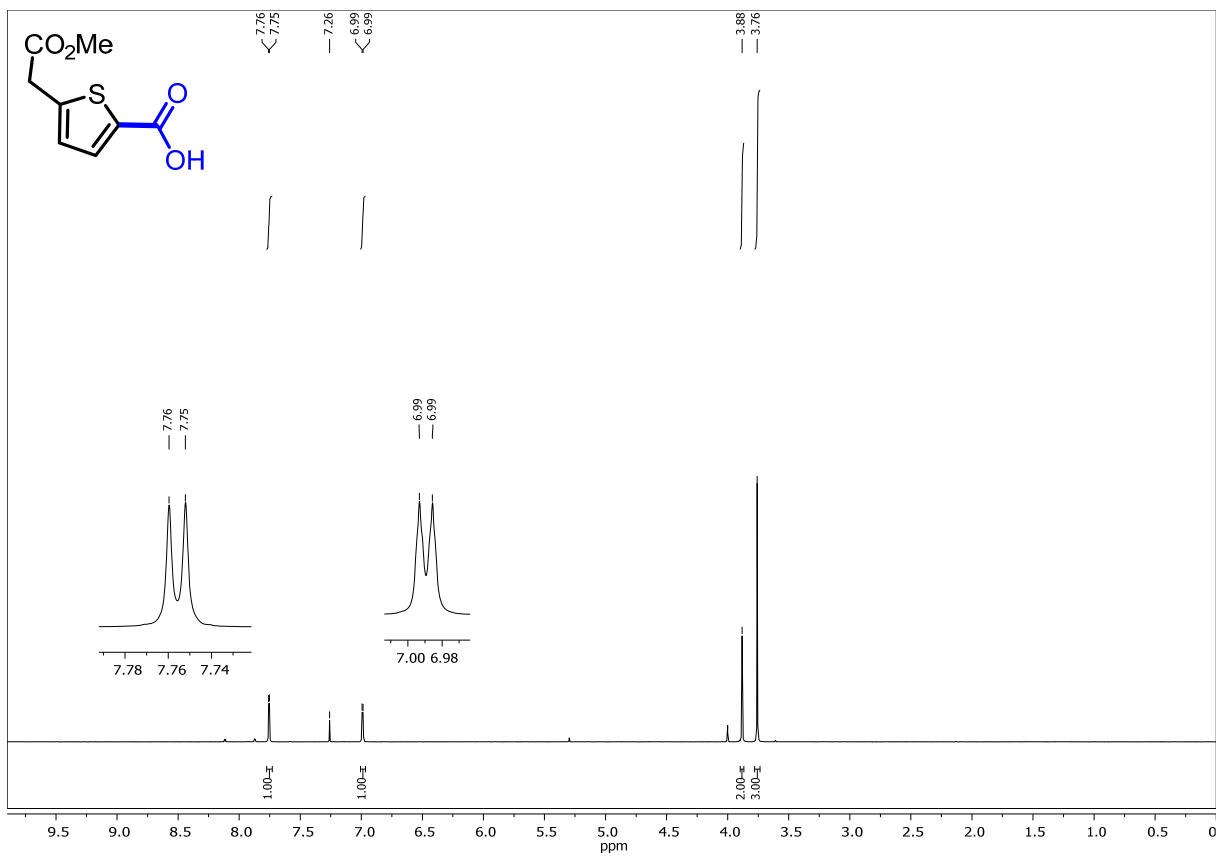


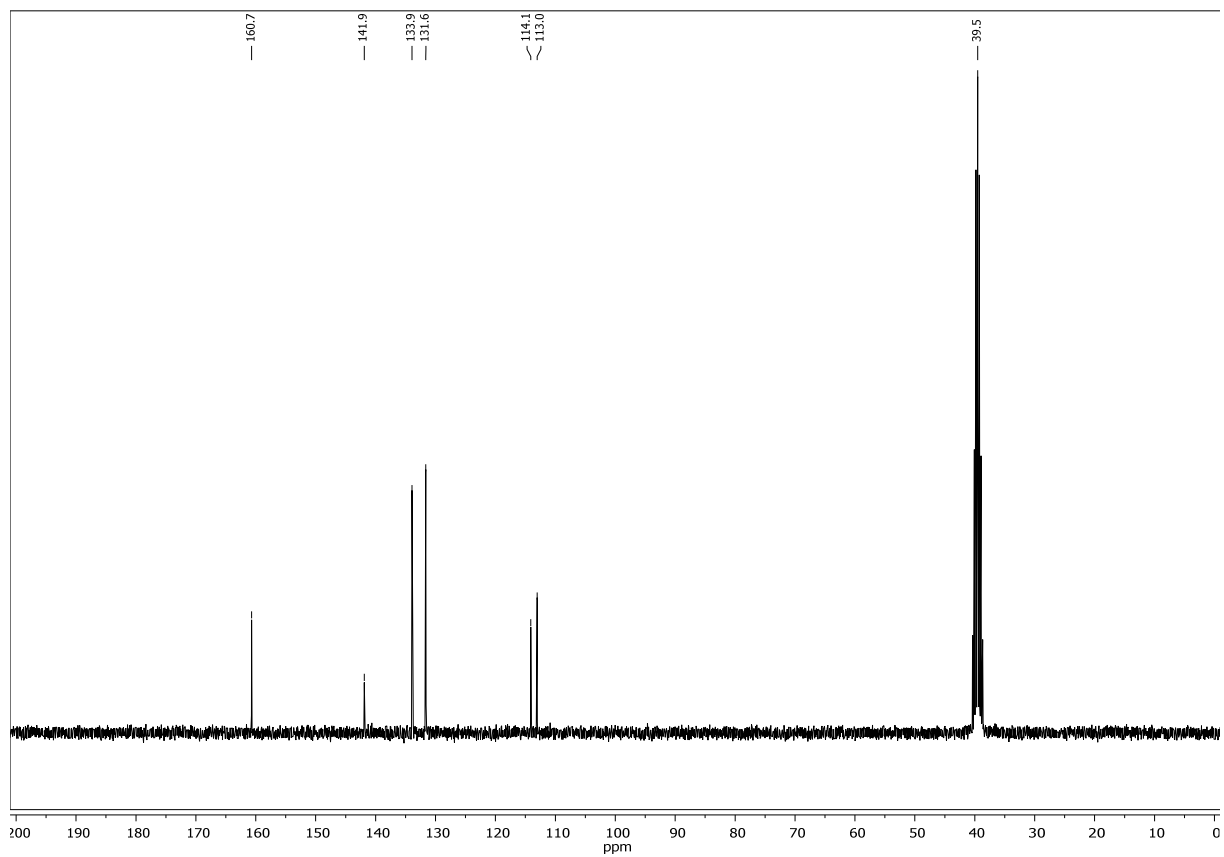
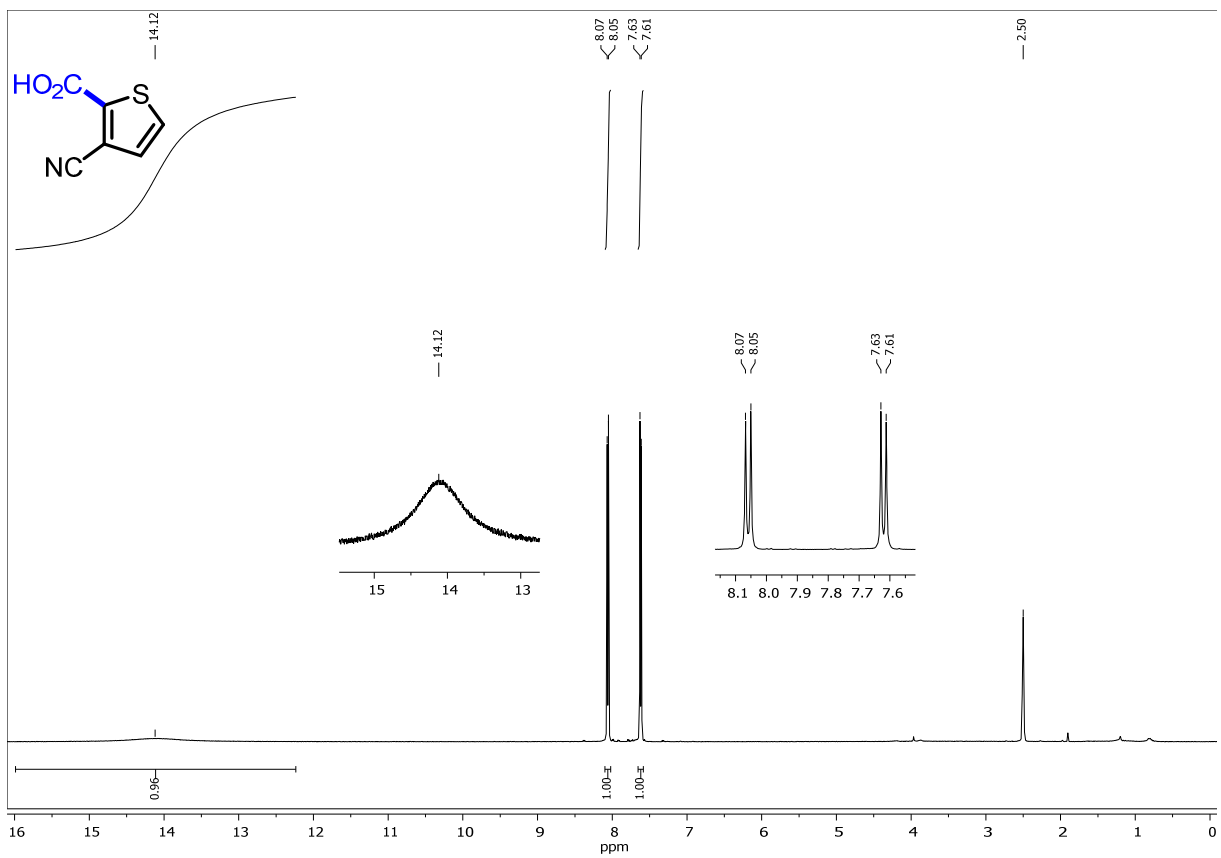


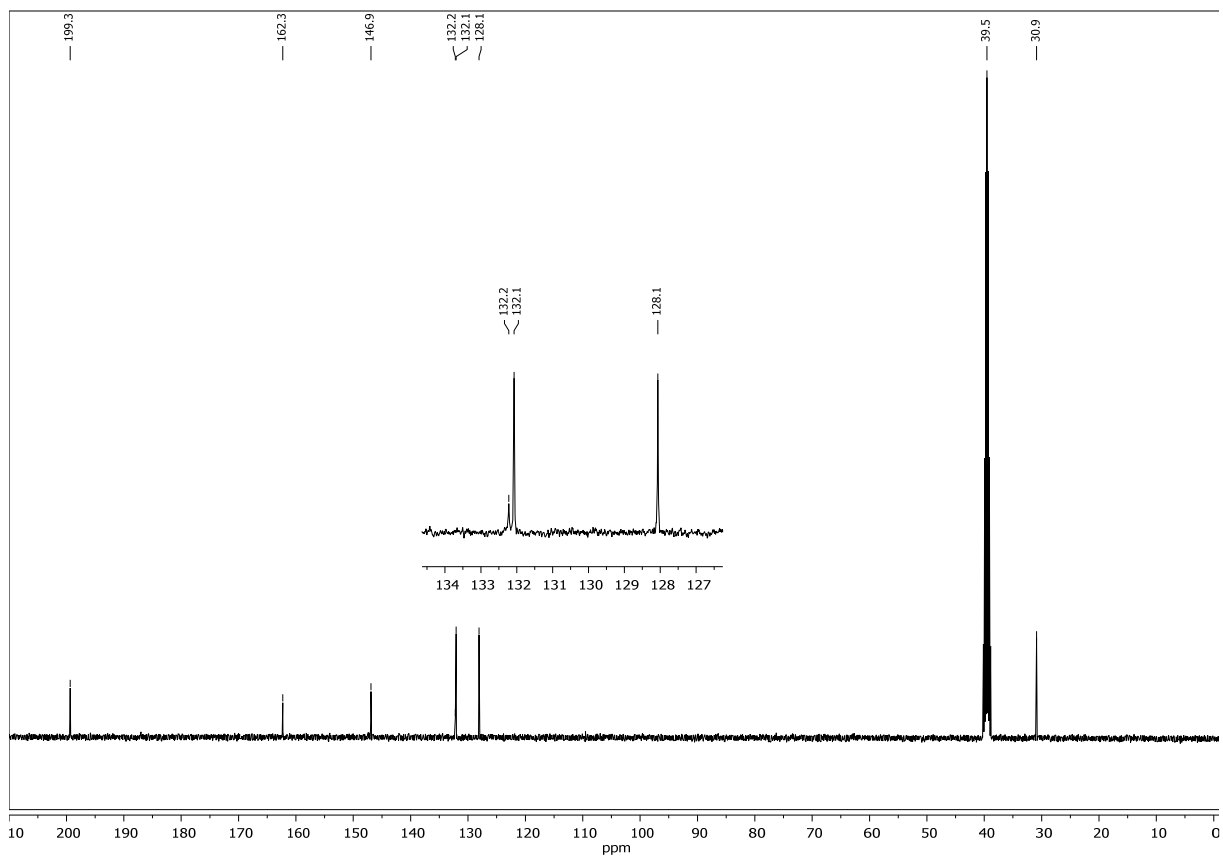
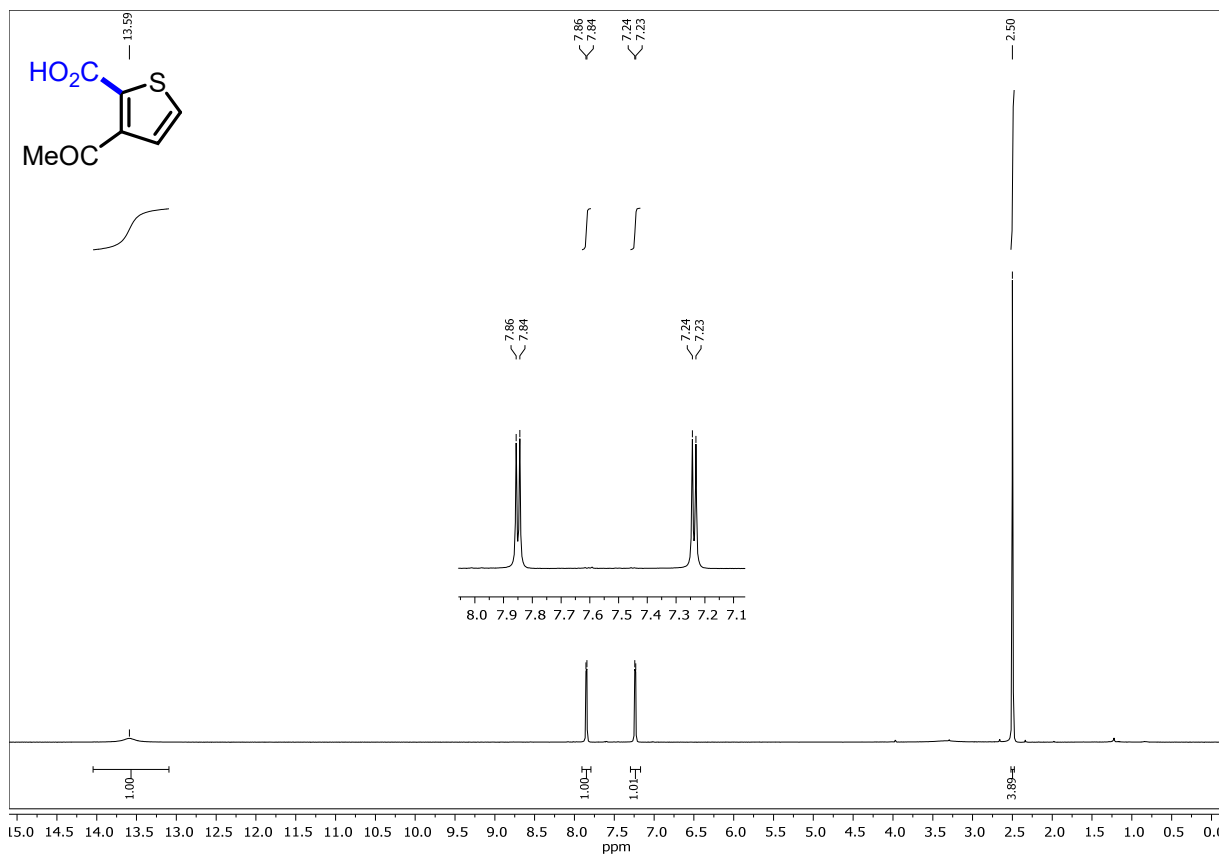


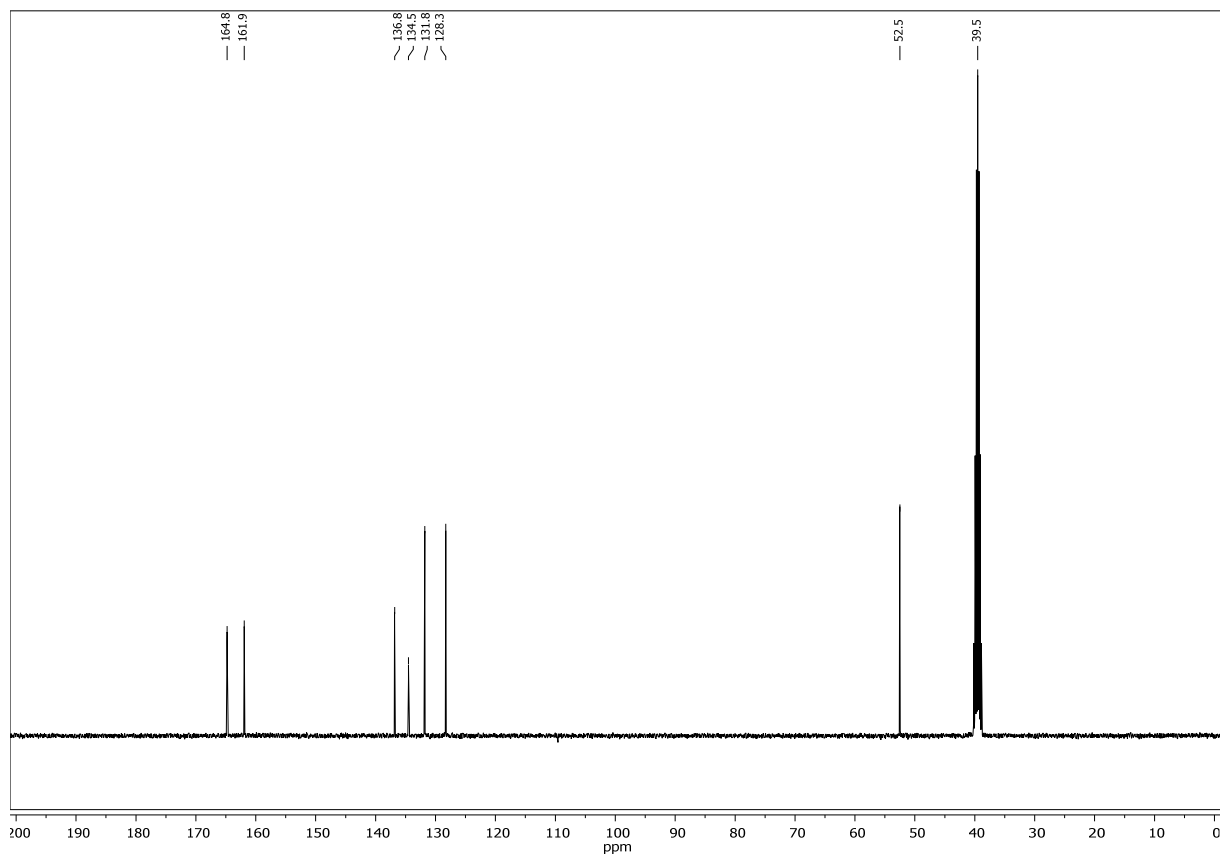
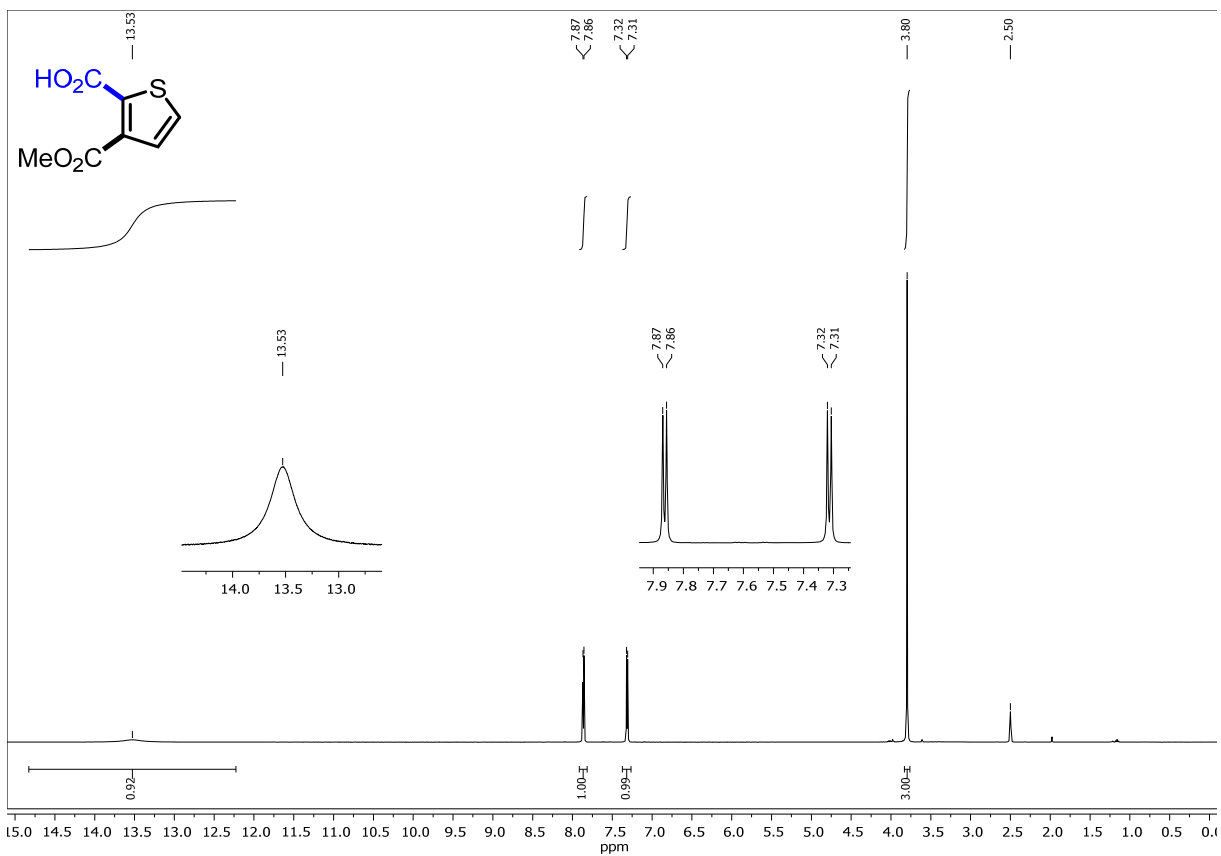


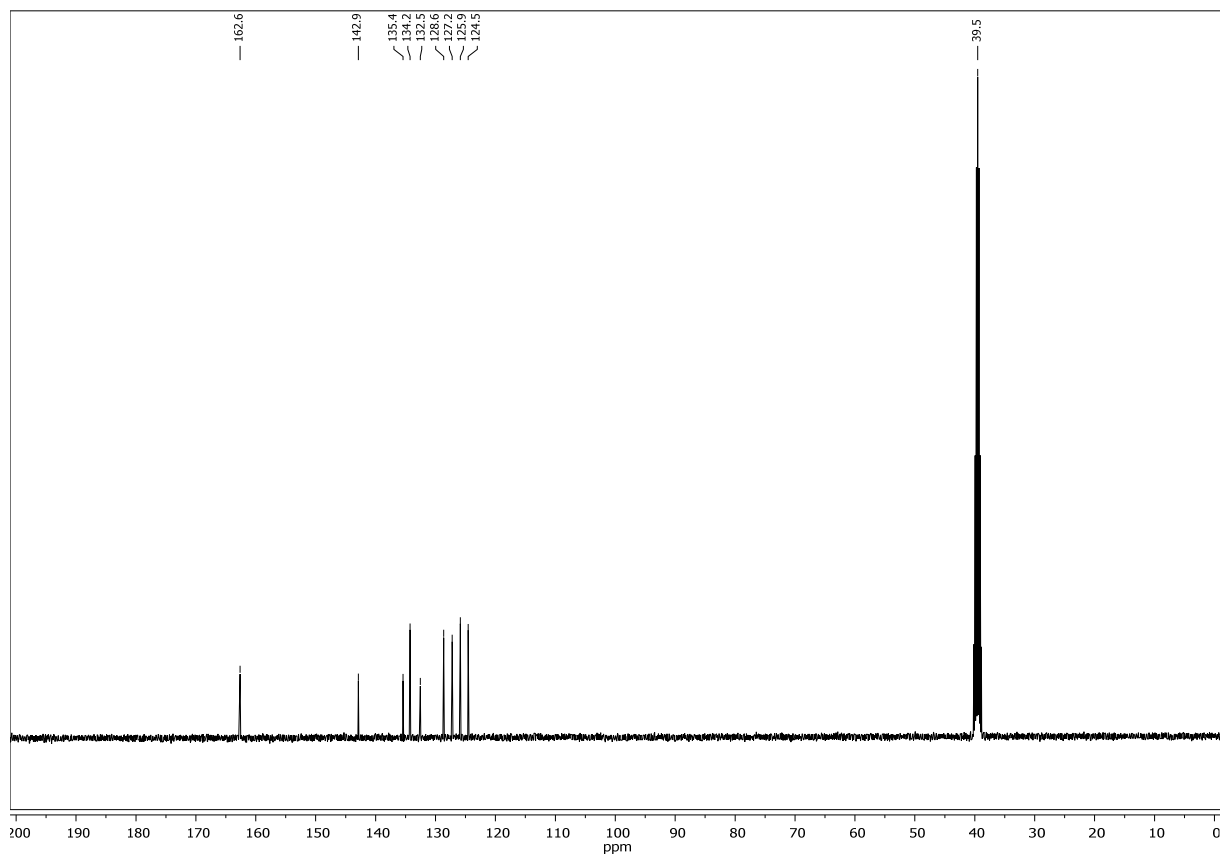
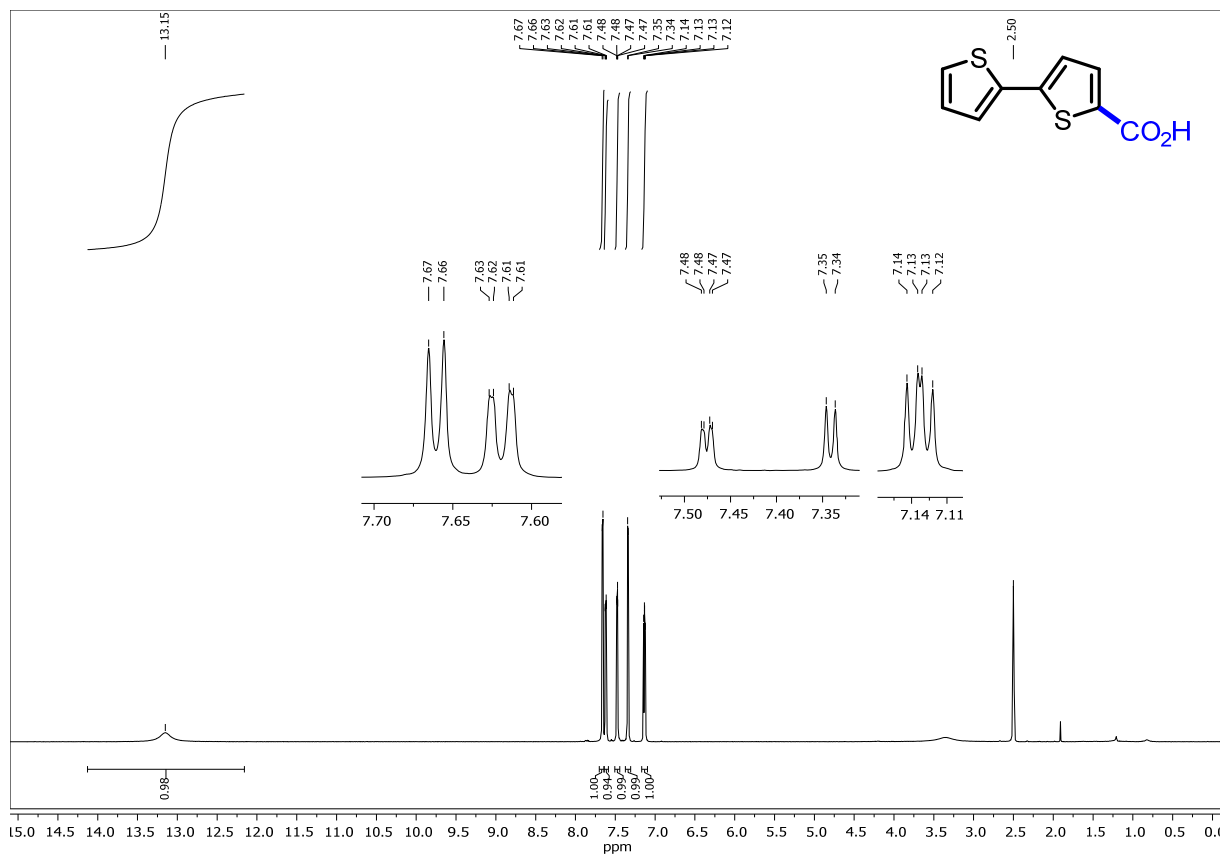


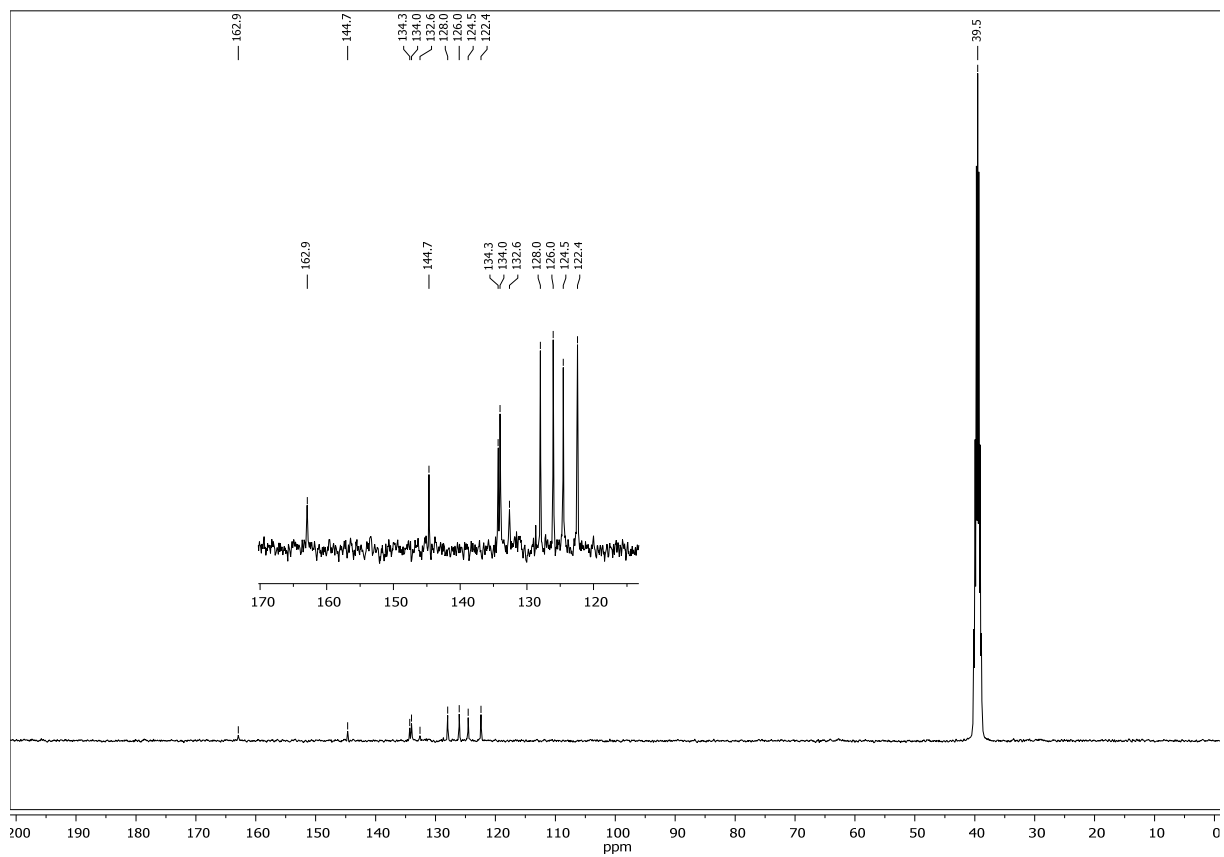
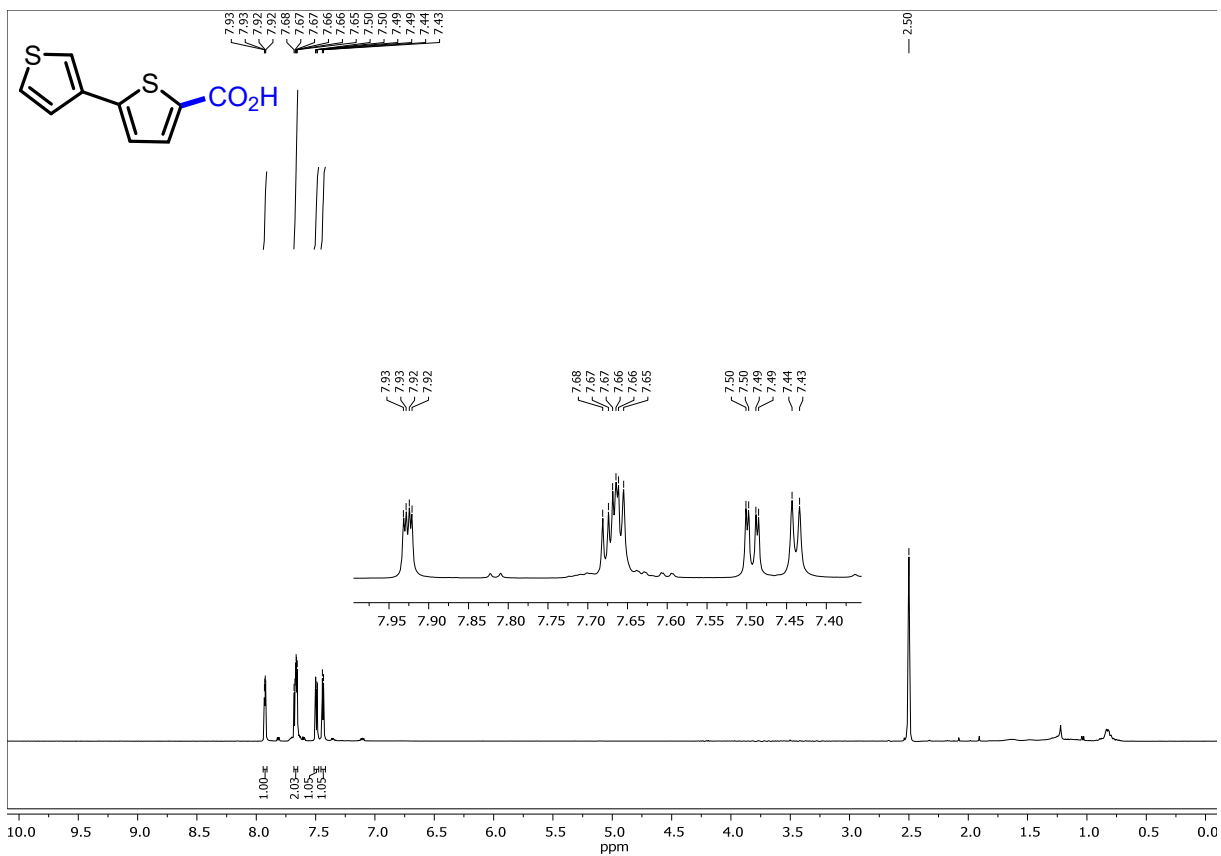


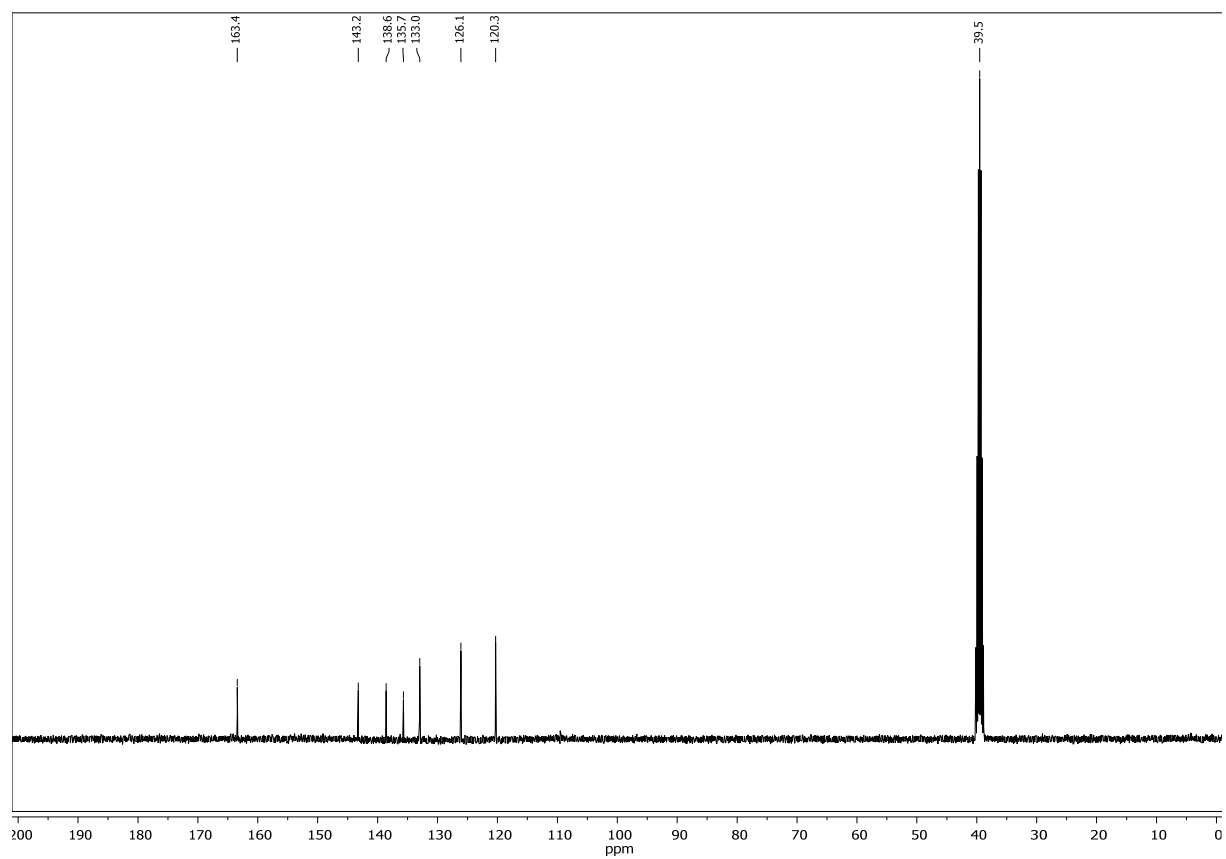
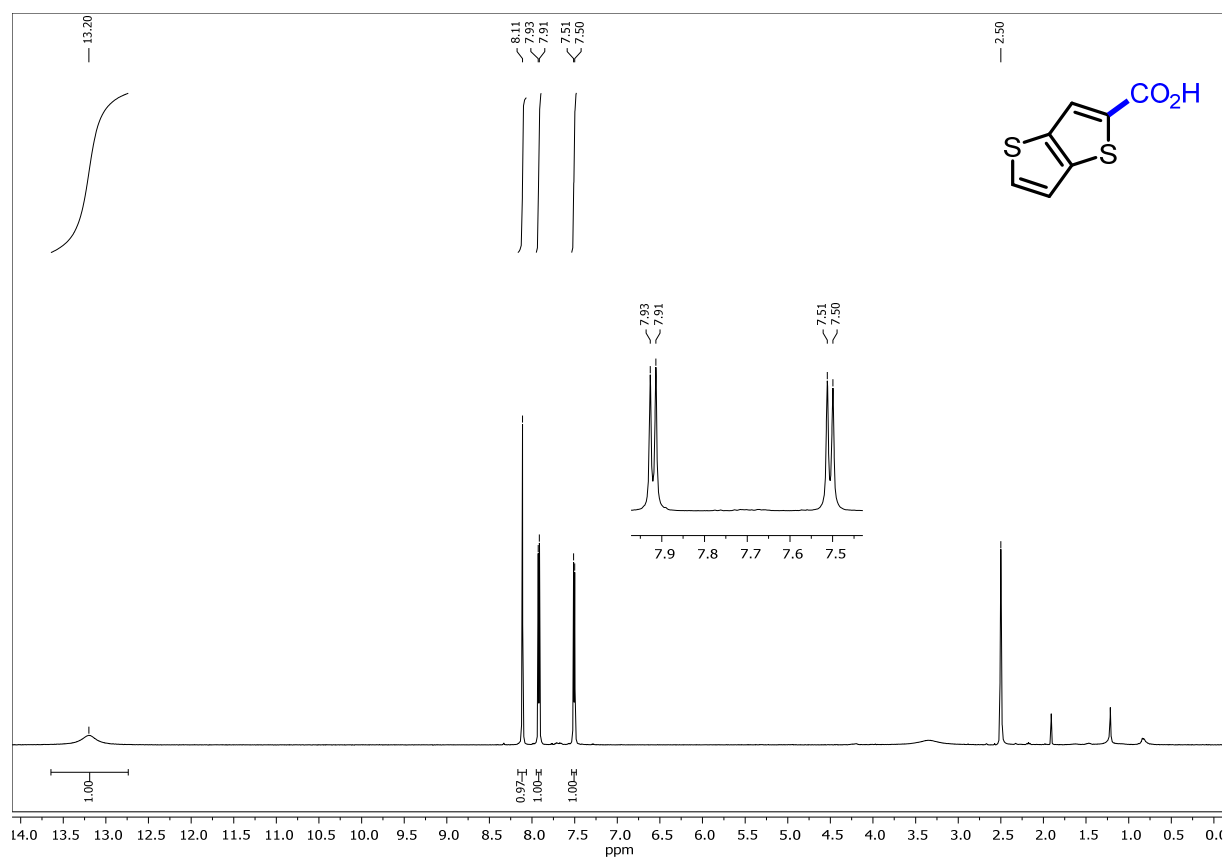


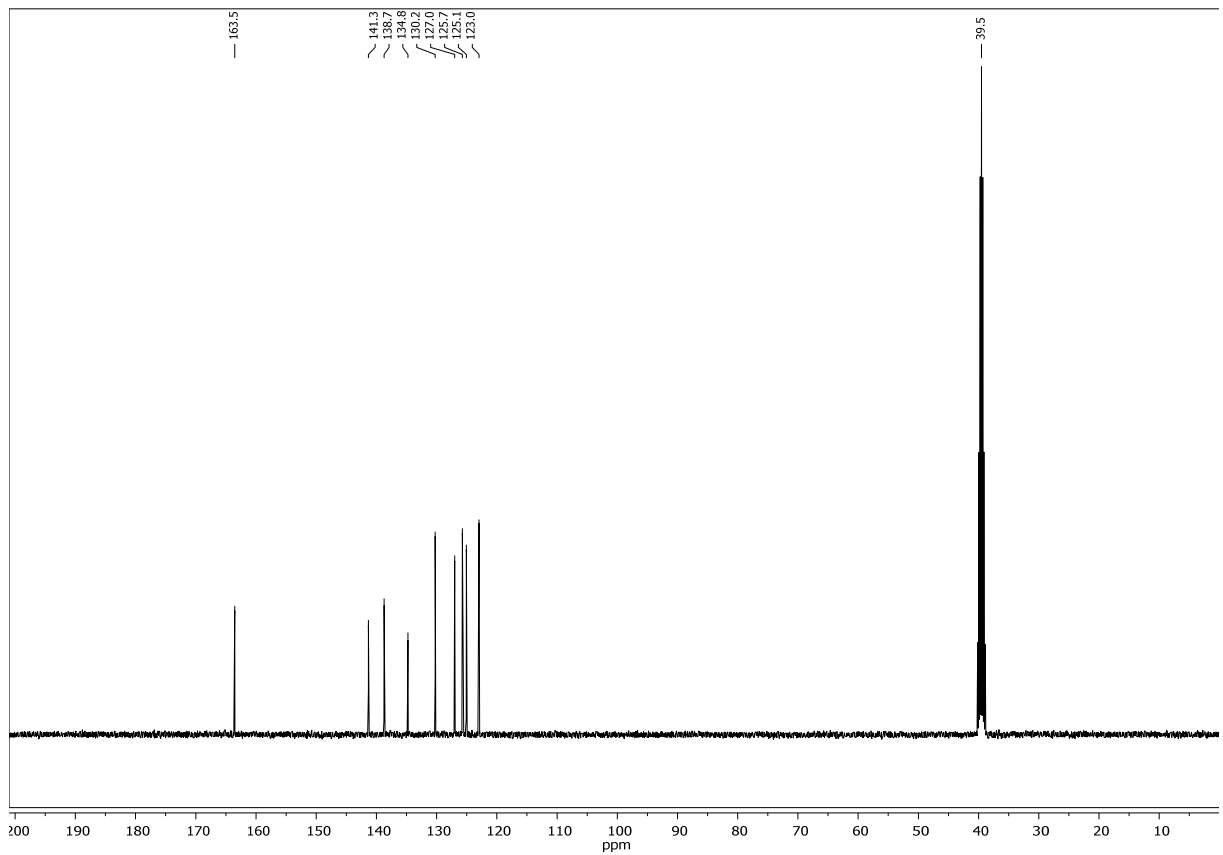
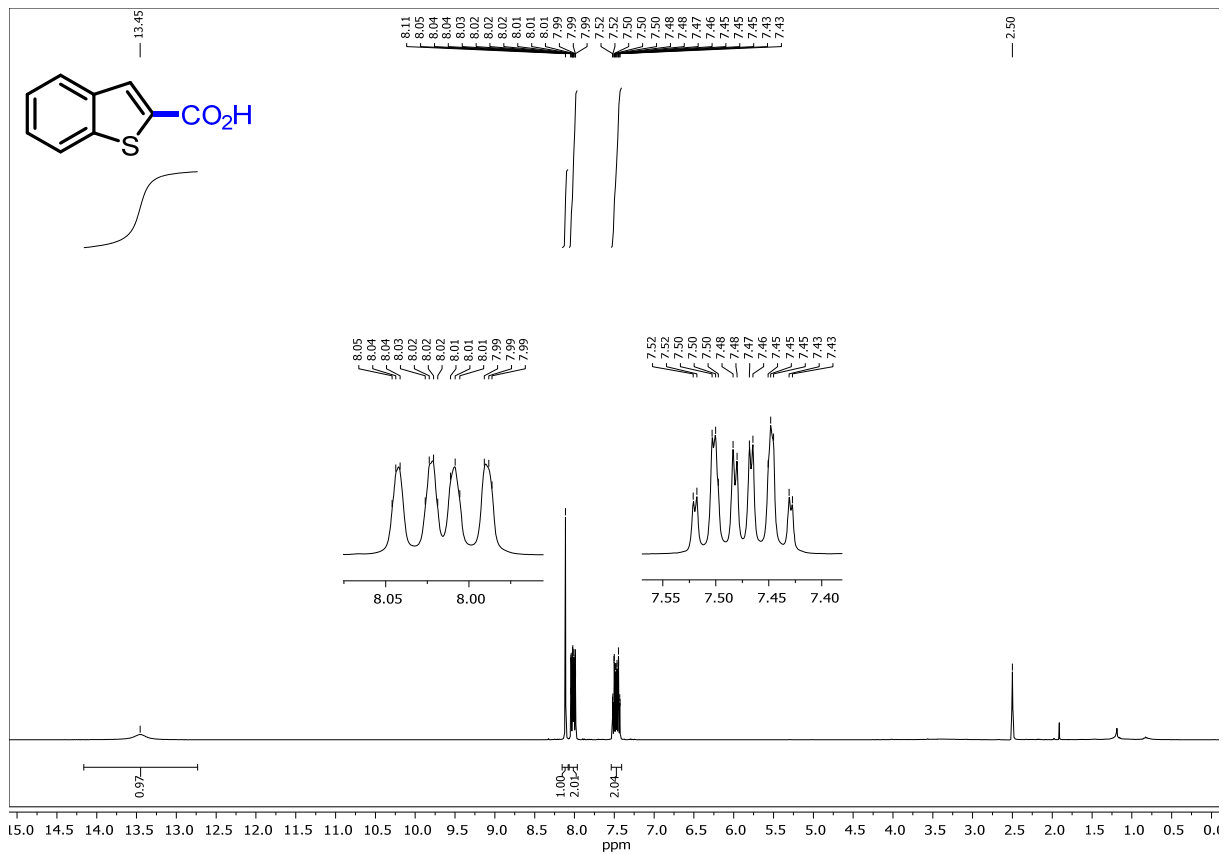


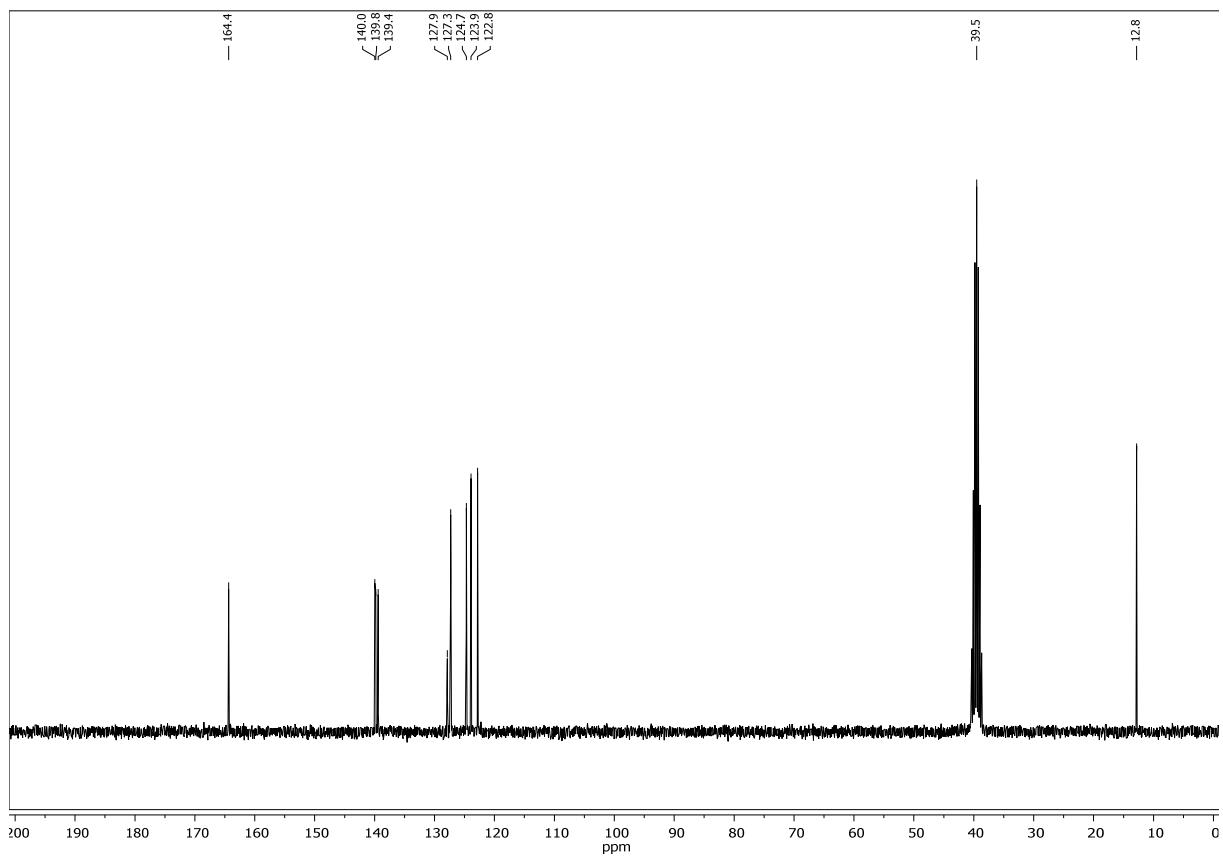
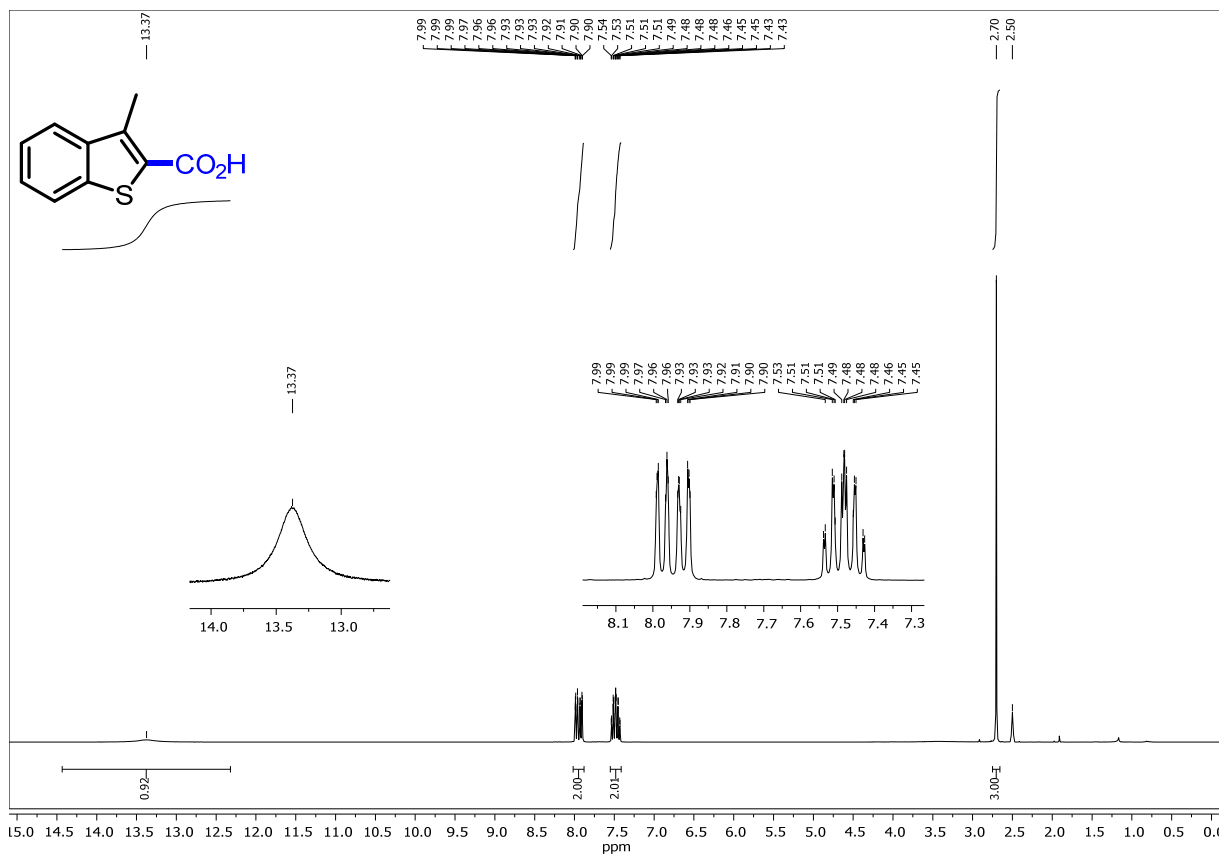


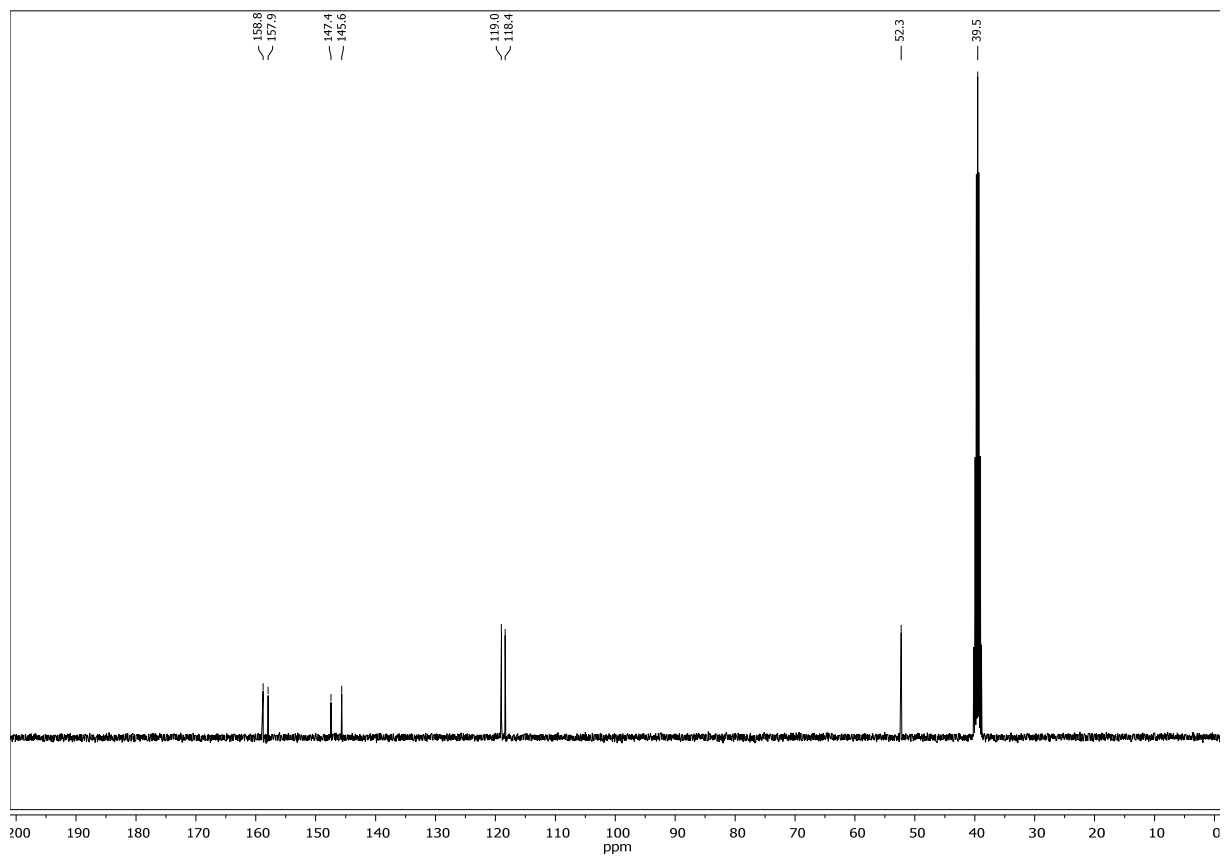
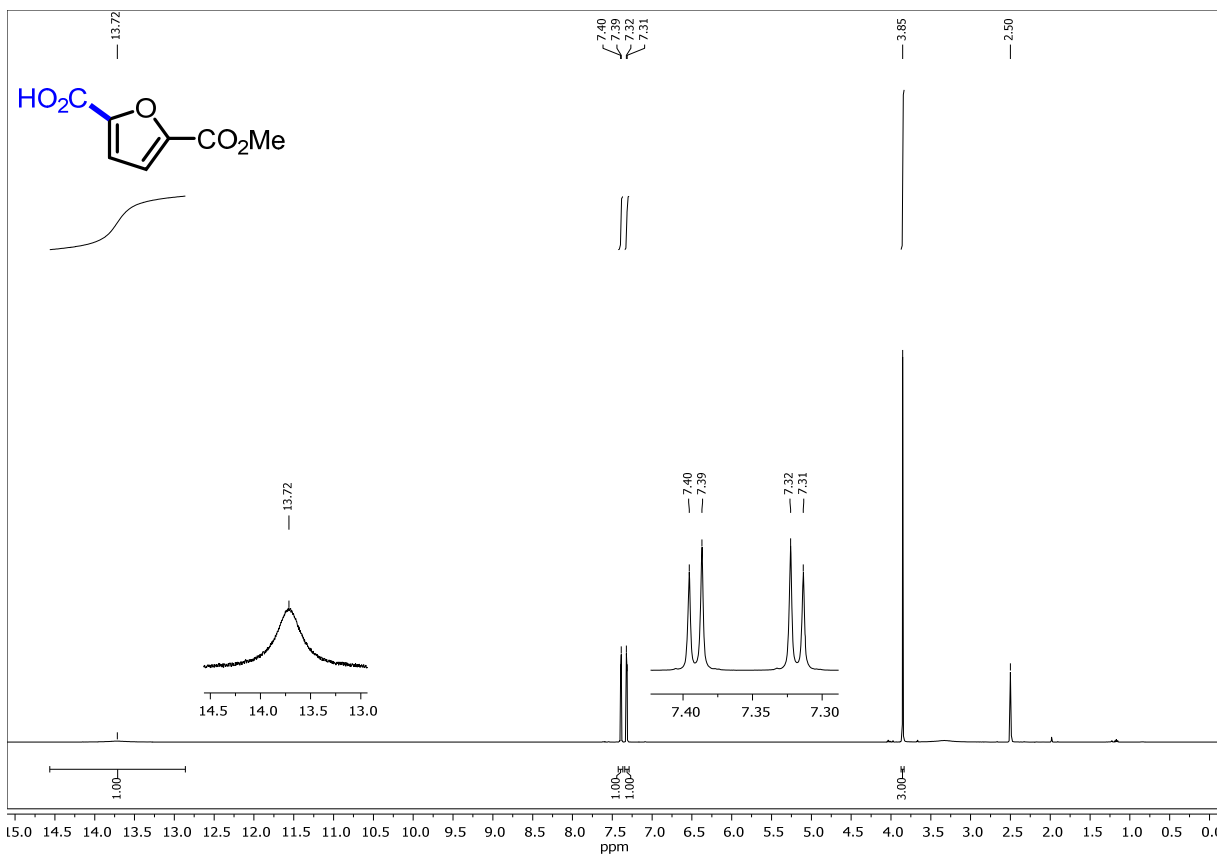


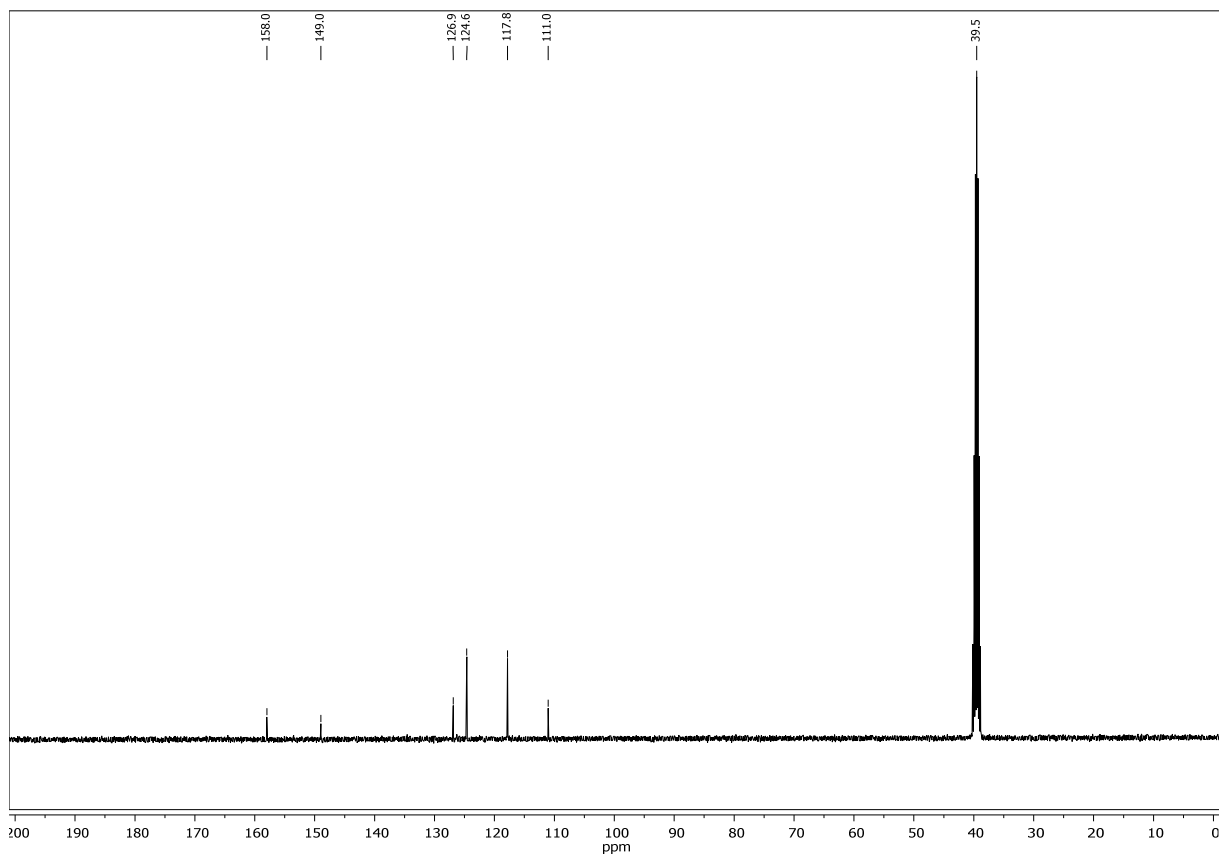
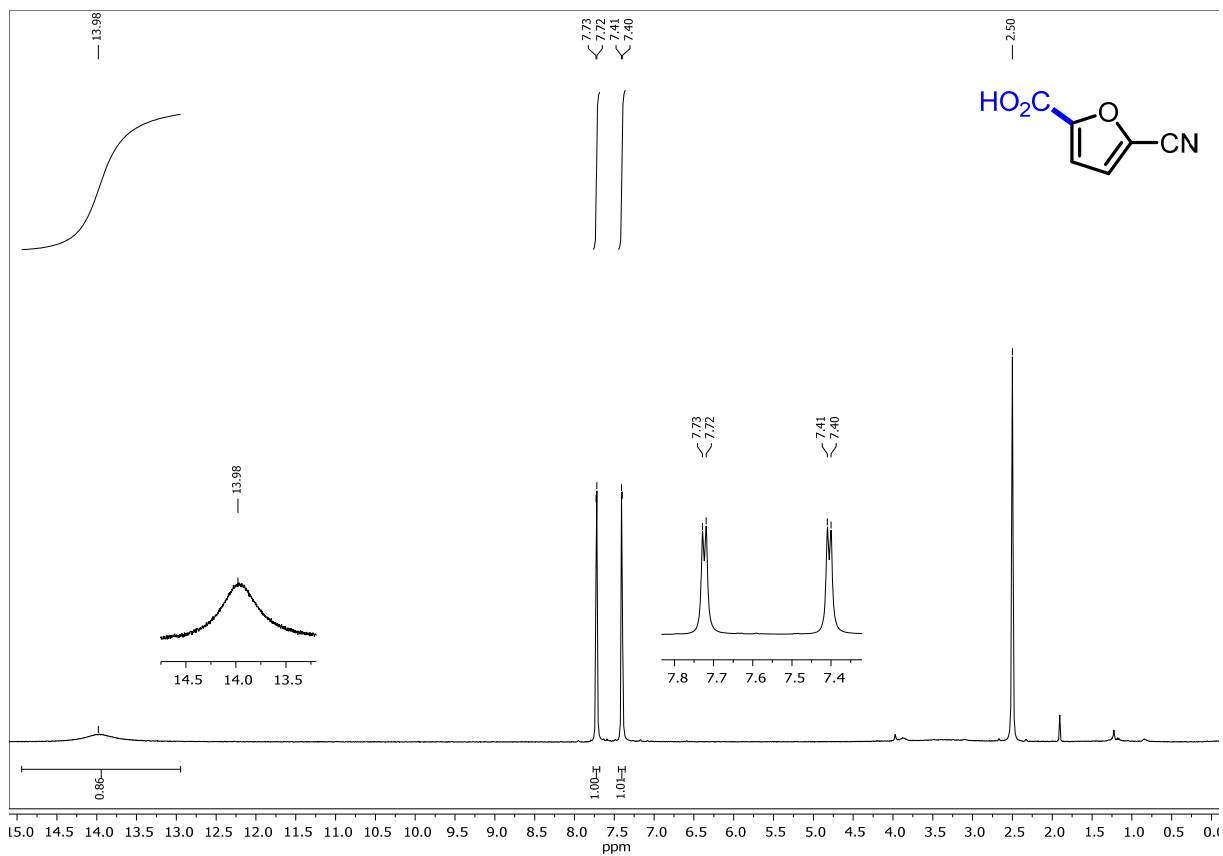


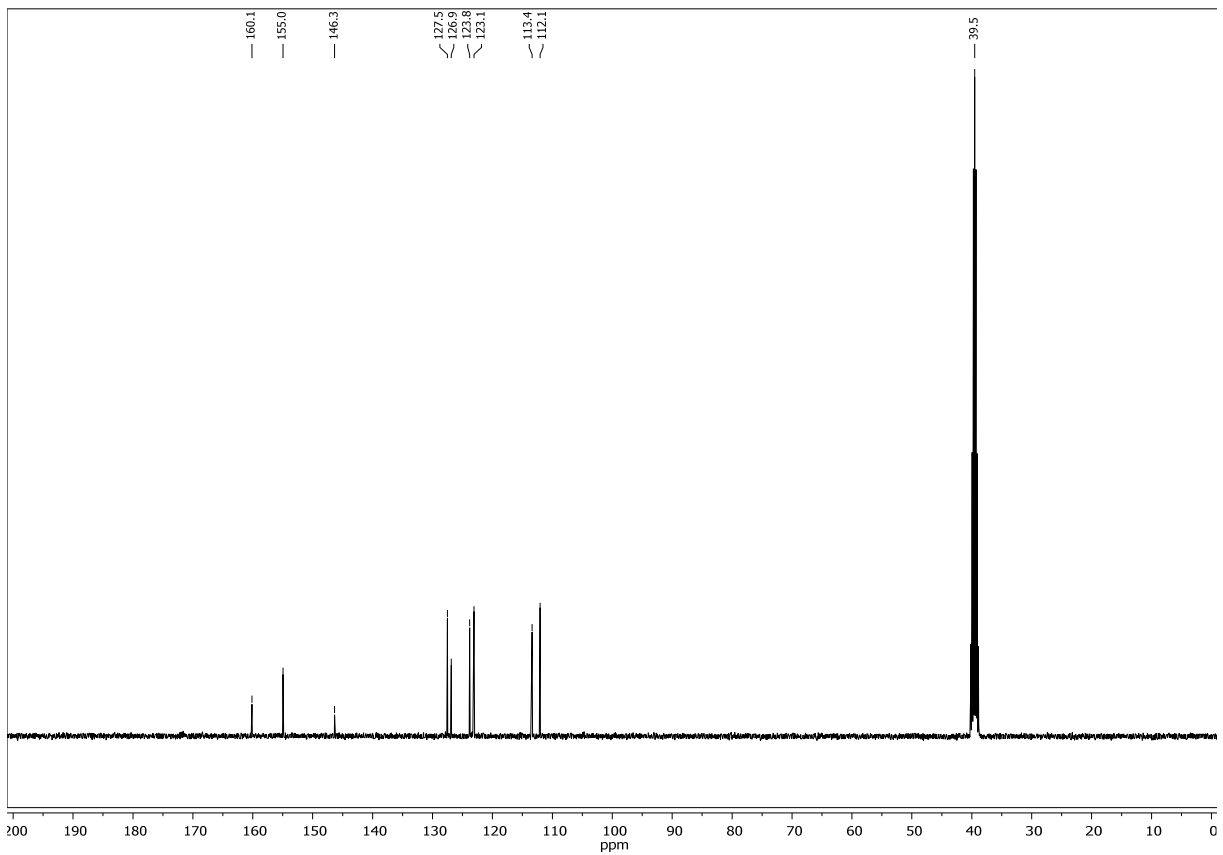
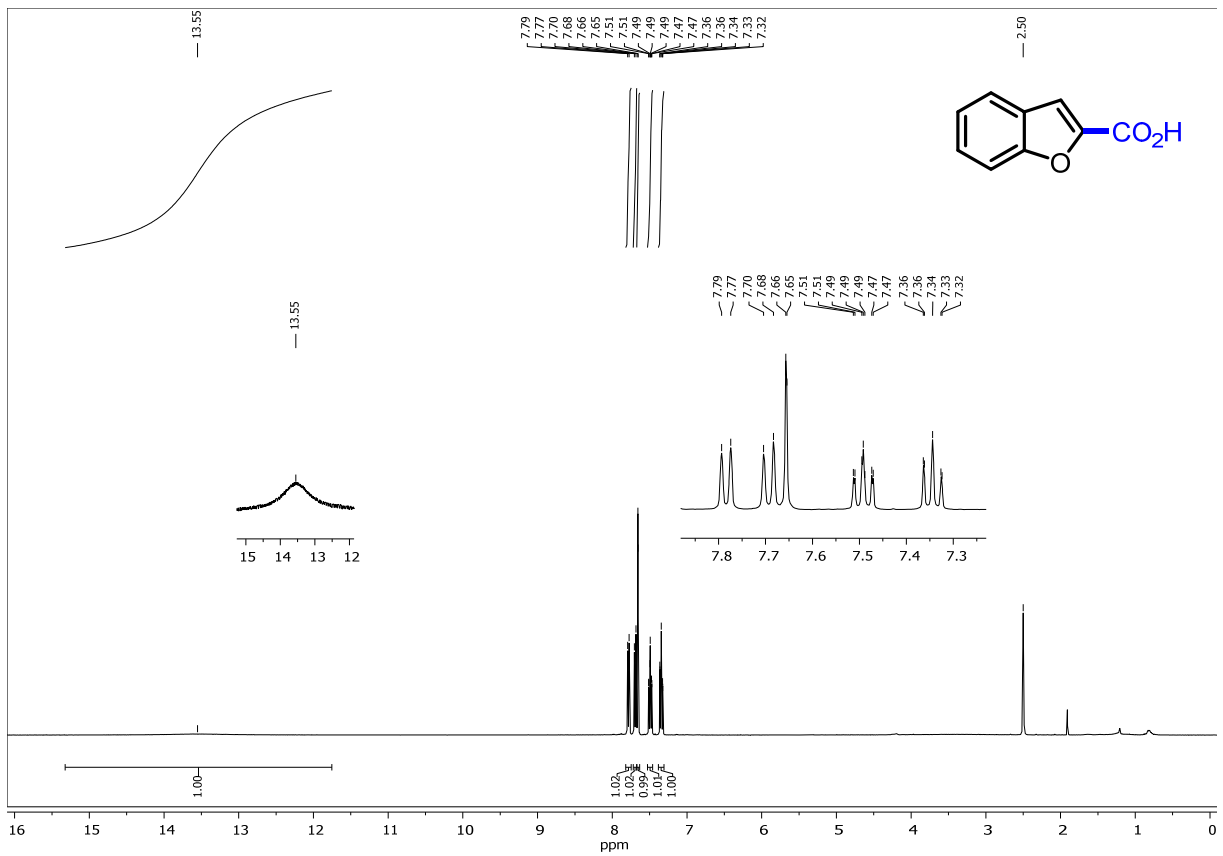


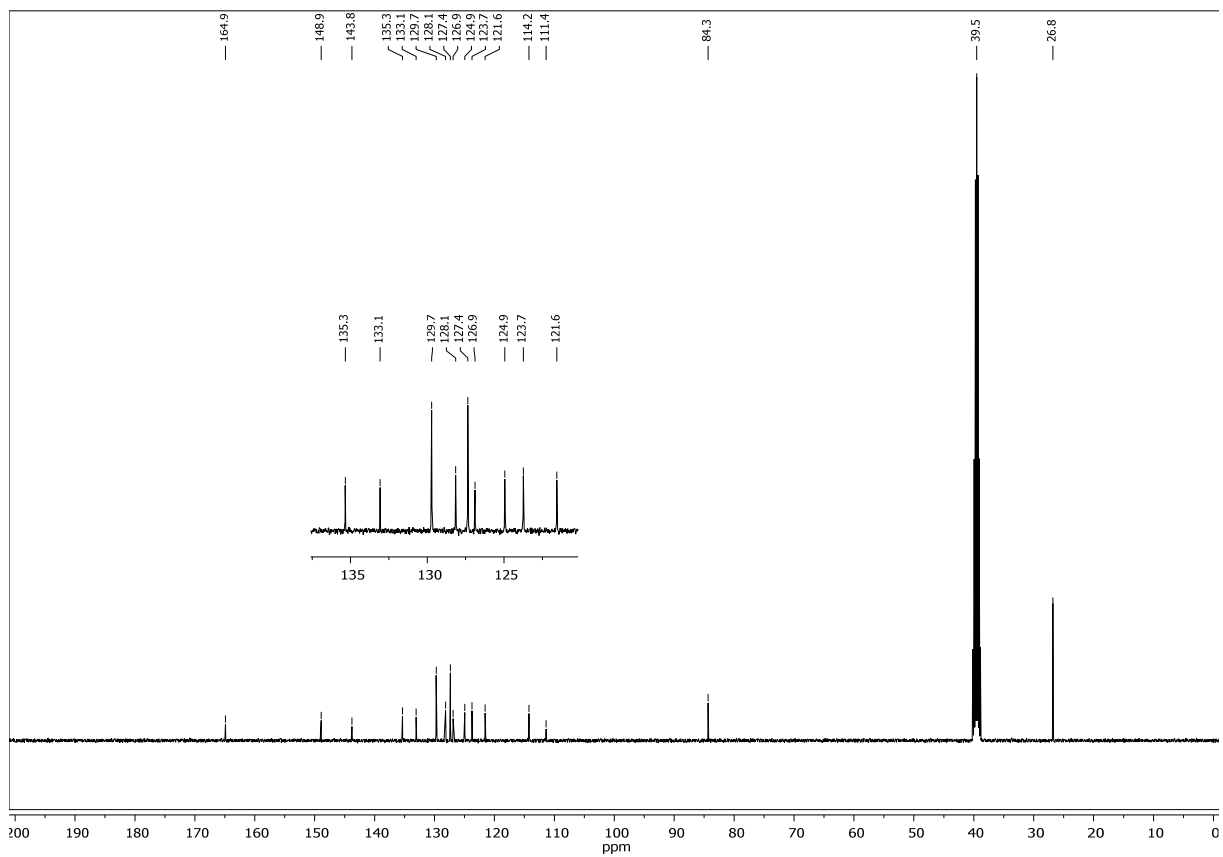
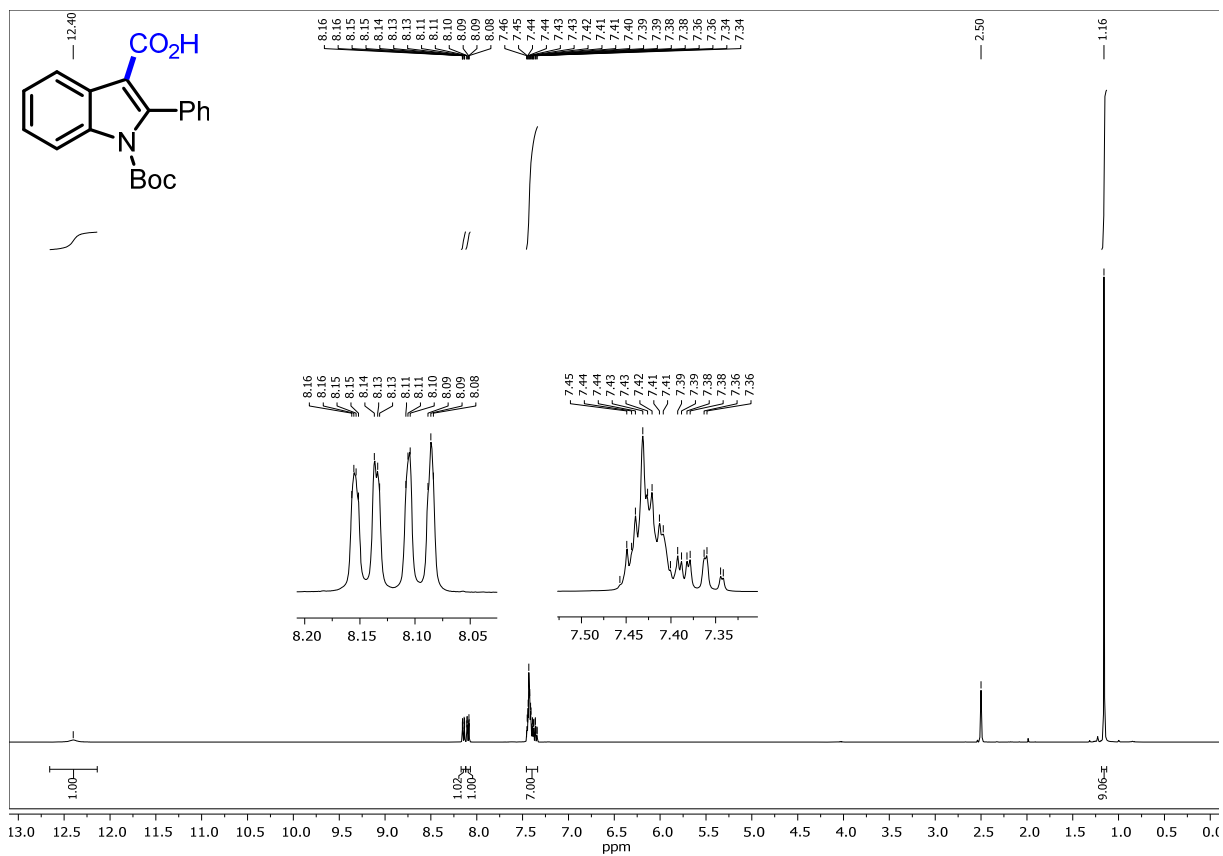


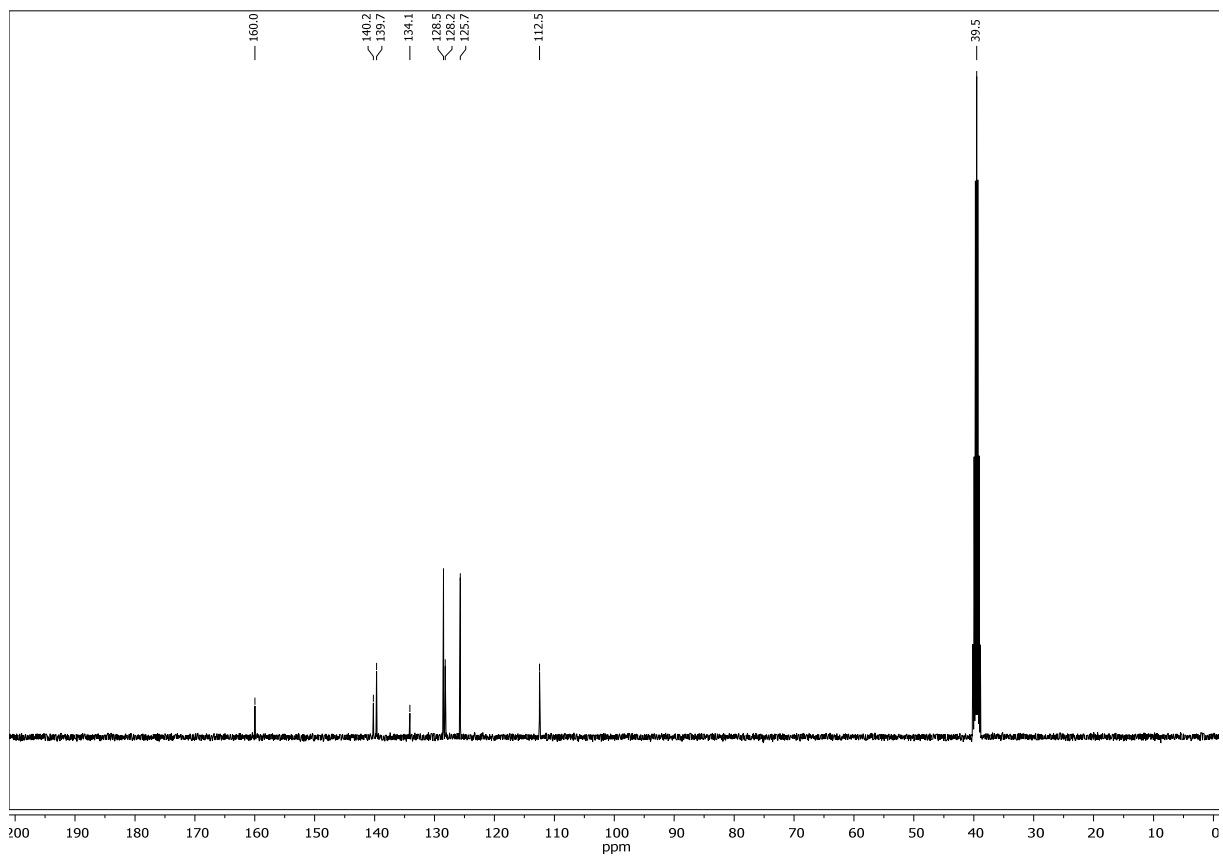
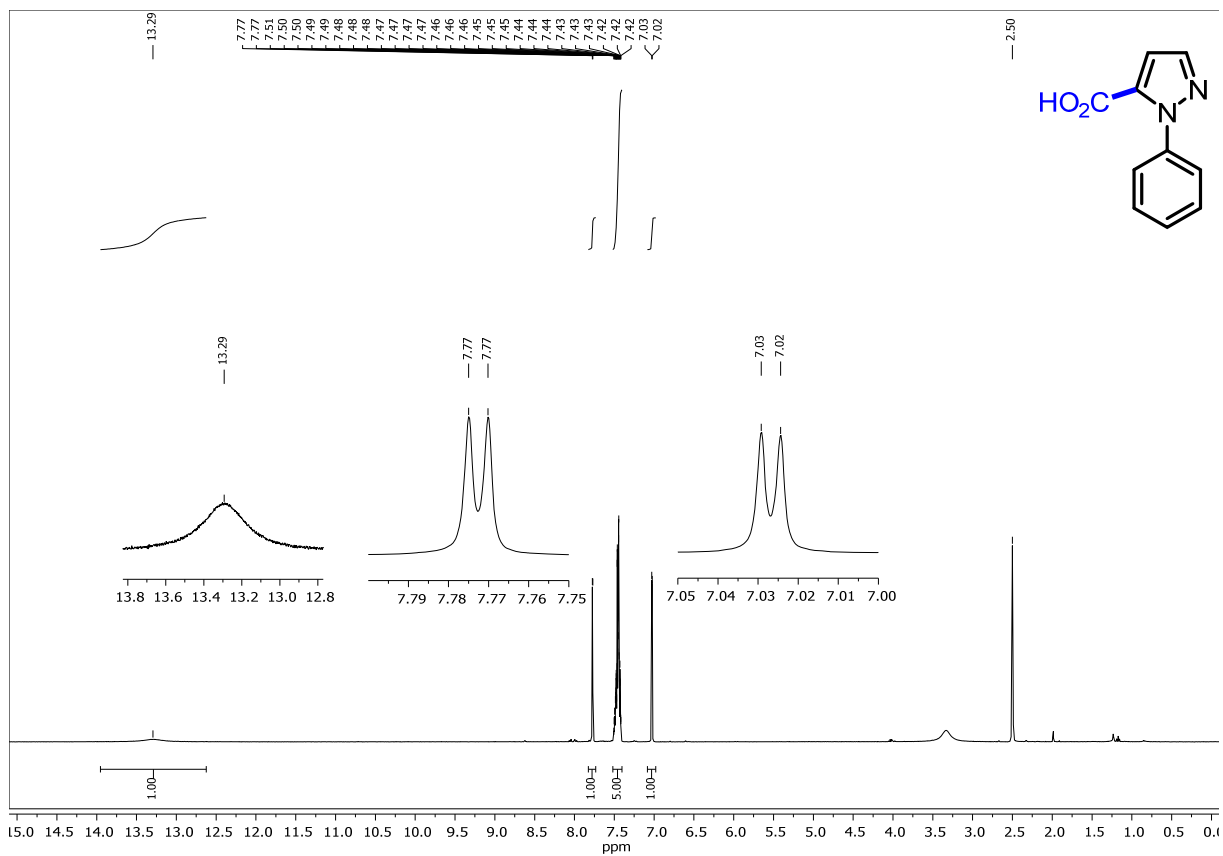


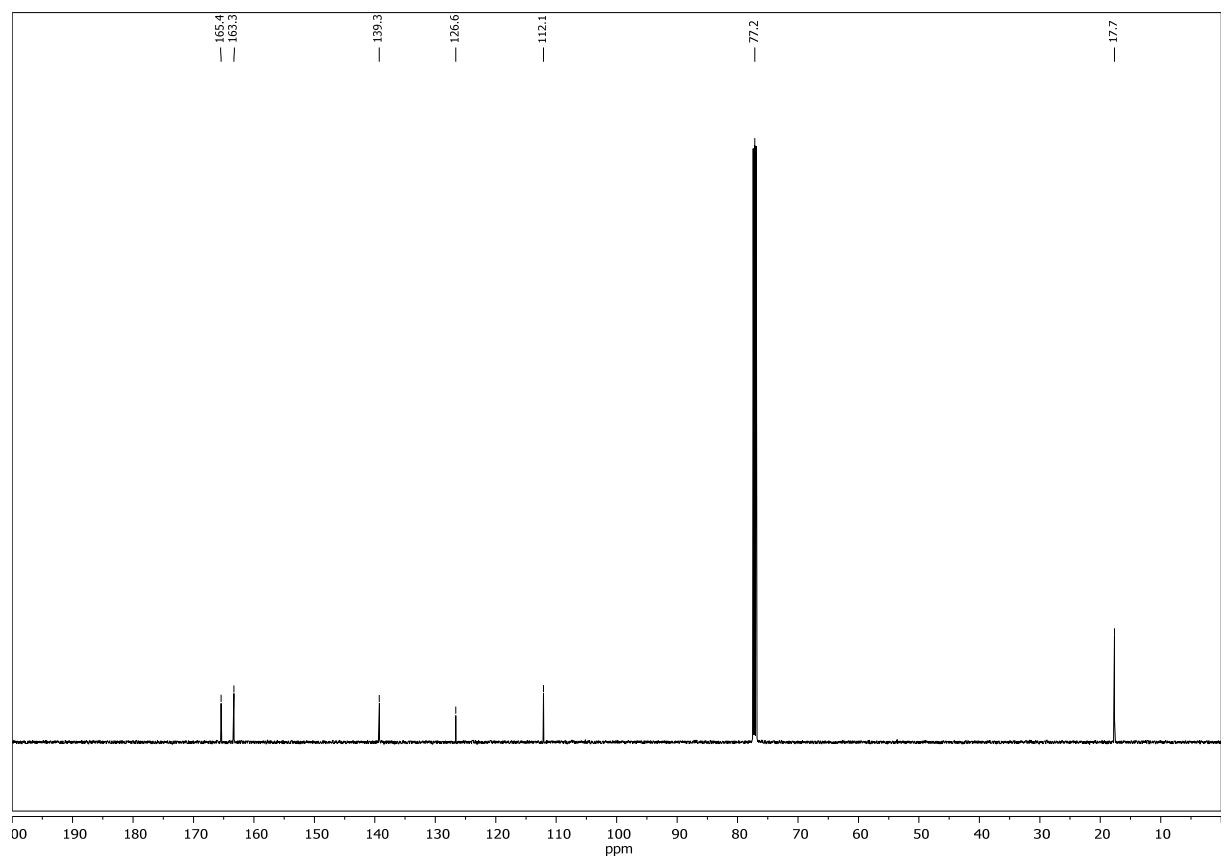
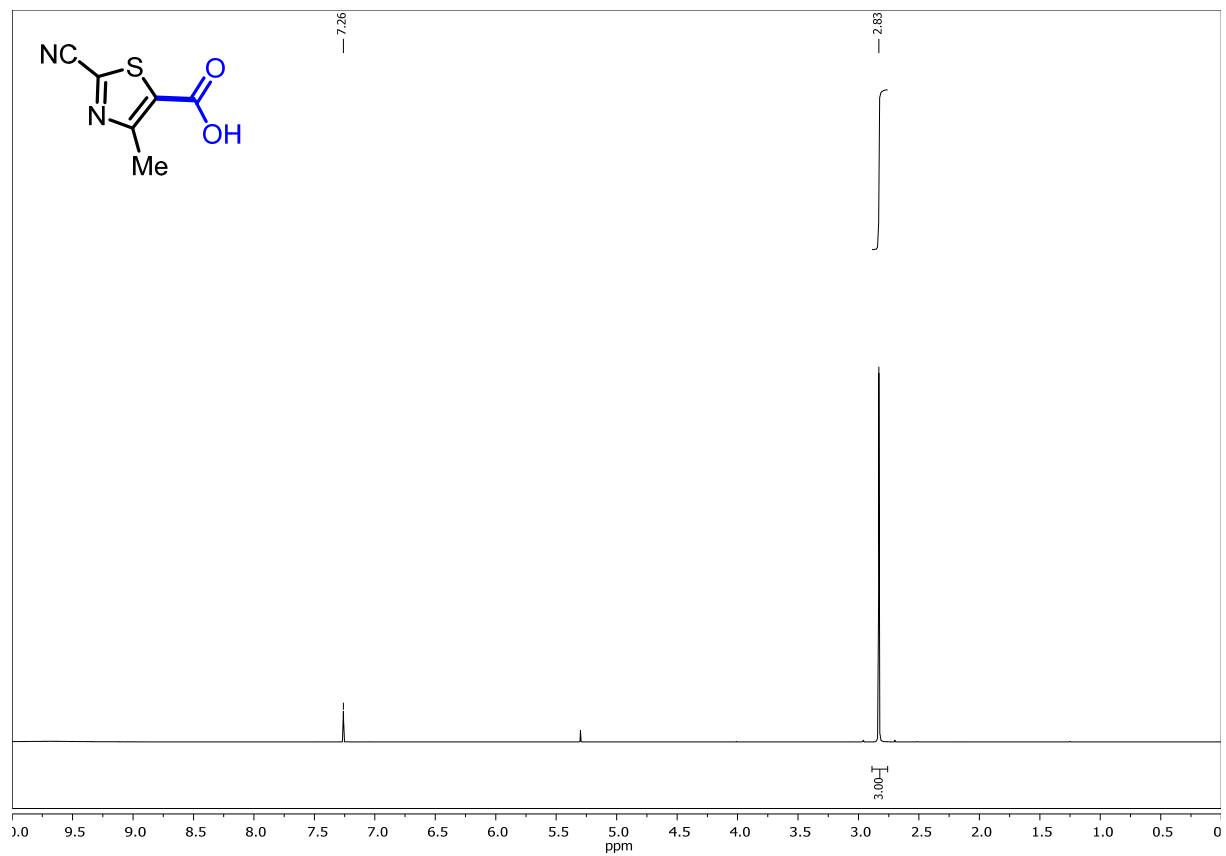


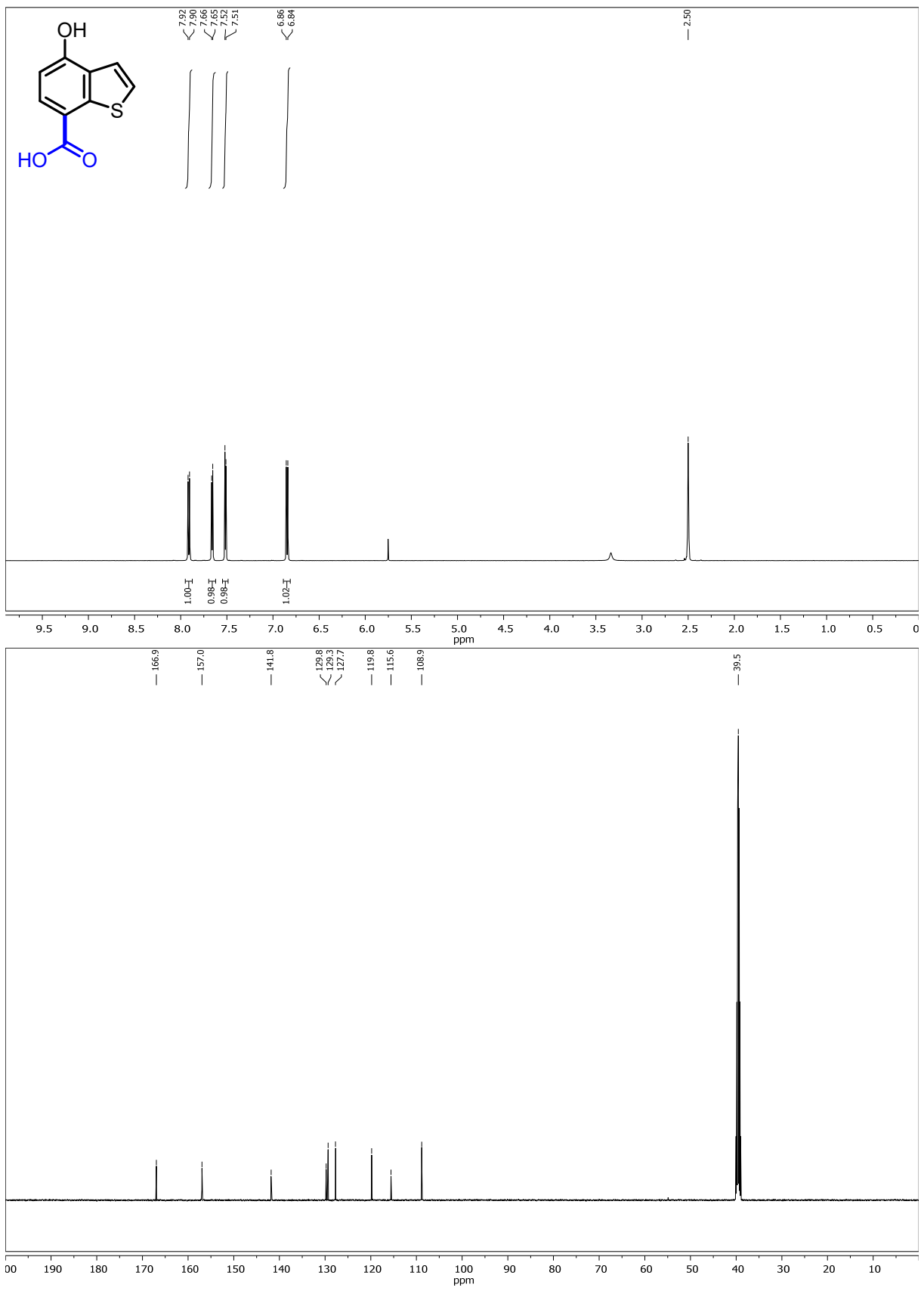


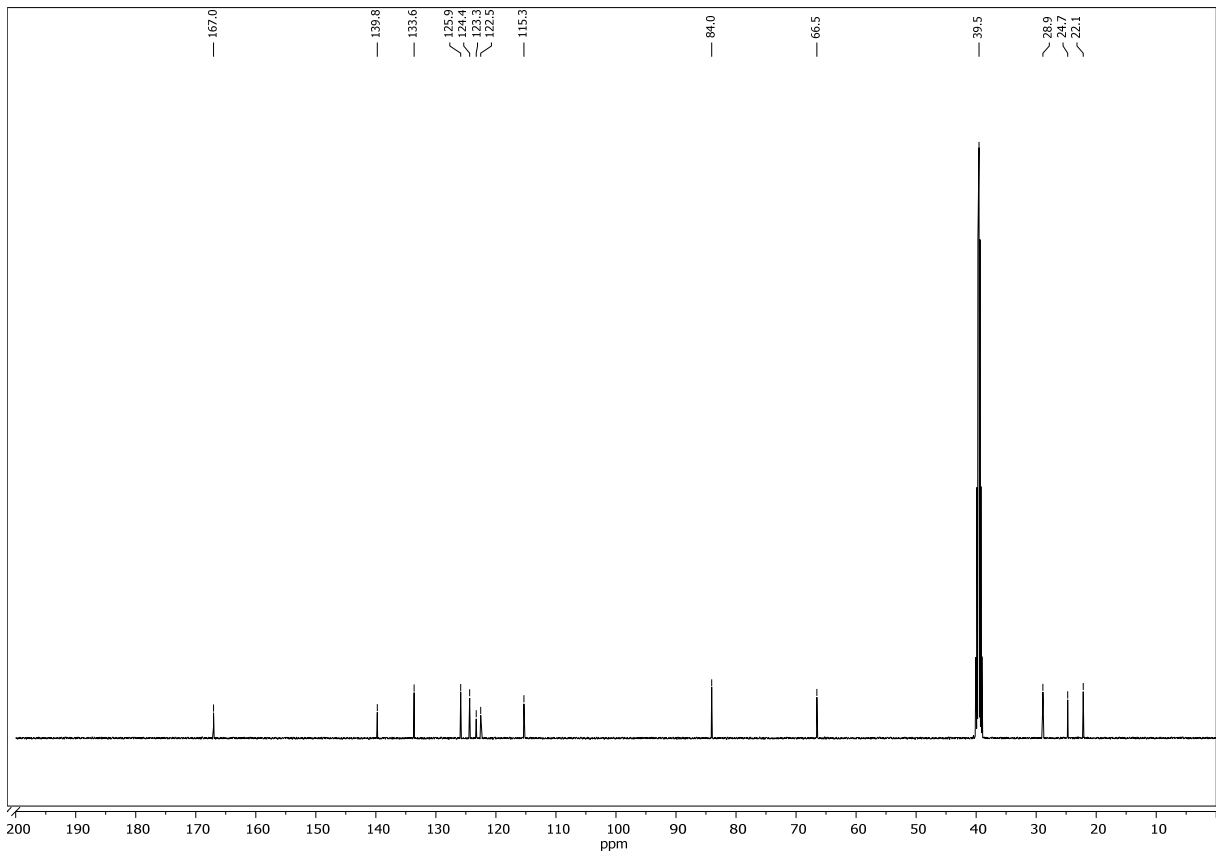
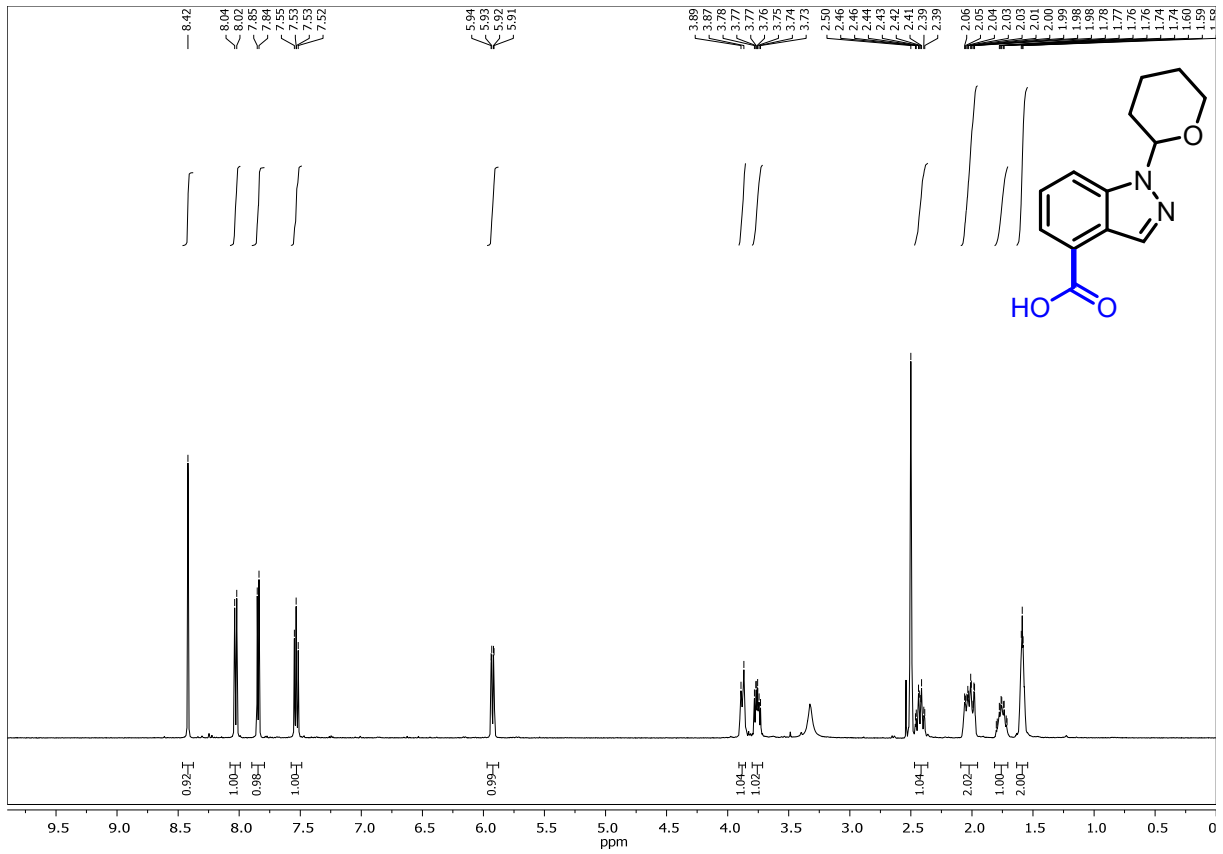


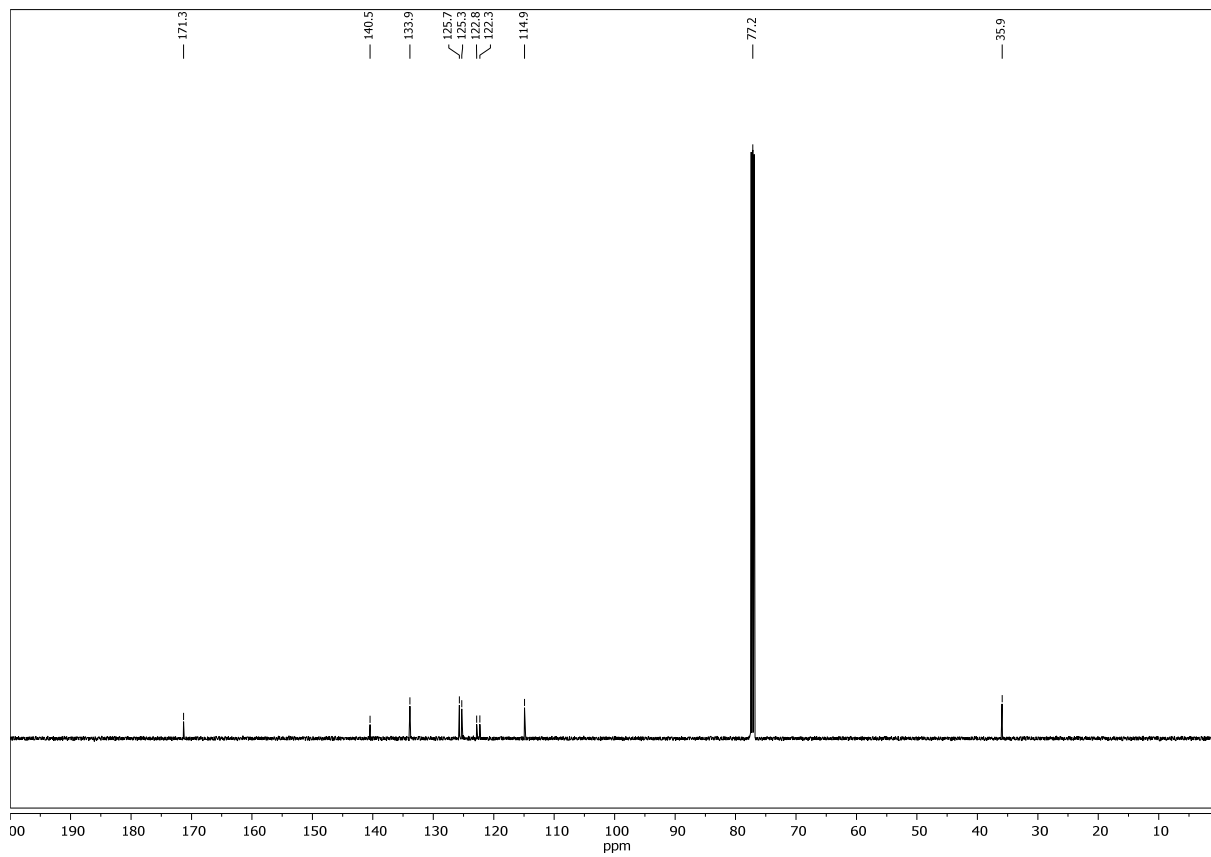
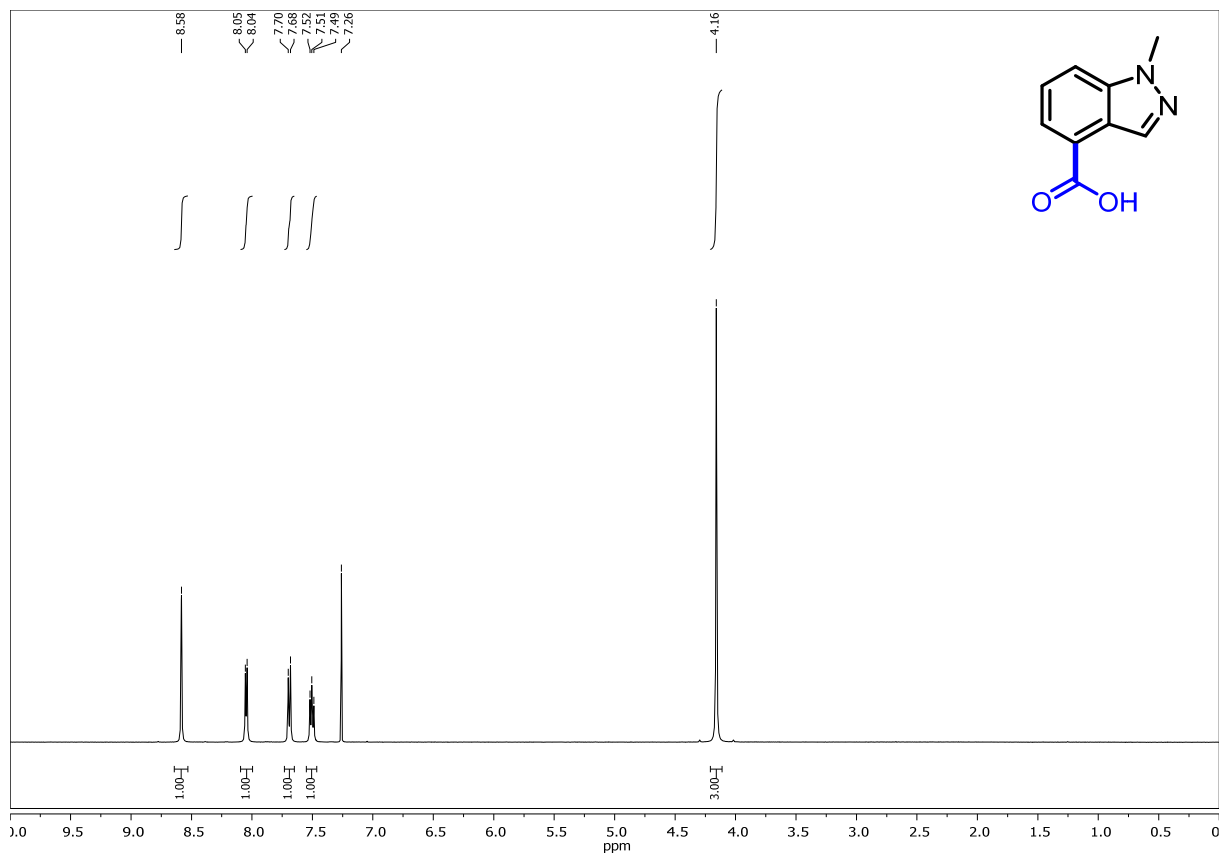


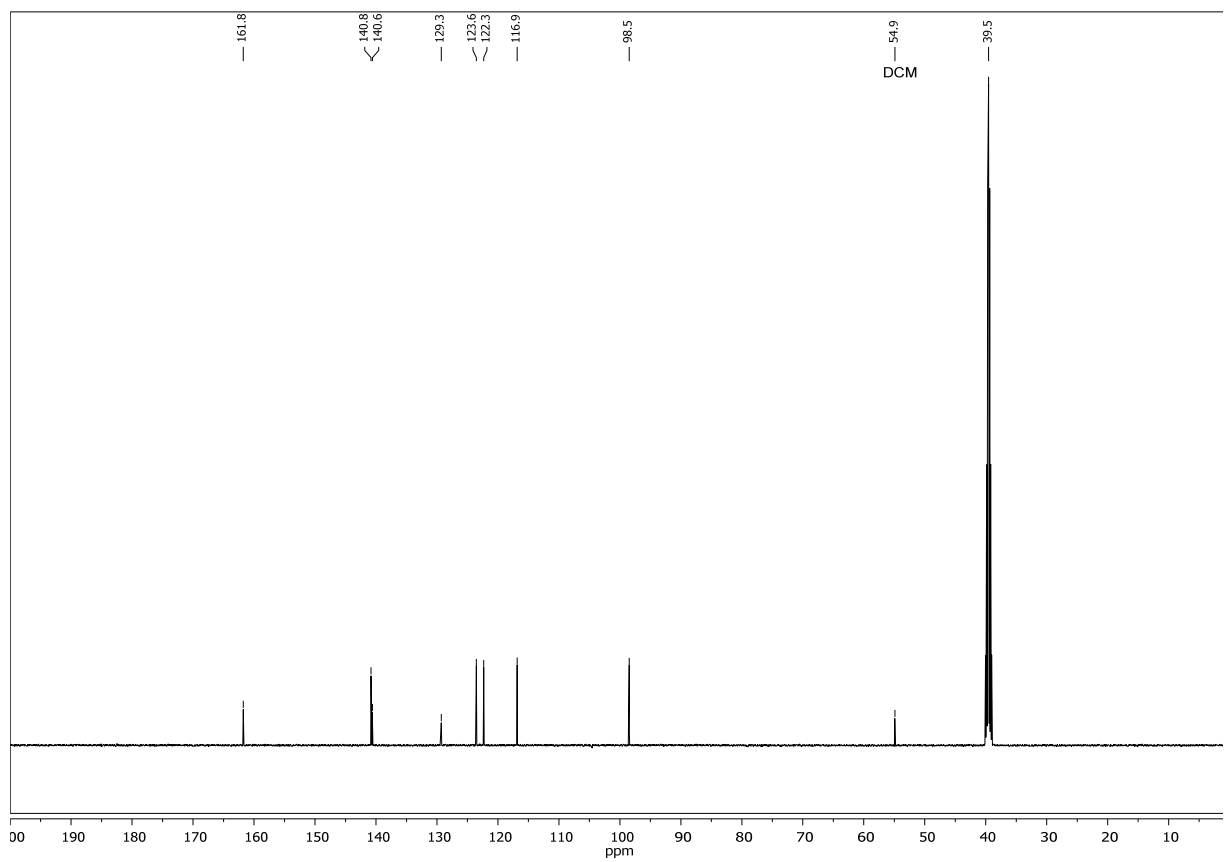
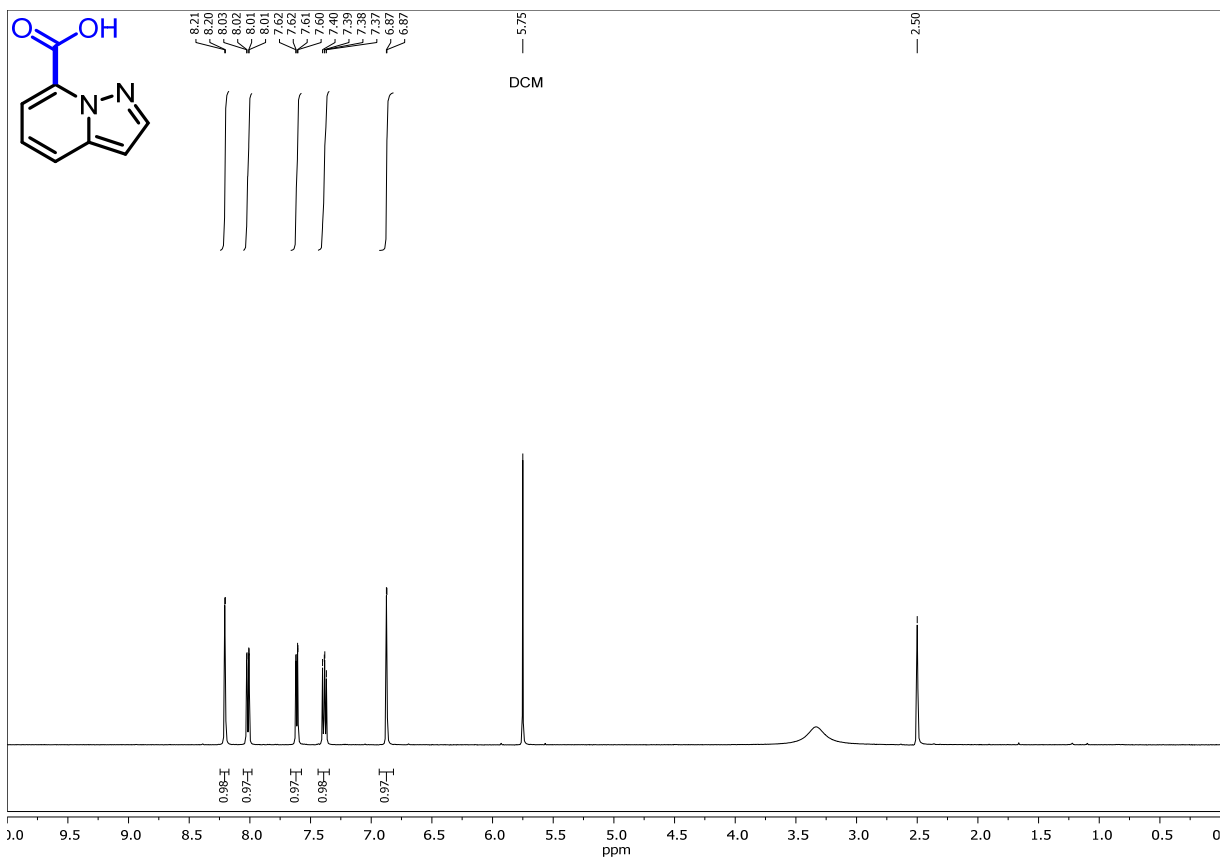


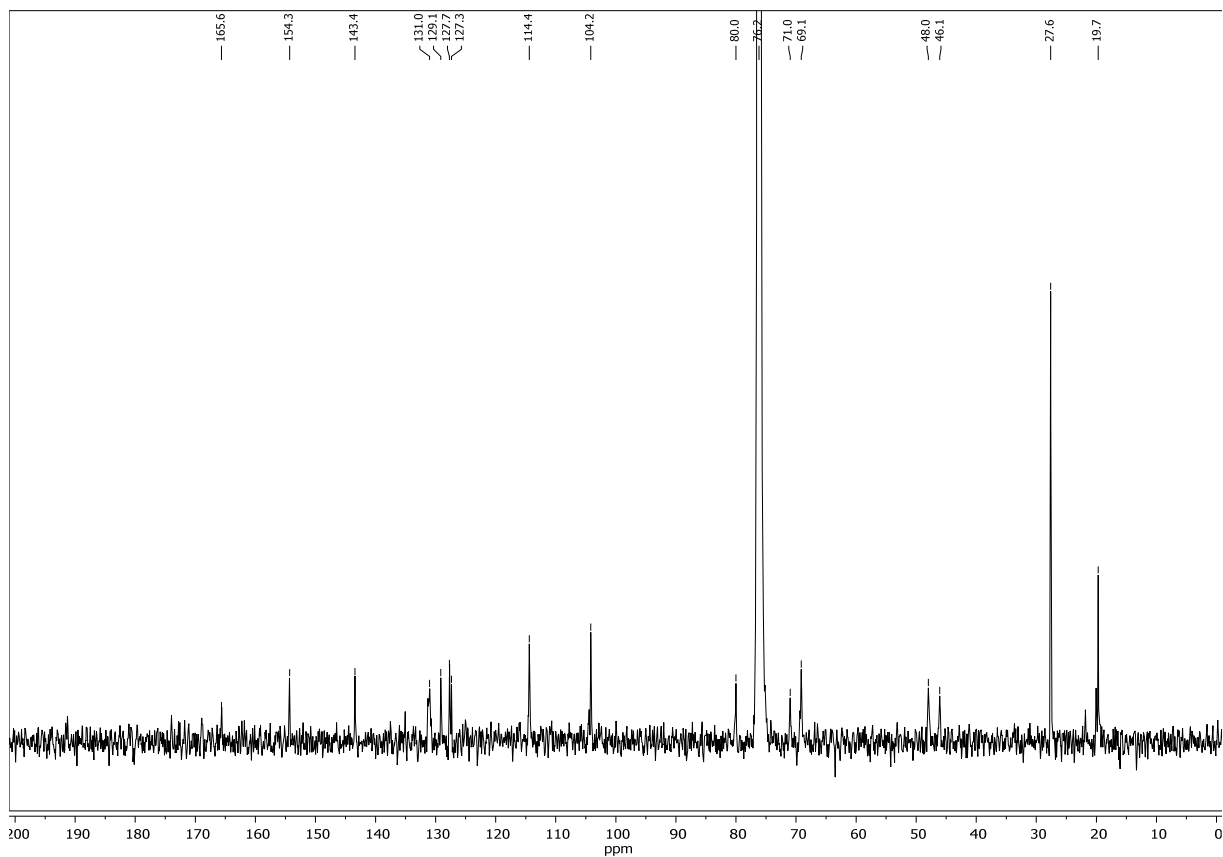
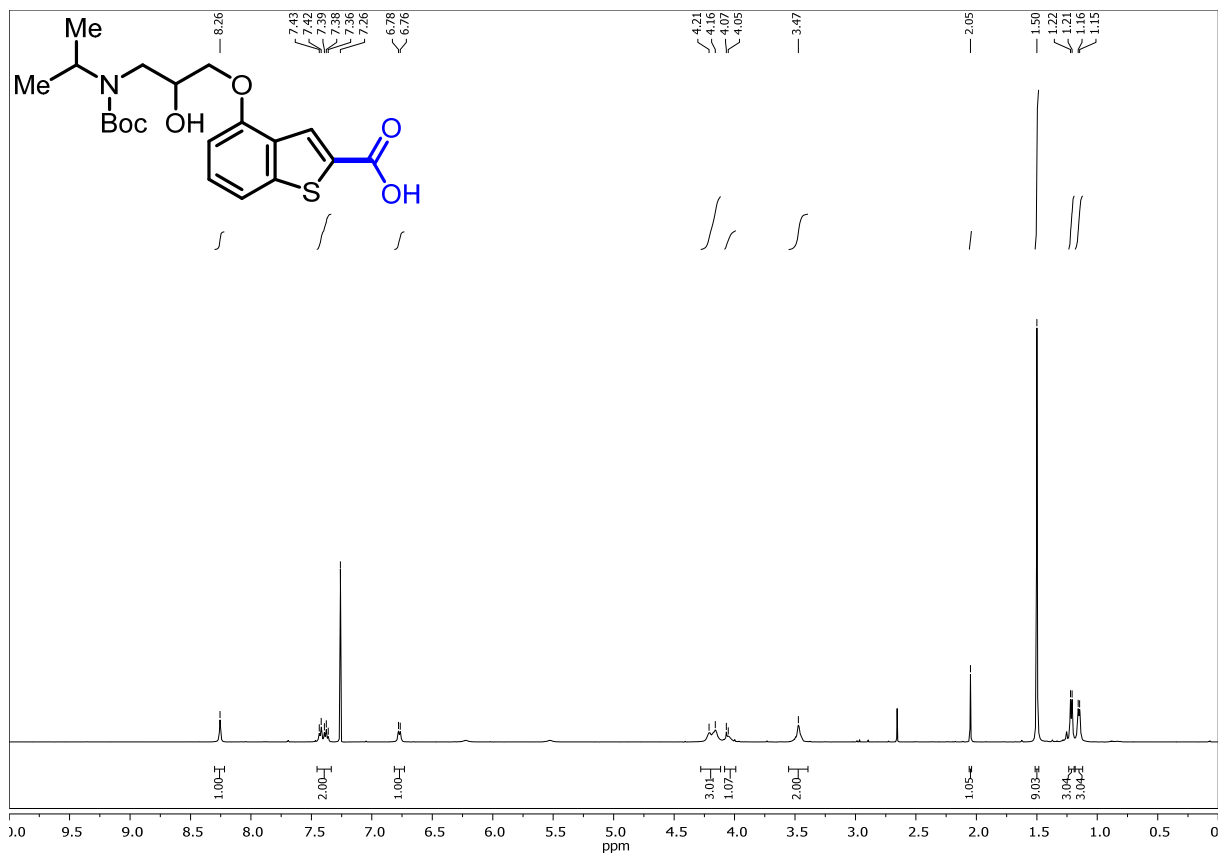


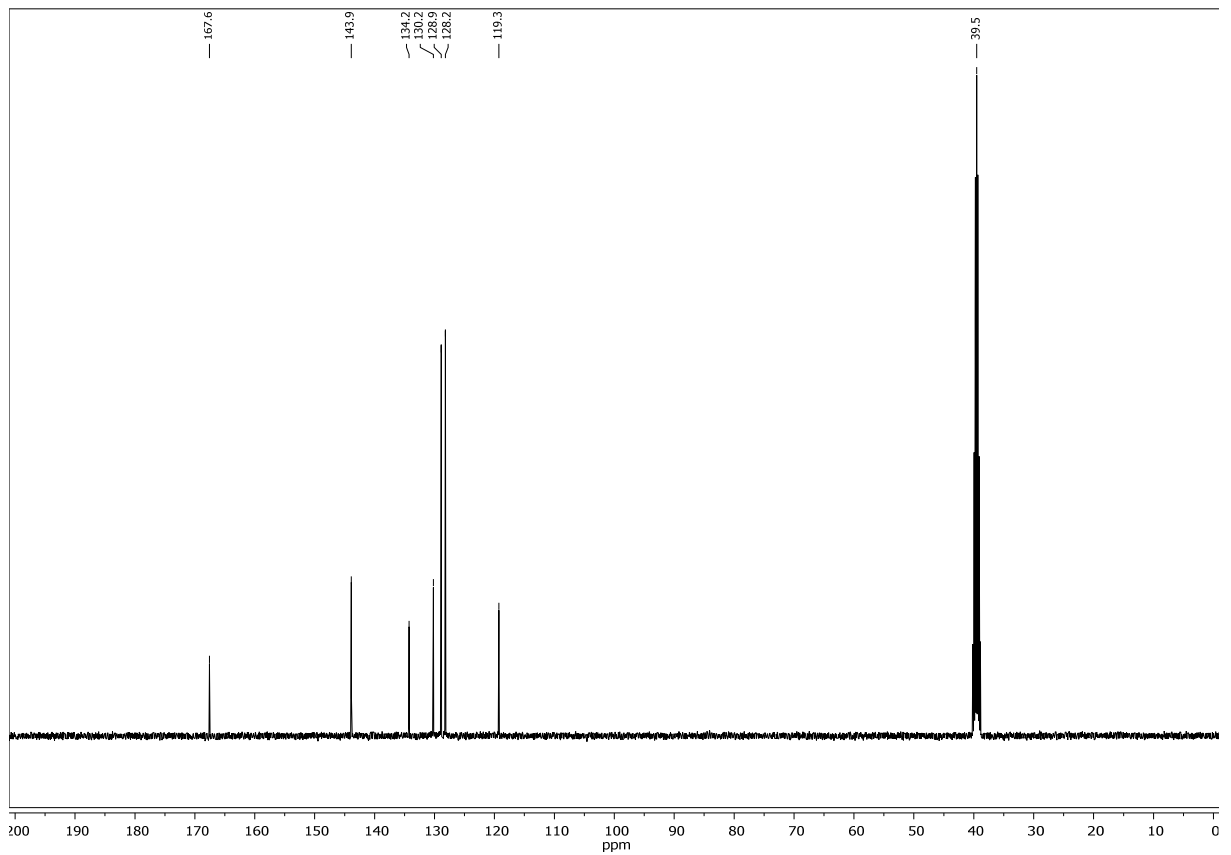
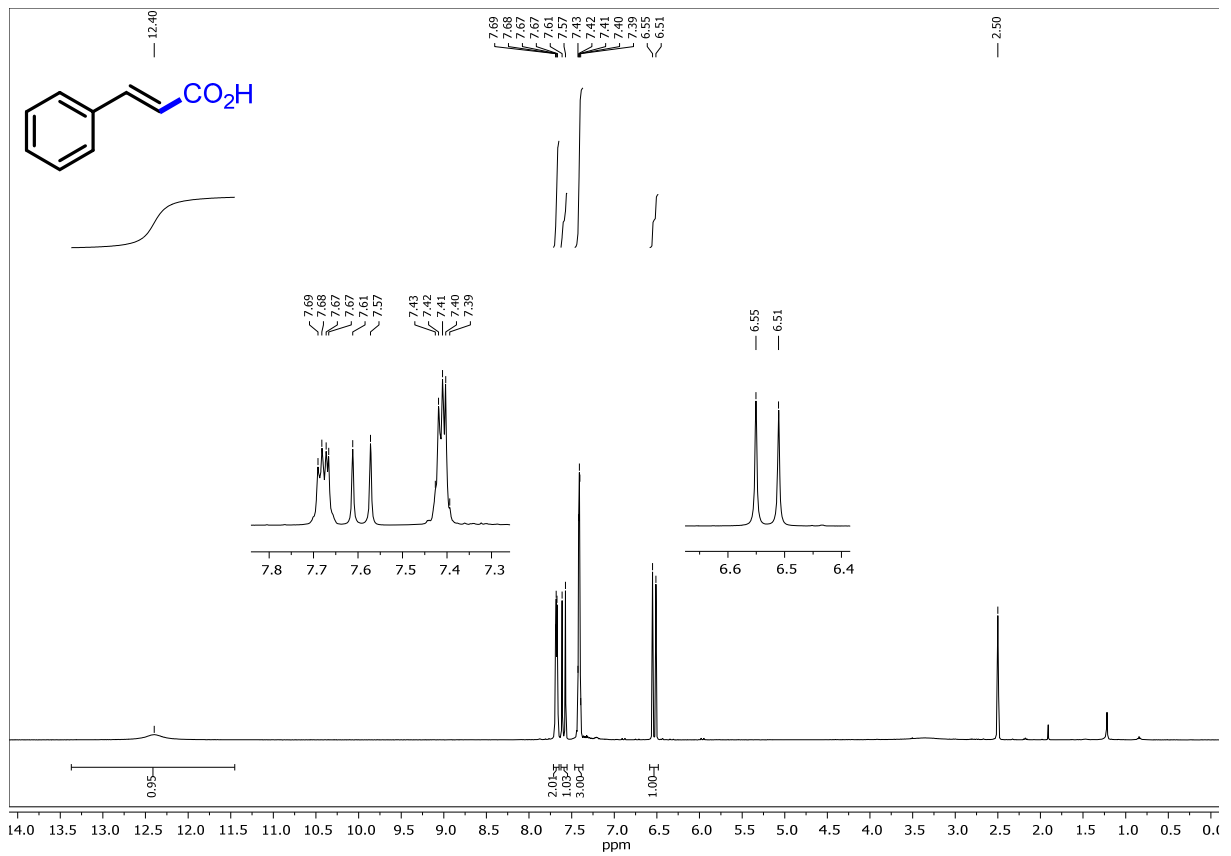


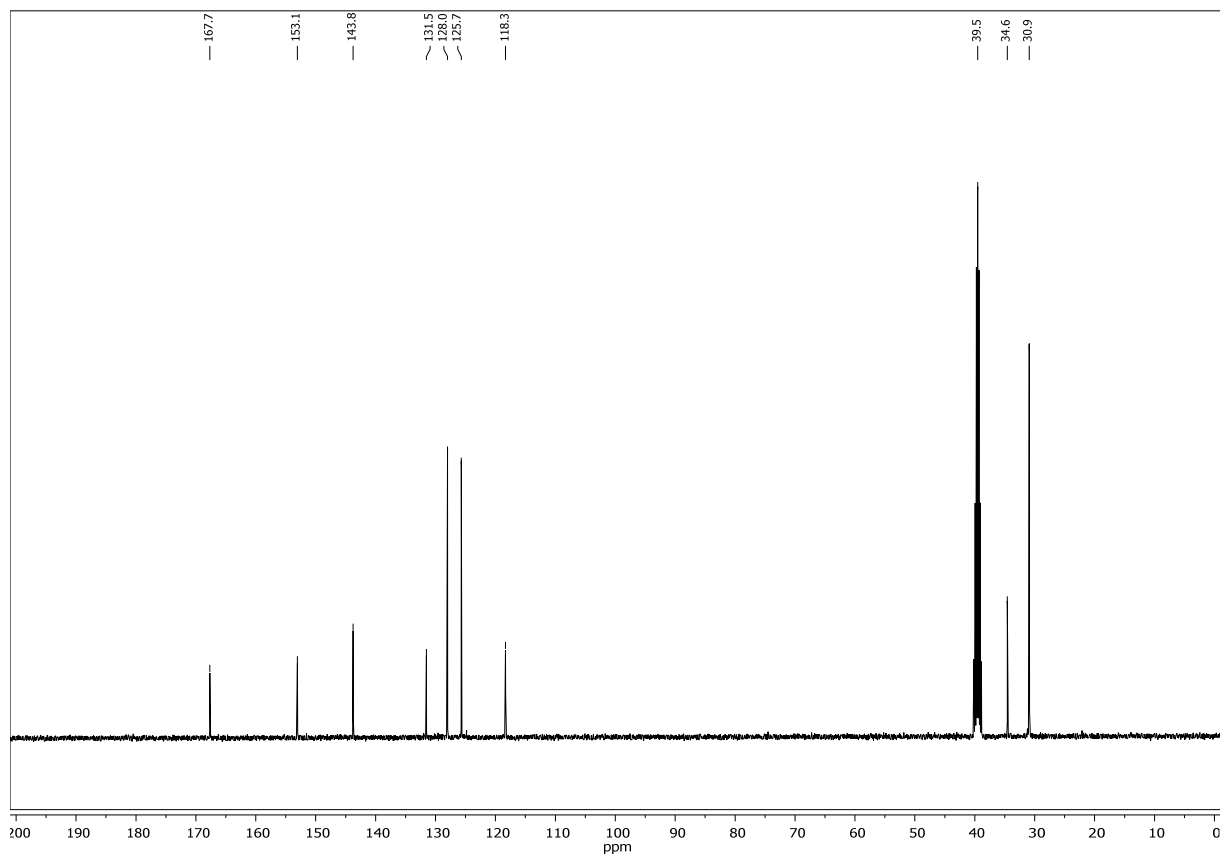
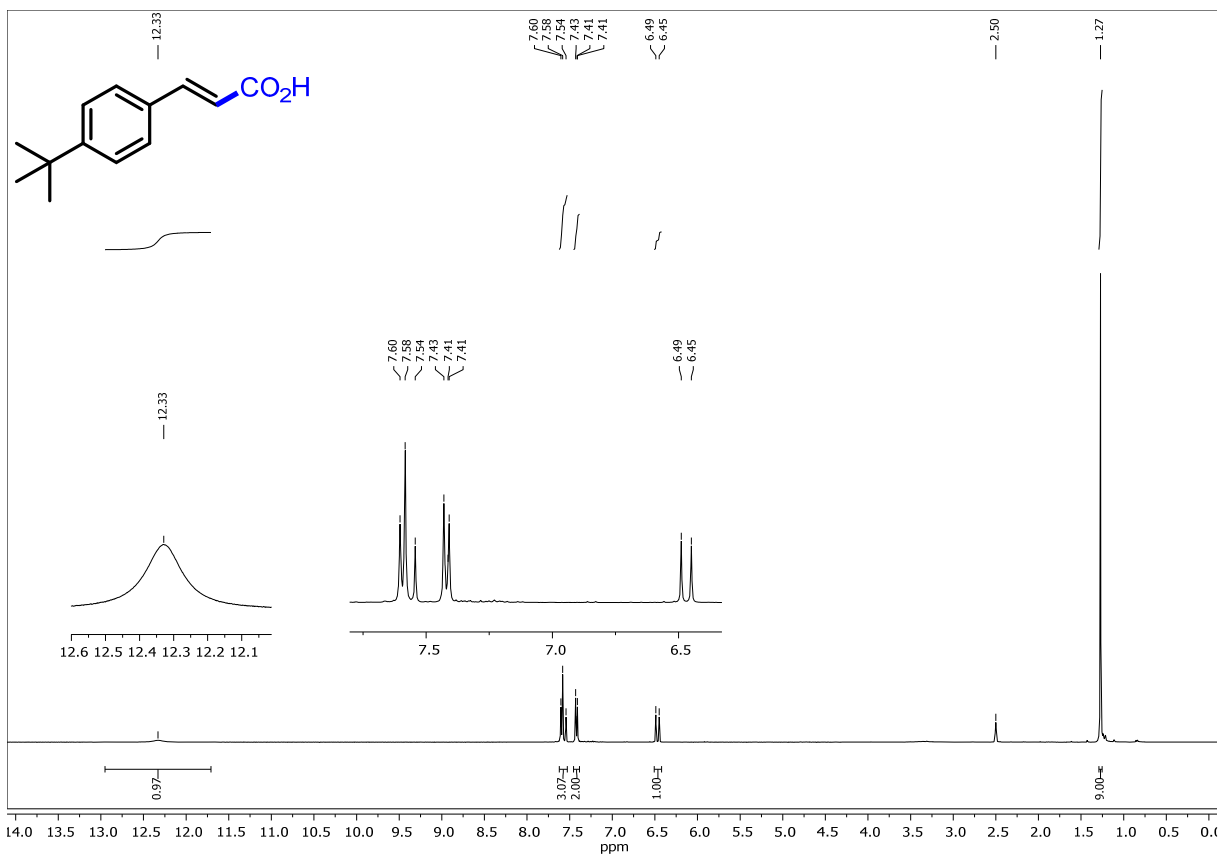


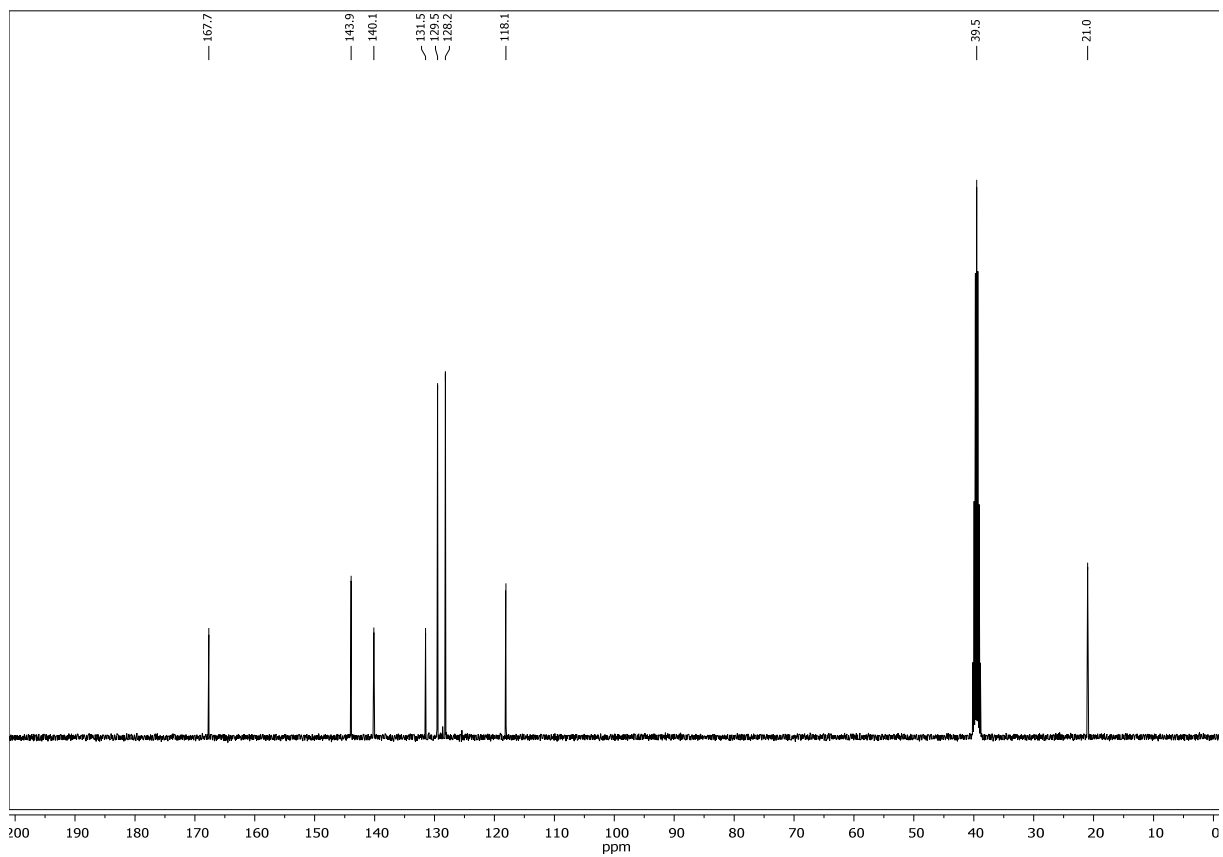
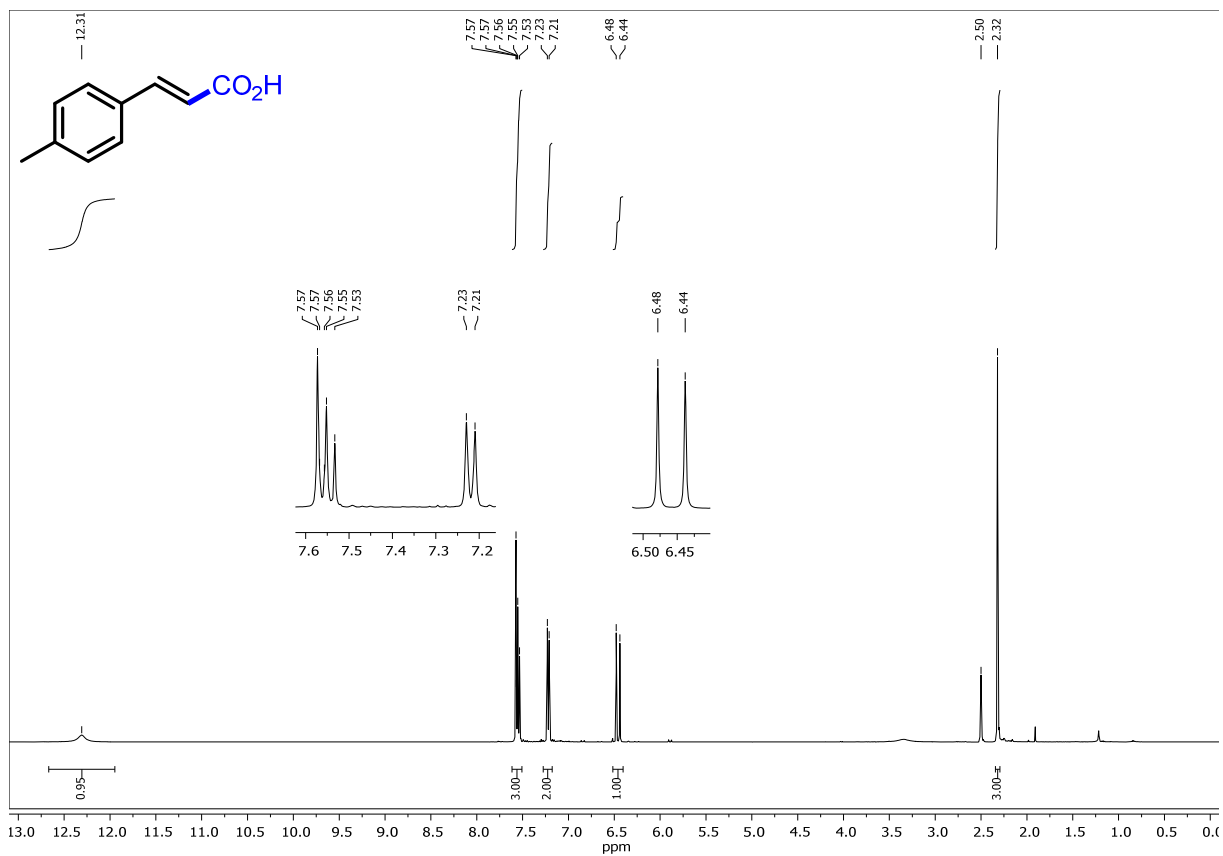


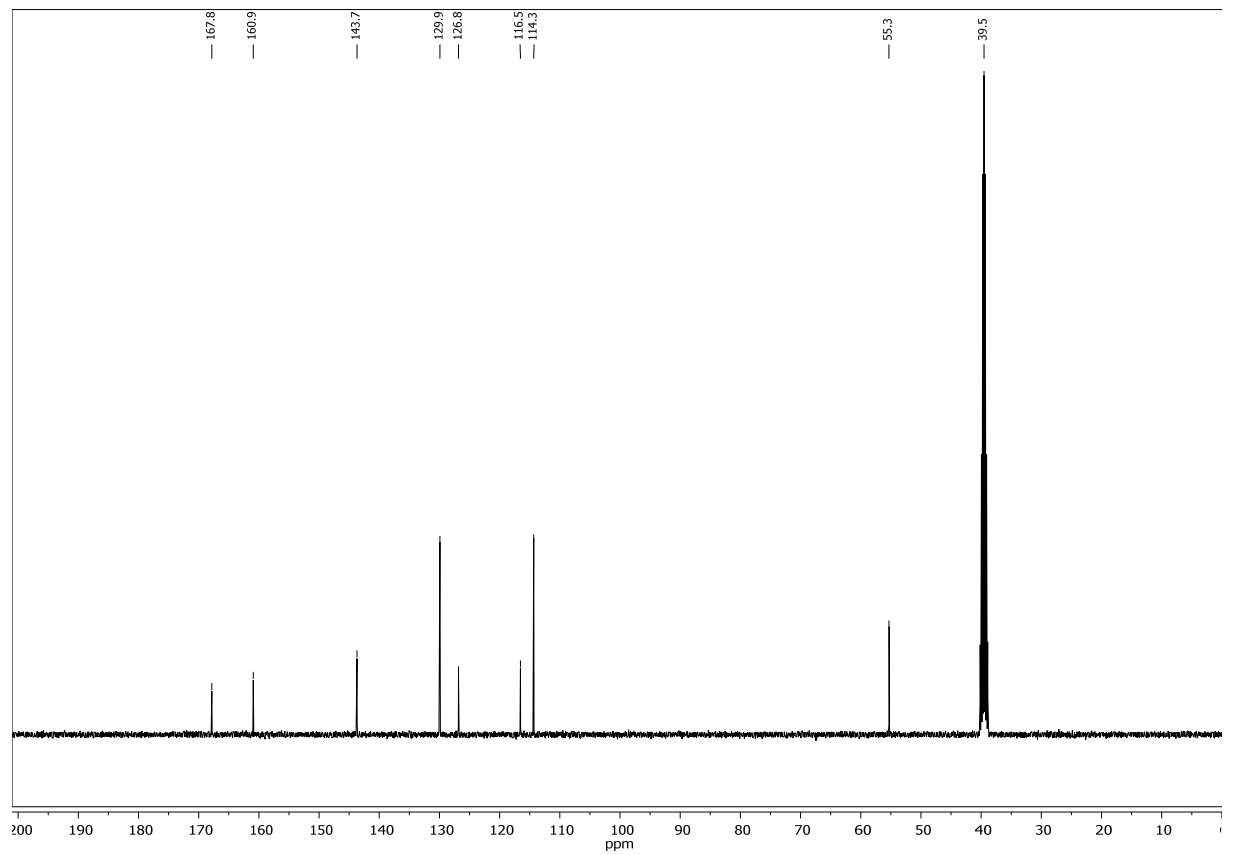
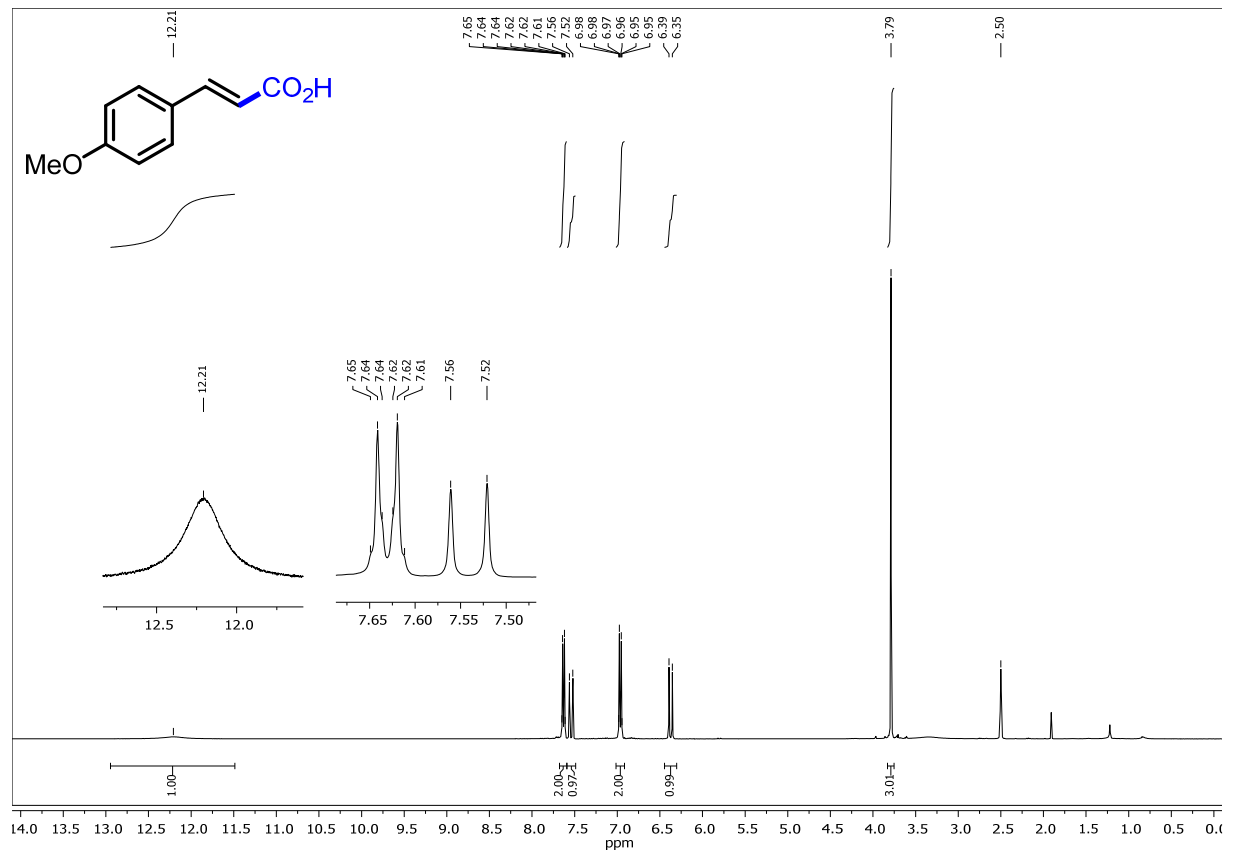


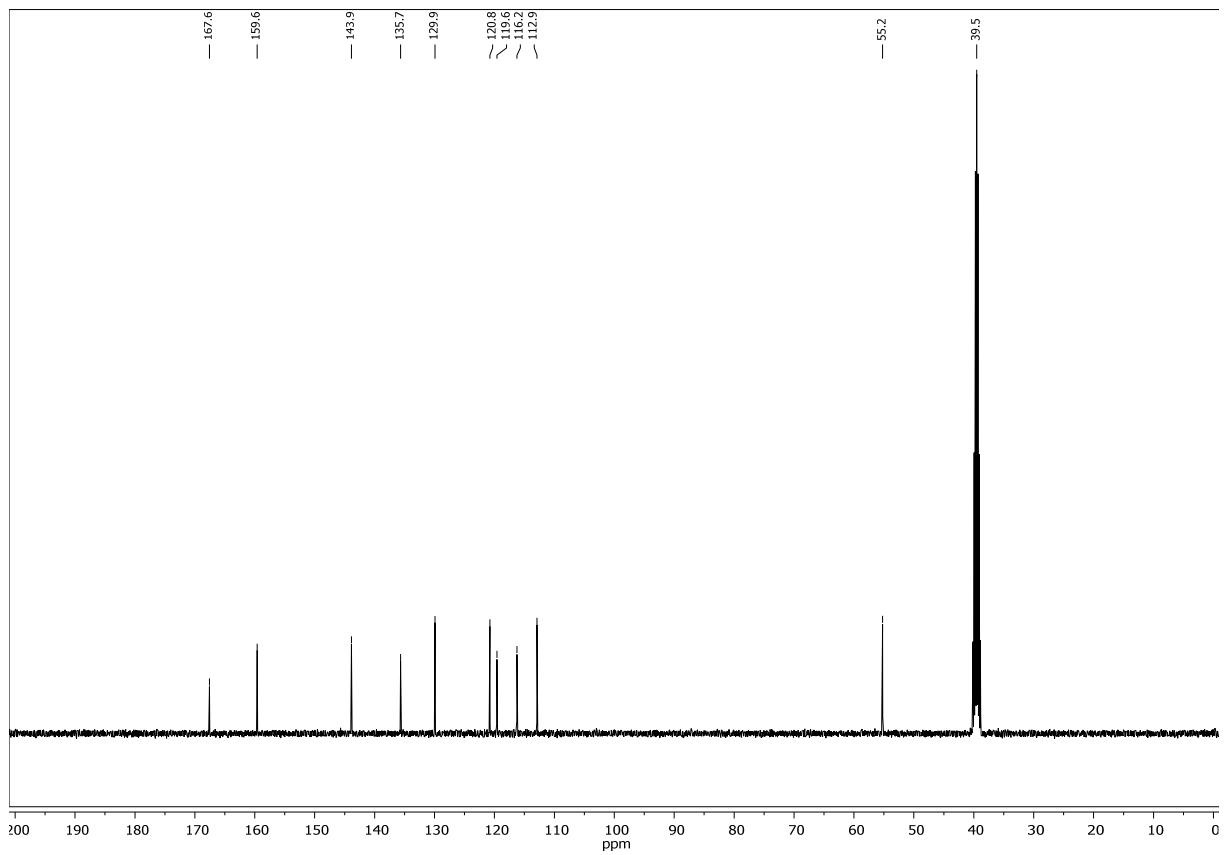
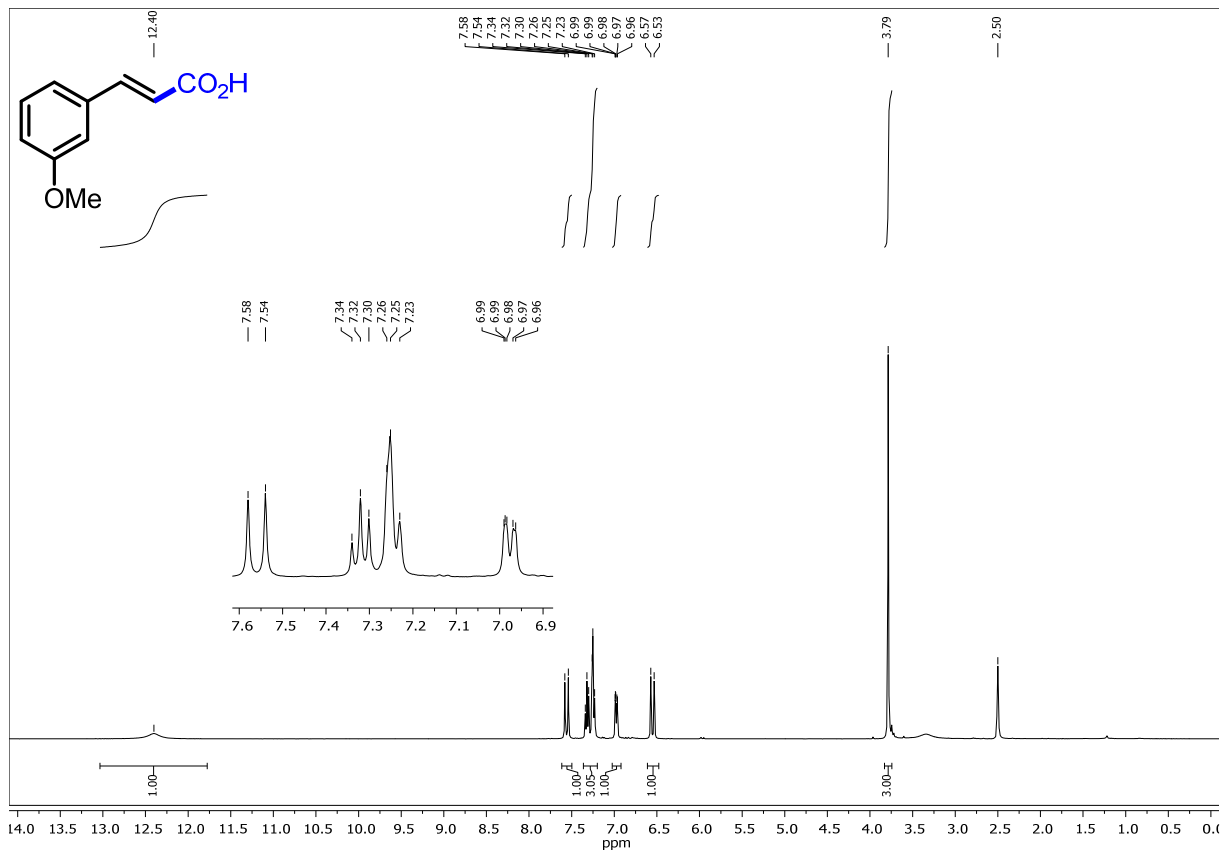


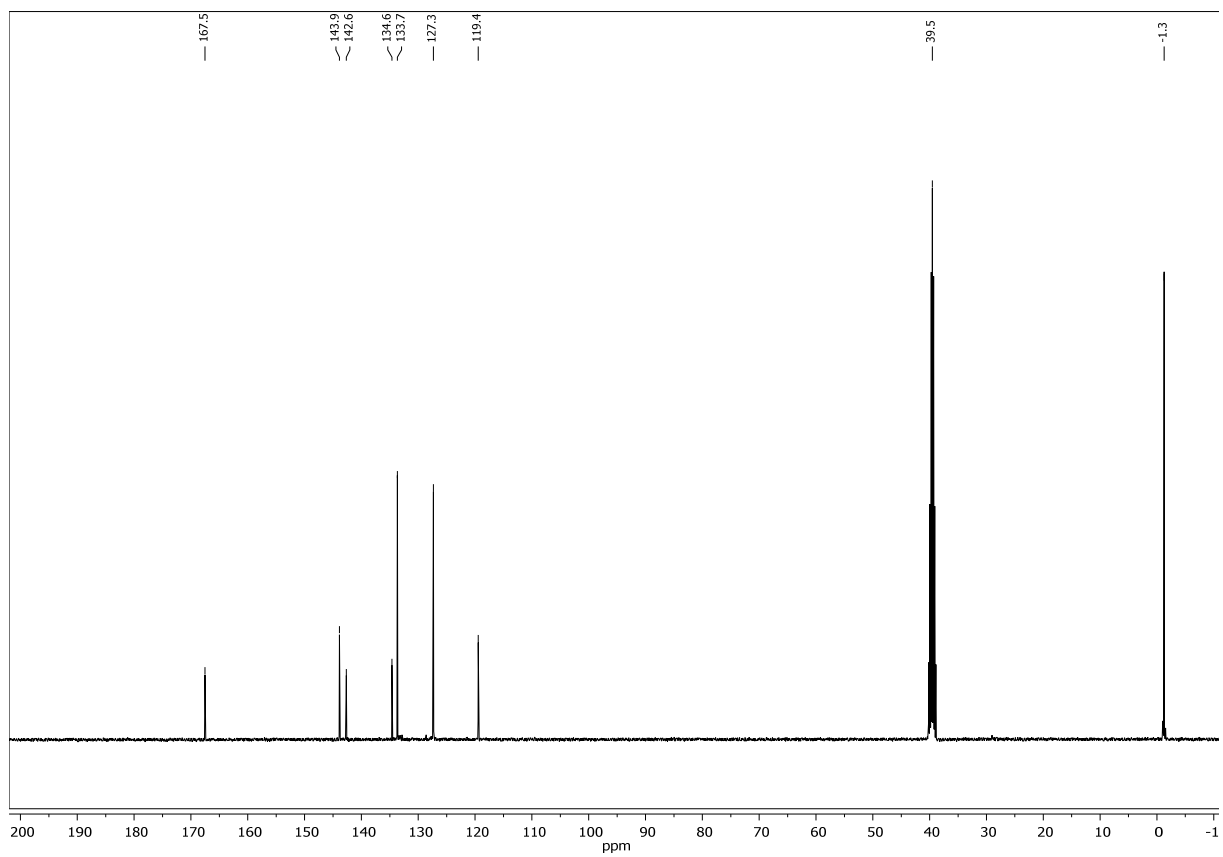
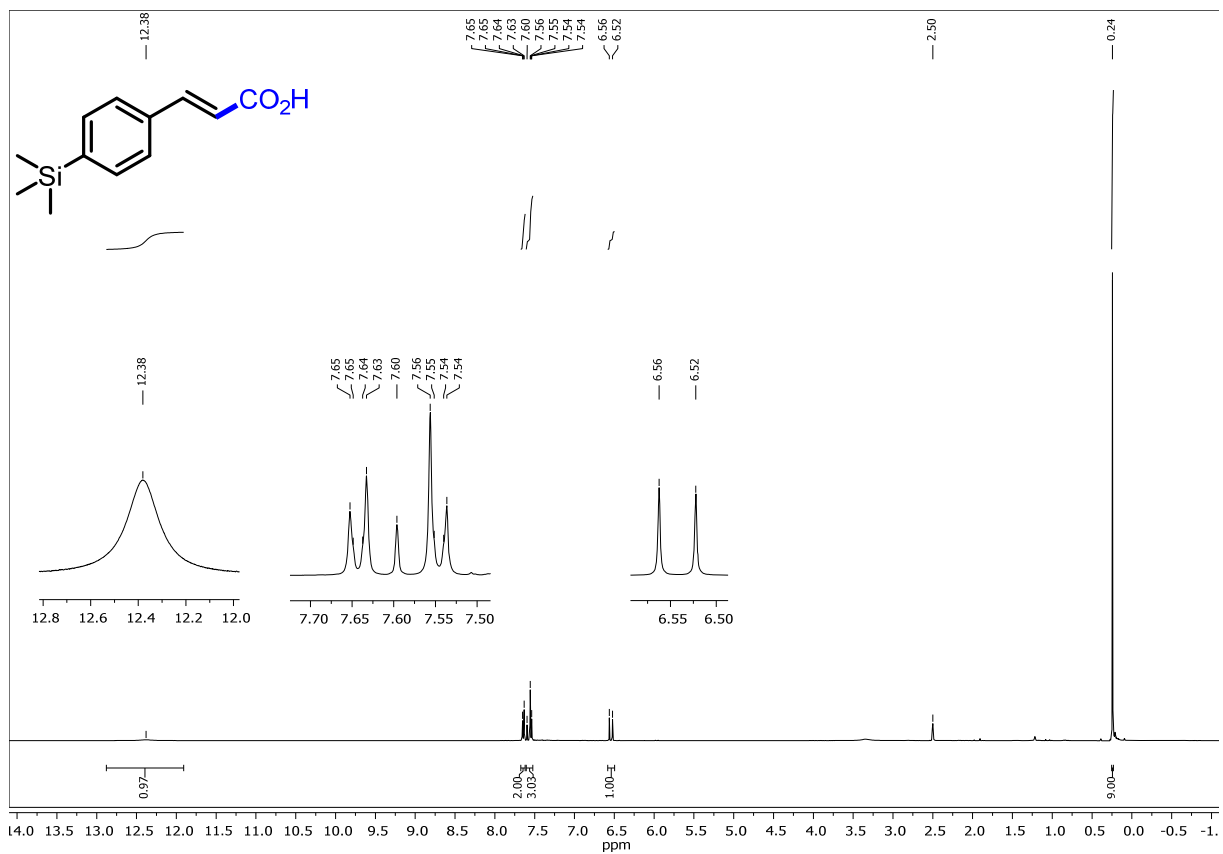


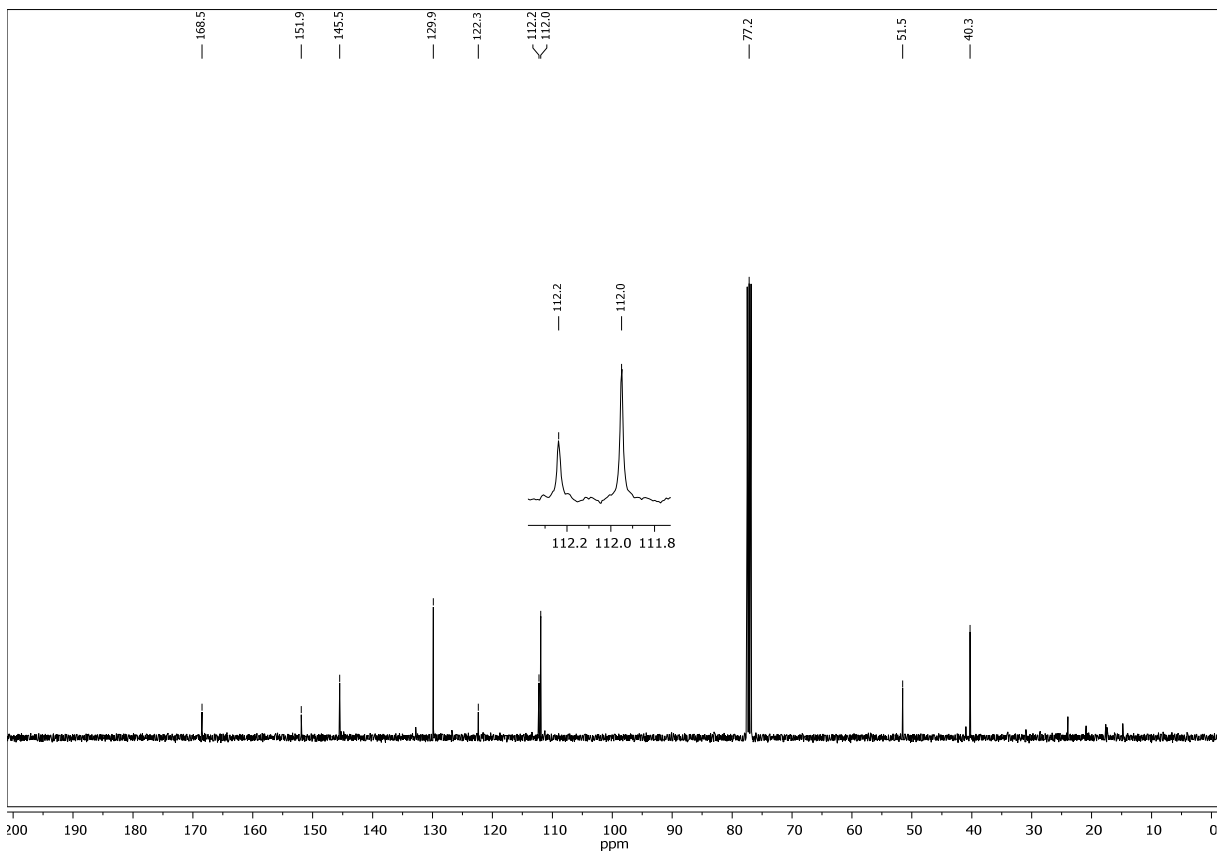
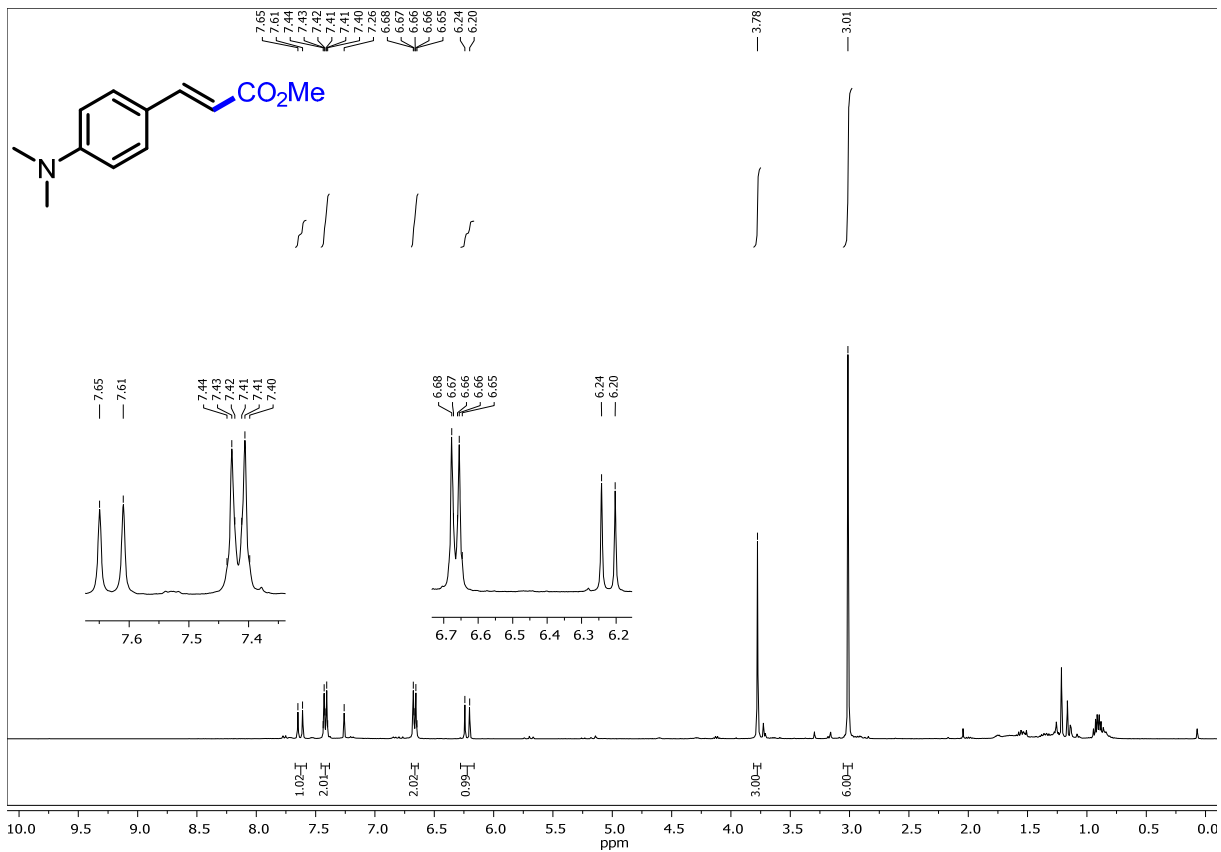


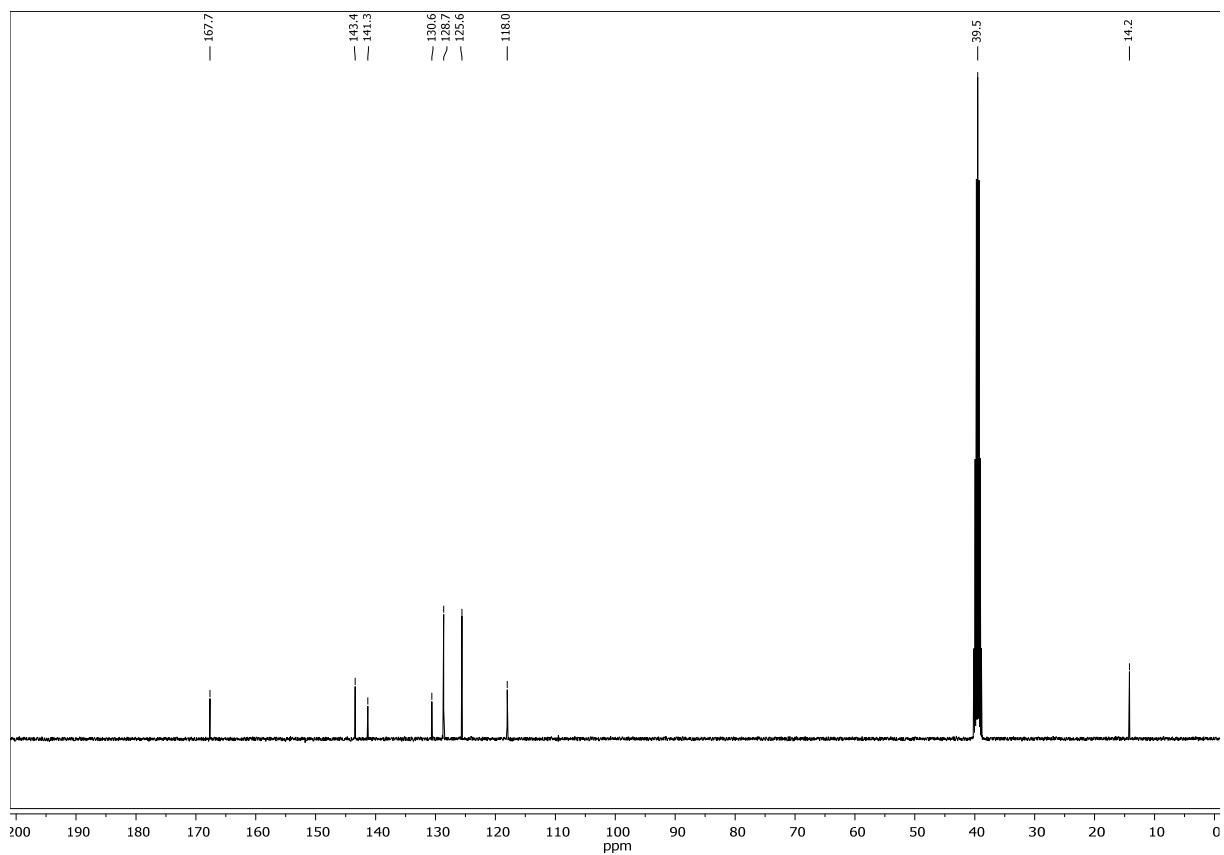
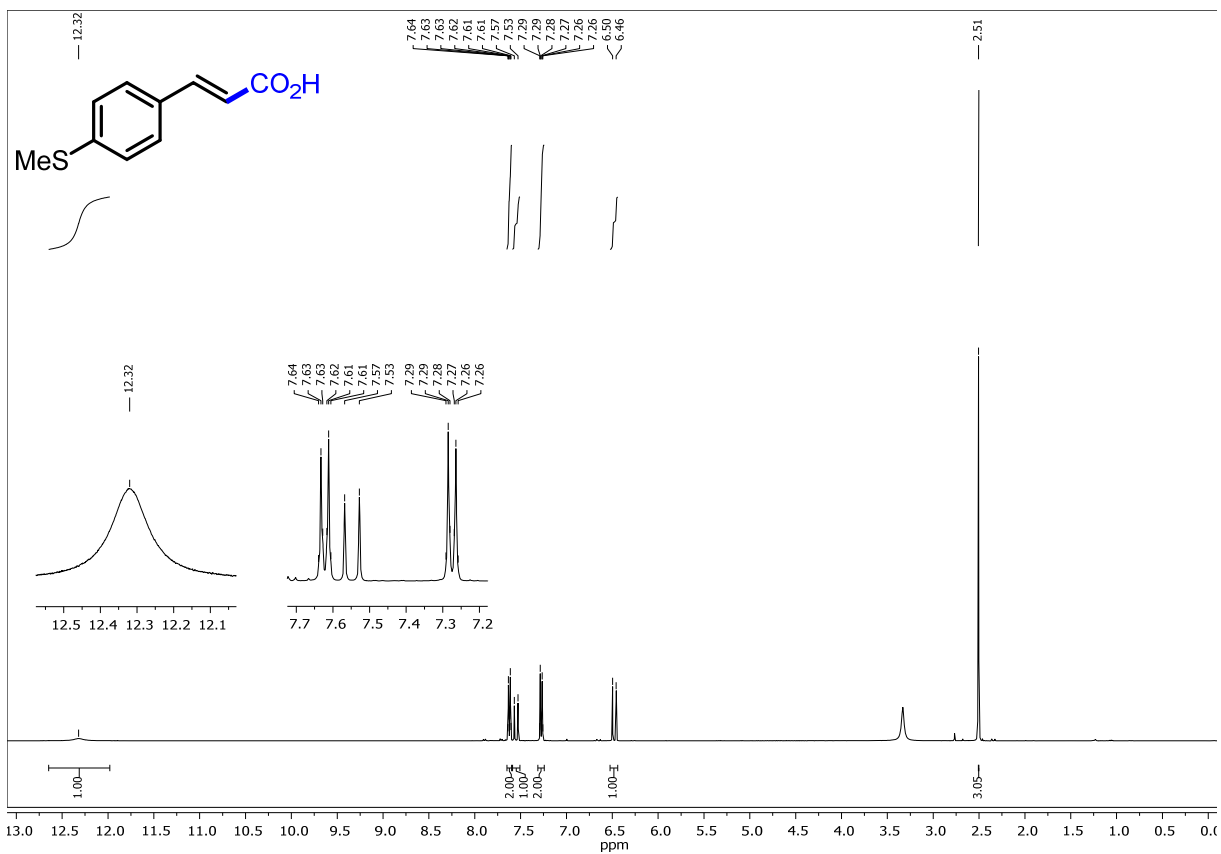


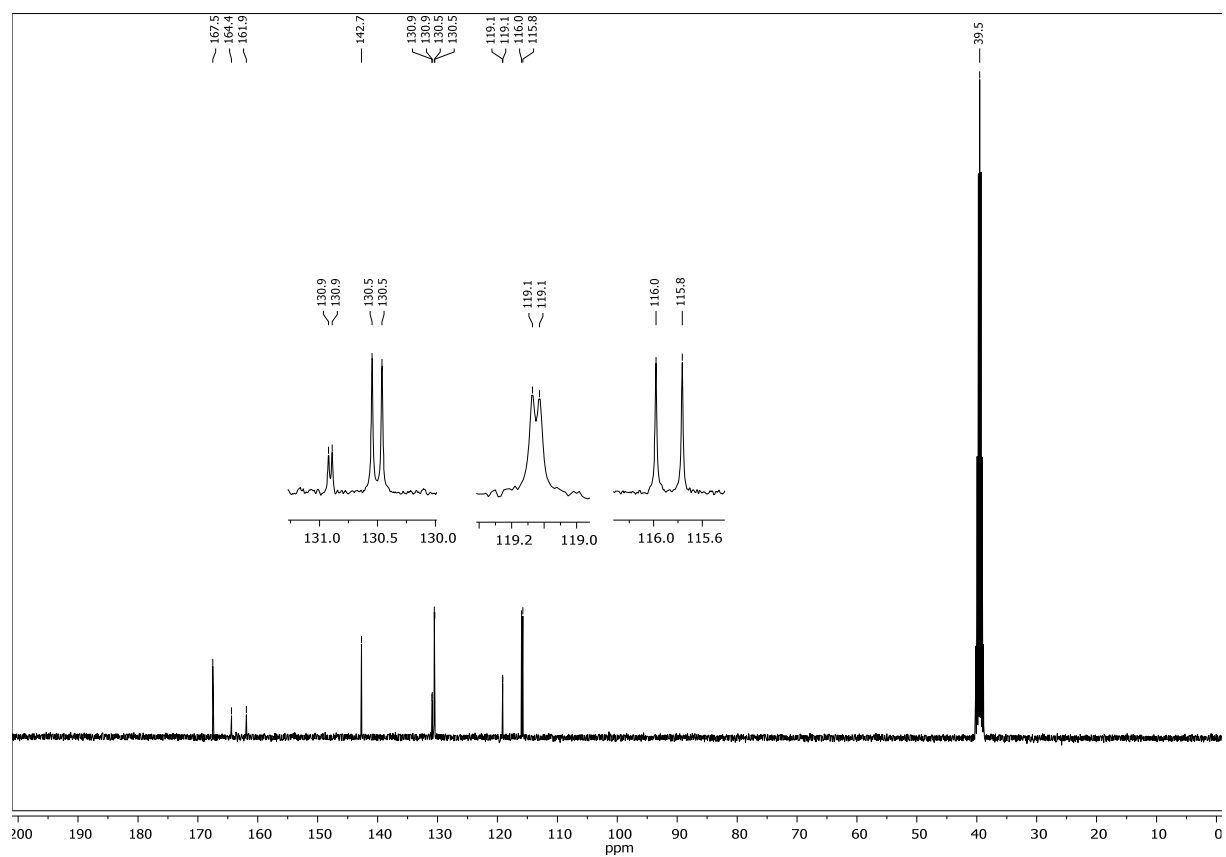
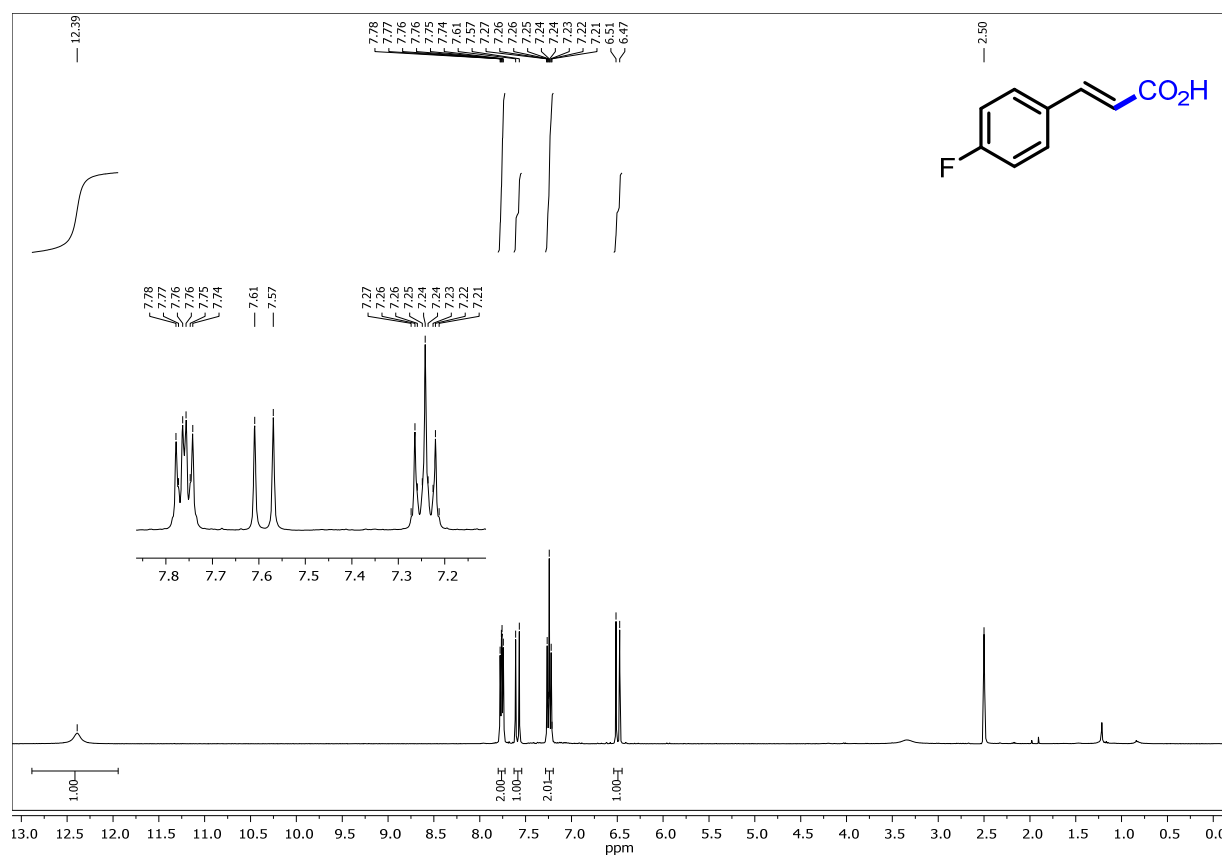


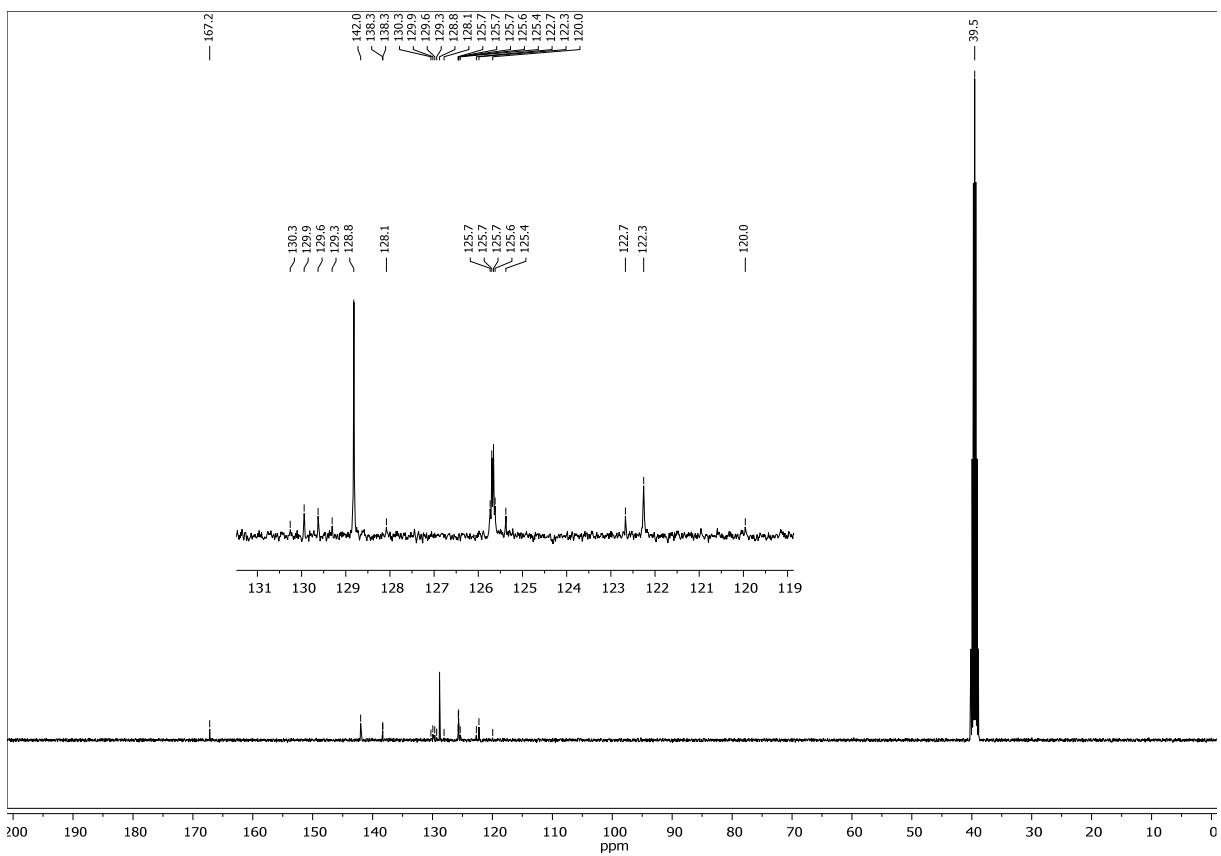
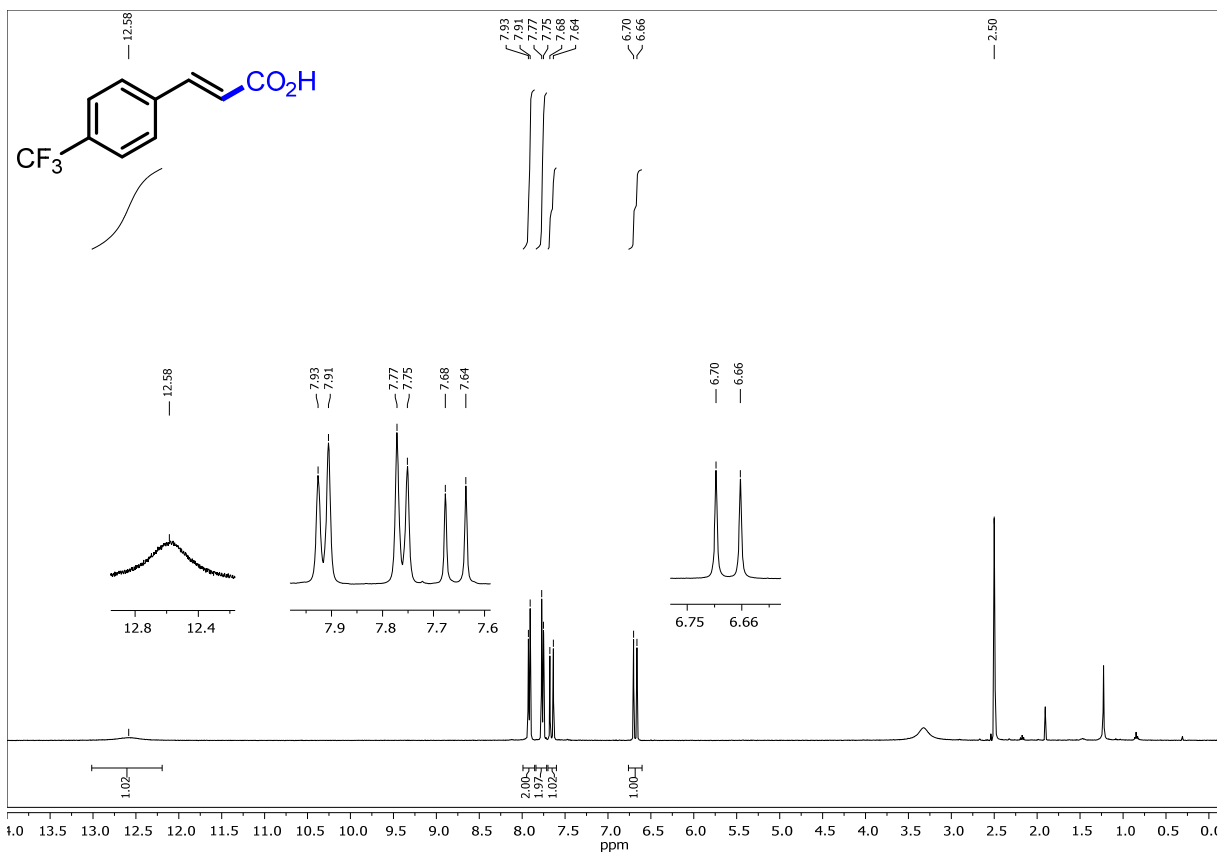


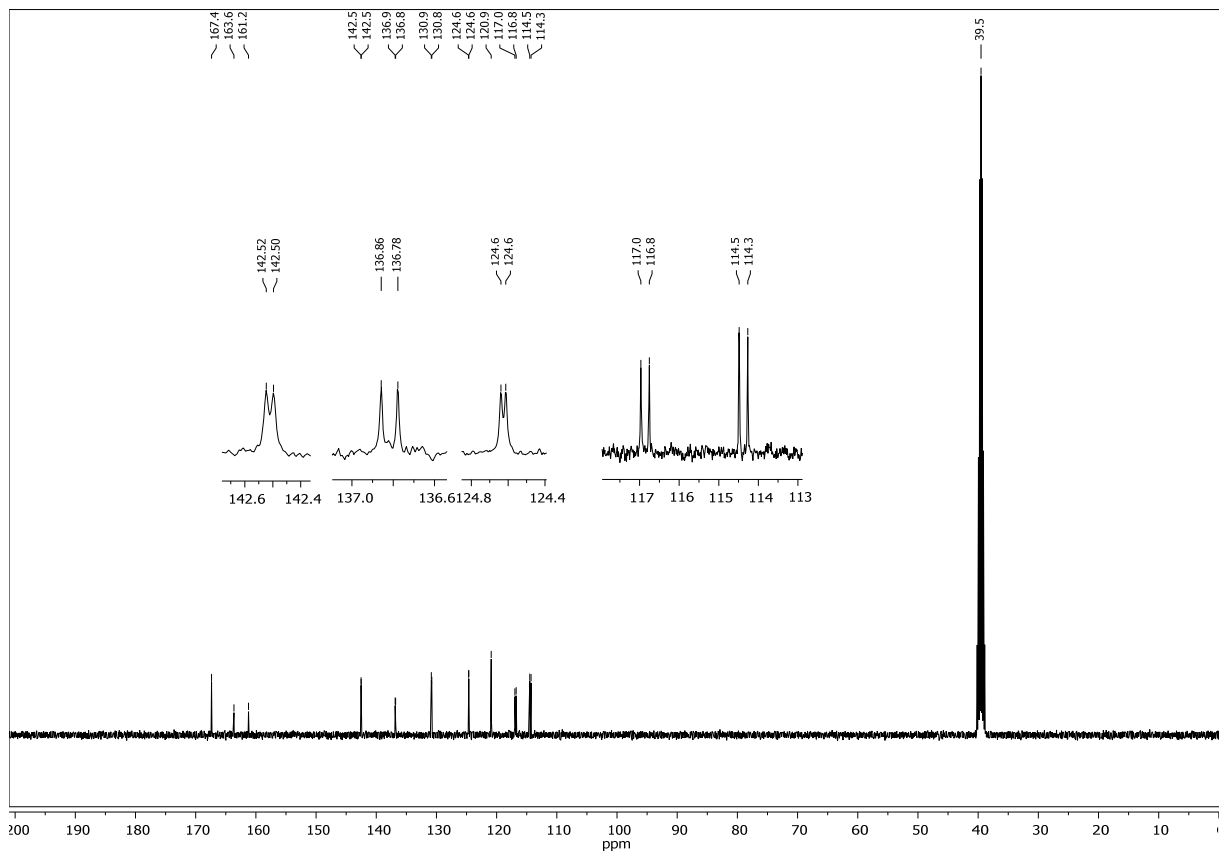
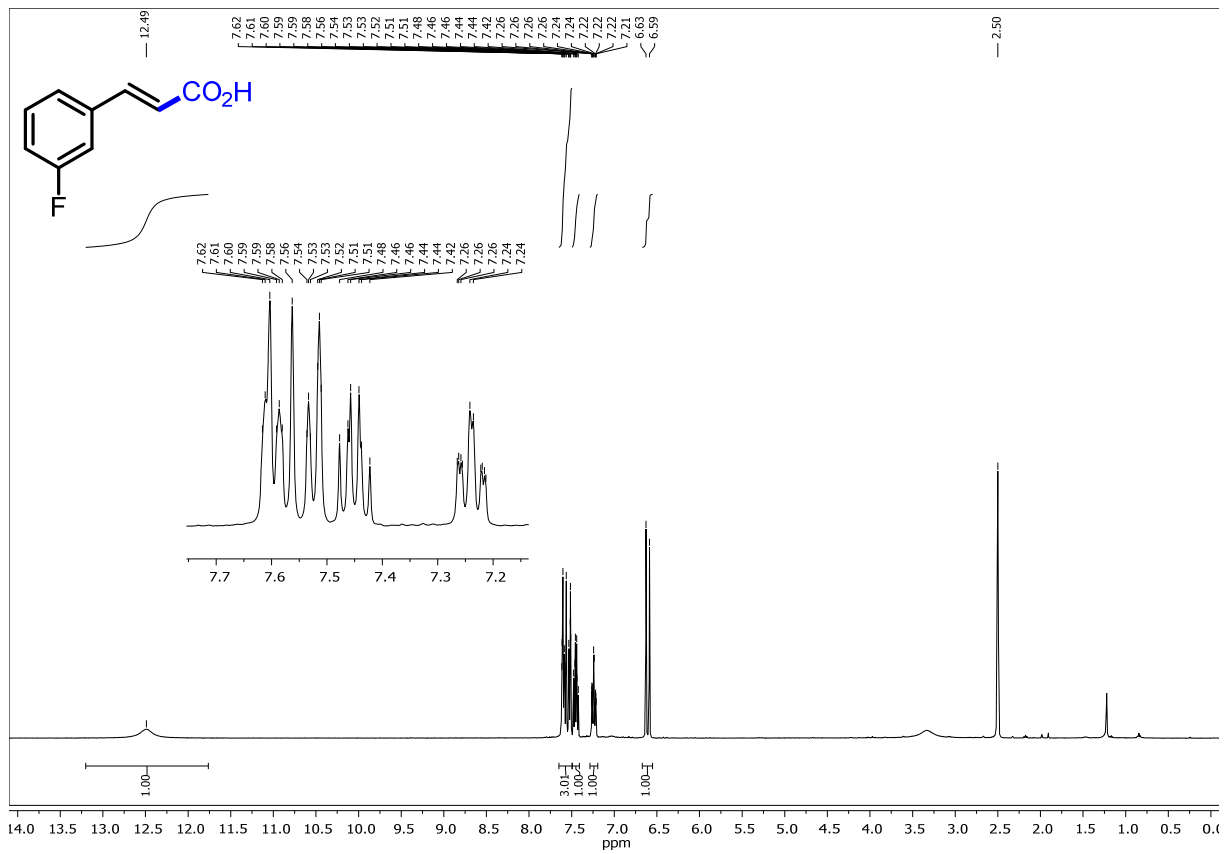


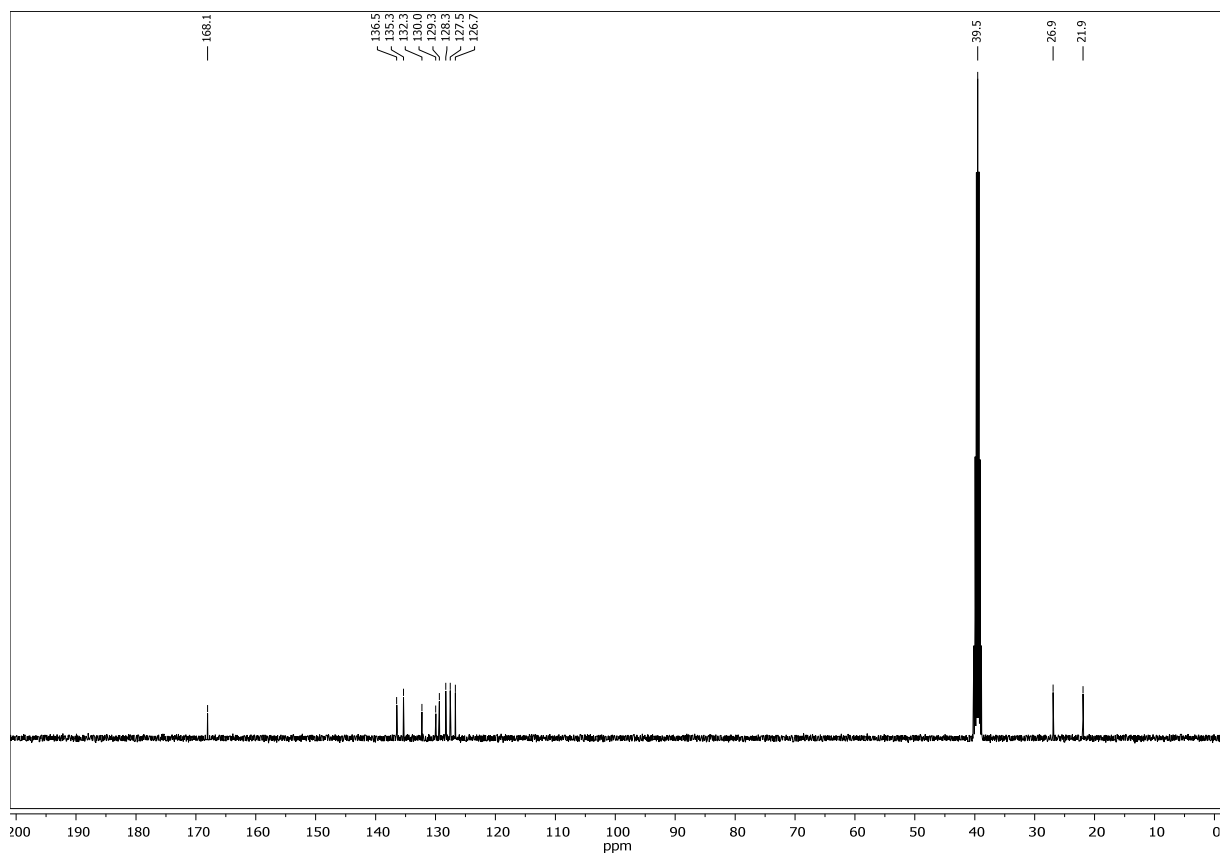
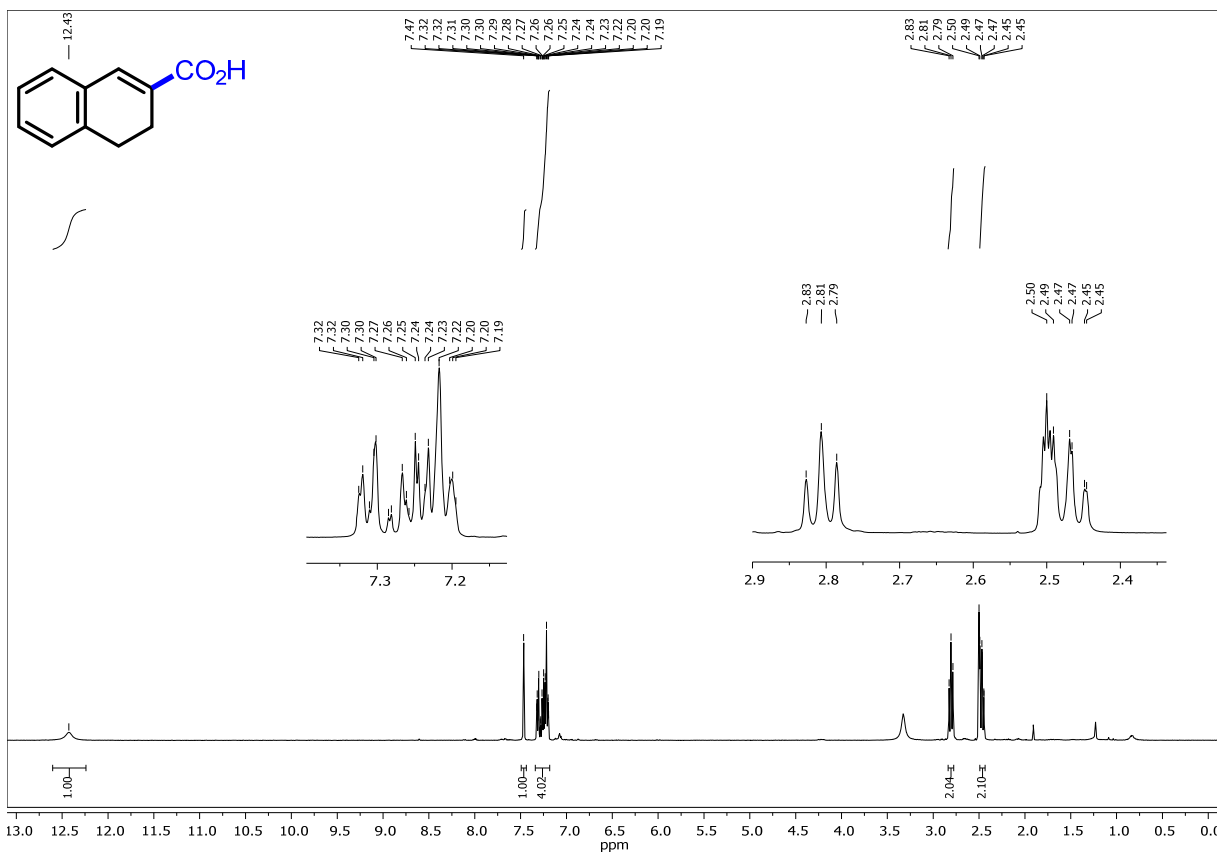


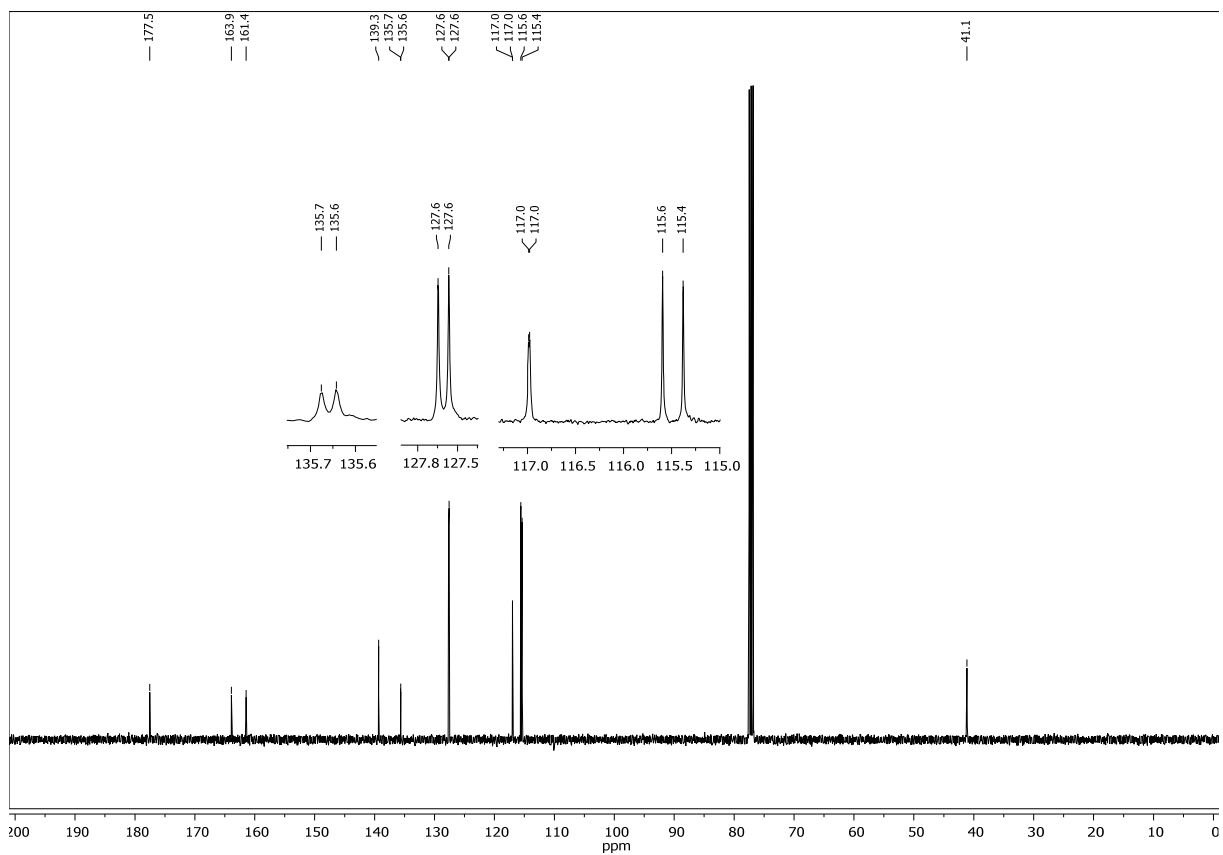
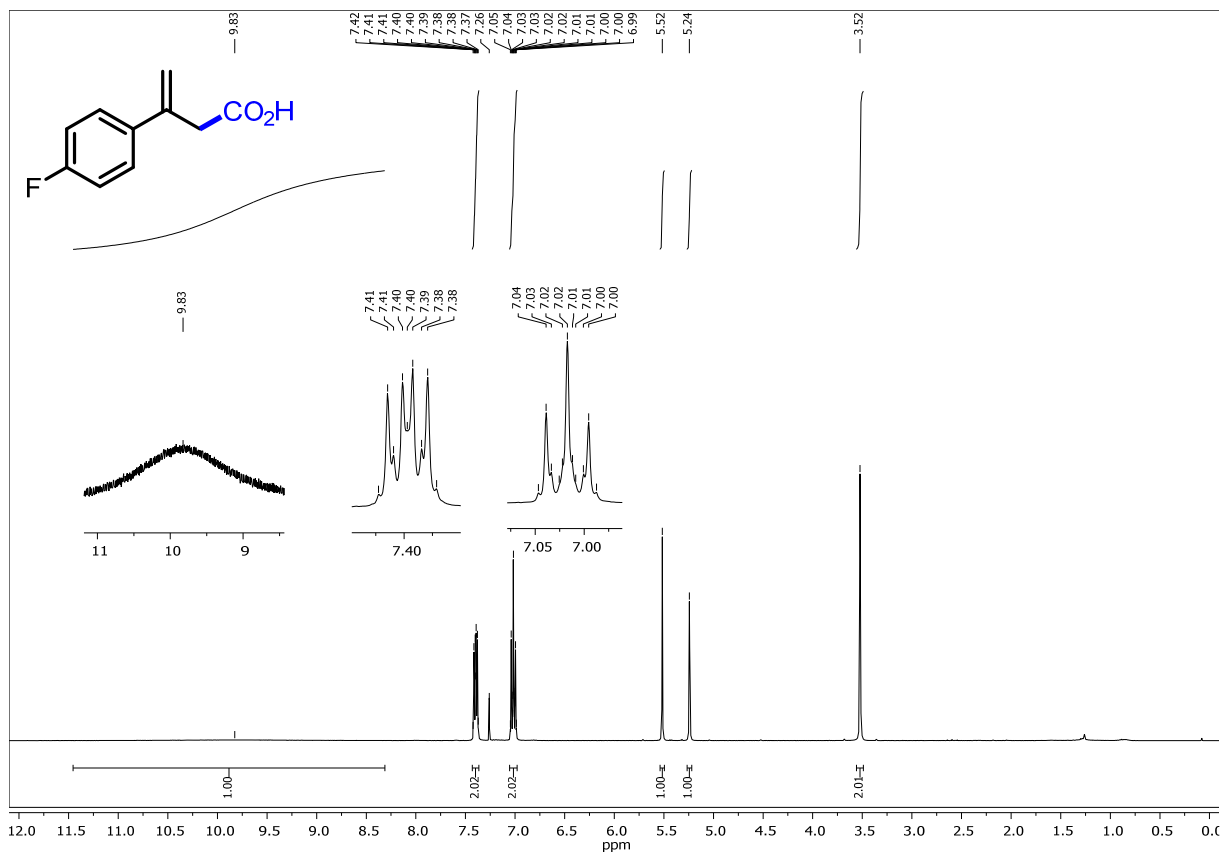


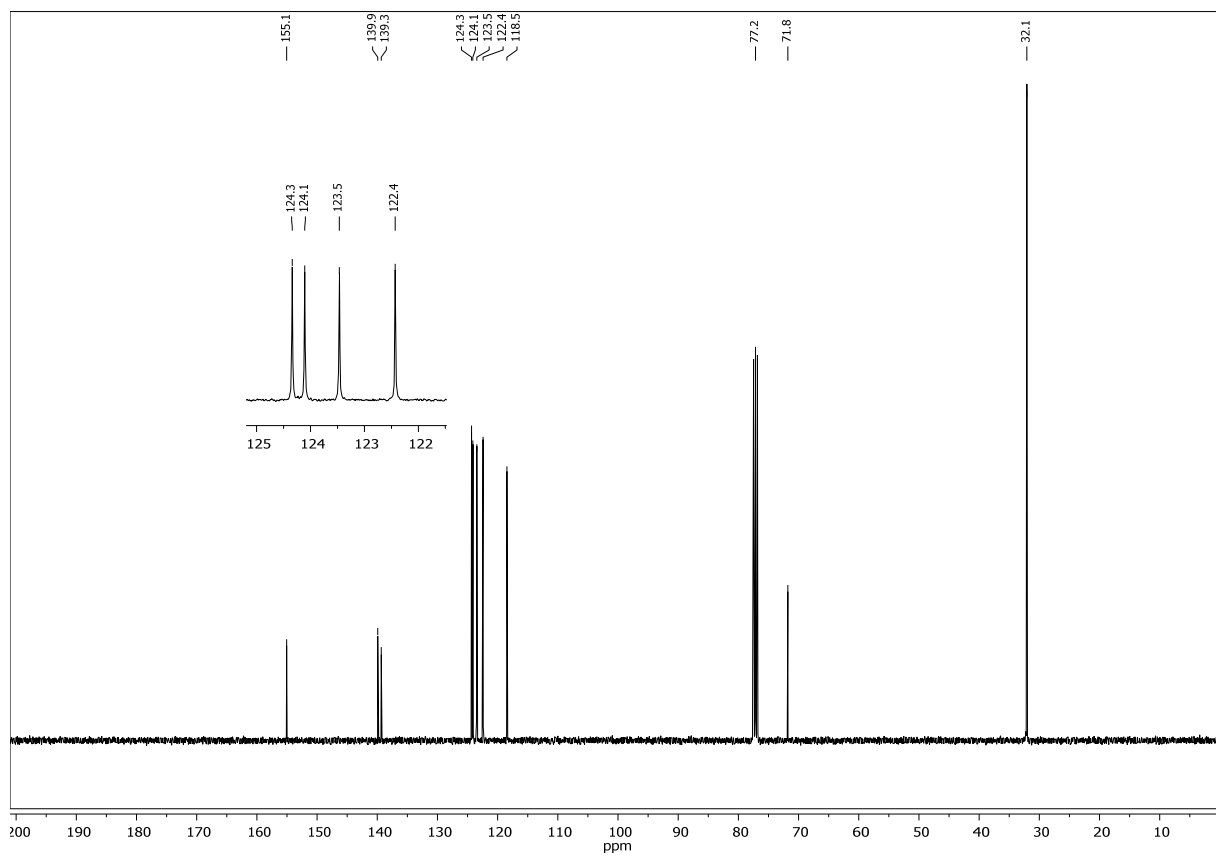
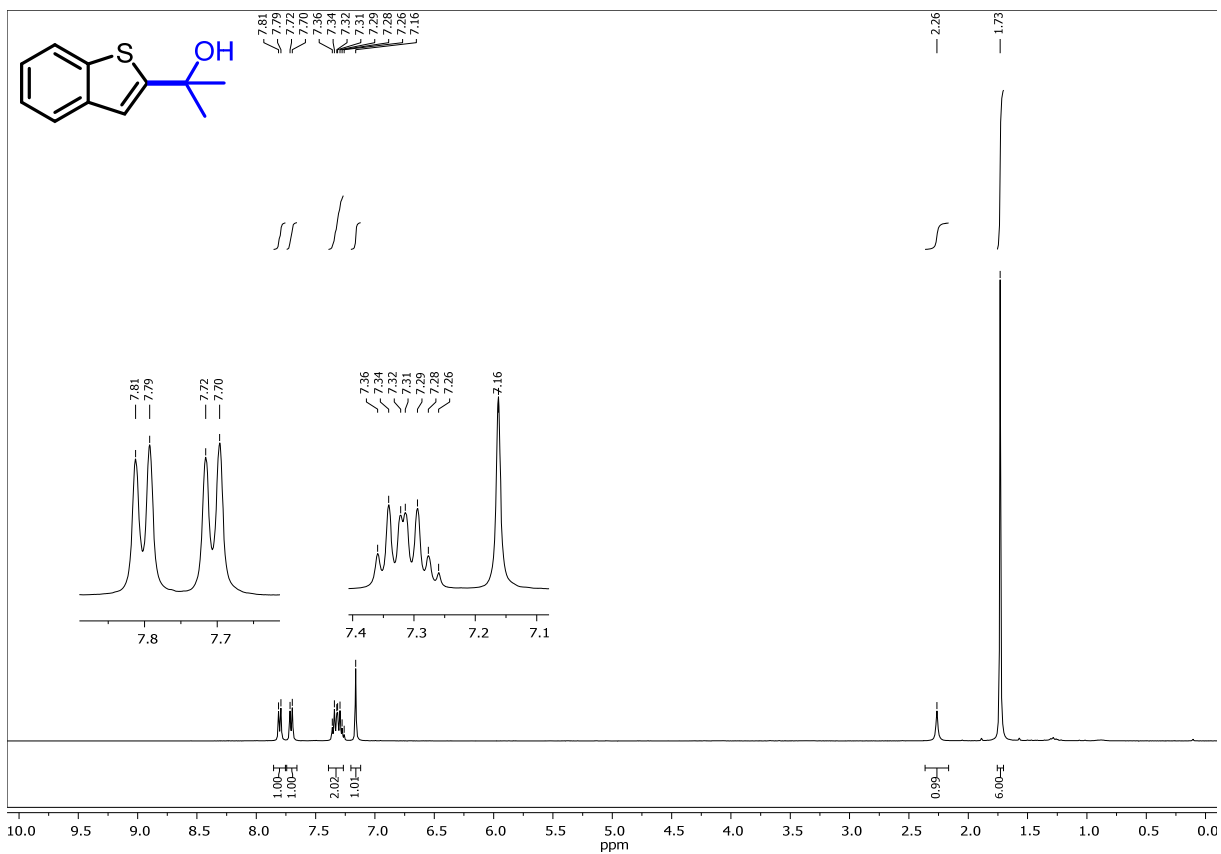


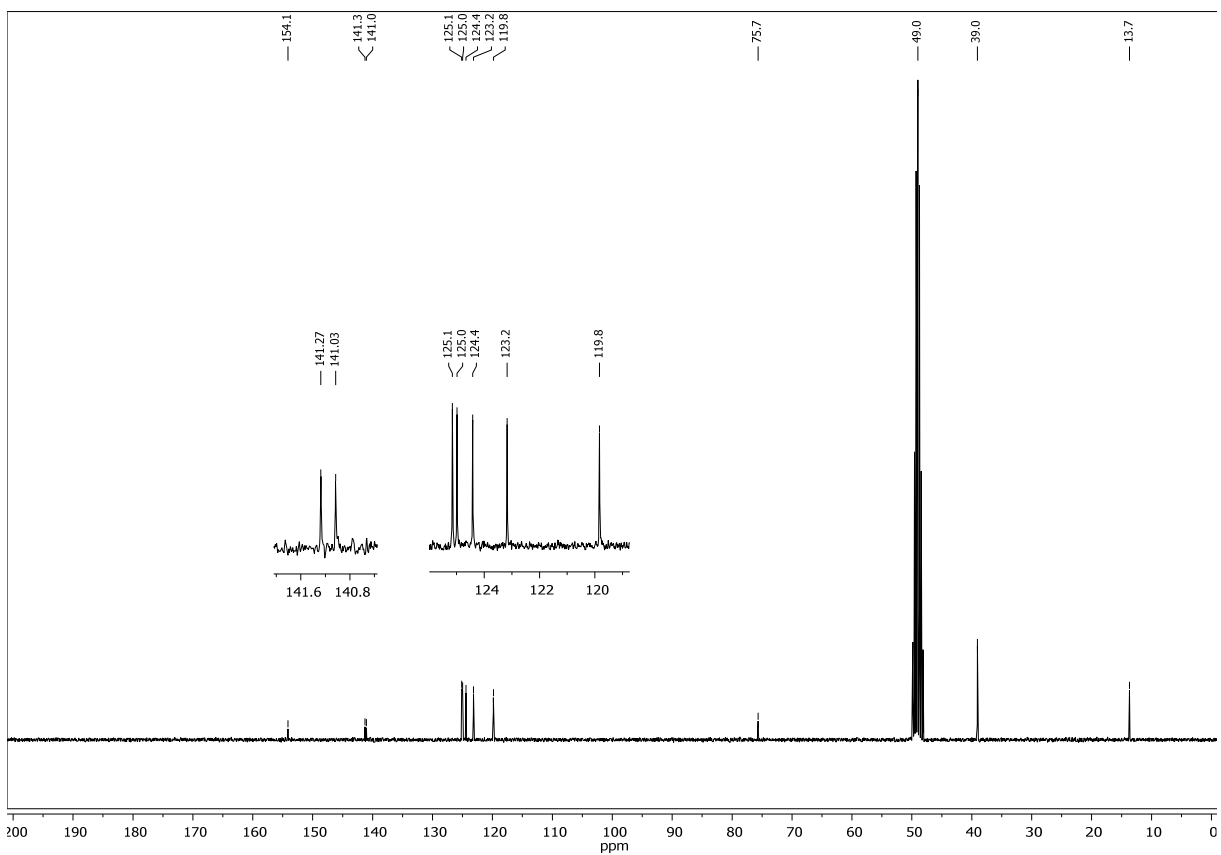
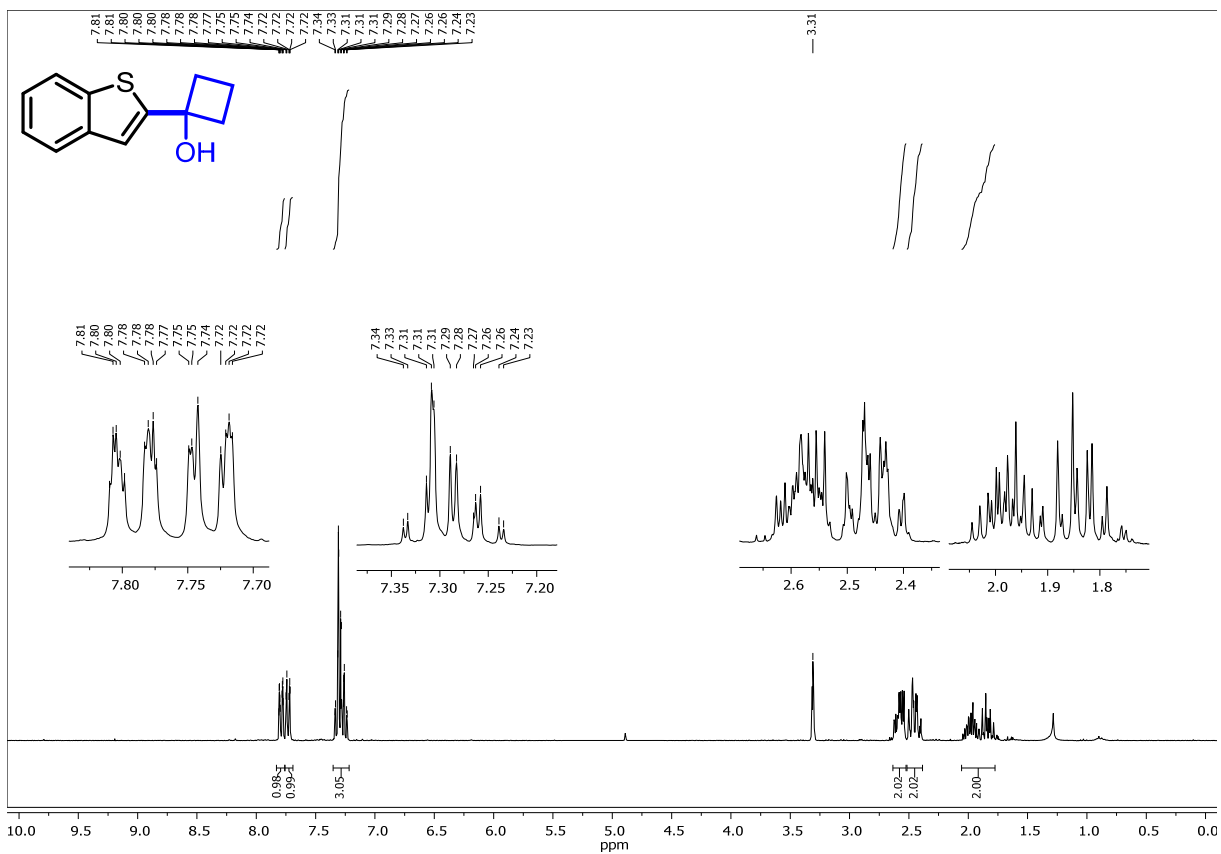


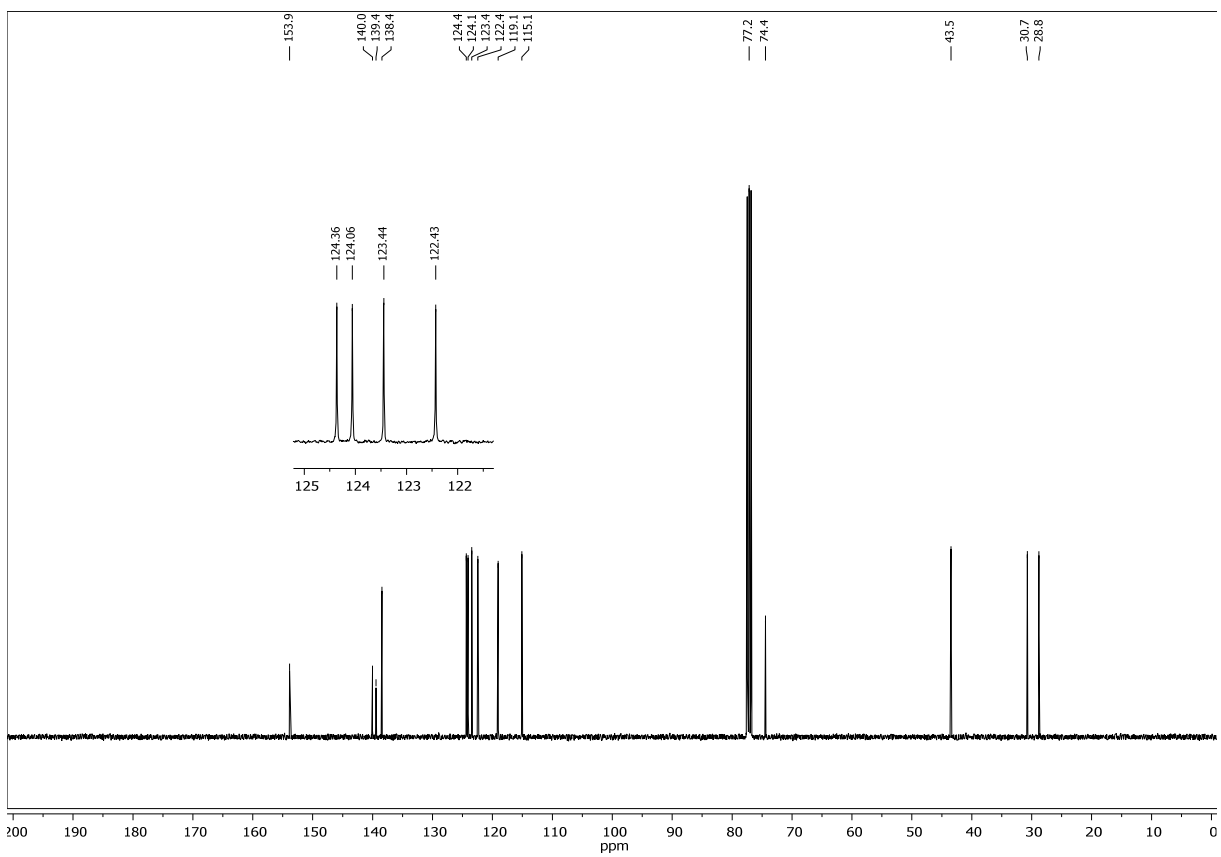
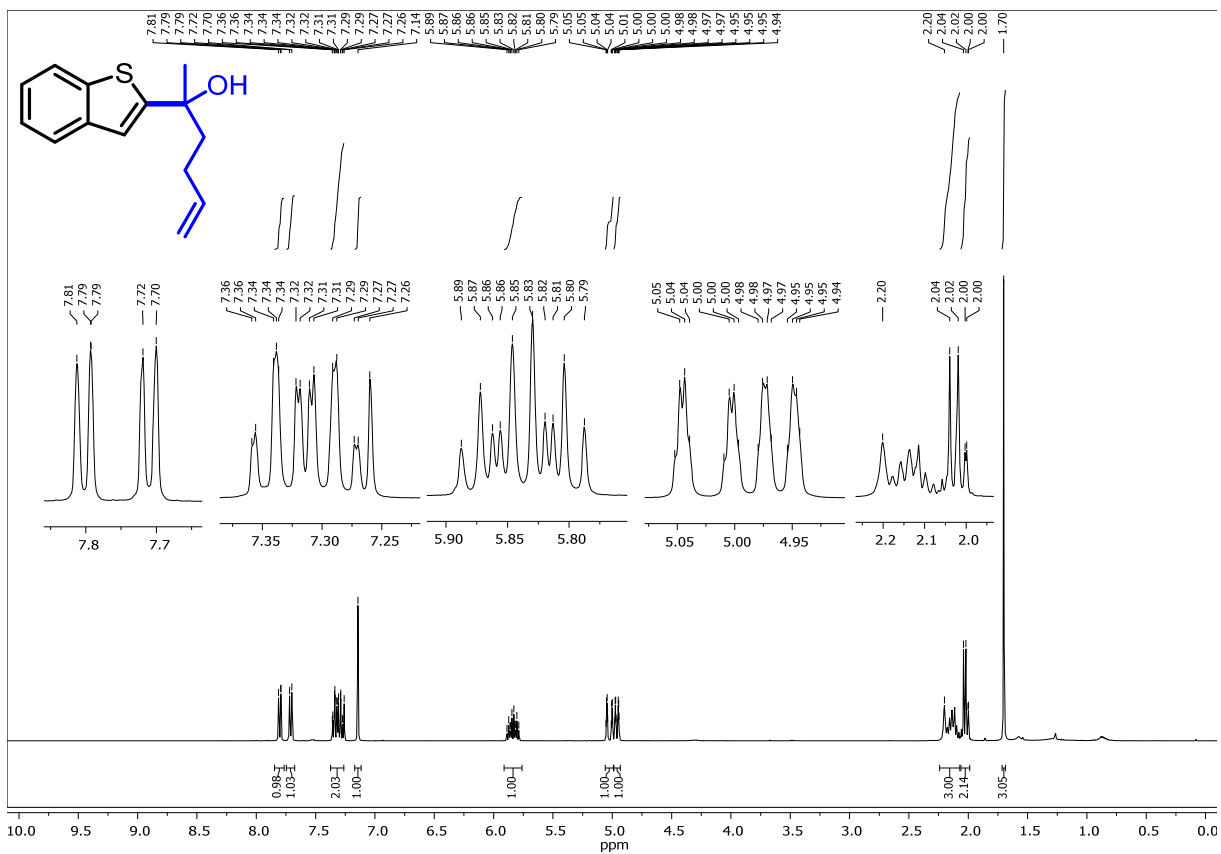












6 - Mechanistic Studies

6.1 - General Procedure for High-throughput Screening of Arenes

To a paradox 96-well plate fitted with 0.5 mL glass vials containing magnetic stirrer bars was added the arene (0.03 mmol) and 2,3,6,7-tetramethoxyanthracen-9(10*H*)-one (2.0 mg, 20 mol%). The vials were partially-sealed and transferred to a glovebox antechamber after the vial had evacuated and refilled with N₂ (3×) within the antechamber. DMSO (0.3 mL) was dispensed to each of the vials followed by 1,1,3,3-tetramethylguanidine (11 μL, 0.09 mmol) and the plate was sealed with the plate lid, two rubber mats and a Teflon TFA film. The plate was then removed and transferred to a glove-bag filled with an over-pressure of CO₂. The plate was then unsealed and placed on a stirrer plate with 3×456 nm Kessil lamps clamped overhead. The vial was then irradiated from above by two kessil lamps (vials approximately 10 cm away from the light source). After 18 hrs the irradiation was stopped and the plate was removed from the glove bag and quenched with aq. HCl (0.2 mL, 0.5M) and samples were taken and filtered before being placed on a plastic 96 well plate for HPLC analysis.



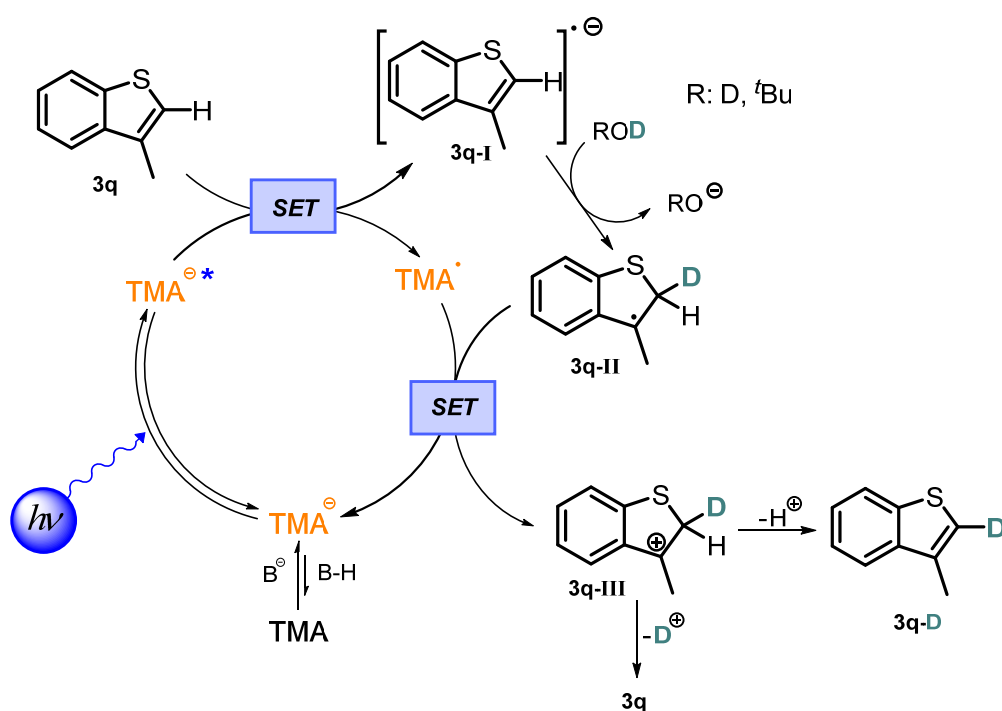
Figure S9. a) photo showing the removal of the plate lid within the CO₂ glove-bag for mass screening of substrates. b) 96 well plate reactions running in the CO₂ glove-bag set up.

6.2 - Deuterium Labeling Experiments

Upon formation of an arene radical anion **3q-I** we envisioned a H/D exchange reaction giving rise to **3q-II** in presence of a deuterium source. After reoxidation and deprotonation **3q-D** would be formed (Scheme S3).

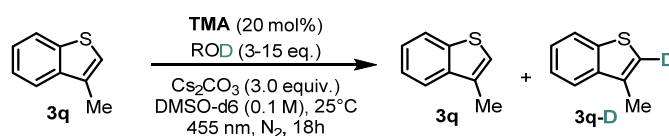
To a dry flat-bottomed crimp vial (5 mL) equipped with stirring bar, was added **3q** (0.1 mmol) and 2,3,6,7-tetramethoxyanthracen-9(10*H*)-one (6.3 mg, 0.02 mmol, 20 mol%, only for entry 1-3 Table S3). Cs₂CO₃ (98 mg, 3 equiv.) was quickly added and the vial was sealed with a Supelco aluminium crimp

seal with septum (PTFE/butyl). The vial was then evacuated and refilled with N_2 ($5\times$) *via* syringe needle. The reaction mixture was dissolved in DMSO- d_6 (1 mL, dry and degassed by bubbling with N_2) and the deuterium source was added *via* syringe. The vial was then irradiated from the bottom side with blue LED light and a constant reaction temperature (25°C) was maintained by employing a water-cooling circuit connected to a thermostat. After 18 hrs of reaction time the reaction was quenched by the addition of water and the crude mixture was extracted with Et_2O ($3\times$). The combined organic layers were dried over Na_2SO_4 , concentrated and purified *via* flash silica column chromatography using a mixture of hexanes and DCM (95:5) as eluent. The obtained product was dried in vacuo and analyzed by $^1\text{H-NMR}$ (Table S3 and Figures S10a-b) and GC-MS (Figure S10c).



Scheme S3. Proposed mechanism for the deuterium labeling experiments using **3q** as substrate.

Table S3. Deuterium labeling experiments



entry	catalyst	λ [nm]	D-source (eq.)	D-incorporation [%] ^a
1	TMAH	455	D_2O (3)	10
2	TMAH	455	D_2O (15)	14
3	TMAH	455	$^t\text{BuOD}$ (10)	15
4 ^b	-	dark	D_2O (15)	<1

^a determined by $^1\text{H-NMR}$ integration upon isolation and purification of the reaction mixture; ^b reaction was stirred in the dark.

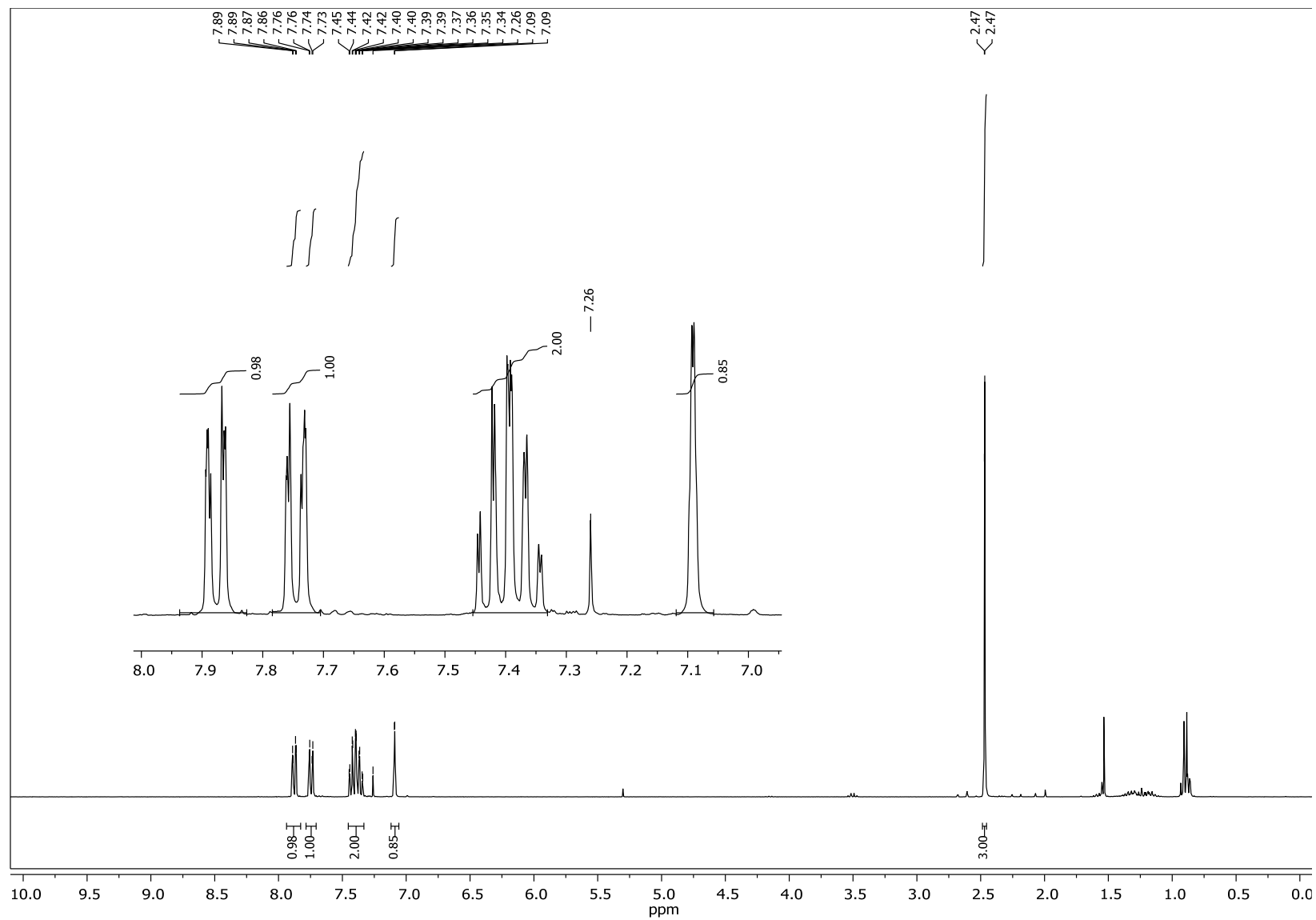


Figure S10a. $^1\text{H-NMR}$ recorded after reaction work-up and column chromatography according to entry 3, Table S3. The signal at 7.1 ppm corresponds to the proton in position 2 of **3q**. Peak integration revealed a slightly reduced value of 0.85. The signal at 7.75 ppm served as reference and was set to integral 1.00.

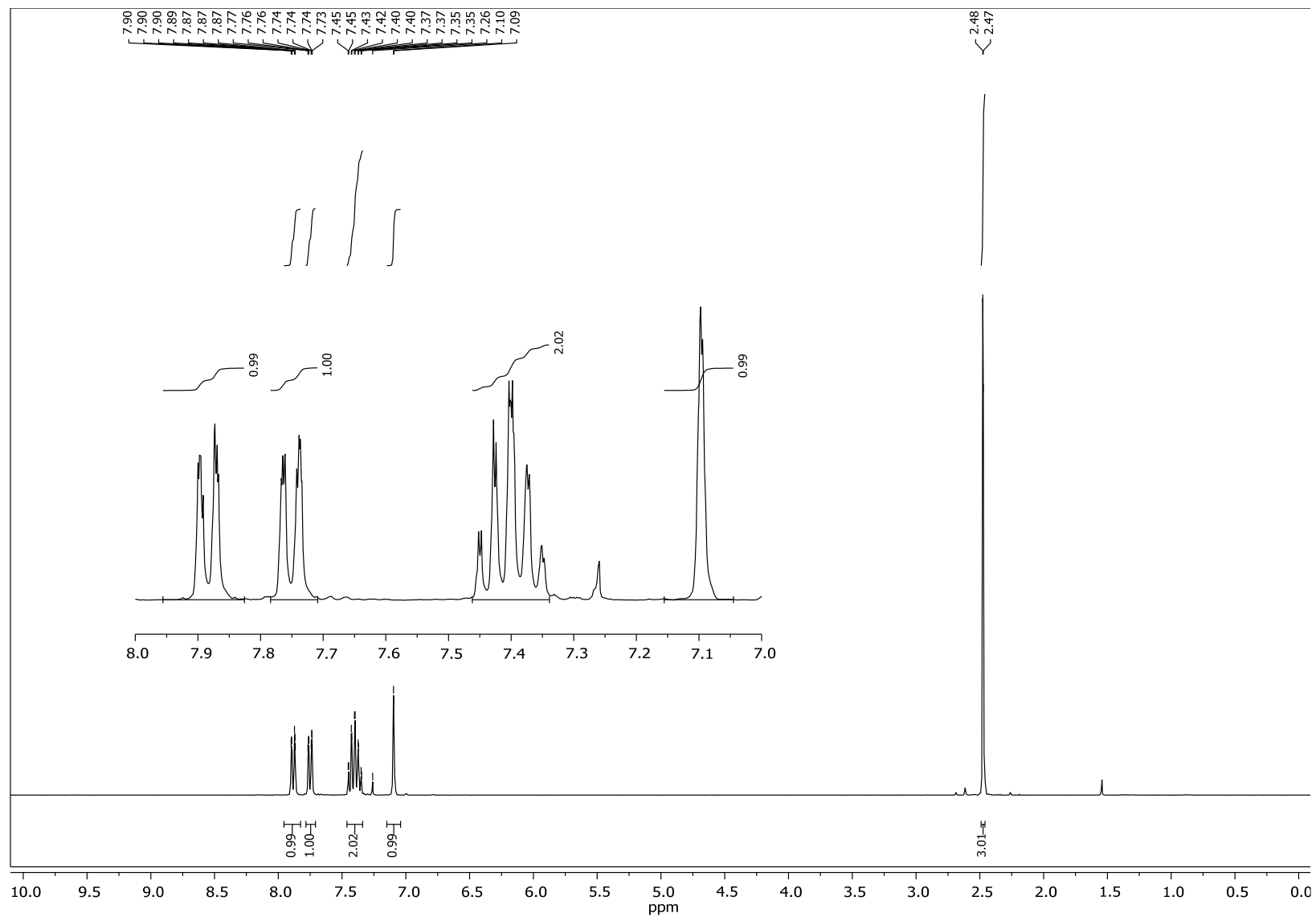


Figure S10b. $^1\text{H-NMR}$ recorded after reaction work up and column chromatography according to entry 4, Table S3. The signal at 7.1 ppm corresponds to the proton in position 2 of **3q**. Peak integration revealed a value of 0.99. The signal at 7.75 ppm served as reference and was set to integral 1.00.

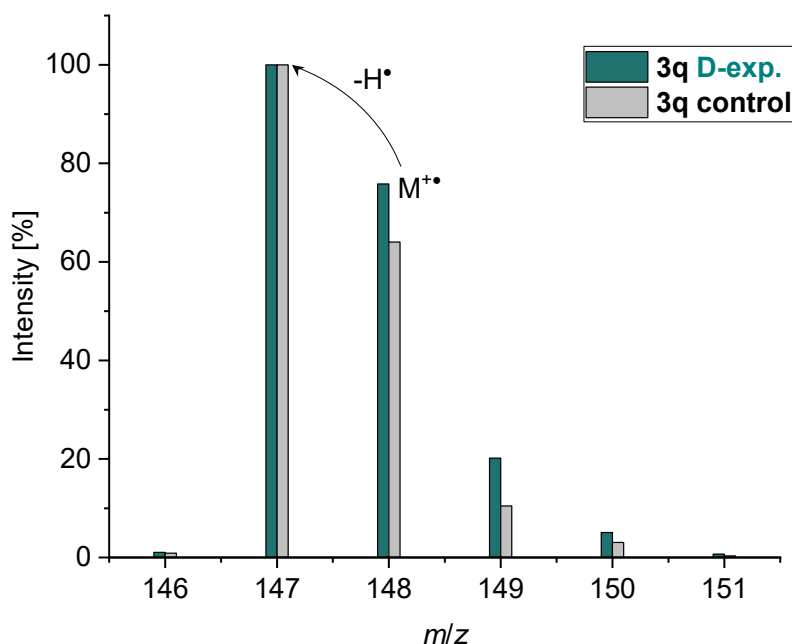


Figure S10c. GC-MS analysis after reaction work up and column chromatography according to entry 3 from Table S3 (green) and purchased **3q** (grey). Mass spectra was recorded upon electron impact ionization (70 eV). The ionized **3q** is prone to lose a hydrogen atom causing the most intense peak at m/z 147.

Figure S10a shows the $^1\text{H-NMR}$ spectrum from the isolated product of the deuterium labeling experiment in presence of $t\text{BuOD}$ (entry 3, Table S3). Integration over the signal at 7.1 ppm, which corresponds to the proton in position 2 of benzothiophene **3q**, revealed a slightly decreased value (0.85 instead of 1.00). This deviance can be explained by the partial exchange of hydrogen by deuterium.

Figure S10b shows the $^1\text{H-NMR}$ spectrum from the isolated product of the control reaction (entry 4, Table S3). Integration over the signal at 7.1 ppm gave a value close to unity and suggests no or only traces of incorporated deuterium.

In addition to $^1\text{H-NMR}$ analysis, the incorporation of deuterium was verified by GC mass. Compared to the set of peaks caused by the purchased starting material **3q** (Figure S10c, grey), the different ratios in the isotope pattern suggest the partial incorporation of deuterium into the product isolated upon deuterium labeling reaction (entry 3, Table S3).

6.3 - Time-resolved Luminescence Quenching studies

A first prediction regarding possibly working substrates was made by time-resolved luminescence quenching of the photoexcited catalyst. If there is an interaction between the excited PC and the substrate (electron transfer is proposed), the luminescence lifetime is shortened. Such processes can be easily followed by luminescence lifetime analysis and from the data obtained a Stern-Volmer plot of the time-resolved experiment was developed (Figure S11a-d and S13). A linear correlation between concentration of quencher [Q] and $\tau_0 \times \tau^{-1}$ indicates a dynamic luminescence quenching. The luminescence lifetime was recorded in dry, degassed DMSO in presence of cesium carbonate by using a quartz cuvette (1×1 cm) with septum screw cap. The cuvette was degassed *in vacuo* and backfilled with N₂ (5×) before the stock solution of quencher and the catalyst solution were added *via* syringe. A TMAH concentration of c(TMAH) = 40 μM in the cuvette was used for all experiments. For excitation of the sample, a 452 nm laser diode was used and an optical longpass filter (cut-on wavelength 500 nm) was installed before the detection unit. The time range for the measurement was set to 400 ns. The experimental data were fitted with a mono-exponential function. The quenching experiment using CO₂ as quencher was recorded as described above using a CO₂-saturated DMSO solution. The approximated concentration of dissolved CO₂ was calculated from literature data.⁴¹

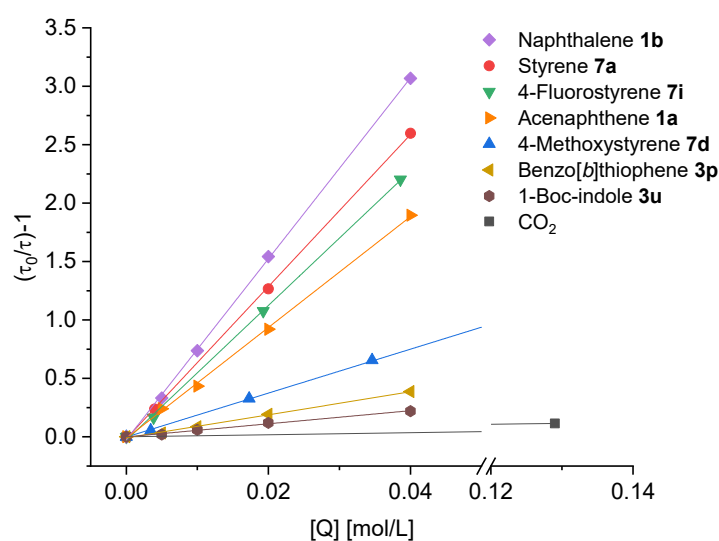


Figure S8a. Stern-Volmer plot developed with data obtained from time-resolved quenching experiments of TMAH in presence of Cs₂CO₃ with tolerated substrates and a CO₂-saturated solution of DMSO.

Thiophene derivatives **3c**, **e**, **j** are excellent quenchers and are tolerated in the carboxylation reaction whereas benzo[*b*]thiophene (**3p**) was found to quench the excited state of TMA⁻, however less efficiently. No quenching was observed in presence of thiophene and no carboxylation occurred when thiophene was used as substrate under the optimized reaction conditions (Figure S11b). The tested N-heteroarenes containing at least one nitrogen are quenching the excited photocatalyst. However, carboxylation products were only obtained using **3u** (Figure S11a) or **3w** (Figure S11c). Using acetone

9a as electrophile instead of CO₂ gave rise to the respective tertiary alcohol **9pa**. Quenching studies revealed that adding acetone (up to 2000 eq. regarding to catalyst concentration) does not quench the photoexcited TMA⁻ (Figure S11d), supporting the hypothesis of a nucleophilic arene radical anion which attacks the electrophile.

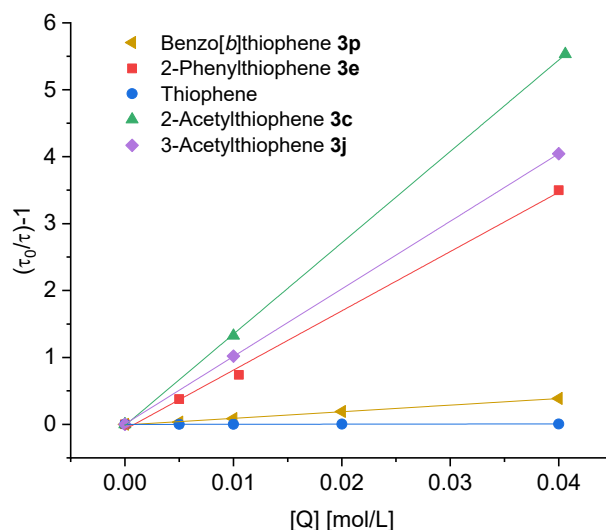


Figure S9b. Stern-Volmer plot developed with data obtained from time-resolved quenching experiments of TMAH in presence of Cs₂CO₃ with thiophene derivatives. In case of thiophene, no quenching was observed. No carboxylation occurred using thiophene as substrate under the optimized reaction conditions.

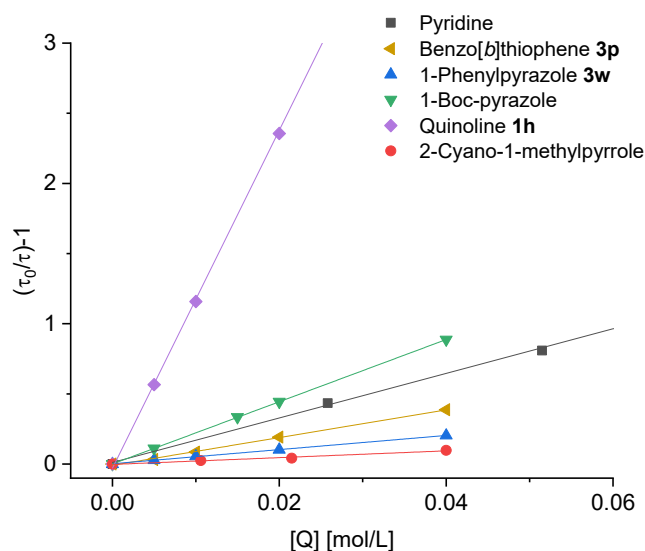


Figure S10c. Stern-Volmer plot developed with data obtained from time-resolved quenching experiments of TMAH in presence of Cs₂CO₃ with *N*-heteroarenes and benzo[*b*]thiophene as reference.

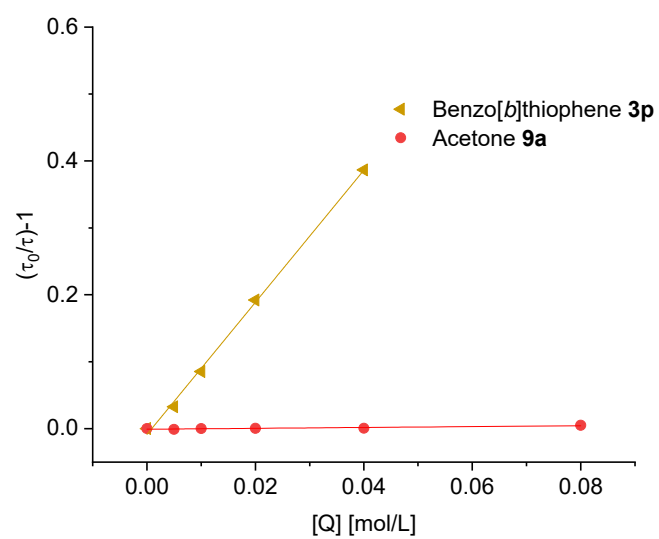


Figure S11d: Stern-Volmer plot developed with data obtained from time-resolved quenching experiments of TMAH in presence of Cs₂CO₃ with acetone and benzo[*b*]thiophene as reference.

6.4 - Computational Analysis

Screening density functional theory (DFT) calculations were performed on substrates and radical anions to derive molecular and atomic properties that could rationalize the reaction outcomes. Geometries were optimized using the B3LYP-D3⁴² *a posteriori*-corrected hybrid functional⁴³ with the LACVP**+ basis set, and final energies and atomic properties were calculated using B3LYP-D3/LACV3P**+ together with the PBF solvation model⁴⁴ for DMSO. The calculations were performed within the Schrödinger Small-Molecule Drug Discovery Suite 2019-2 using Jaguar version 10.4.⁴⁵ To facilitate convergence to a minimum, any apparent symmetry in the starting geometry was ignored in the optimizations (isymm=0). To facilitate SCF convergence for some radical anions the use of the pseudospectral method was turned off during all calculations (nops=1; **J** and **K** operators constructed from analytic two-electron integrals; no grid used). For each substrate and radical anion, Atomic Fukui indices, Mulliken charges and the spin population were calculated. The electron affinity for each substrate was roughly estimated by the direct DFT energy difference between the radical anion and the substrate and are given in kcal mol⁻¹.

As seen in Figures S10-13, there is a strong correlation with reactivity and a positive outcome and calculated atomic descriptors and estimated electron affinities. However, there are also substrates that seem to fall within the acceptable range of estimated electron affinity, atomic charge, spin distribution and nucleophilicity that does not yield the desired products. This could be due to subsequent spontaneous decarboxylation as for **3u** (requiring trapping the carboxyl acid as an ester) or the presence of non-tolerated functional groups. According to the calculations, the regioselectivity is most strongly correlated to the Mulliken spin population.

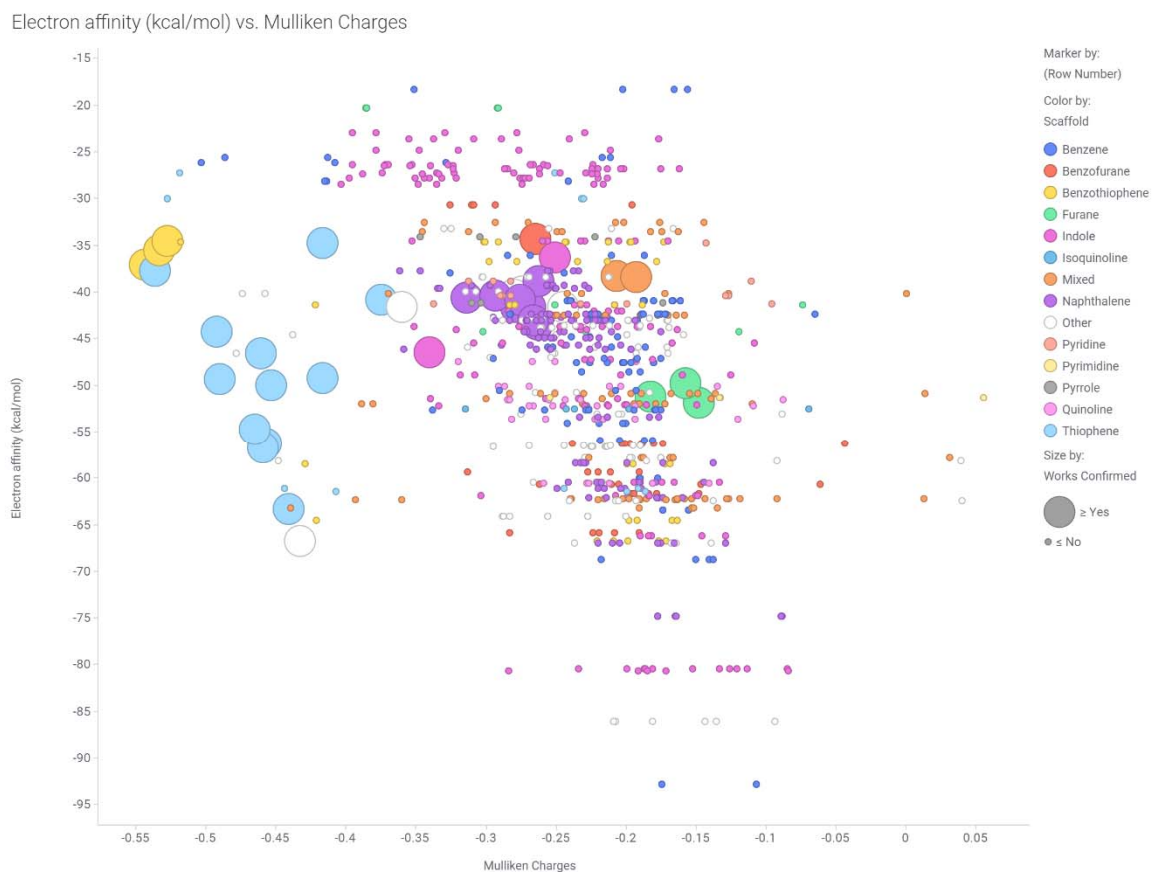


Figure S12a. A plot of the DFT estimated electron affinities (kcal mol^{-1}) vs. Mulliken charges of the radical anions for the carbons reacting with CO_2 and for all CH carbons in the aromatic rings of non-reacting substrates, highlighting that most of the reactive substrates are located within a triangle. Three reacting furanes coloured in green are outliers.

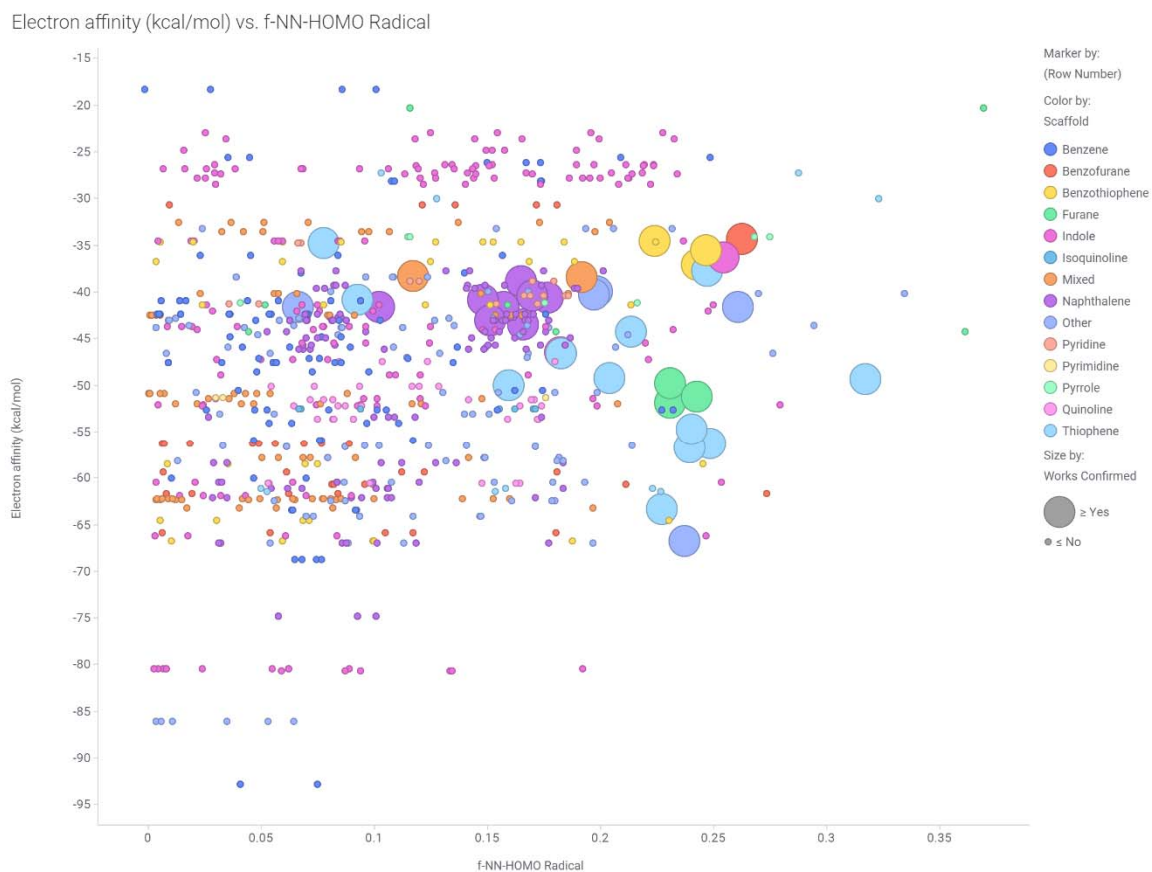


Figure S12b. A plot of the DFT estimated electron affinities (kcal mol^{-1}) vs. the Fukui f-NN-index (describing nucleophilicity) of the radical anions for the carbons reacting with CO_2 and all CH carbons in the aromatic rings of non-reacting substrates illustrating that most of the reactive substrates have more nucleophilic radical anions.

Mulliken Charges vs. f-NN-HOMO Radical



Figure S12c. A plot of the DFT Mulliken charges of the radical anions vs. Fukui f-NN-index of the radical anions for the carbons reacting with CO₂ and all CH carbons in the aromatic rings of non-reacting substrates illustrating that most of the non-reactive carbons are less negatively charged and have lower predicted nucleophilicity.

Electron Affinity (kcal/mol) vs. Mulliken Spin Population

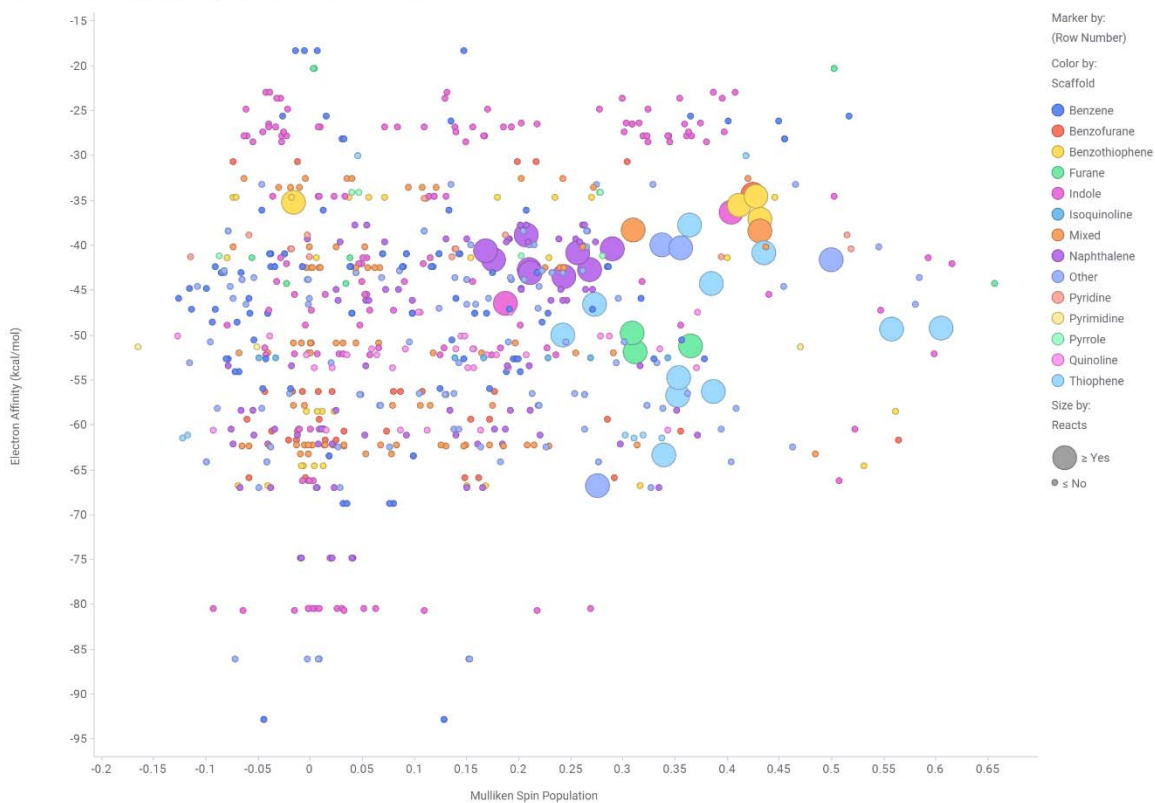
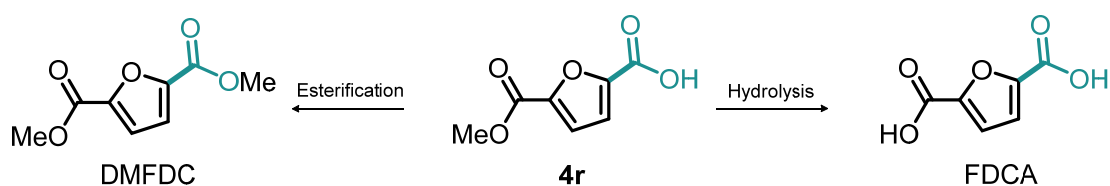


Figure S12d. A zoom in plot of the DFT Mulliken charges of the radical anions vs. Fukui f-NN-index of the radical anions for the carbons reacting with CO₂ and all CH carbons in the aromatic rings of non-reacting substrates including only compounds with DFT estimated electron affinities within the values among the substrates that react. Highlighted are substrates with required electron affinities and nucleophilicity but not reacting due to non-compatible functional groups.

7 - Miscellaneous

7.1 - Synthetic route towards FDCA and DMFDC

Modifying the conditions during reaction work-up allows for the direct transformation of the crude reaction mixture of **4r** to either 2,5-furandicarboxylic acid (FDCA) or dimethyl 2,5-furandicarboxylate (DMFDC). Both are important monomers for the manufacture of polyesters derived from biomass (Scheme S4). The reaction work-up with conc. HCl would cause the hydrolysis of the ester giving rise to the dicarboxylic acid FDCA. In contrast, the addition of MeI after releasing the CO₂ overpressure allows for the formation of dimethyl dicarboxylate DMFDC.



Scheme S4: Synthetic route towards FDCA and DMFDC starting from crude reaction mixture of **4r**.

7.2 - Carboxylation of biphenyl

Biphenyl acts as a good quencher but the resulting carboxylation product [1,1'-biphenyl]-4-carboxylic acid was only obtained in low yield (6%). Nevertheless, this result shows that also benzene derivatives can be activated towards a C–H carboxylation with our method. The thermodynamic driving force for this transformation with CO₂ however seems to be low.

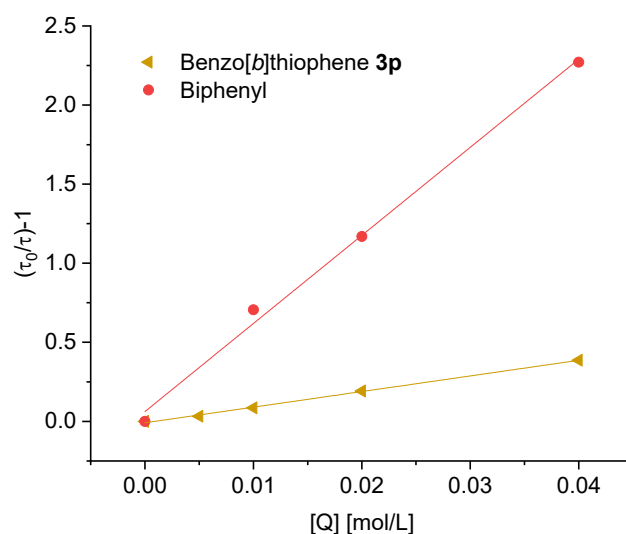


Figure S13. Stern-Volmer plot developed with data obtained from time-resolved quenching experiments of **TMAH** in presence of Cs₂CO₃ with biphenyl and benzo[*b*]thiophene **3p** as reference.

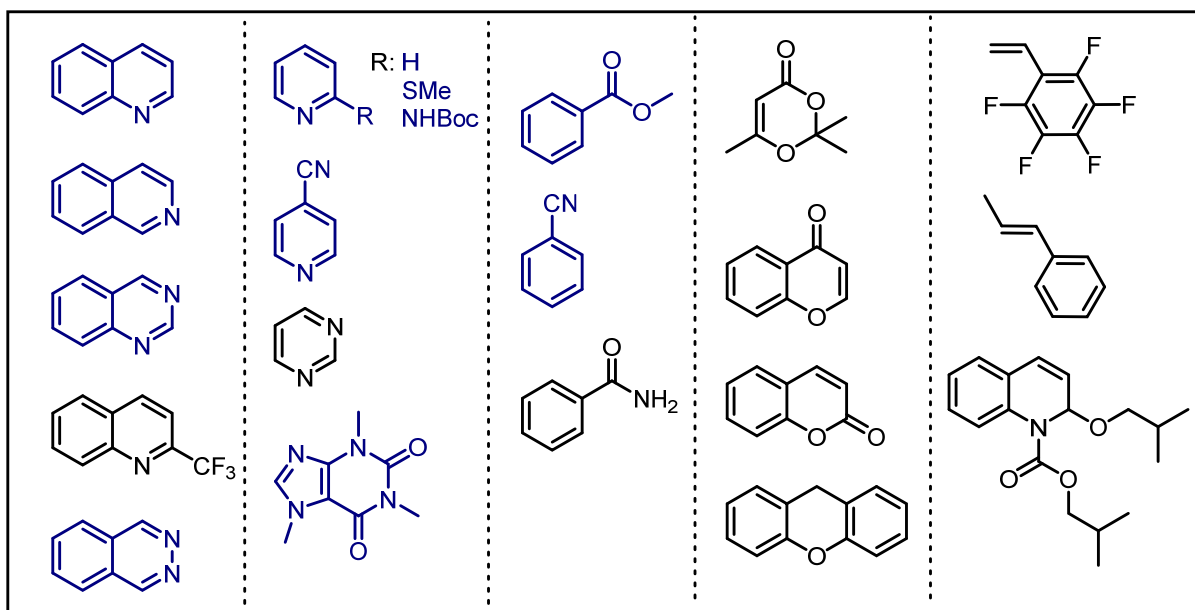


Figure S14c. Non-tolerated quinolines, pyridines, benzenes, benzopyrans, styrenes and related compounds.

8 - References

- Müller, A., Raltschewa, M., and Papp, M. (1942). Über die Dimerisation des Isoeugenolmethyläthers (Harzphenole I). *Ber. Dtsch. Chem. Ges. A* 75, 692–703.
- Stewart, P., Renney, C.M., Mooibroek, T.J., Ferheen, S., and Davis, A.P. (2018). Maltodextrin recognition by a macrocyclic synthetic lectin. *Chem. Commun.* 54, 8649–8652.
- Miao, Q., Nguyen, T.-Q., Someya, T., Blanchet, G.B., and Nuckolls, C. (2003). Synthesis, Assembly, and Thin Film Transistors of Dihydrodiazapentacene: An Isostructural Motif for Pentacene. *J. Am. Chem. Soc.* 125, 10284–10287.
- Keller, F., and Rüchardt, C. (1998). Bimolecular formation of radicals by hydrogen transfer. 14: The uncatalyzed transfer hydrogenation of α -methylstyrene by 2,6-disubstituted 9,10-dihydroanthracenes. *J. prakt. Chem.* 340, 642–648.
- Pavlishchuk, V. V., and Addison, A.W. (2000). Conversion constants for redox potentials measured versus different reference electrodes in acetonitrile solutions at 25°C. *Inorganica Chim. Acta* 298, 97–102.
- Romero, N.A., and Nicewicz, D.A. (2016). Organic Photoredox Catalysis. *Chem. Rev.* 116, 10075–10166.
- Rehm, D., and Weller, A. (1970). Kinetics of Fluorescence Quenching by Electron and H-Atom Transfer. *Isr. J. Chem.* 8, 259–271.
- Tolbert, L.M., Nesselroth, S.M., Netzel, T.L., Raya, N., and Stapleton, M. (1992). Substituent effects on carbanion photophysics. 9-Arylfluorenyl anions. *J. Phys. Chem.* 96, 4492–4496.
- Legros, B., Vandereecken, P., and Soumillion, J.P. (1991). Electron transfer photoinduced from naphtholate anions: anion oxidation potentials and use of Marcus free energy relationships. *J. Phys. Chem.* 95, 4752–4761.
- Vásquez-Céspedes, S., Chepiga, K.M., Möller, N., Schäfer, A.H., and Glorius, F. (2016). Direct C–H Arylation of Heteroarenes with Copper Impregnated on Magnetite as a Reusable Catalyst: Evidence for CuO Nanoparticle Catalysis in Solution. *ACS Catal.* 6, 5954–5961.
- Yu, X., Park, E.-J., Kondratyuk, T.P., Pezzuto, J.M., and Sun, D. (2012). Synthesis of 2-arylindole derivatives and evaluation as nitric oxide synthase and NF κ B inhibitors. *Org. Biomol. Chem.* 10, 8835.
- Discekici, E.H., Treat, N.J., Poelma, S.O., Mattson, K.M., Hudson, Z.M., Luo, Y., Hawker, C.J., and de Alaniz, J.R. (2015). A highly reducing metal-free photoredox catalyst: design and application in radical dehalogenations. *Chem. Commun.* 51, 11705–11708.
- Yamada, S., Flesch, K.N., Murakami, K., and Itami, K. (2020). Rapid Access to Kinase Inhibitor Pharmacophores by Regioselective C-H Arylation of Thieno[2,3-*d*]pyrimidine. *Org. Lett.* 22, 1547–1551.
- Pospech, J., Tlili, A., Spannenberg, A., Neumann, H., and Beller, M. (2014). Regioselective Ruthenium-Catalyzed Carbonylative Direct Arylation of Five-Membered and Condensed Heterocycles. *Chem. Eur. J.* 20, 3135–3141.
- Mäsing, F., Mardyukov, A., Doerenkamp, C., Eckert, H., Malkus, U., Nüsse, H., Klingauf, J., and Studer, A. (2015).

- Controlled Light-Mediated Preparation of Gold Nanoparticles by a Norrish Type I Reaction of Photoactive Polymers. *Angew. Chem. Int. Ed.* *54*, 12612–12617.
16. Chen, X., Yin, Y., Tanaka, K., Kita, H., and Okamoto, K.-I. (2006). Synthesis and Characterization of Novel Sulfonated Polyimides Derived from Naphthalenic Dianhydride. *High Perform. Polym.* *18*, 637–654.
 17. Zhang, X., Zhang, W.Z., Shi, L.L., Guo, C.X., Zhang, L.L., and Lu, X.B. (2012). Silver(I)-catalyzed carboxylation of arylboronic esters with CO₂. *Chem. Commun.* *48*, 6292–6294.
 18. Meyers, A.I., and Higashiyama, K. (1987). Asymmetric Additions to Chiral Naphthalenes. 4. An Asymmetric Synthesis of the AB-Ring of Aklavinone. *J. Org. Chem.* *52*, 4592–4597.
 19. Berger, P., Bessmerlykh, A., Caille, J.C., and Mignonac, S. (2006). Palladium-catalyzed hydroxycarbonylation of aryl and vinyl bromides by mixed acetic formic anhydride. *Synthesis* *2006*, 3106–3110.
 20. Nemoto, K., Yoshida, H., Egusa, N., Morohashi, N., and Hattori, T. (2010). Direct Carboxylation of Arenes and Halobenzenes with CO₂ by the Combined Use of AlBr₃ and R₃SiCl. *J. Org. Chem.* *75*, 7855–7862.
 21. Mori, S., Simkhada, D., Zhang, H., Erb, M.S., Zhang, Y., Williams, H., Fedoseyenko, D., Russell, W.K., Kim, D., Fler, N., et al. (2016). Polyketide Ring Expansion Mediated by a Thioesterase, Chain Elongation and Cyclization Domain, in Azinomycin Biosynthesis: Characterization of AziB and AziG. *Biochemistry* *55*, 704–714.
 22. Suerbaev, K.A., Aldabergenov, M.K., and Kudaibergenov, N.Z. (2015). Carboxylation of hydroxyarenes with metal alkyl carbonates. *Green Process. Synth.* *4*, 91–96.
 23. Wang, S., Dupin, L., Noël, M., Carroux, C.J., Renaud, L., Géhin, T., Meyer, A., Souteyrand, E., Vasseur, J.-J., Vergoten, G., et al. (2016). Toward the Rational Design of Galactosylated Glycoclusters That Target *Pseudomonas aeruginosa* Lectin A (LecA): Influence of Linker Arms That Lead to Low-Nanomolar Multivalent Ligands. *Chem. Eur. J.* *22*, 11785–11794.
 24. Abarbri, M., Thibonnet, J., Bérillon, L., Dehmel, F., Rottländer, M., and Knochel, P. (2000). Preparation of new polyfunctional magnesiated heterocycles using a chlorine-, bromine-, or iodine-magnesium exchange. *J. Org. Chem.* *65*, 4618–4634.
 25. Chalker, J.M., Wood, C.S.C., and Davis, B.G. (2009). A convenient catalyst for aqueous and protein Suzuki-Miyaura cross-coupling. *J. Am. Chem. Soc.* *131*, 16346–16347.
 26. Kaizerman, J.A., Gross, M.I., Ge, Y., White, S., Hu, W., Duan, J.X., Baird, E.E., Johnson, K.W., Tanaka, R.D., Moser, H.E., et al. (2003). DNA binding ligands targeting drug-resistant bacteria: Structure, activity, and pharmacology. *J. Med. Chem.* *46*, 3914–3929.
 27. Dai, J.J., Xu, W.T., Wu, Y.D., Zhang, W.M., Gong, Y., He, X.P., Zhang, X.Q., and Xu, H.J. (2015). Silver-Catalyzed C(sp²)-H Functionalization/C-O Cyclization Reaction at Room Temperature. *J. Org. Chem.* *80*, 911–919.
 28. Kilbinger, A.F.M., Schenning, A.P.H.J., Goldoni, F., Feast, W.J., and Meijer, E.W. (2000). Chiral aggregates of α,ω -disubstituted sexithiophenes in protic and aqueous media. *J. Am. Chem. Soc.* *122*, 1820–1821.
 29. Hagishita, S., Yamada, M., Shirahase, K., Okada, T., Murakami, Y., Ito, Y., Matsuura, T., Wada, M., Kato, T., Ueno, M., et al. (1996). Potent inhibitors of secretory phospholipase A2: Synthesis and inhibitory activities of indolizine and indene derivatives. *J. Med. Chem.* *39*, 3636–3658.
 30. Frizler, M., Schmitz, J., Schulz-Fincke, A.C., and Gütschow, M. (2012). Selective nitrile inhibitors to modulate the proteolytic synergism of cathepsins S and F. *J. Med. Chem.* *55*, 5982–5986.
 31. Podlesný, J., Pytela, O., Klikar, M., Jelínková, V., Kityk, I. V., Ozga, K., Jedryka, J., Rudysh, M., and Bureš, F. (2019). Small isomeric push-pull chromophores based on thienothiophenes with tunable optical (non)linearities. *Org. Biomol. Chem.* *17*, 3623–3634.
 32. Baillie, S.E., Bluemke, T.D., Clegg, W., Kennedy, A.R., Klett, J., Russo, L., De Tullio, M., and Hevia, E. (2014). Potassium-alkyl magnesiates: Synthesis, structures and Mg-H exchange applications of aromatic and heterocyclic substrates. *Chem. Commun.* *50*, 12859–12862.
 33. Shang, R., Ilies, L., and Nakamura, E. (2016). Iron-Catalyzed Ortho C-H Methylation of Aromatics Bearing a Simple Carbonyl Group with Methylaluminum and Tridentate Phosphine Ligand. *J. Am. Chem. Soc.* *138*, 10132–10135.
 34. Paridala, K., Lu, S.M., Wang, M.M., and Li, C. (2018). Tandem one-pot CO₂ reduction by PMHS and silyloxy carbonylation of aryl/vinyl halides to access carboxylic acids. *Chem. Commun.* *54*, 11574–11577.
 35. Kubota, K., Hayama, K., Iwamoto, H., and Ito, H. (2015). Enantioselective Borylative Dearomatization of Indoles through Copper(I) Catalysis. *Angew. Chem. Int. Ed.* *54*, 8809–8813.
 36. Magalhães, J., Franko, N., Annunziato, G., Welch, M., Dolan, S.K., Bruno, A., Mozzarelli, A., Armao, S., Jirgensons, A., Pironi, M., et al. (2018). Discovery of novel fragments inhibiting O-acetylserine sulphhydrylase by combining scaffold hopping and ligand-based drug design. *J. Enzym. Inhib. Med. Chem.* *33*, 1444–1452.
 37. Bettinetti, L., Schlotter, K., Hübner, H., and Gmeiner, P. (2002). Interactive SAR studies: Rational discovery of super-potent and highly selective dopamine D₃ receptor antagonists and partial agonists. *J. Med. Chem.* *45*, 4594–4597.
 38. Takaya, J., Tadami, S., Ukai, K., and Iwasawa, N. (2008). Copper(I)-catalyzed carboxylation of aryl- and alkenylboronic esters. *Org. Lett.* *10*, 2697–2700.

39. Nogi, K., Fujihara, T., Terao, J., and Tsuji, Y. (2015). Cobalt- and Nickel-Catalyzed Carboxylation of Alkenyl and Sterically Hindered Aryl Triflates Utilizing CO₂. *J. Org. Chem.* *80*, 11618–11623.
40. Liu, R., Yang, Z., Ni, Y., Song, K., Shen, K., Lin, S., and Pan, Q. (2017). Pd(II)/Bipyridine-Catalyzed Conjugate Addition of Arylboronic Acids to α,β -Unsaturated Carboxylic Acids. Synthesis of β -Quaternary Carbons Substituted Carboxylic Acids. *J. Org. Chem.* *82*, 8023–8030.
41. Fogg, G.T., P. (1992). Carbon Dioxide in Non-Aqueous Solvents At Pressures Less Than 200 KPA. In IUPAC Solubility Data Series 50, J. W. Lorimer, H. L. Clever, and C. L. Young, eds. (Pergamon Press), p. 362.
42. Grimme, S., Antony, J., Ehrlich, S., and Krieg, H. (2010). A consistent and accurate ab initio parametrization of density functional dispersion correction (DFT-D) for the 94 elements H-Pu. *J. Chem. Phys.* *132*, 154104.
43. Becke, A.D. (1993). Density-functional thermochemistry. III. The role of exact exchange. *J. Chem. Phys.* *98*, 5648–5652.
44. Marten, B., Kim, K., Cortis, C., Friesner, R.A., Murphy, R.B., Ringnalda, M.N., Sitkoff, D., and Honig, B. (1996). New model for calculation of solvation free energies: Correction of self-consistent reaction field continuum dielectric theory for short-range hydrogen-bonding effects. *J. Phys. Chem.* *100*, 11775–11788.
45. Bochevarov, A.D., Harder, E., Hughes, T.F., Greenwood, J.R., Braden, D.A., Philipp, D.M., Rinaldo, D., Halls, M.D., Zhang, J., and Friesner, R.A. (2013). Jaguar: A high-performance quantum chemistry software program with strengths in life and materials sciences. *Int. J. Quantum Chem.* *113*, 2110–2142.